The University Of Sheffield.

Hypoxia and Reactive Oxygen Species Modulate the Interaction Between Human Neutrophils and *Staphylococcus aureus*.

Natalia Helena Hajdamowicz

The University of Sheffield

Department of Infection, Immunity and Cardiovascular Disease. The Florey Institute.

Thesis submitted for the degree of

Doctor of Philosophy

July 2021

Table of Contents

List of Figures

List of Tables

Abstract

Hypoxia and Reactive Oxygen Species Modulate the Interaction Between Human Neutrophils and *Staphylococcus aureus*.

Neutrophils are crucial to host defence, and when their function is impaired, the result is increased susceptibility to infection with a range of pathogens; *Staphylococcus aureus* (*S. aureus*) is a leading and sometimes life-threatening problem in this setting. Sites of infection are characterised by low oxygen availability, caused by consumption of oxygen by both bacteria and infiltrating immune cells, contributing to profound tissue hypoxia, which may alter the bactericidal capacity of neutrophils. Limited evidence suggests the resulting lack of oxygen to fuel the 'oxidative burst' may contribute to failure to control staphylococcal infection. We hypothesised that hypoxia modulates the host-pathogen interaction by influencing the generation of reactive oxygen species (ROS) by the NADPH oxidase in human neutrophils. The main aim of this study is to determine the impact of physiological hypoxia and pharmaceutical inhibition of ROS generation on neutrophil function, in particular the phagosomal environment and killing of ingested *S. aureus.*

In the work reported in this thesis, I demonstrated that in hypoxia, neutrophil apoptosis was diminished, and hypoxia-regulated genes (BCL2 interacting protein 3-BNIP3 and glucose transporter 1- GLUT1) are up-regulated, results that confirmed establishment of a hypoxic environment. Hypoxia limited the growth of *S. aureus* in nutrient-limited brain heart infusion (BHI), but bacteria grew slowly in nutrient-limited Roswell Park Memorial Institute (RPMI) cell culture medium, irrespective of oxygen tension. Importantly, levels of hypoxia typical of sites of infection markedly reduced the ability of neutrophils to kill *S. aureus* (Wood 46 and SH1000 strains) in a HIF-independent fashion, reduced the generation of ROS at the phagosomal membrane, and led to changes in phagosomal morphology (the formation of smaller 'tight' phagosomes), confirmed by transmission electron microscopy. Treatment with the NADPH oxidase inhibitor diphenyleneiodonium iodide (DPI) also impaired neutrophil-mediated killing of *S. aureus* and had a similar effect on phagosomal morphology, also modifying phagosomal pH (enhancing acidification). Using bafilomycin on DPI-treated neutrophils normalised the pH experienced by intracellular bacteria to a level observed

in control cells but did not restore normal phagosomal morphology or killing of *S. aureus*.

Modulation of intracellular transport processes, including recruitment of cytoplasmic oxidase components to the phagosome by inhibition of Class III PI3 kinases, led to reduced ROS production and changes in phagosomal morphology of phagosomes containing *S. aureus.* Use of vacuolar protein sorting 34 (VPS34) inhibitor restrained ROS production, changed the phagosomal morphology and very surprisingly, increased killing of *S. aureus* by human neutrophils, an effect that is not at present understood.

These findings shed light on an important host-pathogen interaction, highlighting the importance of ROS in combating staphylococcal infection. I have shown that physiological/pathological (hypoxia) and pharmacological (DPI) inhibition of ROS generation impairs killing of *S. aureus* by reducing ROS generation at the phagosome, associated with changes in phagosomal morphology and intraphagosomal pH. Manipulation of these processes by selected inhibitors may enable enhanced killing of this pathogen in hypoxic environments and could help treatment of deep-seated staphylococcal infections.

Acknowledgements

Firstly, I would like to thank my supervisors Prof. Alison Condliffe and Prof. Simon Foster for giving me the opportunity to study PhD under their supervision and for all the support given to me throughout this time. It has been a privilege to do research in your laboratories. Thank you very much Alison for your belief in me and all the personal support which you offered to me in my most challenging moments.

I would also like to thank my co-supervisor Dr Philip Elks for all of your support during the pandemic. It is much appreciated that you agreed to become my supervisor and offered helpful meetings in those weird and challenging times.

I would like to gratefully thank my unofficial supervisor and most importantly my friend, Dr David Buttle. I got to know the surrounding area of Sheffield in a completely new, colourful way! I learnt a lot about wildlife support, how to grow my own vegetables and work on an allotment! Thank you for being a part of my chosen family, your support, motivation, and strong belief in me!

I would not manage without friends. Special thanks to Emma Brudenell (Emska) and Nathan Wong (Thański) with whom I developed lifelong friendships and experienced the best holiday in my life visiting Vietnam and Singapore. Your emotional support, scientific discussions, helping each other are memories which will be with me forever!

Huge thank to other lab members of the Condliffe group: Charlotte Burton, Ben Durham, Kirsty (Krysia) Leigh Bradley, Katja Vogt, Rebecca Hull and Clare Stokes for all your input into my work, training in dealing with neutrophils but also for your all support when needed. Thank to other lab groups such as F18, Renshaw's group, Prince's group, Parker's group, Shaw's group, and Sayer's group within IICD (Grace Manley, Joanne McKenzie, Yin Xin Ho, Becky Dowey, Domen Zafred, Stavroula Louka, Ernesto Felix Diaz).

Thanks to the sponsor of my PhD the Florey Institute for funding my studies but also to the management team and members for the great time that I spent while being a

part of the FIRF! Thanks to being a member, I met fantastic people (mentioning only a few: Laia, Ruairidh, Sophie, Alex, Lucia) and I gained soft skills experience! It was a pleasure to work with you and have fun at the same time!

Words of appreciation also to our IICD technical support team (Janine, Katie, Jon, John, Ben, Mark, Linda) for all your training, support and help when most needed.

I have many lovely people outside the University that I made friends with during my life in Sheffield. Thank you all Cubana friends for providing a lot of fun into my intense PhD life, your understanding, listening and dances! I learnt how to dance salsa, bachata and kizomba!

Special thanks to my friend “Captain Will Healy” without whom my social English would be very poor, and I would not learn so many idioms! Your love, support and wiping of tears helped a lot and I will never forget the meaning of our friendship!

I would not manage in both my personal and PhD life without my beloved Family! Thanks to my sister Anna, brother Marcin and my best mother/friend/therapist Małgorzata! I would not be where I am without your constant support, believe and encouragement!

I dedicate this thesis to my beloved grandma who sadly passed away during my PhD. I love you and miss you a lot!

List of abbreviations:

AdoR- adenosine receptor

agr- Accessory Gene Regulator

AhpC- alkyl hydroperoxide reductase

ARNT- aryl hydrocarbon receptor nuclear translocator

Aur- aureolysin

BHI- Brain Heart Infusion

BNIP3- BCL2 interacting protein 3

CGD- chronic granulomatous disease

CHIPS- chemotaxis inhibitory protein of S. aureus

Clf- clumping factor

Cna- collagen adhesin

Coa- coagulase

CXCL1/2/5- C-X-C motif chemokine ligand 1/2/5

DAMPs- damage-associated molecular patterns

DMOG- dimethyloxallyl glycine

DPI- diphenyleneiodonium iodide

Ebp- elastin-binding protein

EDTA- ethylenediaminetetraacetic acid

FAD- flavin adenine dinucleotide

FBS- fetal bovine serum

FcRs- Fc receptors

Fe2+- iron ions

FIH- factor inhibiting HIF

FMLP- N-formylmethionine-leucyl-phenylalanine

FnBP- fibronectin-binding protein

G-CSF- granulocyte colony-stimulating factor

GLUT1- glucose transporter 1

GMP- granulocyte-monocyte progenitor

GPCRs- G protein-coupled receptors

H2O2- hydrogen peroxide

HIF- hypoxia inducible factor

HSC- hematopoietic stem cells

iNOS- inducible nitric oxide synthase

KatA- catalase

LAP- LC3-associated phagocytosis

LPMP- lymphoid-primed multipotent progenitor

LPS- lipopolysaccharide

MAP1Lc3- microtubule-associated proteins 1A/1B

MIP-1β- macrophage inflammatory protein-1β

mmHg- millimetres of Mercury

MMP- matrix metalloproteinase

MPO- myeloperoxidase

MPP- multipotent progenitor

MRSA- methicillin resistant Staphylococcus aureus

MRSA- methicillin-resistant S. aureus

MSCRAMMs- microbial-surface components recognising adhesive matrix molecules

MTD- mitochondrial DAMPs

NADPH- nicotinamide adenine dinucleotide phosphate

NETs- neutrophil extracellular traps

NFK β - nuclear factor-kappa β

NO- nitric oxide

NOX- NADPH oxidase

$O2^{-}$ - superoxide

OatA- peptidoglycan O-acetylase

ODD- oxygen- dependent domain

$OH^{\bullet}$- hydroxyl radicals

PAMPS- pathogen-associated molecular patterns

PBMCs- peripheral blood mononuclear cells

PBS- phosphate-buffered saline

PHDs- prolyl hydroxylases

PI3K- phosphoinositide 3-kinase

PIP2- Phosphatidylinositol-(4,5)-bisphosphate

PIP3- Phosphatidylinositol-(3,4,5)-trisphosphate

PKC- protein kinase C

PLD- phospholipase D

PMN- polymorphonuclear

PPP- platelet poor plasma

PRP- platelet rich plasma

PRR- pattern recognition receptor

PSMs- phenol- soluble modulins

RBCs- red blood cells

ROS- reactive oxygen species

RPMI- Roswell Park Memorial Institute

RT- room temperature

sar- Staphylococcal Accessory Regulator

SGD- specific granule deficiency

SIRS- systemic inflammatory response syndrome

SodA/M- superoxide dismutase A/M

SpA- staphylococcal protein A

SSL- staphylococcal superantigen-like protein

SSTI- skin and soft tissue infections

TEM- transmission electron microscopy

TLRs- Toll-like receptors

TNBS- trinitrobenzenesulfonic acid

TNF- tumour necrosis factor

VEGF- vascular endothelial growth factor

VHL- von Hippel-Lindau tumour suppressor protein

VRSA- vancomycin-resistant *S. aureus*

WBCs- white blood cells

1 Introduction and Overview

Staphylococcus aureus (*S. aureus*) is a Gram-positive coccal bacterium, which colonizes around 30% of the population worldwide (Thammavongsa *et al.*, 2015). It causes frequent infections of the skin, but also can act as an opportunistic pathogen causing severe and even life- threatening human infections if mucosal surfaces are breached. *S. aureus* possesses numerous virulence factors which help it to cross the skin barrier and access deeper tissues, thereby causing a spectrum of diseases from local skin and soft tissue infections (including superficial abscesses, furuncles, and cellulitis) to more severe metastatic conditions with high mortality, such as osteomyelitis, endocarditis and septicaemia (Tong *et al.*, 2015). The importance of *S. aureus* as a human pathogen is enhanced by its multidrug resistance profile. In the pre-antibiotic era *S. aureus* bloodstream infection was fatal in about 80% of cases, but this outlook was dramatically improved by the introduction of penicillin. However, *S. aureus* rapidly acquired penicillinase to destroy this antibiotic. Although further antibiotics have been developed, resistance has again evolved. There are now different strains resistant to most available antibiotics e.g., methicillin-resistant *S. aureus* (MRSA) and vancomycin-resistant *S. aureus* (VRSA) (Gardete and Tomasz, 2014). MRSA/VRSA are listed as Priority 2 pathogens (requiring urgent research and drug development) by the World Health Organisation (https://www.who.int/medicines/publications/WHO-PPL-Short_Summary_25Feb-ET_NM_WHO.pdf); only 3 pathogens are listed in the more critical Priority 1 category. They are also classed as a 'Serious Threat' by the Centre for Disease Control (https://www.cdc.gov/drugresistance/biggest-threats.html; only 5 pathogens are on the 'Critical Threat' list above this). Thus *S. aureus* is a major worldwide healthcare problem and research is needed to understand it and design new ways of treating it.

In addition to its ability to respond to evolutionary pressures from antibiotics, *S. aureus* has also evolved to combat the antimicrobial mechanisms of professional phagocytic cells such as polymorphonuclear leukocytes (PMNs or neutrophils) and macrophages. Neutrophils are crucial for human defence against staphylococcal infections, as highlighted when neutrophil function is defective (see Section 1.3.6). Of importance, *S. aureus* may persist inside the neutrophil despite the high-grade bactericidal

functions these cells command, such as production of reactive oxygen species (ROS), and discharge of granule proteases and antimicrobial peptides (Lu *et al.*, 2014; Leliefeld *et al.*, 2018). Many factors contribute to the resistance of *S. aureus* to host-mediated killing, including the propensity of this pathogen to infect areas of relative tissue hypoxia. Whilst in healthy tissues the oxygen tension is commonly 20-70 mm Hg (2.5-9% O_2), infection sites show much lower oxygen levels, often <10 mm Hg (<1% oxygen), measurements of fluids from patients clinically documented with abdominal or anorectal infection (Simmen and Blaser, 1993). The efficacy of innate immune cells to handle this pathogen is thus at least partly dependent on their ability to operate in low-oxygen environments. Of note, under low oxygen tension *S. aureus* is still highly successful as a pathogen in causing infections.

There is incomplete understanding of interactions between innate immune cells and *S. aureus*, and how these interactions may result in pathogen death, containment, or dissemination. It is essential to study host-pathogen interaction under conditions that resemble those present in humans during bacterial invasion, such as hypoxia.

1.1 Innate and Adaptive Immunity

Immunity is divided into two main ‘compartments’, determined by the speed and specificity of the response to infection. They are called the innate and adaptive systems, although there is some interaction and cross-over between these two components. Innate immunity consists of physical (e.g., skin barrier), chemical (e.g., secretion of antimicrobial peptides) and cellular (e.g., macrophages and neutrophils) barriers. The innate immune response is rapid (constitutively present to several hours) and non-specific, in comparison to the adaptive immune responses which take longer to develop (several days to weeks), are highly specific, evolve with the pathogen, and establish a memory component. Although not antigen- specific, the innate immune system is able to distinguish between foreign (‘’non-self’’) particles and the body’s own molecules (‘’self’’). This is achieved by phagocytic cells (macrophages and neutrophils) possessing pattern recognition receptors (PRRs), which recognise structures that are present on microbes (but not on host cells) and are called pathogen-associated molecular patterns (PAMPS), for example Toll-like receptors (TLRs). Engagement of PRRs by PAMPs activates the innate immune cells, initiating

antimicrobial responses. Adaptive immunity utilizes antigen- specific receptors present on T and B lymphocytes to direct targeted effector reactions against pathogens. It takes time to develop this type of immunity, but the mechanisms, once activated, fight pathogens effectively and specifically by antibody production and cytotoxic T cell responses (Parkin and Cohen, 2001).

1.2 Macrophages

Macrophages (Mφ) are highly plastic innate immune cells, which can develop phenotypic and functional characteristics on a spectrum between pro-inflammatory (M1) and anti- inflammatory (M2). Resident macrophages patrol tissues such as the lung and constitute an immediate defensive platform. In the setting of infection, circulating monocytes are recruited to tissues and differentiate into macrophages, which adopt a phenotype on the M1-M2 spectrum according to local conditions (Accarias *et al.*, 2016). These professional phagocytes are long-lived, mobile cells, often named (and developing specialised features) according to their residence in different organs, for instance liver macrophages are known as Kupffer cells, whilst brain-resident macrophages are known as microglia.

Macrophages recognise foreign particles, interact with, and ingest (phagocytose) them, killing them where possible and presenting processed antigens to other immune cells to initiate adaptive immunity (antigen presentation). However, staphylococci have been found to persist within macrophages (Kubica *et al.*, 2008), particularly in the setting of certain diseases such as cystic fibrosis (Li *et al.*, 2017) where their function is compromised. Whilst macrophages have undoubted significance in anti-staphylococcal immunity, the focus of this thesis is on neutrophils, since impaired neutrophil functions are associated with enhanced occurrence of, and severe outcomes from, staphylococcal infections (Section 1.3.6). Hence, these cells will be further described, with reference to their interactions with *S. aureus*, in the following sections.

1.3 Neutrophils

Neutrophils or PMNs are one of three types of granulocytic white blood cells (the others being eosinophils and basophils) which are part of the innate immune system.

They are produced from hematopoietic stem cells in the bone marrow (Fig 1.1), where they undergo several transformations before becoming mature cells ready to be released to the blood circulation (Görgens *et al.*, 2013). More than 10^{11} cells are produced every day (Dancey *et al.*, 1976). The process of generation of neutrophils is known as granulopoiesis. Hematopoietic stem cells differentiate into multipotent progenitors which then transform into lymphoid-primed multipotent progenitors. These latter cells differentiate into granulocyte-monocyte progenitors which, under the control of granulocyte colony-stimulating factor (GCF), then transform into myeloblasts. From this point they mature through the stages of promyelocyte, myelocyte, metamyelocyte, band cell and finally become a mature neutrophil (von Vietinghoff and Ley, 2008); see Fig. 1.1). Throughout differentiation, the developing neutrophil nucleus changes from a round shape into a banded and then a lobulated morphology (which may enhance its ability to navigate through narrow capillaries) as well as the expression of several receptors. Mature neutrophils contain antimicrobial granules and secretory vesicles that are formed as differentiation proceeds. There are three types of granules namely primary (azurophil), secondary (specific) and tertiary (gelatinase) granules. They store an arsenal of antimicrobial enzymes such as myeloperoxidase, defensins, elastase and matrix metalloproteinases that are used to destroy pathogens (Häger *et al.*, 2010).

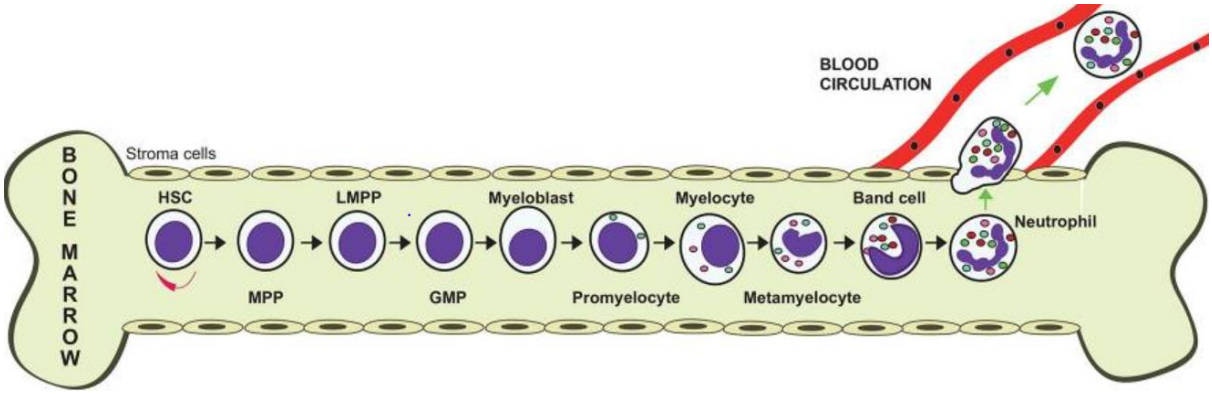

Figure 1.1 Granulopoiesis

Neutrophils are generated in the bone marrow from the hematopoietic stem cells (HSC). From HSC a multipotent progenitor (MPP) cell is formed. Next, MPPs develop into lymphoid-primed multipotent progenitors (LPMP) which differentiate to granulocyte-monocyte progenitors (GMP). Under the control of granulocyte colony-stimulating factor (G-CSF) GMPs leads to neutrophil generation by transforming to myeloblasts which then undergo a maturation process through the stages of promyelocyte, myelocyte, metamyelocyte, band cell and finally, mature neutrophil (adapted from Rosales, 2018).

Neutrophils from the bone marrow enter the bloodstream and are the most plentiful circulating leukocytes (around 70% of total white blood cells). Thanks to the fine balance between production and elimination, known as neutrophil homeostasis, the number of those cells in circulation stays relatively steady except in infection, when increased neutrophil production and release from the bone marrow occurs. Once neutrophils reach the end of their lifespan they are either removed from the blood by the spleen, or in tissues they are cleared by resident macrophages and dendritic cells through phagocytosis of apoptotic cells ('efferocytosis'; (Bratton and Henson, 2011).

Neutrophils are not classically tissue-resident cells but transmigrate on demand to the site of an infection or inflammation, exiting the circulation by the process known as the leukocyte adhesion cascade (Vogt *et al.*, 2019). Neutrophils are rapidly responsive, are the fastest moving cells in the body, but are also short-lived (although their lifespan may be prolonged by inflammatory mediators and by hypoxia in the setting of infection). Their role is to recognise the invading pathogens, transmigrate to the site of an infection, phagocytose and kill bacteria (by deployment of pre-formed antimicrobial granules and *de novo* generation of reactive oxygen species (ROS) by the NADPH oxidase complex).

1.3.1 Neutrophil killing mechanisms

Host cells including PMNs recognise multiple pathogen-associated molecules such as peptidoglycan, lipoproteins, lipoteichoic acids, lipopolysaccharide or flagellin, whether integral to, or secreted by bacteria. These molecules represent pathogen-associated molecular patterns (PAMPs) and are recognised by receptors, e.g., toll-like receptors (TLRs), which are present on the surface of immune cells including neutrophils (Sabroe *et al.*, 2003). Amongst the TLRs, only TLR3 seems not be expressed by human neutrophils as indicated by lack of responses when its agonist Poly I:C was applied (Hayashi *et al.*, 2003).

Receptor ligation to PAMPs triggers a range of host cells to produce various proinflammatory cytokines and chemokines, such as interleukin (IL)-8, IL-1alpha and beta, CXCL1, CXCL2, CXCL5, tumour necrosis factor (TNF), and granulocyte-macrophage colony stimulating factor (G-MCSF) (Adams *et al.*, 2021). These molecules act as chemoattractants, recruiting neutrophils to the infected tissues

(reviewed by (Kobayashi *et al.*, 2018). Recognition of PAMPs (or of host factors that bind them) by recruited neutrophils is essential for subsequent phagocytosis. Phagocytosis is a complex process linking cell surface receptors such as TLRs, scavenger receptors ans C-type lectin to microbial PAMPs or host-derived antibodies. Pathogens may also be coated by opsonins (such as complement components and antibodies produced by the adaptive response), which engage opsonic receptors such as CR1 and CR3 for C3b and FcγRII and FcγRIII for IgG. These interactions lead to alterations in neutrophil membrane conformation, changes in phospholipid metabolism and actin cytoskeleton rearrangement, culminating in the formation of pseudopodia around the pathogen (reviewed by (van Kessel *et al.*, 2014). This eventually leads to the formation of a membrane-bound phagosome within which pathogens become enclosed and where most microorganisms are effectively killed (Fig. 1.2).

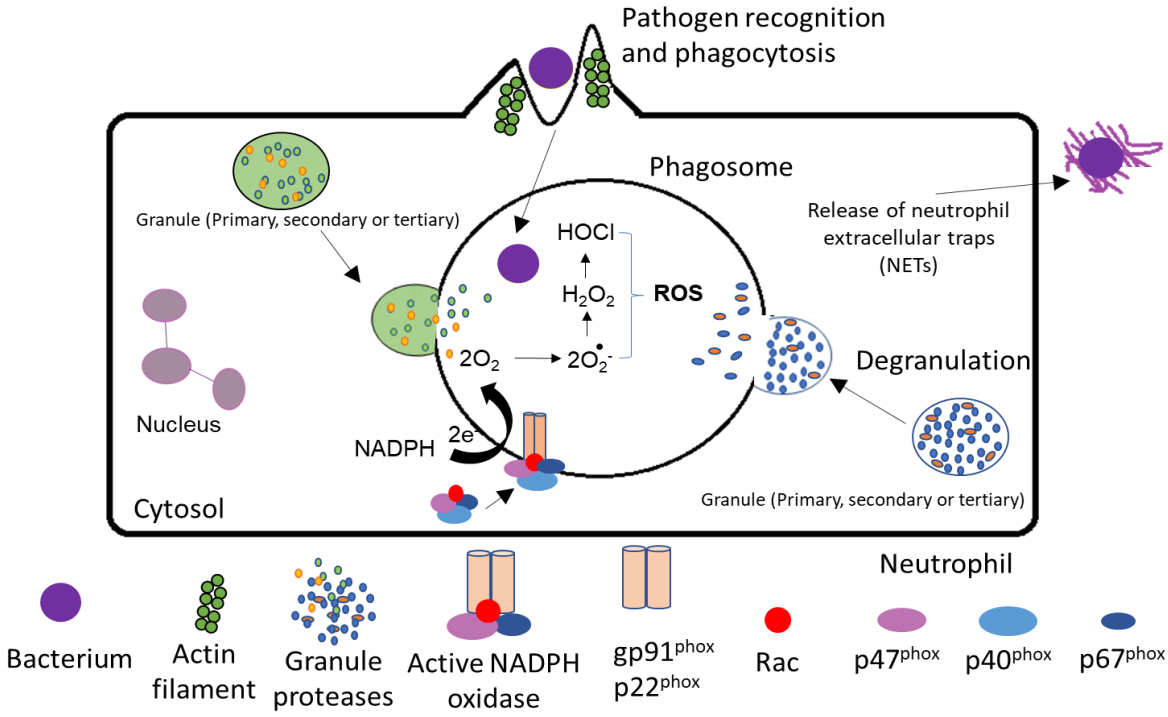

Figure 1.2 Bacterial killing mechanisms of an activated neutrophil

The neutrophil, activated by phagocytosis, engages multiple (oxidative and non-oxidative) mechanisms to kill engulfed bacteria. At the phagosomal membrane, the components of the NADPH oxidase are assembled to form an active complex producing ROS. Neutrophils also contain many granule populations, which fuse with the phagosome to release antimicrobial peptides such as lactoferrin, myeloperoxidase (MPO) or elastase. When the target microorganism is too large to be internalised, neutrophils release neutrophil extracellular traps (NETs) to kill bacteria extracellularly (adapted from Ulfig and Leichert, 2021)

1.3.2 Maturation of the phagosome

Immediately after formation, the phagosome does not have bactericidal ability, rather its membrane resembles the plasma membrane, and its fluid contents are a sample of the extracellular medium. However, not long after (or even prior to) sealing, the vacuole undergoes massive changes in its composition as a progressive maturation process occurs. Unlike macrophage phagosomes, neutrophil phagosomes do not acidify, as V-ATPases do not accumulate efficiently on phagosomes when the NADPH oxidase is active (El Chemaly *et al.*, 2014). This may reflect the fact that neutrophil phagosomal maturation is less dependent on endosomal/lysosomal fusion events. Studies on neutrophils reveal that their phagosomal pH is in fact somewhat alkaline at 8.5-9 for the first 30 minutes (mins) following phagocytosis (Levine *et al.*, 2015; Segal *et al.*, 1981). This alkalisation together with the influx of potassium ions (Reeves *et al.*, 2002) leads to activation of the neutral proteases that are released into the phagosome from the cytoplasmic granules, which are mobilised by calcium fluxes and microtubule dynamics to fuse with the phagosomal membrane (Nordenfelt and Tapper, 2011). This early alkalisation is maintained by the activity of NADPH oxidase, with electron transfer and consumption of protons in the phagosomal space (Segal *et al.*, 1981; Foote *et al.*, 2019). Proton channels such as Hv1 (also called HVCN1) prevent neutrophil phagosomal acidification by sustaining the high-level ROS production that inhibits V-ATPase accumulation on phagosomes until later time points (El Chemaly *et al.*, 2014). Foote *et al.* also reported the increase in alkalinity of the phagosome milieu correlated with increased oxidase activity (Foote *et al.*, 2019).

The NADPH oxidase is activated and regulated by the combined action of intracellular signalling pathways, including phosphoinositide 3-kinase (PI3K), protein kinase C (PKC) and phospholipase D (PLD) (Condliffe *et al.*, 2005). Neutrophils express all PI3K classes (I, II, III). It has been shown that class I PI3Ks are responsible for generation of PtdIns(3,4,5)P_3 (PIP_3) that has a major effect on regulation of the oxidase in human neutrophils by stimulation with N-formylmethionine-leucyl-phenylalanine (FMLP) (van Kessel *et al.*, 2014; Yasui and Komiyama, 2001). The role of PI3Ks in the oxidative burst is described in more detail in Section 1.3.4.

Another intracellular antimicrobial pathway called LC3-associated phagocytosis (LAP) has been shown to play a role in maturation of phagosomes in some settings. LAP

incorporates certain features of autophagy (lipidation of LC3, but not generation of a double-membrane structure) into the phagocytic pathway. The hallmark of LAP is decoration of the single membrane phagosome (containing internalised bacteria) with lipidated LC3; this is in contrast to canonical autophagy which is characterised by double membrane LC3-decorated autophagosome formation. Most studies on LAP have been done on macrophages, with microorganisms such as *Aspergillus fumigatus, Listeria monocytogenes and Mycobacterium tuberculosis;* collectively, these studies have suggested an important role for LAP at the early stages of infection with certain pathogens (Lam *et al.*, 2013; Lerena and Colombo, 2011; Huang *et al.*, 2009). LAP seems to occur at the earlier timepoints *in vivo* than autophagy and has been suggested to provide an intracellular niche for staphylococci within neutrophils in a zebrafish model (Prajsnar *et al.*, 2021). It was demonstrated by Prajsnar *et al.* that ingested Staphylococci were present (as early as 1 hour post-infection - hpi) within LC3-positive, spacious 'LAPosomes' in zebrafish neutrophils. Importantly, bacteria were able to proliferate and escape from these structures to the cytoplasm, where they could trigger canonical autophagy with microbicidal effect (Gibson *et al.*, 2020).

1.3.3 Non- oxidative killing by PMNs

Neutrophils are granulocytes, containing abundant granules that can be termed peroxidase positive (azurophil or primary) and negative (specific or secondary and gelatinase or tertiary) granules, based on their enzymatic content (Bainton and Farquhar, 1968; Bainton *et al.*, 1971). They are formed by the process known as granulopoiesis, which begins between the myeloblast and promyelocyte stages and proceeds over 4 to 6 days (Summers *et al.*, 2010; Bainton *et al.*, 1971). Granulopoiesis begins with the genesis of primary (azurophilic) granules, followed by production of specific granules with gelatinase granules formed during the transition into band neutrophils. Neutrophil granulopoiesis is completed with the development of ficolin-1-positive granules and secretory vesicles, at the stage when the neutrophil nucleus acquires its characteristic multi-lobed phenotype (Kennedy and DeLeo, 2009; Faurschou and Borregaard, 2003). The granules' contents can be released by either intracellular or extracellular degranulation (Fig. 1.3).

Fusion of granules with the phagosome is critical for the killing of many pathogens and hence is tightly regulated. Extracellular degranulation is hierarchical, with progressive release of tertiary, secondary and finally primary granules depending on the degree of elevation of intracellular calcium levels, but granule fusion with the phagosomal membrane is less well understood. Electron micrographs of both events are shown below (Fig. 1.3.). The early granule-phagosome fusion events are dependent on calcium but this does not seem to be the case for the fusion of azurophilic granules with phagosomes at later stages (Nordenfelt and Tapper, 2010). Rab proteins (e.g., Rab5, 7 and 11) are important regulators of phagosome fusion events, promoting recognition of membranes that are destined to fuse, with SNARE proteins (e.g., syntaxins 7, 8 and 13 and VAMPs 3, 7 and 8) helping to enact fusion at a molecular level (reviewed by (Haas, 2007).

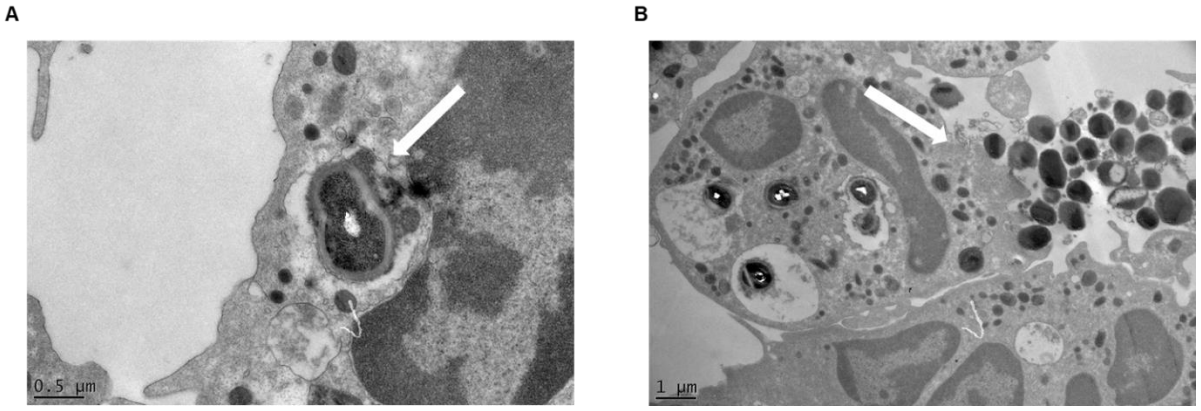

Figure 1.3 Intra- and extracellular degranulation in the human neutrophil in response to *S. aureus* infection

Electron microscopic images acquired in this study (see Materials and Methods Section 2.8). Briefly, neutrophils were infected with S. aureus at MOI 10 and fixed at 0.5 h post infection prior to processing. ***(A)*** *Intracellular degranulation showing the fusion of granules (denoted by the white arrow) with the phagosome which contains an ingested S. aureus particle,* ***(B)*** *Extracellular degranulation of the neutrophil denoted by the white arrow. Scale bars are 0.5 µm for A and 1 µm for B.*

Myeloperoxidase (MPO) is the protein that defines peroxidase-positive granules (Bainton and Farquhar, 1968). The large, dense azurophil or primary granules also contain digestive enzymes such as the serine proteases, namely proteinase 3, cathepsin G, neutrophil elastase (NE) and the more recently described neutrophil

serine protease 4 (NSP4) (Pereira *et al.*, 1990; Perera *et al.*, 2013). These enzymes and other granule contents are released into the phagosomes. Granule proteins contribute to the toxic bactericidal environment in a manner which is likely both synergistic and pathogen specific. For example, cathepsin G is known to target *S. aureus* (Reeves *et al.*, 2002), and mice lacking both elastase and cathepsin G but not either alone are susceptible to fungal infection (Tkalcevic *et al.*, 2000). Alpha-defensins (peptides abundant in azurophil granules) display broad antimicrobial activity against bacteria, enveloped viruses, and protozoa by creating transmembrane pores in the microbial outer membrane (Faurschou and Borregaard, 2003; Ganz *et al.*, 1985; Wimley *et al.*, 1994). In contrast to the azurophil granules, specific and gelatinase granules are more readily mobilised to the plasma membrane for extracellular release (Bainton and Farquhar, 1968; Leffell and Spitznagel, 1974), but nonetheless their contents are also released in abundance into the phagosome and contribute to the phagosomal environment. Specific (secondary) granules are rich in lactoferrin, which has direct bacteriostatic and bactericidal effect against many pathogens, including Gram-positive bacteria, largely by its iron-chelating effect (Valenti and Antonini, 2005). Specific granules also convey membrane components of the NADPH oxidase to the phagosome. Gelatinase (tertiary) granules contain matrix-degrading enzymes such as gelatinase (also known as matrix metalloproteinase-9 - MMP-9) and also membrane receptors namely CD11b/CD18, CD67, fMLF-R, SCAMP and VAMP2, which play an important role in the earliest phases of the neutrophil inflammatory responses when mobilized to the cell surface (Cowland and Borregaard, 2016; Faurschou and Borregaard, 2003). Overall, infection as exemplified by presence of pathogens within a phagosome is a strong degranulation stimulus, resulting in rapid granule mobilisation (Lodge *et al.*, 2017; Lodge *et al.*, 2020) to the intracellular or extracellular milieu.

1.3.4 Oxidative killing by PMNs

Stimulated PMNs exhibit an abrupt and dramatic increase in oxygen consumption, the so-called neutrophil respiratory or oxidative burst (Reiss and Roos, 1978). The enzyme responsible for the respiratory burst is a multicomponent complex with subunits organised into distinct compartments in the resting neutrophil. Two subunits, $p22^{phox}$ and $gp91^{phox}$ (known as NOX2) form a heterodimer, which comprises the

membrane-localized part of the enzyme, referred to as cytochrome b_{558}. The cytochrome b_{558} is present in the plasma membrane of neutrophils, however the majority of it is expressed in the membrane of specific granules (Borregaard *et al.*, 1983). The cytoplasmic subunits include $p40^{phox}$, $p47^{phox}$ (also called neutrophil cytosolic factor 1, NCF1), $p67^{phox}$ and Rac2 (Groemping and Rittinger, 2005; El-Benna *et al.*, 2008). Mutations in $p22^{phox}$, $gp91^{phox}$, $p47^{phox}$ and $p67^{phox}$ have long been known to cause the primary immune deficiency disease chronic granulomatous disease (CGD) which is characterised by a failure of the phagocyte respiratory burst and extreme susceptibility to infections with *S. aureus* and fungi such as *Aspergillus spp* (Winkelstein *et al.*, 2000). Whilst the importance of $p40^{phox}$ to the oxidative burst was previously uncertain, neutrophils from $p40^{phox-/-}$ mice were shown to exhibit severe defects in the NADPH oxidase-dependent ROS production in response to *S. aureus,* suggesting that $p40^{phox}$ is an essential component in bacterial killing (Ellson *et al.*, 2006). More recently, $p40^{phox}$ loss-of-function mutations in patients with a mild version of CGD have been shown to impair phagocytosis-induced ROS generation (but not the PMA-induced oxidative burst) and to impair the killing of *S. aureus* but not fungi (Geer *et al.*, 2018). This may reflect the critical importance of phagosomal ROS in killing *S. aureus*, or an alternative pathogen-specific function of $p40^{phox}$. Study of Hsu P. A *et al*. (2019), has shown that dominant activating mutation in Ras-related C3 botulinum toxin substrate 2 (RAC2), the small GTPase, in patients leads to lymphoid and myeloid defects. Mice with a gain-of-function of Rac2 (E62K) display similar to the T- and B- cell lymphopenia, leading to activation of neutrophil superoxide production by its interactions with reduced NADPH-oxidase component $p67^{phox}$, demonstrating the important role of Rac2 in hematopoietic cells (Hsu *et al.*, 2019).

ROS are harmful to the host cell and tissues; hence NADPH oxidase activation must be strictly regulated in time and space to limit ROS production. NADPH oxidase assembly and activation (see Figure 1.4) is regulated by processes such as binding of $p47^{phox}$ and $p40^{phox}$ to phospholipids, phosphorylation of its components, and activation of the GTPase Rac2. Binding of the membrane phospholipid phosphadylinositol-3-phosphate (PI3P) to the PX (Phox homology) domain of $p40^{phox}$ was found to be important for oxidase assembly and activation at the phagosome in response to both *S. aureus* and *E coli.*; the phagosomal PI3P responsible for this binding was found to be synthesised predominantly by the Class III PI3K known as

VPS34 (Anderson *et al.*, 2008), although PI3P is also produced by sequential dephosphorylation of PIP_3 (produced in abundance at the phagosomal membrane by the activation of Class 1 PI3Ks). The PX domain of $p47^{phox}$ binds to phosphatidylinositol 3,4 bisphosphate ($PI(3,4)P_2$) (Kanai *et al.*, 2001), which is generated at the phagosome either by dephosphorylation of PIP_3 (produced by the activation of Class 1 PI3Ks) or *de novo* by Class II PI3Ks. However, use of R90A mutations in the $p47^{phox}$ PX domain that result in loss of phosphoinositide binding, resulted in marked impairment of ROS generation in response to soluble stimuli, but only a minor reduction in the response to a number of particulate stimuli including *S. aureus* (Li *et al.*, 2010). This work was done in mouse neutrophils using opsonized prey but does suggest that at the *S. aureus* containing phagosome, the interaction between PI3P and $p40^{phox}$ is predominant in mediating recruitment and activation of the oxidase.

The phox components of the oxidase all become phosphorylated on neutrophil activation, and many of these phosphorylation events are important for oxidase assembly and activation (for a recent review of this extensive literature, see (Belambri *et al.*, 2018). It should be noted that the majority of studies have been performed on neutrophils stimulated by soluble stimuli, particularly PMA; since PMA activates protein kinase C (PKC), which is responsible for many of the phosphorylation events detected, it is possible that not all of the detected events are relevant to phagosomal oxidase assembly. Work by Garcia and Segal in 1988 compared protein phosphorylation in normal and flavocytochrome b_{558}- deficient neutrophils from X-linked CGD patients, demonstrating that $gp91^{phox}$ and $p22^{phox}$ are phosphorylated in PMA- and IgG opsonized latex particle stimulated neutrophils (Garcia and Segal, 1988). *In vitro* studies revealed that phosphorylation of $p47^{phox}$ induces its interaction with $p22^{phox}$ (Fontayne *et al.*, 2002; Groemping and Rittinger, 2005). $gp91^{phox}$/NOX2 and $p22^{phox}$ are phosphorylated by PKC in human neutrophils to promote the assembly and catalytic activity of the multimeric complex (Raad *et al.*, 2009; Regier *et al.*, 1999), whilst phosphorylation of $gp91^{phox}$ by the ataxia telangiectasia-mutated (ATM) kinase seems to limit oxidase activation (Beaumel *et al.*, 2017). A range of $p47^{phox}$ phosphorylation events regulate NADPH oxidase activation and are summarised by Belambri *et al.* (2018). Pro-inflammatory cytokines such as TNF-alpha and GM-CSF do not activate the NADPH oxidase directly, but they prime its activation in response

to a secondary stimulus as the bacterial tripeptide fMLF. These priming molecules induce the phosphorylation of $p47^{phox}$ specifically on Ser345 by p38MAPK, and this event plays a critical role in the priming of ROS production in neutrophils (Dang *et al.*, 1999; Dewas *et al.*, 2003; Dang *et al.*, 2006).

During the activation of neutrophils, the cytoplasmic subunits of NADPH oxidase translocate to the membrane and assemble a functional electron transport machinery, regulated as noted above by phosphorylation event and lipid binding. Upon activation, electrons from cytoplasmic NADPH are transported across the membrane to the cytochrome via flavin adenine dinucleotide (FAD) to molecular oxygen, that is thereby reduced to superoxide (O_2^-; one electron reduction), first of the formed ROS. Superoxide rapidly dismutates to form hydrogen peroxide (H_2O_2; two electron reduction). Starting with the production of superoxide and hydrogen peroxide, the oxidative burst of PMNs initiates the generation of a cascade of labile reactive oxygen species (ROS). Reaction of superoxide anion with nitric oxide (NO) leads to formation of strongly cytotoxic peroxynitrite. In the presence of ferrous ions (Fe^{2+}), hydrogen peroxide is converted into strongly reactive hydroxyl radicals (OH•) by the 'Fenton reaction'. Hydroxyl radicals induce peroxidation of lipids in cell membranes, affecting their fluidity, and have been shown to kill *S. aureus* directly in culture *in vitro* (Repine *et al.*, 1981). Released by degranulation, myeloperoxidase (MPO) from azurophil granules catalyses the reaction of hydrogen peroxide with halide molecules (Cl_2, Br_2 and J_2) leading to formation of highly toxic hypohalides (OCl^-, OBr^- and OJ^-), and hypohalous acids. Whilst it is currently impossible to study the complex (and in some cases highly ephemeral) mixture of ROS and ascribe individual functions to the various species, hypochlorous acid has been incorporated into a wound irrigation system currently undergoing clinical trials in human patients requiring skin grafts (in whom *S. aureus* infection may be devastating and lead to graft failure), and was found to induce a 50% decrease in *S. aureus* growth in biofilms *in vitro* (Burian *et al.*, 2021). *In vivo*, all forms of ROS are likely to be critical components of the intracellular killing of ingested pathogens; if released into the extracellular milieu they can also be important mediators of the destruction of the healthy tissue (Hampton *et al.*, 1996; Hampton *et al.*, 1998; Weiss, 1989).

ROS production is inhibited by iodonium compounds such as diphenyleneiodonium iodide (DPI), which directly inhibits NADPH oxidase activity, hence leading to inhibition of ROS production in neutrophils. It inhibits the reduction of FAD and cytochrome b_{558} (Cross and Jones, 1986). However, DPI can inhibit other flavoproteins, hence it is not totally specific for the phagocytic NADPH oxidase. It was reported to affect other oxidases, including xanthine oxidase and components of the mitochondrial electron transport chain (Hirano *et al.*, 2015; Holland and Sherratt, 1972). It has been suggested that other compounds may be more specific ROS production inhibitors, such as a small molecule termed GSK2795039 (Hirano *et al.*, 2015), or apocynin which is an inhibitor of the intracellular translocation of two cytosolic subunits of the NADPH oxidase- p47 and p67 (Stolk *et al.*, 1994; Vejrazka *et al.*, 2005). However, apocynin also has off-target effects, for example inhibiting cytokine-mediated ERK1/2 phosphorylation, independently from its action on ROS (Pintard *et al.*, 2020).

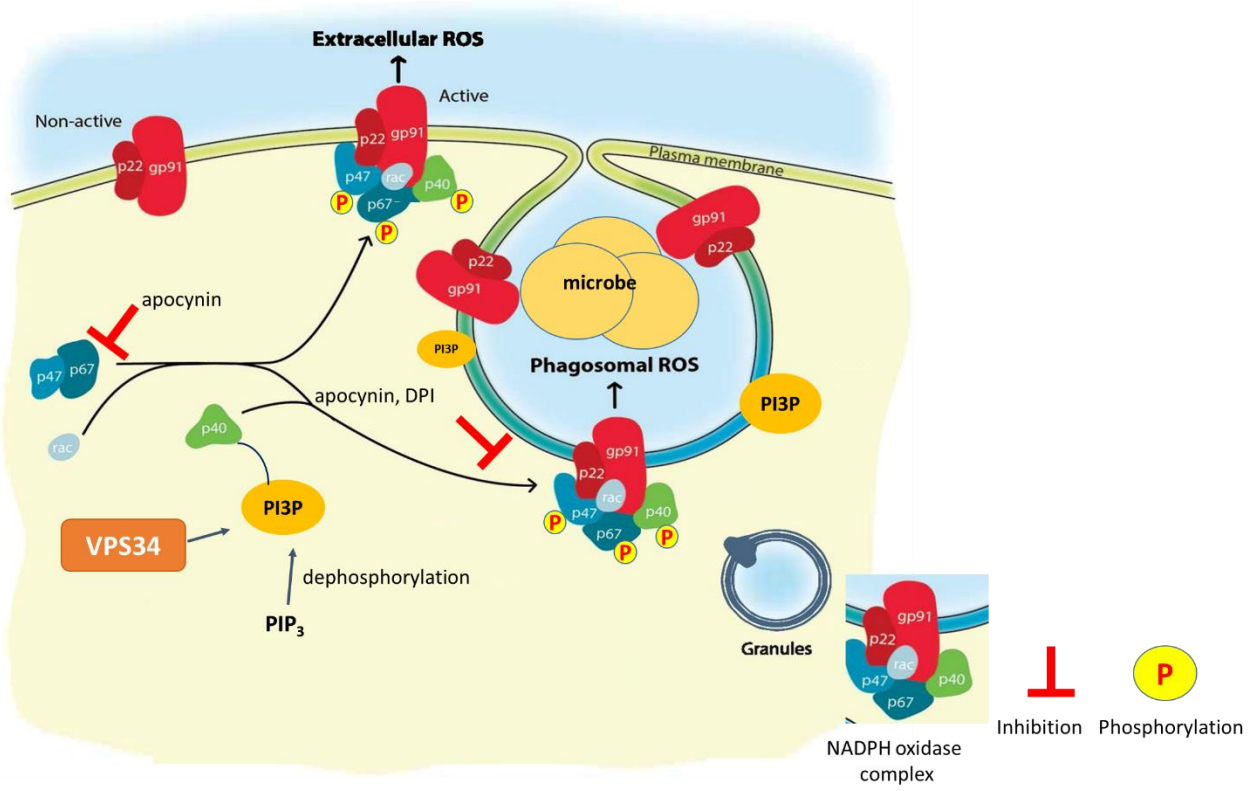

Figure 1.4 Schematic of the NADPH oxidase assembly and its inhibition

NADPH oxidase subunits are divided to the cytosolic and membrane (largely of specific granules) by their localisation within the cell. To become active, all subunits- p40 (binds with PI3P), p47^{phox}, p67^{phox}, p22^{phox}, gp91 and Rac2 are recruited to membranes (dependent on

lipid binding and phosphorylation events). ROS can be produced extracellularly or intracellularly. Activation of the NADPH oxidase complex leads to production of O_2^- and H_2O_2, subsequently converted to hypohalides in a reaction that is catalysed by MPO (azurophil granules). Modified from (Dahlgren et al.*, 2019).*

Neutrophils extracellular traps (NETs) are reticulate formations of extracellular DNA release with associated antimicrobial molecules (mostly granule proteins and histones) and may play a role in innate immune defence (Ab *et al.*, 2012; Goldmann and Medina, 2012). In humans, this process was first described in 2004 (Brinkmann *et al.*, 2004). NETs release is induced by various host or pathogen derived molecular signals such as IL-8 (Keshari *et al.*, 2012), TNF- alpha, LPS, and fMLP, as well as by the pharmacological agent PMA (Brinkmann *et al.*, 2004; Gupta *et al.*, 2005). Neutrophil ROS are an integral part of most reaction cascades leading to the release of NETs (Ab *et al.*, 2012; Kirchner *et al.*, 2012; Arazna *et al.*, 2013). Most NETosis requires ROS formation by the NADPH oxidase complex (Guimarães-Costa *et al.*, 2012; Röhm *et al.*, 2014; Aleyd *et al.*, 2014; Fuchs *et al.*, 2007) and is linked to the autophagy pathway (Mitroulis *et al.*, 2011; Remijsen *et al.*, 2011). NETosis was also shown to be activated when the internalisation of the pathogen is not feasible, therefore allowing the invading pathogens to be killed extracellularly (Rigby and DeLeo, 2012). There are conflicting findings with regards to the killing of pathogens by release of NETs. Brinkmann *et al.* demonstrated that inhibiting neutrophil phagocytosis with cytochalasin D still permitted NETs formation and the ability to kill *S. aureus* was preserved (Brinkmann *et al.*, 2004). Opposite findings were reported by Menegazzi *et al.* where there was no microbicidal effect of NETs against *S. aureus* with release of live bacteria on the addition of DNAse (Menegazzi *et al.*, 2012). Such differences might be related to the timing of DNAse addition to dismantle NETs, or incomplete inhibition of phagocytosis by cytochalasin D. NETs are likely to contribute to tissue damage and have been implicated in lung injury in COVID-19 (Godement *et al.*, 2021).

1.3.5 Neutrophil interactions with *Staphylococcus aureus*

Pathogens have evolved multiple mechanisms to circumvent PMN microbicidal actions (see Fig. 1.5). Pathogen recognition is an important step in the host defence against bacteria, which is often avoided by pathogens. For example, the chemotaxis inhibitory protein of *S. aureus* (CHIPS) binds to C5a and formyl peptide receptors to mask receptor-ligand interactions and inhibit neutrophil activation and chemotaxis (Haas *et al.*, 2004). Also, staphylococcal superantigen-like protein (SSL3) blocks TLR2, preventing recognition by this receptor. Moreover, SSL1 and SSL5 were

demonstrated to inhibit neutrophil matrix metalloproteinases (MMP8 and MMP9), leading to subsequent inhibition of MMP-dependent IL-8 cleavage, and hence inhibiting neutrophil recruitment (Koymans *et al.*, 2016).

Staphylococci are coated by a thick peptidoglycan layer, and in addition several clinical strains (particularly serotypes 5 and 8, Watts *et al.*, 2005), produce slimy capsular polysaccharides. This capsule protects *S. aureus* from being phagocytosed and thereby contributes to its pathogenesis (Thammavongsa *et al.*, 2015). If internalised, some strains of *S. aureus* have the capacity to survive intracellularly, which may facilitate dissemination (Gresham *et al.*, 2000; Kubica *et al.*, 2008). *S. aureus* has been found to remain viable and virulent inside murine PMNs, localised in the cytoplasm, and both within larger vacuoles called ‘’spacious phagosomes’’ or inside small vacuoles termed ‘’tight phagosomes’’ (Gresham *et al.*, 2000). A single neutrophil was noted to contain bacteria in each of these 3 intracellular niches, suggesting it was not an effect specific to an individual neutrophil. Phagocytosis of organisms is not synchronous, and the possibility that this was a temporal effect, with one stage progressing to the next, was not explored. Bacteria within spacious phagosomes (suggested to have formed via macropinocytosis rather than true phagocytosis) were thought to be more likely to survive, perhaps due to failure to deploy the normal killing mechanisms in this setting.

The NADPH oxidase (see Figure 1.4 and Section 1.3.3) is a key executioner of ingested staphylococci, and hence antioxidant defences are likely to be important in bacterial survival. *S. aureus* produces a number of antioxidants in an attempt to mitigate the effect of ROS (Figure 1.5). Staphyloxanthin, superoxide dismutase (SodA/SodM), catalase (KatA) and alkyl hydroperoxide reductase (AhpC) all possess antioxidant functions which can protect *S. aureus* from the oxidative stress induced by intraphagosomal ROS. *S. aureus* lacking the carotenoid staphyloxanthin were more susceptible to killing by exogenous ROS than were isogenic wild type bacteria (Clauditz *et al.*, 2006) and blocking staphyloxanthin biosynthesis *in vitro* rendered *S aureus* more susceptible to killing by human blood (Liu *et al.*, 2008). *S. aureus* produces two superoxide dismutases (SODs), SodA and SodM. Staphylococci isolated from the sputum of patients with cystic fibrosis (a highly inflammatory and oxidising environment) transcribed high levels of sodA and sodM, and both enzymes

promoted survival of *S. aureus* during PMN killing (Treffon *et al.*, 2020). Although catalase has been regarded as a major virulence factor, clinical isolates of catalase positive and negative strains of *S. aureus* were equally virulent in a mouse model of CGD (Messina *et al.*, 2002), perhaps due to residual catalase activity provided by AhpC. Interestingly, although mutation of both *katA* and *ahpC* impaired the ability of *S. aureus* to withstand oxidative stress *in vitro*, the double mutant was not attenuated in *in vivo* infection models, which the authors proposed was due to the low oxygen availability at *in vivo* sites of infection (Cosgrove *et al.*, 2007). Together, this body of data is consistent with an ongoing 'arms race' with *S. aureus* attempting to overcome the oxidative stress within the phagosome or to escape from it.

Within the phagosome, *S. aureus* are exposed to high concentrations of granule proteins, and in response have evolved secreted factors which neutralise granule proteases and antibacterial peptides (Figure 1.5). For example, peptidoglycan O-acetylase A (OatA) protects *S. aureus* from degradation by lysozyme; in a septic arthritis model, mice infected with an OatA-deficient strain developed milder disease than those infected with wild type bacteria. To combat the ability of neutrophil serine proteases to cleave a range of staphylococcal virulence factors, *S. aureus* produces three serine protease inhibitors known as extracellular adherence proteins (EAPs) Eap, EapH1 and EapH2 (Stapels *et al.*, 2014), which also protected the bacteria from NETs (Eisenbeis *et al.*, 2018). Triple EAP mutants generated reduced bacterial loads compared to wild type pathogens in *in vivo* mouse models of infection but were not more susceptible to intracellular killing by neutrophils *in vitro*, suggesting the extracellular effects of these inhibitors are the main mechanism whereby they promote virulence. The huge array of antibacterial peptides and proteases in the phagosomal milieu is difficult to evade, hence the propensity of *S. aureus* to evolve multiple strategies of immune evasion.

S. aureus can escape from neutrophil cytosol or phagosomes by producing phenol-soluble modulins (PSMs), regulated by the *agr* quorum-sensing system, again expressed when they are needed for staphylococcal pathogenesis. It was demonstrated that the main role of PSM (predominantly PSMα) but also leukotoxins and haemolysins, is to cause destruction of neutrophils (Rong *et al.*, 2007). The mechanism of neutrophil death is currently unclear.

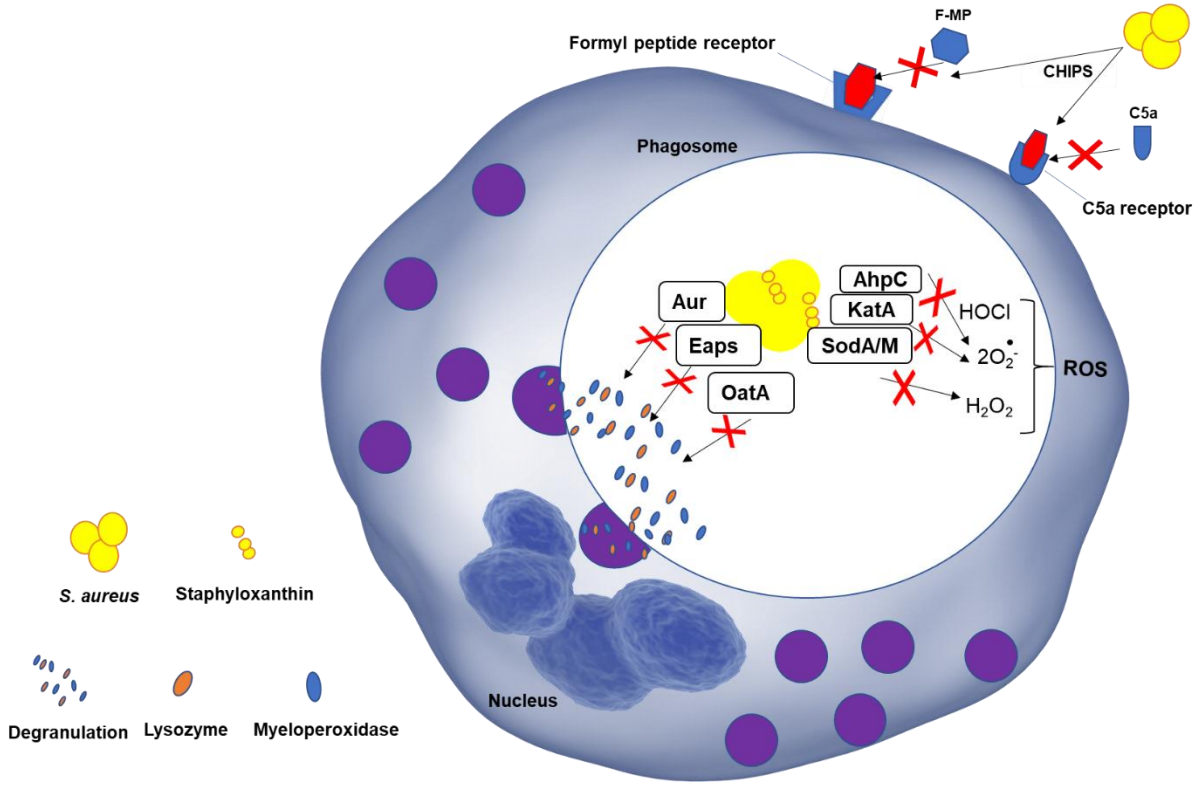

Figure 1.5 *S. aureus* avoids engulfment and killing by neutrophils.

Neutrophil chemotaxis is inhibited by chemotaxis inhibitory protein of S. aureus (CHIPS), which prevents binding of chemoattractants to neutrophil C5a and formyl peptide receptors. The S. aureus capsule is poorly detected by PMNs, reducing internalisation. S. aureus inhibits killing of phagocytosed pathogens by secreting several inhibitors and enzymes. Granule-derived antimicrobial peptides such as lysozyme or MPO are cleaved by aureolysin (Aur). Additionally, DltA-D promotes D-alanyl esterification of teichoic acids and MprF modifies phosphatidylglycerol with alanine or lysine, detoxifying bactericidal peptides. Peptidoglycan O-acetylase (OatA) protects S. aureus from degradation by lysozyme. Extracellular adherence proteins (Eaps) inhibit neutrophil serine proteases elastase, proteinase 3 and cathepsin G through blocking processing and activation of cellular receptors. The adenosine synthesising enzyme (AdsA) impedes degranulation via adenosine receptor (AdoR) signalling. Staphyloxanthin, superoxide dismutase (SodA/SodM), the catalase (KatA) and alkyl hydroperoxide reductase (AhpC) are all antioxidants which protect Staphylococcus from the oxidative stress induced by production of reactive oxygen species (ROS) inside of phagosome (adapted from Guerra et al.*, 2017).*

In addition to surface-related virulence factors, *S. aureus* secretes a wide range of exoproteins, which are vital in the latter stages of infection. *S. aureus* controls the production of its abundant virulence factors through two distinctive interacting regulatory loci, namely the global regulation systems *sar* (Staphylococcal Accessory Regulator) (A. L. Cheung *et al.*, 1992) and *agr* (Accessory Gene Regulator) (Recsei *et al.*, 1986). The secretory phenotype depends on bacterial density, detected by quorum sensing mechanisms. At low densities (early infection), *S. aureus* adopts the "adhesive" phenotype, with upregulation of surface adhesion molecules to facilitate attachment and colonisation. Later in infection, staphylococci switch to an "invasive" phenotype secreting toxins and proteases to promote bacterial dissemination to distant tissues (Dunman *et al.*, 2001). Thus, *S. aureus* adjust their expression of virulence factors to environmental conditions.

1.3.6 Neutrophil dysfunction and staphylococcal infection

The main role of PMNs is to recognise and clear invading pathogens. When this ability is impaired, pathogen success is dramatically increased. Several inherited and acquired neutrophil disorders have been described, often leading to increased susceptibility to staphylococcal infection (Table 1.1). The most common example is neutropenia, where the number of neutrophils is markedly reduced, for example by cancer chemotherapy; because neutrophils are short-lived they must be rapidly replenished; chemotherapy targets rapidly dividing cells such as neutrophil precursors in the bone marrow (Jin *et al.*, 2017).

The importance of the neutrophil, and in particular the oxidative burst, in anti-staphylococcal immunity was dramatically highlighted when chronic granulomatous disease (CGD) was first described, and its cause identified (for a recent review, see (Yu *et al.*, 2021). Neutrophils from CGD patients are unable to produce ROS from molecular oxygen, because of inactivating mutations in the phox components ($gp91^{phox}$, $p22^{phox}$, $p47^{phox}$ $p40^{phox}$ or $p67^{phox}$) of the NADPH oxidase enzyme. CGD patients are highly susceptible to infections caused by microorganisms such as *Staphylococcus* spp., *Aspergillus* spp., *Salmonella* spp., and *Serratia* spp. (Winkelstein *et al.*, 2000) since the defective oxidative burst leads to a failure of

pathogen killing. CGD neutrophils also release 2- to 4- fold higher levels of interleukin-8 (IL-8) than those isolated from healthy volunteers, contributing to enhanced and delayed resolution of inflammation (Lekstrom-Himes *et al.*, 2005). Aberrant clearing of cellular debris further promotes granuloma formation in CGD patients (Kobayashi *et al.*, 2004; Okura *et al.*, 2015).

In contrast, the neutrophil dysfunction in HyperIgE syndrome (HIES) is complex and poorly understood. These patients also have increased susceptibility to staphylococcal and fungal infections, but the main defect seems to relate to impaired Th17-mediated immunity (Park and Liu, 2020), with reduced neutrophil chemotaxis perhaps secondary to reduced generation of chemoattractants (Soderberg-Warner *et al.*, 1983) but preserved intracellular killing of relevant pathogens. Surprisingly, myeloperoxidase deficiency confers only minor increased susceptibility to infection in only a few affected patients (Nauseef, 1988), although *in vitro* killing of *S. aureus* was reported to be somewhat compromised (Kitahara *et al.*, 1981), again illustrating the redundancy of the extensive antibacterial protease arsenal of the neutrophil. In contrast, neutrophils lacking the entire specific granule population due to mutations in the transcription factor C/EBPε are profoundly susceptible to staphylococcal infection (Kyme *et al.*, 2012). This may relate to both impaired recruitment of the membrane phox components of the NADPH oxidase as well as the role of the specific granule proteins.

Understanding rare diseases such as CGD and specific granules deficiency have thus shed light on normal immune cell function and identified possible pathways to target to improve host immunity.

Table 1.1 Clinical Features of Neutrophil Disorders

Disease	Defect	PMN Dysfunction	Clinical outcomes
Neutropenia	Decreased PMN numbers, either congenital (e.g., elastase deficiency) or acquired (most commonly drug-induced such as cancer chemotherapy).	Insufficient PMN numbers to respond to invading pathogens, life-threatening Gram-negative and Gram-positive infections.	Life-threatening infections during periods of neutropenia, susceptibility reduced when neutrophil count recovers.
Chronic granulomatous disease (CGD)	Mutations in NADPH oxidase components; reduced or absent ROS formation.	Reduced killing of certain pathogens e.g., *Staphylococcus aureus, Aspergillus fumigatus*, Gram- negative bacilli.	Life-threatening infections with *Staphylococcus* and *Aspergillus*; aberrant healing (granulomas).
Hyper IgE Syndrome (formerly Job's syndrome)	Mutations in STAT3 (signal transducer and activator of transcription 3) or DOCK 8 (Dedicator of cytokinesis 8).	Reduced killing of certain pathogens e.g., *Staphylococcus aureus, Aspergillus fumigatus.*	Staphylococcal and fungal skin infections, pulmonary and joint infections, 'cold' abscess formation (reduced cytokine release).
Myeloperoxidase deficiency	Decreased or lack of MPO/HOCl system.	Increased chronic conditions mediated by adaptive immunity, decrease NET killing of microbes.	Mild susceptibility to chronic infections caused by *Candida albicans, S. aureus.*
SGD (Specific Granule Deficiency)	Azurophil granule lack of defensins. Absence of specific granules, bilobed neutrophils nuclei.	Impaired chemotaxis, disaggregation, reduced respiratory burst, and deficient bactericidal activity (mainly to *S. aureus*).	Severe staphylococcal infections, aberrant skin lesion healing.
Leukocyte Adhesion Deficiency (LAD)	Integrin or integrin-ligand defects.	Failure of neutrophil recruitment to infection, increased circulating PMN numbers.	Infection, aberrant wound healing, periodontitis.

1.4 Hypoxia in health and disease

Hypoxia implies an imbalance between oxygen supply and demand rather than being defined by a specific oxygen tension. Physiological oxygen gradients exist within and across tissues, as shown by directly measured oxygen tensions; this 'physiological hypoxia' is heightened by disease processes such as inflammation and infection leading to 'pathological hypoxia'.

1.4.1 Physiological hypoxia

Local tissue 'hypoxia' is normal in the healthy organism. The oxygen level in tissue environments differs considerably from that of inspired air (pO_2 about160 mm Hg). Circulating neutrophils repeatedly transit between a pO_2 of approximately 100 mmHg in major arteries, 50 mmHg in arterioles and 20-30 mmHg in capillaries. Since oxygen must diffuse from capillaries to the surrounding environments, the oxygen tension in normal tissues can be even lower – 'physiological hypoxia'. The availability of oxygen in tissues is dependent on previous oxygen extraction and distance from the closest capillary (Sitkovsky and Lukashev, 2005). Tissue oxygenation can be measured using micro-electrodes or by staining with compounds such as pimonidazole, which binds to thiol groups at oxygen tensions below 10 mmHg. It has been reported in a mouse model, using the OxyLite PO_2 system (which determines the O_2-dependent fluorescent lifetime of ruthenium chloride) that the pO_2 in the healthy thymus is approximately 10mm Hg and around 16mm Hg in the spleen (Braun *et al.*, 2001). This physiological tissue hypoxia is amplified in pathological settings (see Section 1.5). To enable appropriate responses to the challenges presented by low oxygen levels, a complex and accurate oxygen sensing system has evolved.

1.4.2 Oxygen sensing at the molecular level

The molecular response to hypoxia is controlled by the family of hypoxia-inducible factor (HIF) transcription factors (Jaakkola *et al.*, 2001). There are two phases of regulation of the HIF-1α subunit (Fig. 1.6); hydroxylation and subsequent degradation when molecular oxygen is accessible (normoxia), and stabilisation and nuclear translocation in decreased oxygen settings (hypoxia).

Functional HIFs are heterodimers formed of one of 3 alpha subunits (although HIF-3α is restricted to neuronal tissue and is not further discussed) with a single beta subunit, aryl hydrocarbon receptor nuclear translocator (ARNT). *In vitro studies have shown that HIF-1α protein only accumulates after incubation in ≤3% oxygen, whilst HIF-1β is constitutively expressed irrespective of oxygen status. Whilst HIF-1α protein is stabilised in hypoxia, levels drop rapidly following re-oxygenation* (Huang *et al.*, 1996). HIF-1/2 α stability is post-transcriptionally regulated by molecular oxygen, via oxygen-sensitive Prolyl Hydroxylases (PHDs), which hydroxylate the oxygen- dependent domain (ODD) of HIF-α (McDonough *et al.*, 2006). When dioxygen is available, PHDs are catalytically active and hydroxylate HIF-α, targeting it for ubiquitination and hence proteasomal degradation, a process facilitated by von Hippel-Lindau (VHL) tumour suppressor protein (Maxwell *et al.*, 1999; McDonough *et al.*, 2006). Another oxygen-dependent enzyme, Factor Inhibiting HIF (FIH), hydroxylates critical asparagine residues to silence the HIF-α transactivation domains. This hydroxylation blocks the association of HIFs with transcriptional co-activators CBP/p300, and prevents transcriptional activation (Lando *et al.*, 2002).

When molecular oxygen in the cytoplasm is reduced, PHD and FIH activity are impaired, HIF-1α subunits accumulate in the cytoplasm, heterodimerise with HIF-1β and recruit p300/CBP coactivator family proteins. This regulatory complex transmigrates to the nucleus and binds to hypoxia responsive elements (HREs) to control target genes (e.g., glucose transporter 1- GLUT1; vascular endothelial growth factor- VEGF).

HIF-1 and HIF-2 play both overlapping and somewhat divergent roles in regulating responses to hypoxia by means of differential temporal regulation of stabilisation and overlapping and distinct gene targets. For example, angiogenesis (new vascular development to augment oxygen delivery) in hypoxic conditions is initially HIF-1-dependent. In the middle stage of vasculogenesis both HIFs drive overlapping functions. With the rising oxygen concentrations, maturation of vasculature showed dependency on HIF-2, which is required to finalise the remodelling and stabilisation of the newly established vasculature (Koh and Powis, 2012).

HIF-1 and HIF-2 may have divergent effects on immune-related genes; for example, the balance between HIF-1-regulated inducible nitric oxide synthase (iNOS) and HIF-2-regulated arginase control formation of nitric oxide (NO). Arginase competes with iNOS for a common substrate, L-arginine and therefore inhibits production of NO, a potent antimicrobial. Up-regulation of arginase by HIF2-driven macrophages to the M2 (alternatively activated) anti-inflammatory phenotype (Takeda *et al.*, 2010) and HIF-1 regulates macrophage antibacterial activity via the increased expression of iNOS (Peyssonnaux *et al.*, 2005).

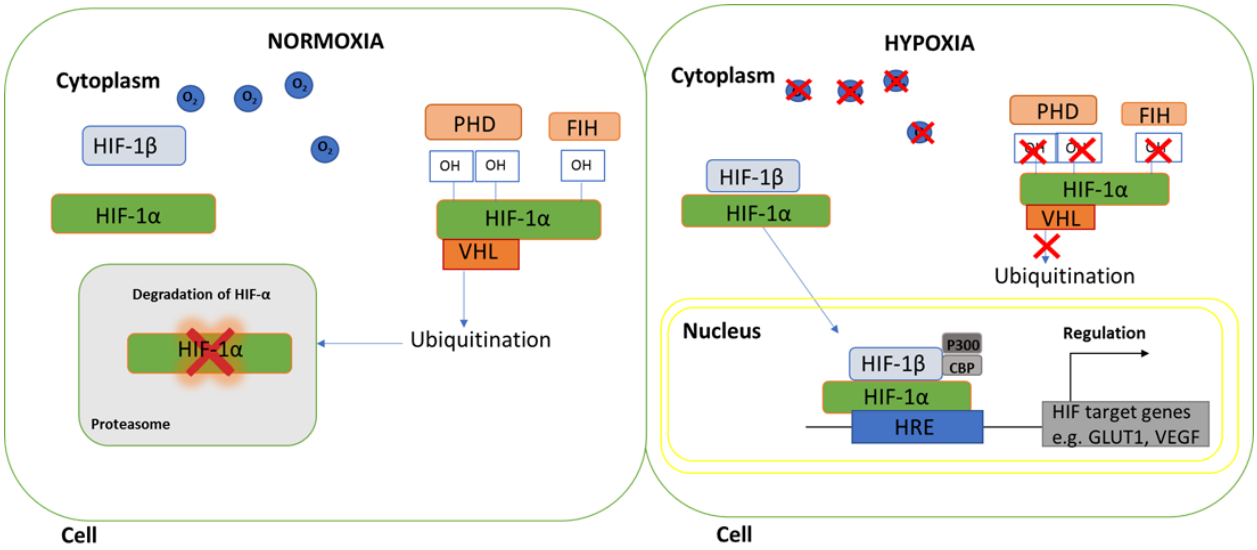

Figure 1.6 Sensing molecular oxygen levels and responses by human cells.

Under normoxia, HIF1/2-α subunit abundance is diminished due to hydroxylation by PHDs, which target HIF-α for pVHL-facilitated proteasomal destruction, and by FIH which blocks interactions with p300/CBP. Under hypoxia HIF-α stabilised and dimerises with its cofactor HIF-1β. The newly formed heterodimer translocates to the nucleus, interacts with p300/CBP and binds to hypoxia-responsive elements (HRE) in promotor regions to regulate target genes e.g., GLUT1 or VEGF (adapted from Elks et al.*, 2015).*

In addition, in a larval zebrafish model of mycobacterial infection, either HIF-1α stabilisation or reduction of HIF-2α reduced bacterial burden via elevated production of NO by neutrophils (Elks et al., 2013). Thus, it appears that HIF-1α to HIF-2α ratio determines the iNOS/arginase production respectively and therefore the NO-dependent bactericidal capacity of phagocytes.

Although HIFs are the canonical effectors of hypoxia signalling, in has more recently become apparent that hypoxia can lead to a range of HIF-independent effects. These may be mediated by PHDs or VHL directly (for example in cancer, reviewed by Nguyen and Durán, 2016; Zhang and Zhang, 2018 respectively), or by lack of molecular oxygen to fuel reactions such as the NADPH oxidase (Hoenderdos *et al.*, 2016). These HIF-independent pathways allow rapid responses to hypoxia, often without the requirement for transcriptional activity.

1.5 Pathological hypoxia

Tissue oxygenation can be compromised by pathological processes, such as atherosclerosis (reduced delivery of oxygenated blood by narrowed vessels), tumour formation (abnormal blood vessels and increased diffusion distance), and infection. Using the trinitrobenzenesulfonic acid (TNBS) colitis model of murine acute colonic inflammation, it has been shown that neutrophil accumulation directly induces inflammatory hypoxia. Infiltration of PMNs depleted local molecular oxygen levels in adjacent intestinal epithelial cells by consuming oxygen to fuel the oxidative burst (Campbell *et al.*, 2014; Monceaux *et al.*, 2016). Bacteria may also contribute to tissue hypoxia, for example *S. aureus* depleted dissolved oxygen in a skin infection model (Lone *et al.*, 2015). Thus, neutrophils must operate in hypoxic environments to control infection; hence it is critical to establish the impact of hypoxia on key neutrophil microbicidal functions. Of note, most data on neutrophil function have been collected by studying isolated cells cultured in atmospheric oxygen (160 mmHg).

1.5.1 The impact of hypoxia on neutrophil accumulation

Neutrophils are key effector cells for the resolution of inflammation and/or infection (Palazon *et al.*, 2014), and transmigrate to compromised microenvironments altered by pathogens. Over-accumulation or excessive activation of neutrophils in the disease setting can be harmful for the host and may lead to tissue injury and chronic inflammation. It is important that neutrophil influx and activation are appropriately regulated to allow their microbicidal function but limit their tissue-damaging properties. Of note, neutrophil functions that enable recruitment, such as sensing, polarisation and migration in the direction of chemotactic stimuli, are fully sustained at low-oxygen

levels (McGovern *et al.*, 2011), suggesting that a hypoxic environment will not prevent the mobilisation of PMN from the circulation.

Hypoxia prolongs the longevity of PMNs by delaying apoptosis (Hannah *et al.*, 1995). Neutrophils cultured *in vitro* under hypoxic conditions stabilise HIF-1/2α with increased mRNA of HIF-targets such as BNIP3 and IKKβ mRNA (Hannah *et al.*, 1995; McGovern *et al.*, 2011; Monceaux *et al.*, 2016). Walmsley *et al.* explored the cause of the diminished neutrophil apoptosis under hypoxia, showing that it is mediated by HIF-1α-dependent nuclear factor-kappa β (NFκβ) expression and activity (Walmsley *et al.*, 2005). Hypoxic neutrophils were also found to release the survival factor cytokine MIP-1β (macrophage inflammatory protein-1β or CCL4), providing a further, indirect mechanism for increased PMN longevity (Walmsley *et al.*, 2005).

1.5.2 The impact of hypoxia on interactions between neutrophils and pathogens

Neutrophils recognise, ingest and execute pathogens rapidly and efficiently by employing their extensive antimicrobial functions. Host- or pathogen-derived priming agents, for instance tumour necrosis factor (TNFα) or bacterial lipopolysaccharide (LPS), make neutrophils more responsive to recruitment and activation signals. Additionally, priming amplifies a range of pathogen internalisation and destruction functions, comprising chemotaxis, phagocytosis, degranulation, ROS generation and release of neutrophil extracellular traps (NETs) (Lu *et al.*, 2014). McGovern *et al*. showed that recruitment-relevant responses to stimuli such as TNFα, the bacterial tripeptide fMLP and LPS are unaltered by hypoxia. Additionally, neutrophil expression of the β2 integrin subunit CD11b, a key factor mediating transmigration, is conserved and even augmented in hypoxic conditions relative to normoxia (McGovern *et al.*, 2011).

Interestingly, neutrophil phagocytosis has been reported to be either unchanged (McGovern *et al.*, 2011) or increased (Fritzenwanger *et al.*, 2011) by hypoxia. These opposing reports likely reflect the methodological differences in the two studies. Fritzenwanger *et al.* isolated blood samples from subjects exposed to hypoxia but then isolated the cells in atmospheric oxygen (which will have re-oxygenated them) and presented them with FITC-labelled zymosan (fungal particle) as prey. The volunteers

in this study were subjected to various oxygen concentrations in an air-conditioned hypoxia chamber that corresponds to oxygen availability at different heights (4000-5500 m). After collecting blood, samples were subjected back to atmospheric oxygen levels (21%) and used for performing assays, using all chemicals without earlier pre-conditioning to hypoxia. That could possibly lead to re-oxygenation, hence enhanced phagocytosis rates. In contrast, McGovern *et al*. isolated blood from volunteers and then incubated the isolated cells in a hypoxic chamber adjusted to 3% oxygen, adding *S. aureus* when the cells had 'acclimatised' to hypoxia. The relevant finding will depend on the situation that is being investigated hence in persistently hypoxic infective settings, phagocytosis may be preserved but not promoted as demonstrated by McGovern *et al*., whilst under conditions of intermittent hypoxia or hypoxia-reperfusion it is likely to be enhanced in keeping with the findings of Fritzenwanger *et al.*

The function of the NADPH oxidase is to generate ROS at the phagosome; with the discharge of granule protease, this generates an environment that is hostile to bacterial survival (Reeves *et al.*, 2003). Molecular oxygen is required for ROS generation and is thus an important mediator of neutrophil microbicidal function (Babior *et al.*, 2014) likely including the killing of *S. aureus* (McGovern *et al.*, 2011). However, not all pathogens are equally susceptible, for example PMN killing of phagocytosed *Escherichia coli* (*E. coli*) is unaffected by hypoxia, suggesting that the neutrophil-mediated killing of this pathogen is largely mediated by non-oxidative mechanisms such as granule proteases or peptides (McGovern *et al.*, 2011). Of note, hypoxia increases stimulated extracellular release of neutrophil microbicidal proteins and proteases, including MPO, lactoferrin, matrix metalloproteinase- 9 (MMP-9) and neutrophil elastase (Hoenderdos *et al.*, 2016). This may impact on tissue destruction and be relevant to certain aspects of staphylococcal pathology, for example abscess formation (see Section 1.6.2).

Neutrophil extracellular traps (NETs) consist of chromatin and granular proteins, which bind to, restrain and kill both Gram- positive and -negative bacteria as well as fungal organisms. NETosis is a form of neutrophil death which differs from apoptosis or necrosis and is predominantly ROS-dependent. CGD neutrophils form few NETs with aberrant morphology (Fuchs *et al.*, 2007). Despite this, NET formation in response to

viable *S. aureus* (wild-type or nuclease-deficient strains) was retained under hypoxia (1% oxygen), suggesting that even trace levels of ROS suffice to signal NETs release (Branitzki-Heinemann *et al.*, 2016).

Prolonged hypoxia thus changes the ability of the host to clear invading pathogens, despite host immune adaptation. These maladaptive responses provide opportunities for researchers to further investigate the interplay between phagocytes and immune cells for therapeutic benefit in staphylococcal infection.

1.6 Hypoxia, neutrophils and staphylococcal infection

1.6.1 Spectrum of staphylococcal infections

Although *S. aureus* is a commensal bacterium it also frequently causes disease. In this section, I will describe how hypoxia and the host immune response interact with this organism to shape some of the typical clinical syndromes of staphylococcal infection, namely abscess formation, infection of prosthetic material, and systemic infection (septicaemia).

1.6.2 Abscess formation

Abscesses are the archetypal manifestation of *S. aureus* infection, with both host and pathogen factors contributing to their formation. Patients with impaired neutrophil function have increased risk of staphylococcal skin abscesses and infections; for example, patients with CGD and Hyper IgE syndrome (Table 1.1) are particularly prone to staphylococcal skin and lung abscesses (Hill *et al.*, 1974). Bacterial virulence factors such as staphylococcal protein A (SpA) and coagulase (Coa) contribute to abscess formation. SpA blocks complement activation and bacterial opsonization, therefore protecting *S. aureus* from recognition and enabling abscess initiation (Hong *et al.*, 2016). The staphylococcal coagulase interacts with the host coagulation cascade protein prothrombin to form staphylothrombin, leading to conversion of fibrinogen to fibrin, resulting in activation of clotting and coating the staphylococcal surface with fibrin. This protects the bacteria from being phagocytosed, and also from other immune defence mechanisms, for example mitigating ROS effects (Guo *et al.*, 2017). Neutrophils are recruited to combat infection, but as noted above (Section 1.3.2.), *S. aureus* secretes a number of leukocidins and haemolysins to lyse

neutrophils. As infection progresses, the abscess consists of a large mass of pathogen which is replicating at the central part of the lesion, then separated by layer of necrotic PMNs killed by staphylococcal virulence determinants, and surrounded by a fibrin capsule (Cheng *et al.*, 2009). This is a hypoxic environment (Werth *et al.*, 2010), and hypoxia in this setting impairs the capacity to mount a neutrophil respiratory burst, compromising the killing of ingested *S. aureus* (McGovern *et al.*, 2011). This allows bacterial persistence and will further increase the likelihood of pathogen-induced neutrophil death, hence contributing to abscess enlargement. Furthermore, augmented secretion of proteases by hypoxic neutrophils will contribute to host tissue breakdown (Hoenderdos *et al.*, 2016). Ultimately, mature abscess cavities reach an equilibrium, which is usually resolved by either spontaneous discharge to release the infectious material, or surgical drainage.

1.6.3 Infection of Prosthetic Material

S. aureus is notorious for causing infections on the surface of indwelling prosthetic materials, for example intravenous cannulae, joint replacements and artificial heart valves. Most such infections are thought to result from skin flora contamination during implantation, or by tracking of infection from the subcutaneous portion of the device to deeper sites. To facilitate these processes, *S. aureus* is equipped with binding surface proteins- microbial-surface components recognising adhesive matrix molecules (MSCRAMMs). MSCRAMMs such as elastin-binding protein (Ebp), fibronectin-binding protein (FnBP), clumping factor (Clf) or collagen adhesin (Cna) allow adherence to different host tissues (Foster and Höök, 1998). The ability of *S. aureus* to form biofilms is key to its ability to colonise and cause persistent infection of indwelling devices. Whilst biofilm formation has been reported to impair host responses, *in vitro* studies suggest PMNs are able to traverse *S. aureus* biofilms, ingesting and killing bacteria as they do so (Günther *et al.*, 2009); however more established biofilms are resistant to phagocytic attack (Guenther *et al.*, 2009). *S. aureus* increased biofilm formation 4-30 fold in response to hypoxia (Mashruwala *et al.*, 2017). Interestingly, hyperbaric oxygen therapy has recently been shown to enhance antibiotic efficiency in a rat model of infective endocarditis (infection of a heart valve, a life-threatening situation that is difficult to detect and to treat, Lerche *et al.*, 2017), but not in a mouse model of implant-associated bone infection - osteomyelitis (Nis Pedersen *et al.*, 2017). These conflicting

results may reflect differences in the models and access of oxygen to the tissues, alternate antibiotic regimens and species differences, but underscore the need to explore hypoxia and hypoxia-signalling in staphylococcal infections.

1.6.4 Disseminated staphylococcal infection

A substantial proportion of invasive staphylococcal infections are associated with spread from indwelling prosthetic material such as intravenous cannulae, and have a high mortality rate (Malanoski *et al.*, 1995). Termed as peripheral intravenous catheters (PIVs) or intravascular devices (IVDs) as one of the main sources accountable for staphylococcal infections, are ongoing life-threatening complications associated with the hospitalisation. More recent study (2010- 2011) by Austin D.E. *et.al.,* (2016) showed that PIV-related staphylococcal bacteraemia was longer in duration and thrombophlebitis at old sites than current PIVs (Austin *et al.*, 2016). The availability of epidemiological data is poor and there are the greatest number of suffering patients available from study done in particular states in the USA. Overall, the percentage of such infections are decreasing with more care in medical care taken over the patients e.g., the material of which the indwelling devices are made of. In The capacity for intracellular survival within phagocytes is a key factor facilitating the dissemination of *S. aureus* from the original site of established infection to other sites in the host. In animal models, a small number of *S. aureus*-infected neutrophils are thought to function as 'Trojan horses', which can be distributed around the body and release pathogens to disseminated infection with widespread abscess formation (Prajsnar *et al.*, 2012).

An important recent insight was garnered from studying a *S. aureus* murine skin infection in different oxygen environments; remarkably, hypoxia converted a minor superficial process to near-universal and rapid fatality. Although enhanced bacterial replication was not found to be responsible, preconditioning animals, in 10 % O_2 defined hypoxia for 12 hours, improved survival. The phenotype was largely due to neutrophil's response to hypoxia, with HIF-1α activation leading to elevated neutrophil glucose requirements, which led to worse outcome in hypoxemic animals including cardiac failure and hypoglycaemia (Thompson *et al.*, 2017). This study encapsulates how relationships between host, pathogen and hypoxia/hypoxic signalling determine the outcome of infection and have pointed research to promising therapeutic targets in the ongoing fight against invading pathogens.

1.7 Hypothesis and aims

Neutrophils are key players determining infection outcomes and are adapted to operate in hypoxic environments. During successful staphylococcal invasion, the innate immune system fails to combat this pathogen and resulting 'pathological hypoxia' may compound this failure, with potentially fatal outcomes. *Hence,* ***I hypothesised that hypoxia affects the interaction between Staphylococcus aureus and neutrophils, permitting intracellular survival by changes in the phagosomal environment due to lack of molecular oxygen to yield the ''oxidative burst''. I further hypothesised that the impact of hypoxia on neutrophil-staphylococcal interactions could be recapitulated by inhibiting the NADPH oxidase.***

The aims of the work presented in this thesis are as follow:

1. To determine the effect of hypoxia on staphylococcal growth and susceptibility to killing by human neutrophils.
2. To explore the effects of inhibition of ROS production on the intraphagosomal environment experienced by *S. aureus*, and how this impacts the neutrophil- *S. aureus* interaction
3. To investigate the impact of *S. aureus* antioxidant virulence factors on the phagosomal environment and on neutrophil microbicidal function

2 Materials and methods

2.1 Cell and Bacterial Culture media

Brain Heart Infusion (BHI; NutriSelect is a trademark of Merck KGaA, Darmstadt, Germany) is a nutrient- rich and a standard medium for bacterial growth, while Gibco™ Roswell Park Memorial Institute (RPMI) 1640 (Life Technologies Europe BV, Bleiswijk, The Netherlands) medium is optimal for incubating neutrophils but contains fewer nutrients than BHI medium. RPMI used in this study: without HEPES (Catalogue# 12633012), and with HEPES (Catalogue# 72400047).

2.1.1 BHI medium

Ingredients	g/L
Brain extract	7.8
Heart extract	9.7
Proteose peptone	10.0
Sodium chloride	5.0
D-Glucose	2.0
Disodium hydrogen phosphate	2.5

Final pH 7.4 +/- 0.2 at 25°C

2.1.2 RPMI 1640 medium

Ingredients	g/L
Wide range of amino acids	
Vitamins	
Inorganic salts:	
Calcium nitrate	0.1
Magnesium sulfate	0.04884
Potassium Chloride	0.4

Sodium Bicarbonate	2.0
Sodium chloride	6.0
Sodium phosphate dibasic	0.8
Other Components:	
D-Glucose (Dextrose)	2.0
Glutathione (reduced)	0.001
Phenol Red	0.005

pH 7.4 +/- 0.2 at 37°C, 5% CO_2

RPMI 1640 additional supplementation details:

RPMI/FBS	supplemented with 10% FBS
RPMI1%P/S	supplemented with 1% penicillin/streptomycin
RPMI/HEPES	supplemented with 25 mM HEPES

2.2 Preparation of human neutrophils

2.2.1 Ethical approval

Primary neutrophils were isolated from the peripheral blood of human healthy volunteers after obtaining fully informed written consent, in accordance with a protocol approved by South Yorkshire Local Research Ethics Committee (REC reference: 05/Q2305/4).

2.2.2 Neutrophil isolation

2.2.2.1 Plasma-Percoll® density gradient centrifugation

Human neutrophils were isolated from healthy volunteer venous blood by Plasma-Percoll® density gradient centrifugation. To avoid neutrophil activation or contamination the procedure was performed with rigorous care, inside a microflow class II microbiology safety cabinet. First, 45 mL of freshly drawn blood was added promptly but gently to 5 mL of sterile 3.8% (w/v) tri-sodium citrate (Martindale Pharmaceuticals, Romford, UK) in a 50 mL polypropylene universal tube, with slow and gentle inverting of a tube to prevent blood from clotting. Blood was spun at 270 g for 20 min at room temperature (RT), and the upper phase - platelet rich plasma (PRP) - was aspirated to a clean 50 mL universal tube. To make platelet poor plasma (PPP), the PRP was spun at 910 g at RT to remove platelets; PPP was transferred to a new universal tube and the pelleted platelets were discarded. The remaining lower phase of cells containing erythrocytes and leukocytes was gently mixed with 6 mL of 6% (w/v) dextran (product # 52194, molecular weight 500,000; Sigma- Aldrich, Poole, UK) and topped up to 50 mL with 0.9% (w/v) sterile sodium chloride solution (Baxter, Newbury, UK; both pre-warmed in 37ºC water bath) with gentle mixing. This step allows the high molecular weight dextran to bind to and sediment red blood cells (RBCs), by leaving the solution to stand at RT for 30 min. After this time, the upper phase containing white blood cells (WBCs) was transferred using a sterile, plastic Pasteur pipette into a clean universal tube and spun at 270 g for 6 min at RT. After centrifugation, the resulting ‘soft’ pellet of WBCs was gently resuspended in 2 mL of the previously prepared PPP.

WBCs were further separated according to cell density by a discontinuous Percoll®+ (catalogue # 17544501, Cytiva, GE Healthcare, Chicago, IL) gradient centrifugation in a 15 mL polypropylene universal tube. The gradient was prepared using accurate measurements of 90% Percoll® stock solution (9 mL of 100% Percoll®+ was made up with 1 mL of 0.9% saline) and PPP. First, two gradient layers of Percoll®+ mixed with PPP solution were prepared; the upper phase at 42% (v/v) Percoll®/ 58% (v/v) PPP (0.84 mL Percoll®+ mixed with 1.16 mL PPP) and the lower phase at 51% (v/v) Percoll®+/ 49% (v/v) PPP (1.02 mL Percoll®+ mixed with 0.98 mL PPP) in separate tubes. The lower density phase of Percoll®+ was slowly overlaid with a sterile, plastic Pasteur pipette onto the higher density Percoll®+ to generate the discontinuous

gradient (Fig. 2.1.A). Following this step, the resuspended pellet of WBCs was transferred carefully onto the upper layer of Percoll®+, avoiding mixing of the layers. The gradient was then spun at 225 g for 11 min at RT with no brake applied on deceleration. This step yields three separate layers of cells (Fig. 2.1.B); the top peripheral blood mononuclear cells (PBMCs) layer comprised of monocytes and lymphocytes, the middle layer contained neutrophils, eosinophils and basophils and the bottom consisted of the remaining un-sedimented red blood cells. If the layers did not separate correctly the cells were discarded; the most common issue encountered was RBC retention in the neutrophil layer, the presence of which suggests the neutrophils were activated and hence had upregulated adhesion molecules.

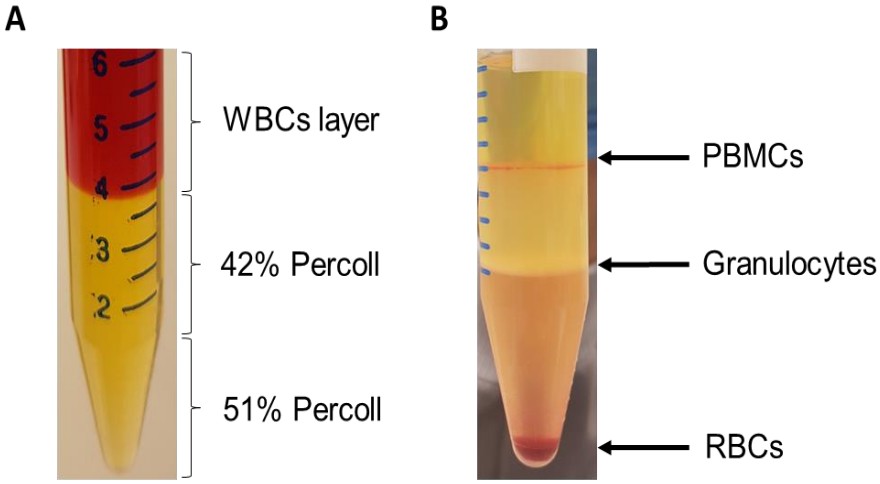

Figure 2.1 Discontinuous Plasma- Percoll® gradient centrifugation

*The left-hand panel (**A**) shows the gradient layers (cellular layer overlying 42% and 51% Percoll®+) prior to centrifugation. The right-hand panel (**B**) shows three distinct layers of blood cells peripheral blood mononuclear cells (PBMCs), granulocytes and red blood cells (RBCs) formed after spinning the gradient at 225 g for 11 min at RT with no brake. The arrows indicate different cells populations with middle layer (granulocytes) containing neutrophils.*

The PBMC layer was removed first using a 2 mL plastic Pasteur pipette and either discarded or used for separate experiments minimising waste. The granulocyte layer was then carefully aspirated with 2 mL plastic Pasteur pipette to a fresh 50 mL Falcon tube with the addition of 10 mL of PPP and was topped up to 40 mL with 1x Hanks' Balanced Salt Solution (HBSS; Gibco™) without Mg^{2+} and Ca^{2+} (to avoid activation of clotting proteins and inadvertent activation of neutrophils). 10 µL of the suspension was removed to count neutrophils under the light microscope using a haemocytometer, before a final centrifugation at 420 g for 6 min. Cells were counted manually in one set of 16 squares on the grid lines of a haemocytometer and the concentration (cells/mL) was calculated by multiplying counted cells by 10,000 (10^4). Neutrophils were resuspended in RPMI/FBS medium supplemented with L- glutamine and 10% (v/v),10% heat inactivated Fetal Bovine Serum (FBS) and (for prolonged incubations) 1% (v/v) penicillin/streptomycin (P/S) at the desired cell concentration. When neutrophils were used for co-incubation with bacteria, RPMI without P/S was used (to avoid the antibiotics killing the bacteria).

2.2.2.2 Immunomagnetic negative selection

During the COVID pandemic, the pool of available donors was restricted, and more frequent blood draws from the reduced pool of available volunteers necessitated a reduction in the blood volume taken at each donation. To enable a higher yield of cells from the available blood, a negative selection immunomagnetic separation method was used.

The EasySep™ Direct Human Neutrophil Isolation Kit (StemCell) consists of two reagents: Isolation Cocktail which is a combination of monoclonal antibodies including Fc receptor blocking antibody in PBS, and RapidSpheres™, a cocktail of magnetically labelled particles with monoclonal antibodies that bind 'unwanted' cell types such as lymphocytes and monocytes, which can thus be removed from whole blood with use of a magnet.

First, 10 mL of freshly drawn venous blood from a healthy volunteer was placed in a 50 mL universal tube containing 122 µL of UltraPure 0.5 M ethylenediaminetetraacetic acid (EDTA; Life Technologies Europe BV, Bleiswijk, The Netherlands) to bind calcium in the blood and prevent it from clotting. The tube was gently inverted to mix blood with the EDTA. Next, 500 µL of Isolation Cocktail from the EasySep™ Direct Human Neutrophil Isolation Kit was added to the whole blood followed by the addition of 500 µL of vortexed RapidSpheres™. The tube was then gently inverted three times to mix cells and incubated for 5 minutes at room temperature. After this time, freshly prepared DPBS/1 mM EDTA (100 µL of EDTA per 50 mL of DPBS) was used to top up the blood sample to 50 mL and the tube was gently inverted three times to mix evenly. Then, the universal tube (with lid loosened) was inserted into the EasySep™ magnet and incubated for 10 minutes at RT to allow magnetic separation of unwanted (non-neutrophil) blood cells from the neutrophil-enriched fraction (Fig. 2.2). The whitish layer of cells separated from other blood cells by virtue of sticking to the wall of the universal tube on the side of contact with the magnet, was then transferred to a fresh 50 mL universal tube without disturbing the bottom blood layer. Again, 500 µL of vortexed RapidSpheres™ was added to the newly transferred cells suspension followed by gentle inversion of the tube for three times to mix and incubate for a further 5 minutes at RT. Next, the tube was placed into the magnet for 5 more minutes of incubation. The neutrophil-enriched fraction was then transferred to the new universal tube and a further 500 µL of RapidSpheres™ was added, following a 5 minutes RT

incubation a third and final separation was performed for 10 minutes in the magnet. This extra step is required to yield very pure neutrophils without any contamination from non-bound cells to beads and clear beads from the suspension by additional use of magnet.

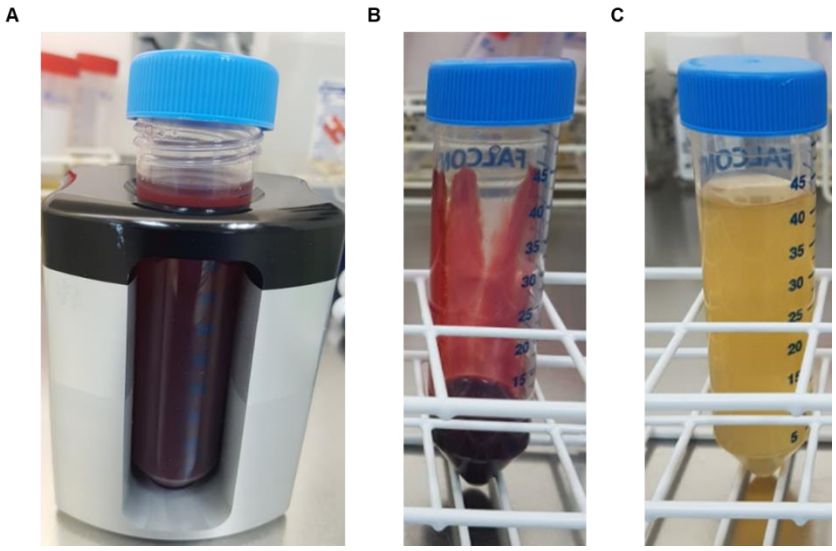

Figure 2.2 Magnetic cells isolation

First incubation in the Magnet of freshly withdrawn blood mixed with the Isolation cocktail and RapidSpheres and freshly prepared DPBS with EDTA ***(A)****. Universal tubes with separated blood and other blood cells* ***(B)*** *from whitish neutrophil- enriched layer* ***(C)****.*

Finally, the neutrophils were removed to a fresh falcon tube with 10 µL used for cell counting using a haemocytometer. After isolation cells were centrifuged at 300 g for 6 minutes at acceleration setting 7 and break 7 (MSE MISTRAL 3000i centrifuge). Cells were washed in 10 mL of DPBS and pelleted again by centrifugation. Finally, cells were resuspended in the calculated volume of RPMI/FBS at the desired cell density.

2.3 Neutrophil incubation

2.3.1 Incubation in normoxia

'Normoxia' is used to refer to the atmospheric oxygen tension, which is approximately 21% (19.6 kPa). Neutrophils resuspended in RPMI (+10% FBS, +/- 1% P/S) at $5x10^6$ cells/mL concentration (unless otherwise stated) were transferred to polystyrene, 96-well plates (# 650180, Greiner CELLSTAR®) and cultured for 0-24 hours at 37ºC, 5% CO_2 humidified incubator, comprising normoxic incubation.

2.3.2 Incubation in hypoxia

A SCI-tive Hypoxia Workstation from Baker Ruskinn (Fig. 2.3) was used to deliver and maintain hypoxic environment. This chamber has three glove ports (to allow the operator to manipulate the experimental components within the chamber) and an interlock (allowing items to be placed within the hood); both glove ports and interlock are flushed with nitrogen to prevent re- oxygenation when adding or removing items. The chamber is equipped with three electrical power sockets, which allow the use of devices such as an 1.5 mL centrifuge tube ThermoMixer and a vortex mixer inside.

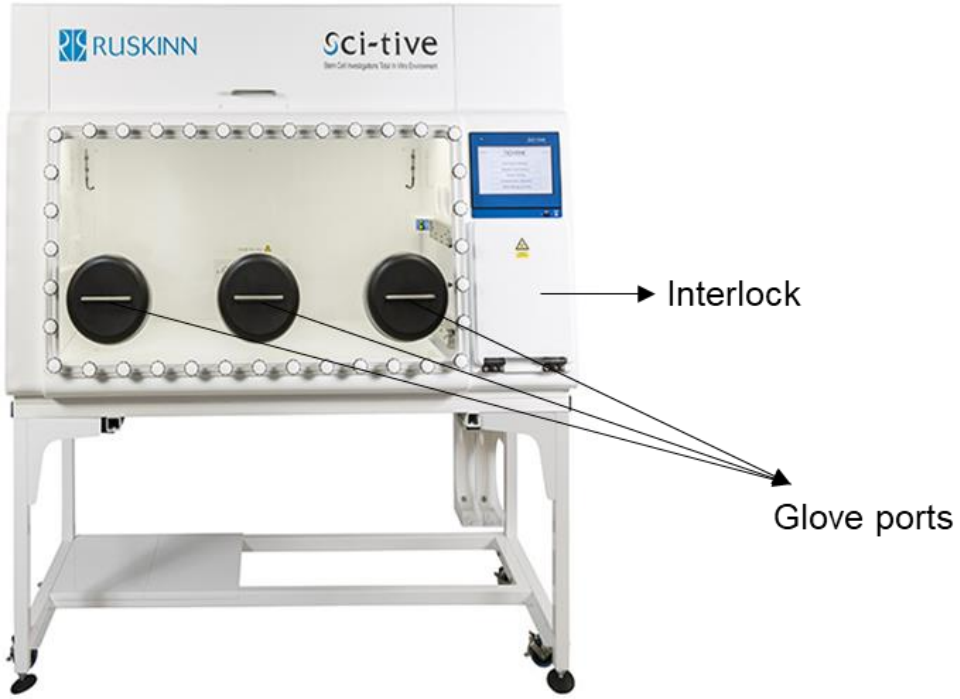

Figure 2.3 SCI-tive Ruskinn Hypoxic Workstation

Image depicts a hypoxic workstation; arrows show an interlock and glove ports (https://www.bakerco.com/sites/default/files/product_files/SCI-tive/sci-tive-front-stand_C9C0006.jpg; Accessed on 17/10/2017).

During bacterial infections, the sites of infection can show considerably lower oxygen levels than surrounding tissues (<1%) (Simmen and Blaser, 1993), thus the hypoxic chamber was set to maintain 0.8% oxygen tension, 5% CO_2 and ~70% humidity to mimic infected tissue hypoxia. These settings were previously shown to be optimal for maintaining media at a pH of approximately 7.4 and oxygen tensions of approximately 3 kPa (McGovern *et al.*, 2011). Before commencing experiments in the chamber, all media were pre-equilibrated in hypoxic conditions overnight to ensure they were at the designated oxygen tension. Incubation conditions were otherwise precisely as for the normoxic incubations.

2.3.3 Cytospin preparations

Freshly isolated neutrophils prepared as described in Section 2.1.2 were routinely checked after isolation for cell purity and viability (see Section 2.4.1.) using a light microscope. Cytospins also allowed visualisation of cell morphology and bacterial

ingestion. To transfer the cells onto glass slides, 70 µL samples of neutrophils (at $5x10^6$ cells/mL) were inserted into the funnel of the Cytospin centrifuge (Shandon Cytospin4, Thermo, Waltham, MA) in duplicate and spun at 400 g for 3 min. Thereafter, slides were air-dried and fixed with 1 drop of 100% methanol. Once dry, slides were submerged sequentially into Quick-Diff Red (Reagena, Toivala, Finland) and Kwik Diff Solution 3 (Blue) (Thermo, Waltham, MA) dyes for 3 min each to stain cells. After staining, slides were rinsed with water to remove the excess stain and allowed to dry completely. Then, in a fume hood, a small drop of distrene-80 plasticiser xylene (DPX) (Fisher Scientific, Loughborough, UK) was added onto each slide and a glass coverslip was gently lowered, excluding air bubbles. Left in the fume hood overnight, slides were ready for light microscopy observation using a Nikon Eclipse TE 300 Inverted Microscope at x100 oil immersion objective. For purity assessment, 300 cells were counted manually from each slide.

2.3.4 Neutrophil purity obtained by plasma-Percoll® centrifugation and EasySep™ isolations

Several neutrophil isolation methods have been described, such as Ficoll-Hypaque, and plasma-Percoll® density gradient centrifugation and negative selection (Haslett *et al.*, 1985; Kuhns *et al.*, 2015; Roth *et al.*, 2020). Several previously published studies indicate that plasma-Percoll® density gradient centrifugation yields ≈95% pure neutrophils which are not pre-activated ('primed') (e.g., Haslett *et al.*, 1985; Parker *et al.*, 2009), and this methodology was therefore initially adopted. Before performing experiments using freshly *ex vivo* isolated human neutrophils it was important to confirm the purity of the plasma-Percoll®-isolated cells to be used in my experiments. If the purity is substantially less than expected it might confound calculations of killing efficiency. Of note, the plasma-Percoll® gradients should separate granulocytes (neutrophils plus eosinophils and basophils) from mononuclear cells (lymphocytes and monocytes) but cannot further separate populations of granulocytes (as their densities are too similar).

Returning to the lab after COVID-19 pandemic restrictions were eased presented a number of challenges with the preparation of neutrophils by Percoll®-density centrifugation including restricted access and hence a greatly reduced donor pool requiring frequent lower volume blood draws, and in many cases the neutrophils we

obtained appeared to be somewhat activated (sticking to the red cells in the gradient). For some experiments we therefore needed to change the method of preparation of neutrophils and adopted a negative selection approach (described in the Section 2.2.2.2 of Materials and Methods). This method allows isolation of highly pure neutrophils using considerably low amount of blood (30 million neutrophils from 10 mL of whole blood) which does not require exposure to a gradient and reduce number of centrifugation steps to just one.

From 6 consecutive independent neutrophil isolations from single healthy donors (see Section 2.2.2.1 for Plasma-Percoll and 2.2.2.2 Immunomagnetic negative selection), neutrophils were transferred onto glass slides, Quick-Diff stained and observed under a light microscope (Section 2.3.3.). The number of neutrophils (characterised by the presence of multi-lobed nuclei) was manually quantified together with that of other contaminating blood cells. As can be seen in Figure 2.4.A, 89.1% ± 2.8% (SEM) of isolated cells were neutrophils with 10.83% ± 2.8% (SEM) contamination of eosinophils and less than 1% ± 0.05% (SEM) peripheral blood mononuclear cells (PBMCs). The purity of isolated cells (from 6 independent experiments) using EasySep immunomagnetic negative selection, by the cytospin preparation. The only contaminating cells using this method were monocytes which comprised 6.25 % ± 1.51 % (SEM). The overall % of neutrophils obtained by this method represent 93.75% ± 1.52 % (SEM) (Fig. 2.5.A).

These results show that I have separated mononuclear cells effectively, but I obtained a somewhat higher proportion of eosinophils than expected. This could be due to fact that eosinophil counts are higher during the spring (when these samples were obtained), and/or to some of our donors being atopic. In all subsequent experiments using this methodology I excluded any cell isolations with more than 10% eosinophils to avoid confounding results. For the majority of subsequent experiments eosinophil contamination was <5%.

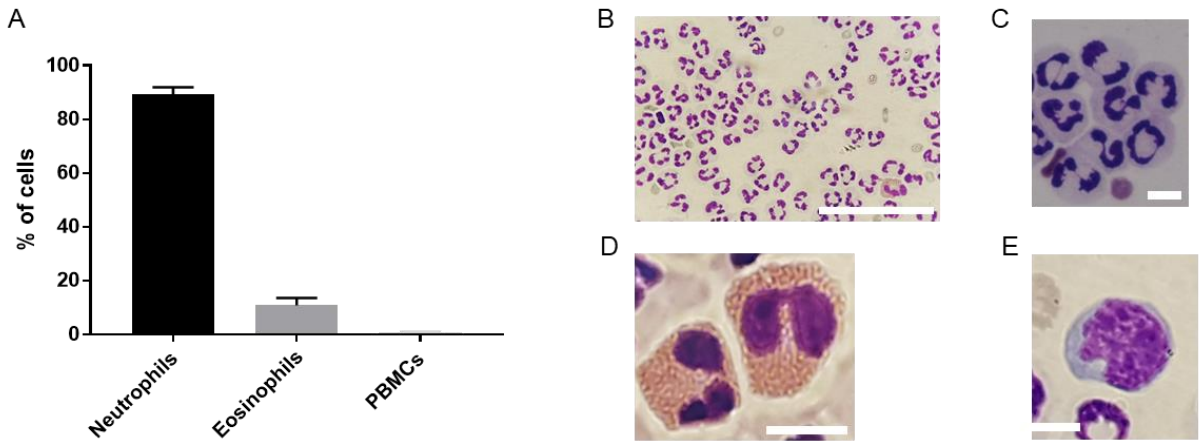

Figure 2.4 Purity of neutrophils prepared by Percoll® gradient centrifugation

***(A)**. Neutrophils isolated by plasma-Percoll® gradient centrifugation were analysed for purity. Diff-Quick stained cytospins were observed using light microscopy and ~300 cells were counted from two slides in each experiment to calculate percentage of neutrophils, eosinophils, and peripheral blood mononuclear cells (PBMCs). **(B).** Micrograph of single counting area. **(C)**. Viable neutrophils with multi-lobed nuclei. **(D)**. Eosinophils with pink granular cytoplasm and bi-lobed nuclei. **(E).** Monocyte with blue cytoplasm and horseshoe-like nucleus. Scale bars represent approximately 100 µm for micrograph B, 10 µm for C-E and 5 µm for F. Error bars represent SEM, n=6.*

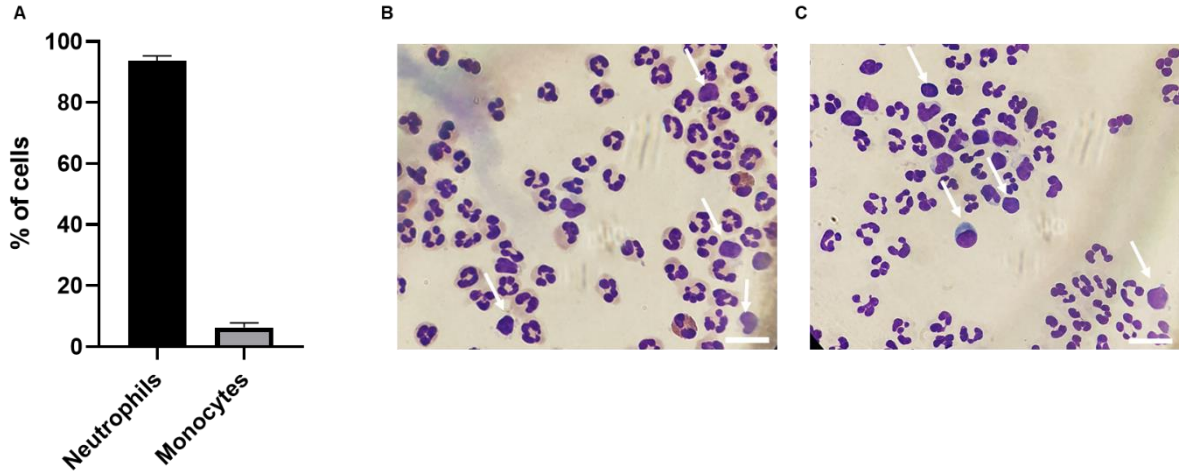

Figure 2.5 Purity of neutrophils prepared by EasySep™ immunomagnetic negative selection.

***(A)**. Neutrophils isolated by EasySep™ immunomagnetic negative selection were analysed for purity. Diff-Quick stained cytospins were observed using light microscopy and ~300 cells were*

counted from two slides in each experiment to calculate percentage of neutrophils and monocytes. ***(B, C).*** *Micrographs of single counting areas with white arrows indicating monocytes containing round and big nuclei. Scale bars represent approximately 10 µm for micrographs. Error bars represent SEM, n=6.*

2.4 Validation of the Hypoxic Chamber Environment

The hypoxic chamber was newly installed, and therefore validation that an appropriate hypoxic environment was established and maintained was required. To this end, neutrophil apoptosis and the transcription of hypoxia-regulated genes were assessed to confirm the impact of hypoxia on those functions of neutrophils with previous literature (McGovern *et al.*, 2011; Walmsley *et al.*, 2005).

2.4.1 Morphological assessment of neutrophil apoptosis

Neutrophils isolated by Plasma-Percoll® gradient centrifugation (see Section 2.1.2) were incubated at $5x10^6$ cells/mL either in normoxia (37ºC, 5% CO_2, 21% O_2) or hypoxia (37ºC, 5% CO_2, 0.8% O_2) in 96-flexiwell vinyl plates for 6 h and 24 h. At these time points, samples were cytocentrifuged, fixed and stained as described in Section 2.3.3, then morphologically examined for apoptosis using oil immersion light microscopy. Based on the characteristic phenotype of apoptotic neutrophils, cells containing darkly stained condensed nuclei (pyknotic) were counted as apoptotic (Fig. 2.4.) with the researcher blinded to the experimental conditions (Murray *et al.*, 1997; Savill *et al.*, 1989). Cytocentrifuge preparations were made in duplicate and approximately 300 cells were counted from each slide.

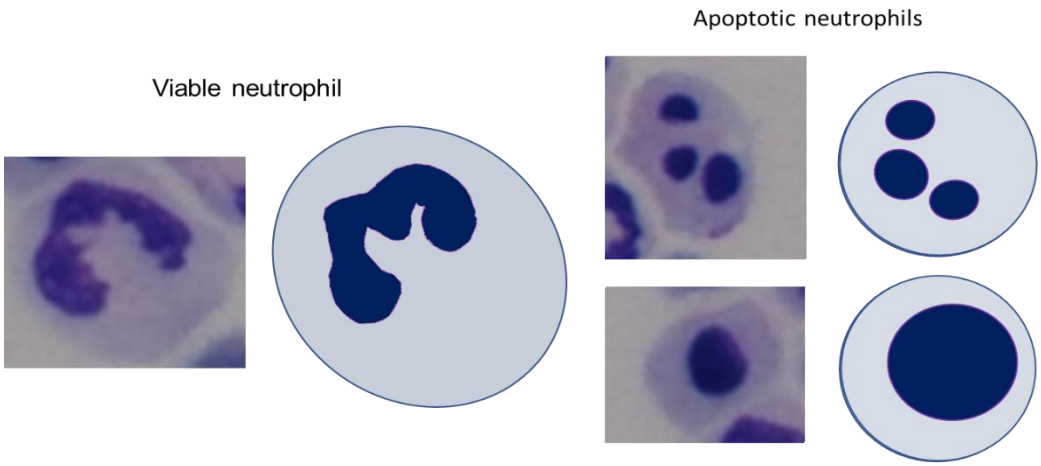

Figure 2.6 Normal and apoptotic nuclear morphology of neutrophils

Quick-Diff-stained fresh viable neutrophils (left) have a multi-lobed nucleus whereas apoptotic neutrophils contain darkly stained condensed (pyknotic) nuclei (right), which may be fragmented.

2.4.2 Polymerase Chain Reaction (PCR)

2.4.2.1 RNA extraction

Neutrophils freshly isolated by Plasma-Percoll® gradient centrifugation (Section 2.2.2.1) were re-suspended at 5 x 10^6 cells/mL in RPMI/FBS medium and cultured in normoxia and hypoxia (exactly as described in Sections 2.3.1 and 2.3.2). At 0, 6, 24 hours post incubation, 1 mL aliquots of neutrophil suspension from both normoxia and hypoxia were transferred to 1.5 mL centrifuge tubes and spun at 300 g for 2 min. The neutrophil pellets were resuspended by vigorous pipetting in 1mL TRI Reagent (a single step total RNA isolation reagent: Sigma- Aldrich, Poole, UK) to lyse cells. 200 µL of chloroform was added, followed by shaking samples vigorously for 15 s and leaving to stand for 10 min at room temperature (RT). Next, samples were spun at 15,294 g for 15 min at 4ºC. After this step, three distinctive phases were formed: the top aqueous layer containing RNA, the middle white interphase containing DNA, and the lower pink organic phase containing protein. The top RNA phase was carefully aspirated, avoiding disturbance of the interphase, and transferred to a clean 1.5 mL centrifuge tube with 500 µL of isopropanol to precipitate the RNA, shaken vigorously for 15 s and left for 10 min at RT. Then, samples were spun at 15,294 g for 10 min at

4ºC, supernatants were removed leaving a small, clear RNA pellet. After washing in 750 µL of 70% v/v ethanol and centrifugation at 5974 g for 5 min at 4ºC, the RNA pellet was left for 5-10 min to dry and was finally dissolved in 20 µL of sterile water.

2.4.2.2 DNase Treatment

The Ambion DNA-*free* ™ Kit (Invitrogen Waltham, MA) was used to purify RNA from any genomic DNA contamination. 2 µL of 10x DNase I Buffer and 1 µL of recombinant DNase I (rDNase I) were added to the RNA and mixed gently. Following incubation at 37ºC in a heat block for 30 min, samples were mixed with 2.3 µL of DNase Inactivation Reagent and incubated for 2 min at RT, mixing 2-3 times during the incubation period. Finally, samples were centrifuged at 10,000 g for 1.5 min, and the supernatant (RNA) was transferred to a fresh tube and stored in a -80ºC freezer.

2.4.2.3 cDNA Synthesis

The concentration of purified RNA (prepared as described above) was measured using a NanoDrop ND-1000 Spectrophotometer (Labtech International, Heathfield, UK). cDNA was generated from 1 µg of total RNA (with added RNase-free water to make the volume up to 20 µL) by using a High-Capacity cDNA Reverse Transcription Kit (Applied Biosystems, Thermo Fisher Scientific). A control (no RNA) sample was prepared by adding 20 µL of MasterMix into 20 µL of water. 20 µL of MasterMix was added to each sample and the resulting mixtures were placed in a Peltier Thermal Cycler – 200 DNA Engine Cycler (BioRad, Hercules, California) for incubation. The samples were repeatedly incubated for 10 min at 25ºC for annealing, 10 min at 37ºC for synthesis, and finally for 5 min at 85ºC for heat inactivation of reverse transcriptase.

2.4.2.4 Quantitative polymerase chain reaction (qPCR)

Relative quantitative PCR (qPCR) was performed using a QuantiTect SYBR Green PCR Kit (Qiagen) and standard QuantiTect Primer Assay primers (Qiagen) (Table. 2.1). The exact primer sequences were not provided by the supplier. Reactions were set up in a 384 well plate. In individual wells, 1 µL of cDNA (prepared as in Section 2.4.2.3) was added to 19 µL of QuantiTect SYBR Green PCR Master Mix (Qiagen) with 2 µL of the appropriate pairs of primers. This was performed twice per sample as

technical duplicates. Primers for 2 'housekeeping' genes Beta-2-Microglobulin (B2M) and 18s ribosomal RNA (RRN18s) which were reported not to change with the hypoxic incubation (Baddela *et al.*, 2014; Foldager *et al.*, 2009), and two experimental hypoxia-regulated target genes BCL2 interacting protein 3 (BNIP3) and Glucose Transporter 1 (SLC2A1) were used (see table 2.1). Subsequently, the plate was placed in a 7900HT Fast Real-Time PCR instrument to repeatedly cycle the reactions initially at 50°C for 2 min and 95°C for 10 min (HotStarTaq DNA Polymerase activation), followed by 40 cycles of 95°C for 15 s (DNA denaturation) and 60°C for 1 min (annealing and extension).

The SDSv2.4 software program was used to analyse data obtained from the qPCR reaction. The relative gene expression was calculated by correcting cycle threshold (CT, number of cycles required for the fluorescence signal to exceed the background level and reach the 'threshold' significantly above background) for the target gene against that of the reference gene RRN18s (ΔCT). Then using the ΔCT values for each timepoint of experimental condition, the difference between the timepoint 0 h and all other timepoints in each condition was determined (ΔΔCT). Relative gene expression (fold change) was expressed as $2^{-\Delta\Delta CT}$.

Gene	Catalogue number
Beta-2-Microglobulin (B2M)	QT00088935
18s ribosomal RNA (RRN18S)	QT00199367
BCL2 interacting protein 3 (BNIP3)	QT00024178
Glucose Transporter 1 (SLC2A1)	QT00068957

Table 2.1 Commercial (Quiagen) primers (Gene globe Quantitect primer assay products) used in this work.

2.5 Bacterial growth and quantification

Bacteria were streaked with a sterile inoculation loop onto BHI agar plates from stocks kept in cryovials at -80°C and incubated overnight at 37°C. 10 mL aliquots of liquid media (BHI; Sigma- Aldrich, Poole, UK; or RPMI; Gibco™ Lonza, UK) in 50 mL sterile universal tubes were inoculated with a single bacterial colony, and subsequently

placed in a rack into a humidified atmosphere incubator at 37°C with 5% CO_2 on a 1.5 mL centrifuge tube ThermoMixer (Stevenage, UK) shaking at 350 rpm for overnight incubation. The following day, bacterial optical density at 600 nm (OD_{600}) was determined by spectrophotometry (Jenway 6100, Stone, UK) and a subculture was made by adding an appropriate volume of the overnight culture to fresh medium to achieve an OD_{600} of 0.05-0.1 to avoid a lag phase (time necessary to recover shock caused by transfer) of bacterial growth.

2.5.1 Staphylococcal strains and storage

S. aureus strains (Table 2.2) were kept at -80°C in Microbank (Pro-lab Diagnostics, Bromborough, UK) cryovials and were inoculated onto BHI agar (Sigma-Aldrich, Poole, UK) plates. For short-term storage (approx. 2 weeks) agar plates were kept at 4°C. For long-term storage, a single colony was transferred from the BHI agar plate using a sterile inoculation loop into Microbank cryovials containing chemically treated beads providing bacterial adhesion, mixed to allow coating of beads with bacteria, and stored at -80°C.

Strain	Description	Reference
SH4276	JE2 (MRSA), USA300 LAC strain cured of plasmids p01 and p03.	(Fey *et al.*, 2013) Obtained from Prof. Simon Foster
SH1000	Functional *rsbU*$^{+}$ derivative of 8325-4	(Horsburgh *et al.*, 2002) Obtained from Prof. Simon Foster
SH4622	Transduction from parent strain RN4220 to SH1000; expressing mCherry under Pma1M (Pma1M-mCherry cloned from pMV158 mCherry).	(Pollitt *et al.*, 2018) Obtained from Prof. Simon Foster
Wood 46	Protein A deficient	ATCC® 10832D5™
MHK10AM	*sodA sodM* mutant in SH1000 parental strain	Needham *et al.*, 2004; Obtained from Prof. Simon Foster
KC043	*katA ahpC* mutant in SH1000 parental strain	(Cosgrove *et al.*, 2007) Obtained from Prof. Simon Foster

Table 2.2 Staphylococcal strains used in this study.

The staphylococcal strain JE2 (SH4276) is derived from the methicillin clinical USA300 strain by removal of two plasmids- p01 (cryptic plasmid) and p03 (conferring resistance to erythromycin). The JE2 strain is the parental strain of a sequence-defined transposon library - the Nebraska Transposon Mutant Library (Fey et al., 2013). SH1000 is methicillin sensitive with a functional rsbU derivative of 8325-4 lineage, the mutation that is known to dramatically reduce sigmaB activity (Horsburgh et al., 2002). The mCherry expressing SH1000 (SH4622) was generated by the phage ϕ11 transduction using pKASBARmCherry plasmid supplemented by EryR (Pollitt et al., 2018). Wood46 was sourced from the American Type Culture Collection (ATCC 10832) and is protein A deficient and spA negative (Balachandran et al., 2017). Double mutant of SH1000 for superoxide dismutase A and M (MHKAM) was constructed by electroporation of plasmids pMK1A and pMK1A into RN4220 then transduced into recipient SH1000 using the ϕ11 (Karavolos et al., 2003). Catalase (KatA) and alkyl hydroperoxide reductase (AhpC) double mutant in SH1000 background (KC043, ahpC katA) was made by transformation of the pSK5630 and pKC2 plasmids into electrocompetent S. aureus RN4220 and then transferred to SH1000 by phage transduction using the ϕ11 (Cosgrove et al., 2007).

2.5.2 Bacterial quantification

To determine the exact number of viable bacteria, the colony forming unit (CFU) counts were determined using the Miles and Misra method (Miles et al, 1938). Briefly, the bacterial culture was serially diluted (1:10) with sterile PBS up to 10^6- 10^8- fold. Three 10 µL drops from each dilution were spotted onto a BHI agar plate and left in the laminar flow hood to dry before overnight incubation at 37°C. On the following day, the colonies from a dilution containing about 20-70 separate colonies (see Figure 2.5) were counted, and the CFUs were determined by the following formula: CFU/mL = (total number of counted colonies per dilution/3) x 100 x dilution factor.

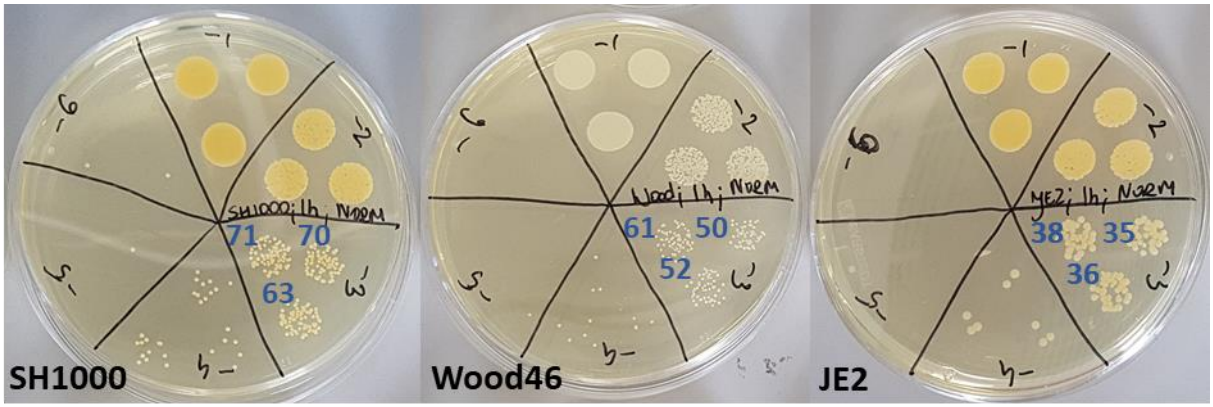

Figure 2.7 Determination of bacterial concentration using Miles and Misra method

*Examples of 10^6-fold serial dilutions for SH1000, Wood46 and JE2 staphylococcal strains. Blue numbers represent counted colonies from informative 10^3 dilutions. Sample concentration (CFU/mL) calculation for SH1000: (71+70+63)/3 *100 *10^3 = 6.8 x 10^6 CFU/mL.*

2.5.3 Measurement of bacterial growth

To determine the effect of culture media and conditions, bacteria were grown as described in Section 2.5. The subculture was grown for 3 h and used to inoculate fresh 10 mL of media at a starting OD_{600} of 0.05 for incubation at 37°C with shaking at 350 rpm, either in normoxia as standard, or in the hypoxic incubator (see Section 2.3). The OD_{600} and CFU were measured at set timepoints in different experiments. To check the growth rate of staphylococcal strains used in this study, OD_{600} was measured

every hour up to 6 h with subsequent Miles and Misra quantification (see Section 2.6). An additional OD_{600} reading was performed at 24 h (Fig. 2.6).

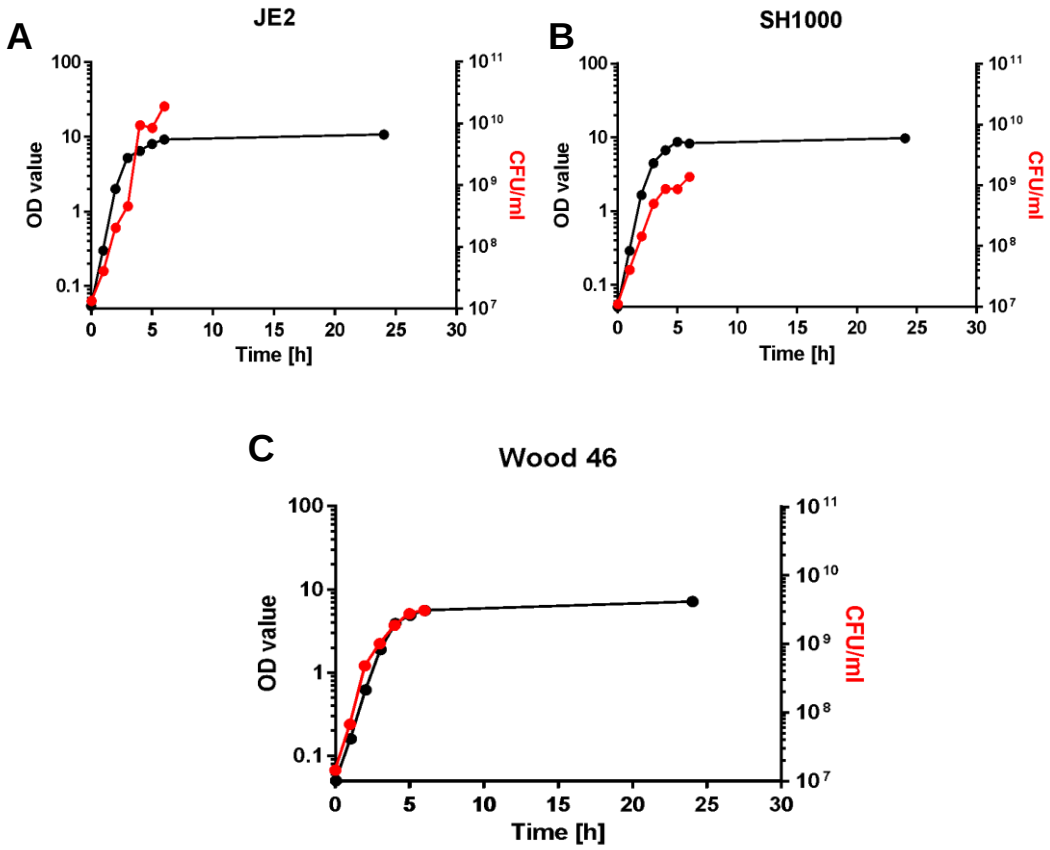

Figure 2.8 Growth kinetics of staphylococcal strains

S. aureus JE2 ***(A)****, SH1000* ***(B)*** *and Wood46* ***(C)*** *strains were grown aerobically in 10 mL of BHI medium for 24 hours, with OD and bacterial enumeration (Miles and Misra) every hour for 6 hours. The red line represents CFU/mL and the black OD value, n=1.*

2.5.4 Preparation of frozen bacterial aliquots

Bacteria were grown to an exponential phase in 10 mL of RPMI/FBS at 37°C with shaking, as described in Section 2.5. The bacterial culture was then aliquoted (500 µL) into 1.5 mL centrifuge tubes and frozen at -80°C. CFU counting (Section 2.5.2) was performed to determine the exact number of bacteria at each time new stocks were prepared.

2.6 Intracellular bacterial killing assay

2.6.1 Antibiotic or enzymatic treatment to kill extracellular bacteria

To quantitate intracellular bacterial killing, it is important to be able to kill non-phagocytosed bacteria quickly and efficiently, to enable enumeration of those bacteria that have been ingested (uneaten bacteria may lead to a high 'background' of un-killed organisms that reflect incomplete phagocytosis rather than failure to kill). Lysostaphin (a metalloendopeptidase that cleaves the crosslinking pentaglycine bridges abundant in the cell wall peptidoglycan of *Staphylococci*; Sigma-Aldrich, Poole, UK) and gentamicin (an aminoglycoside antibiotic that inhibits bacterial protein synthesis by irreversibly binding the 30S subunit of the bacterial ribosome; Sanofi, Guildford, UK) were tested for effective bactericidal activity against the JE2, SH1000 and Wood46 strains. Frozen aliquots of bacteria (Section 2.5.8), were thawed, spun at 5,400 g for 6 min in a microfuge and resuspended in appropriate volume of fresh RPMI/FBS to give a concentration of $1x10^8$ CFU/mL. 10 µL of bacterial suspension was added to lysostaphin or gentamicin (concentrations 5- 40 µg/mL, final volume 200 µL) prepared in RPMI/FBS medium and incubated at 37°C in humidified 5% CO_2 incubator. At the desired timepoints (0- 40 min) the samples were spun at 6,600 g for 2 min, washed once with 1 mL sterile PBS and resuspended in 200 µL of PBS. Following this step, 100 µL was transferred to 900 µL of PBS for serial dilutions up to 10^3 -fold in 96 well plate using a multichannel pipette, and 5 µL was spotted onto BHI agar plate and the CFU was determined using the Miles Misra method (Section 2.5.2).

2.6.2 Neutrophil co- culture with *S. aureus* to assess intracellular bacterial killing

Frozen aliquots of *S. aureus* strains in RPMI/FBS (see Section 2.5.4) were thawed before experiments. The volume containing the correct number of bacteria to achieve the desired multiplicity of infection (MOI) was calculated from the CFU determined prior to freezing. Once thawed, the bacterial suspension was spun at 6,000 g for 7 min and resuspended in the calculated volume of fresh RPMI/FBS (pre- incubated overnight in normoxic and hypoxic conditions) to give the desired MOI. Neutrophils, obtained as described in Sections 2.2.1 or 2.2.2, re-suspended in RPMI/FBS at 2.8 x 10^6 cells/mL were placed (90 µL) into 96 well plate and pre- incubated in normoxia or

hypoxia for 1 h prior to addition of bacteria (10 µL; in normoxic or hypoxic media as appropriate) to give the desired MOI. Bacteria were also incubated in RPMI/FBS without neutrophils (control) so that the exact number of CFU at the beginning and the end of each experiment could be determined. After 30 min of co-incubation, 40 µg/mL of gentamicin was added to kill extracellular bacteria, allowing subsequent intracellular killing to be quantified. At chosen timepoints (15 min- 24 h), samples were centrifuged at 400 g for 3 min to pellet neutrophils and any intracellular bacteria, and neutrophils were then lysed by re-suspension in 1 mL of alkaline water (pH 11) with vigorous pipetting and vortexing. Lysis in alkaline water resulted in more efficient cells lysis than other methods such as 0.1% saponin in PBS, tested by using both methods on recovered CFU of bacteria from cells (data not shown) (Decleva *et al.*, 2006). After 10 min incubation at RT, samples were serially diluted and spotted onto agar plates as described in Section 2.6, allowing the quantification of live intracellular bacteria at each timepoint. The number of internalised bacteria was determined the following day by counting bacterial colonies recovered from lysed neutrophils and calculating the CFUs (see Section 2.5.2). An additional well of the co-culture was prepared in each experiment for the cytospin preparation (Section 2.2.3) and light microscopy.

2.6.3 Use of inhibitors in bacterial killing assays

Bafilomycin, Dimethyloxallyl Glycine (DMOG; Sigma-Aldrich, Darmstadt, Germany) a cell permeable prolyl-4-hydroxylase inhibitor, which stabilises HIF (hypoxia-inducible factor) was dissolved in DMSO at 100 mM working concentration and used in assays at 100 nM. Cycloheximide (CHX, 100 mg/mL in DMSO ready solution; Sigma-Aldrich, Darmstadt, Germany), a controlled protein synthesis inhibitor which was used in killing assays at 1 µg/mL (concentration previously optimised for use in neutrophils in the laboratory, data not shown). 2 µM DPI, 1,5 and 10 µM VPS34N1 with appropriate DMSO vehicle controls were also used. Bafilomycin, DMOG, CHX or vehicle controls were added to neutrophils immediately after isolation and kept till the end of the experiment. DPI, VPS43N1 were added at 50 min of pre-incubation and kept till the end of experiment. Freshly isolated neutrophils at 2.5 x 10^6 cells/mL were placed (90 µL) into 96 well plate and pre- incubated in normoxia (bafilomycin, DMOG, CHX) or hypoxia (CHX only) for 1 h prior to addition of *S. aureus* SH1000 (10 µL) at MOI 5. After 30 min of co-incubation 40 µg/mL of gentamicin was added to kill extracellular

bacteria. At chosen timepoints from the addition of gentamicin (designated t=0 min), namely 180 and 240 min bacterial quantification to determine intracellular killing was undertaken exactly as described in Section 2.6.2.

2.7 Microscopy

These assays were used to image cells and bacteria to obtain information about the host- pathogen interactions, phagosomal maturation, phagosomal acidification, and ROS production by human neutrophils.

2.7.1 Dual staining of bacteria using pHrodo and fluorescein

In order to measure intracellular pH, bacteria they were stained with pH-sensitive dyes pHrodo Red and Fluorescein-5-EX Succinimidyl-ester dyes (Life Technologies, Paisley, UK). Dyes were re-suspended in DMSO to final concentrations of 2.5 mM for pHrodo Red and 16.95 mM for Fluorescein (previously optimised in our group). *S. aureus* strains were grown overnight in 10 mL of BHI, with inoculation of fresh BHI to the OD_{600} 0.05-0.1 on the following day. Bacteria were then grown for about 2 h to achieve exponential growth (OD_{600} of 1). Ten mL of culture was then spun down at 6000 g for 10 minutes. After spinning, the pellet was resuspended in 3.2 mL of PBS pH 9. Two hundred µL of the resulting bacterial suspension was then added to 0.5 µL of pHrodo Red S-ester and 1.5 µL of Fluorescein S-ester (concentrations as above) and pipetted/gently vortexed to mix thoroughly. The bacterial suspension was incubated for 30 min at 37˚C on a rotator protected from the light (the dyes are light-sensitive). To remove unincorporated dye, bacteria were washed sequentially in 1mL PBS pH 8, 1mL 50mM Tris-HCl pH 8.5, 1 mL PBS pH 8, (with centrifugation at 12000 g for 2 min to pellet and aspiration of supernatant after each wash). Finally, the dual-stained bacteria were resuspended in 100 µL of PBS pH 7.4 and stored aliquoted at -80 ˚C until use for the co-incubation with freshly isolated neutrophils. Before each experiment, microscope settings such as exposure time, laser power and sensitivity were optimised by imaging alive, and heat killed bacteria alone resuspended in acidic (pH of 3) or alkali (pH of 8) pH (Fig. 2.7.).

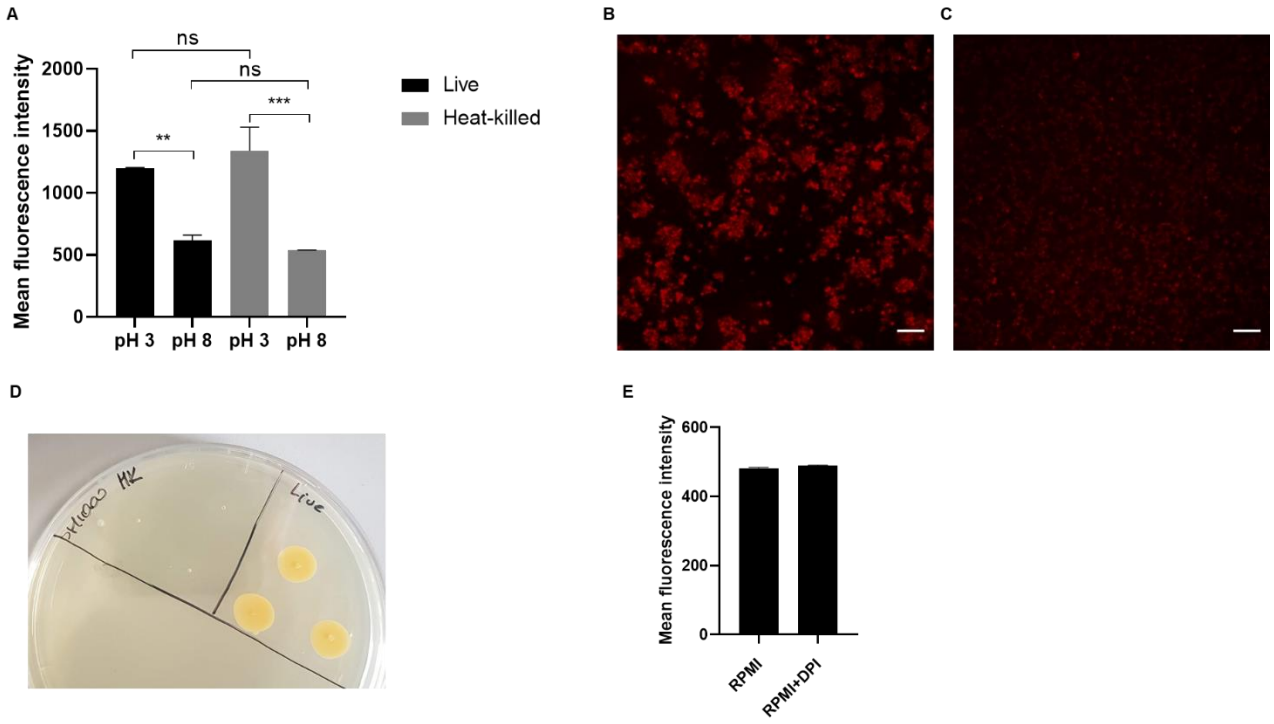

Figure 2.9 Optimisation of pHrodo red- stained *S. aureus.*

*Bacteria were stained with pHrodo red, heat-killed for 20 minutes at 80˚C or live and suspended in media at pH 3 and pH8 to measure mean fluorescence intensity (MFI) at 532 nm wavelength using spinning disk microscopy at 60x oil immersion magnification; Data represent mean +/- SEM, n=3; ns p >0.05, *** p=0.0008, ** p=0.0058 tested by one-way ANOVA with Sidak's Multiple Comparison Test **(A)**. Representative images of bacteria at pH 3 **(B)** and pH 8 **(C)** media. Before each experiment heat-killed bacteria were confirmed to be dead by Miles and Misra method **(D)**. Mean fluorescence intensity of pHrodo red stained S. aureus suspended in RPMI/FBS and RPMI/FBS with addition of 2 µM DPI; Data represent mean +/- SEM, n=1 performed in triplicate **(E)**.*

This procedure allowed changes in pHrodo and fluorescein fluorescence intensity to be measured at different pHs and to adjust settings for the laser power to use for imaging bacteria with neutrophils. In some cases, pHrodo staining was undertaken without the fluorescein, with an otherwise identical protocol (Fig. 2.7). Single stained bacteria were stored exactly as above.

2.7.2 Spinning disk confocal microscopy

2.7.2.1 Dichlorofluorescin (DCF) assay to measure reactive oxygen species (ROS)

Freshly isolated neutrophils at 2.25 x 10^5 cells/180 µL were placed in an 8-well glass bottom Ibidi chamber (Thistle Scientific LTD, Uddingston, Glasgow) to incubate for 1 h prior to the addition of bacteria. After 30 min 5 µM of 2',7' –dichlorofluorescin diacetate (DCFDA) (Sigma Aldrich, Pool, UK), which is oxidised to a fluorescent dye 2', 7' –dichlorofluorescein (DCF) resulting in the development of a green signal when ROS are present. Samples were protected from light as the signal is light-sensitive and fades in ambient light conditions. After 1 h total incubation, *S. aureus* SH1000 mCherry-expressing 1.12 x 10^6 CFU/20 µL) or pHrodo stained strains were added to inhibitor or DMSO (controls) treated neutrophils. Imaging was performed using Perkin Elmer spinning disk confocal microscope (Wolfson Light Microscopy Facility) at 60 x oil immersion magnification.

2.7.2.2 Use of ROS- production inhibitors

To inhibit neutrophil ROS production, the NADPH oxidase inhibitors diphenyleneiodonium chloride (DPI, Sigma Aldrich, Gillingham, UK) or apocynin (Sigma Aldrich, Gillingham, UK) were used. After 50 min pre- incubation (10 min prior to adding bacteria) either DPI (final concentration 2 µM) or apocynin (final concentration 300 µM) or DMSO vehicle control were added to neutrophils. In other experiments, Class I PI3-kinase inhibitors were added, again after 50 min incubation and using appropriate vehicle controls: IC87114 (PI3Kδ inhibitor; BioVision, Milpitas, CA; final concentration 10 µM), AS605240 (PI3Kɣ inhibitor; LKT Laboratories, Inc., St. Paul, USA; final concentration 5 µM), and LY294002 (pan-PI3K inhibitor; Calbiochem®; final concentration 20 µM). These inhibitor concentrations have previously been optimised in the laboratory for inhibition of neutrophil functions with minimal off-target effects. Finally, the Vacuolar Protein Sorting 34 (VPS34) inhibitor VPS34-IN1 (Merck KGaA, Darmstadt, Germany; dissolved in DMSO at 10 mM) was used at concentrations 10, 5 and 1 µM, added at the outset of the experiments. Imaging of DCF and ingested bacteria was carried out exactly as above.

2.7.2.3 Imaging dually stained bacteria with pH sensitive dyes to assess phagosomal acidification

Freshly isolated neutrophils (2.25 x 10^5 cells/180 µL) were placed in 8-well glass bottom Ibidi chamber to incubate for 1 h before addition of bacteria with or without 0.1 µM bafilomycin (Sigma-Aldrich, St. Louis, USA) or vehicle control. DPI 2 µM or vehicle control or other inhibitors (PI3Ks, VPS34N1) were added at t=50 min, and dually stained with fluorescein and/or pHrodo-stained (Section 2.7.1.) *S. aureus* SH1000 (1.12 x 10^6 CFU/20 µL) were added at 60 min. After this time samples were incubated for further 1h before live imaging using spinning disk confocal microscope at 60 x oil immersion magnification (numerical aperture 1.35). Detection of colours green for fluorescein excitation wavelength of 488 nm and red excitation wavelength of 532 nm channel for pHrodo.

2.7.2.4 Analysis of ROS production and acidification in ImageJ

Oxidised DCF green signal or green for fluorescein and red for pHrodo were quantified using a Macro Analysis script written by Dr Nick Van Hateren in ImageJ 2.0.0-rc-69/1.52; Java 1.8.0_172 [64-bit] designed to read mean fluorescent intensity signals from each neutrophil with red bacteria inside, defined by size in pixels. Each parameter was measured from two fields per each experiment.

A

MacroAnalyseParticles-whole-dataset (1).ijm

```
run("Bio-Formats Macro Extensions");
dir = getDirectory("Choose a Directory to Save Analysis");
//choose file, initialise it and get seriesCount
path = File.openDialog("Select a File to Process");
//run("Bio-Formats", "open=[&path] autoscale color_mode=Default rois_import=[ROI manager] view=Hyperstack stack_order=XYCZT series_1");
Ext.setId(path);
Ext.getSeriesCount(seriesCount);

//setBatchMode(true);
//loop over seriesCount, open each series in turn and process

for (i = 1; i < seriesCount; i++) {
    print("Processing series " + i + "/ " + seriesCount);
run("Bio-Formats", "open=[&path] autoscale color_mode=Default rois_import=[ROI manager] view=Hyperstack stack_order=XYCZT series_" + i);

name = getTitle();
//if (name != "") {

print("name = " + name);
run("Set Scale...", "distance=1 known=0.115 pixel=1 unit=microns global");

run("Make Substack...", "channels=1-2");
run("Split Channels");

selectWindow("C2-" + name + "-1");
```

B

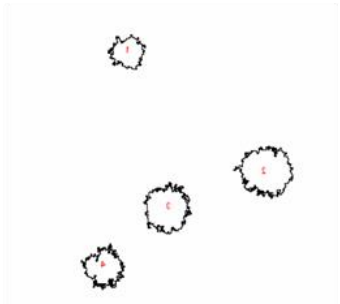

C

	Area	Mean	StdDev	Min	Max
1	10.223	539.358	13.202	494	585
2	25.048	610.263	187.079	503	2189
3	22.641	548.586	15.689	500	608
4	17.113	851.353	688.474	508	5218

Figure 2.10 Analysis of ROS production using macro written in Fiji software

*The macro script was written in Fiji software to analyse intensity of different channels in defined region of interest (ROI). Software was trained to analyse particles of defined pixel size to exclude artefacts **(A)**. After each completed analysis drawings of analysed cells were generated to navigate from which cells each reading has been performed **(B)**. Data acquired from running the macro include the area of each cell (µm^2), mean of fluorescence intensity, standard deviation, and minimum and maximum intensity **(C)**. In each experiment readings of mean fluorescent intensity (MFI) of different channels were acquired to plot figures.*

2.7.3 Nitro-blue tetrazolium (NBT) staining of neutrophils for ROS detection

To enable the assessment of ROS generation in hypoxia (the DCF methodology required unfixed cells and cannot be undertaken in the hypoxic hood, and removal of cells from the hood results in rapid re-oxygenation which nullifies the experiment), the nitro-blue tetrazolium (NBT) method was used. Nitro-blue tetrazolium chloride (Sigma Aldrich, St. Louis, USA) was dissolved in sterile water at 1 % concentration and stored

in aliquots at -20 ˚C. Freshly isolated neutrophils were resuspended in normoxic or hypoxic RPMI/FBS/HEPES at 2.5 x 10^6 cells/mL and placed (180 µL) in wells of 8-well glass bottom Ibidi chamber to pre-incubate for 1 h in normoxia and hypoxia in parallel. After 50 min, DPI at 2 µM was added to normoxic neutrophils (negative control). Phorbol 12-myristate 13-acetate (PMA; Sigma P1585-1MG, dissolved in DMSO at 10 µM) at 50 nM was used as a positive control. *S. aureus* SH1000 mCherry-expressing at 1.12 x 10^6 CFU were added (20 µL) at 1 h and a further 1 h of co-incubation was used to enable phagocytosis and ROS production. Next, RPMI was aspirated from each well and replaced with 200 µL of 0.1 % NBT for 15 min. The NBT was removed, and samples were washed with 1x DPBS and fixed with 100% methanol for 3 min, which was then replaced by 1x DPBS. Samples were then observed under the Perkin Elmer spinning disk microscope at 40x oil immersion magnification under brightfield illumination, with the observer blinded as to the experimental conditions. Cells that had developed grey staining due to the oxidation of NBT to formazan (see Figure 2.8) were designated ROS positive. and counted to get the % of ROS positive cells in different treatments. Approximately 30 cells from the field of view were counted from two different fields per experiment.

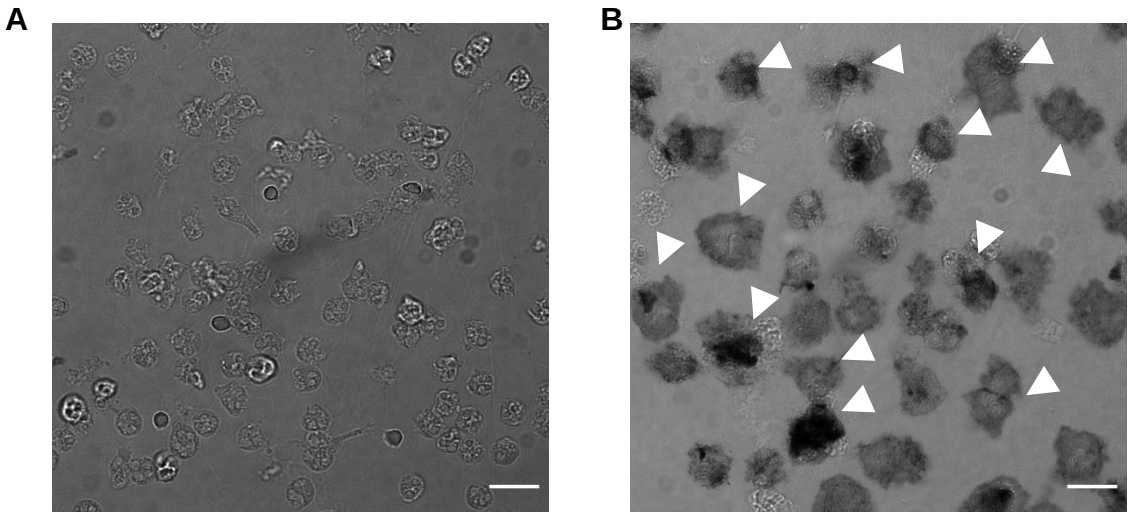

Figure 2.11 NBT assay for ROS detection.

Human neutrophils after 1 h of incubation in normoxia stained with 0.1% NBT. ***(A)*** *Unstimulated (DMSO vehicle control) cells,* ***(B)*** *PMA- treated cells (positive control) White arrowheads indicate cells containing formazan precipitates formed upon reduction of NBT by ROS. Scale bars represent 10 µm.*

2.8 Transmission electron microscopy (TEM) of neutrophils to assess phagosomal morphology

2.8.1 Preparation of neutrophils for TEM

Freshly isolated neutrophils were co-incubated for 30 or 60 min with *S. aureus* SH1000 at a MOI of 10, with gentamicin added after 30 min at 40 µg/mL to kill extracellular bacteria. Specimens ($1.12x10^6$ neutrophils with $1.12x10^7$ bacteria) were spun down and the pellet was fixed in fresh 3% Glutaradehyde[NB] in 0.1 M Phosphate buffer and left overnight at 4^0C. From this stage, samples were processed by Mr Christopher Hill (Electron Microscopy Officer, University of Sheffield). The specimens were washed in 0.1 M phosphate buffer twice at 15 min intervals at 4^0C. Secondary fixation was carried out in 2% aqueous osmium tetroxide for 1-2 hour at RT, washed in 0.1 M phosphate buffer. The samples then underwent dehydration through a graded series of ethanol incubations at room temperature as follows:

1) 75% ethanol for 15 min

2) 95% ethanol for 15 min

3) 100% ethanol for 15 min

4) 100% ethanol for 15 min

5) 100% twice ethanol dried over anhydrous Copper sulphate for 15 mins.

The specimens were then placed in an intermediate solvent, propylene oxide, for two incubations each of 15 mins duration. Infiltration was accomplished by placing the specimens in a 50/50 mixture of propylene oxide/Araldite resin (see table 2.4). The specimens were left in this 50/50 mixture overnight at room temperature on a rotating mixer. The specimens were incubated in full strength Araldite resin for 6-8 hours at room temperature on a rotating mixer after which they were embedded in fresh Araldite resin for 48-72 hours at 60 ˚C.

Araldite resin	mL per mixture
CY212 resin	10 mL
DDSA hardener	10 mL
BDMA accelerator	1 drop per 1 mL of resin mixture

Table 2.3 Araldite resin components.

Semi-thin Sections approximately 0.5 µm thick were cut on a Reichert Ultracut E ultramicrotome and stained with 1% Toluidine blue in 1% Borax. Ultrathin Sections, approximately 70-90 nm thick, were cut on a Reichert Ultracut E ultramicrotome and stained for 25 min with 3% aq Uranyl Acetate followed by staining with Reynold's Lead Citrate for 5 min prior to imaging.

All the mentioned chemicals above (apart from ethanol-SLS scientific Lab Supplies) were purchased from Agar Scientific Ltd, Parsonage Lane, Stansted, Essex.

2.8.2 TEM imaging and analysis

The sections were examined by myself following training from Mr Chris Hill, using a FEI Tecnai Transmission Electron Microscope at an accelerating voltage of 80 Kv.

Electron micrographs were taken using a Gatan digital camera under several magnifications. Analysis of imaging has been performed using ImageJ 2.0.0-rc-69/1.52; Java 1.8.0_172 [64-bit] software, manually measuring the area of bacteria (μm^2) inside of the vacuoles (phagosomes) and area of phagosomes (μm^2) then ratios were made: (area of bacterium/area of phagosome) x 100%= percentage of phagosome area occupied by bacterium (Fig. 2.10).

A

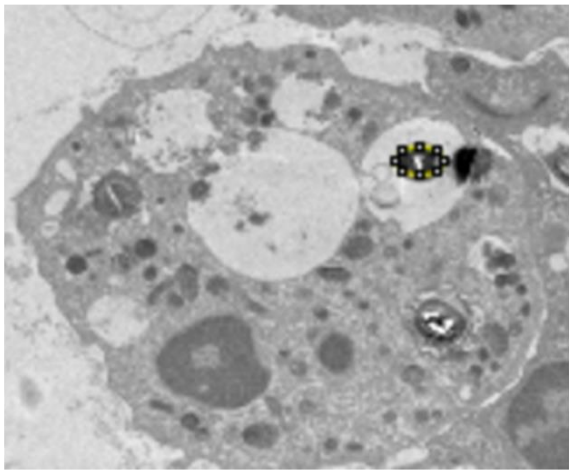

B

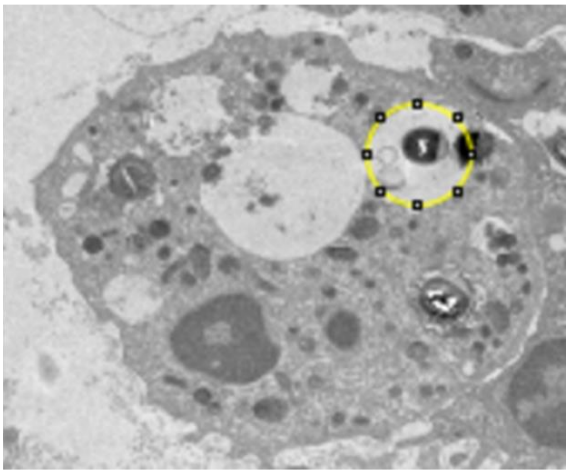

C

	Area	Mean	StdDev	Min	Max
1	0.275	5835.997	1227.169	4505.456	16022.836
2	2.323	7220.985	1081.047	3609.073	16022.836

Figure 2.12 Area measurement of the bacterium and phagosome using ImageJ 2.0.0.

*TEM of neutrophil containing bacteria, with manually pointed area of bacterium **(A)**, and phagosomes in which bacterium is entrapped with its manually pointed area **(B)**. Measurements analysed using ImageJ software with area number 1 being bacterium area and area number 2 being phagosomal area **(C)**. Calculation for ratio is bacterium area/phagosome area x 100% to get percentage of bacteria of phagosome size. Example: 0.275/2.323 x 100%= 11.83 %.*

Classification of phagosomes in terms of their size in ratio with bacteria occupying their space is shown in Table 2.4:

Phagosome shape:	% of bacteria area (μm^2) to phagosome area (μm^2):
Spacious*	<50%
Tight*	>50%

Table 2.4 Classification of phagosomes by shape.

*Spacious phagosome -bacteria occupy less than 50% of area of the phagosome.

*Tight phagosome - bacteria occupy more than 50% of area of the phagosome.

2.9 Statistical analysis

Presented data are expressed as mean ± SEM (standard error of the mean) of the number (n) of independent experiments. Statistical significance for normally distributed data was tested by one-way ANOVA (Analysis of Variance) with a Holm-Sidak's multiple comparison post-test or two-way ANOVA with Tukey's post-test, using the Prism 7.0 statistics software (GraphPad Software, Inc, US) for 2 or more groups. If only 2 groups were compared the Student t-test was used for normally distributed data (Shapiro Wilk test) and a Mann-Whitney U test was employed when data were not normally distributed (Prism 7.0 software). Values of $p<0.05$ were considered significant and are indicated in figure legends.

3 Characterisation of the effect of hypoxia on growth of *S. aureus* and their killing by human neutrophils

3.1 Introduction

A total of 12,784 *S. aureus* bacteraemia cases were reported to Public Health England in 2017/18; whilst methicillin-resistant infections are decreasing due to infection control and public health initiatives they remain difficult to treat, and serious infections due to methicillin-sensitive organisms continue to increase (Public Health England, https://assets.publishing.service.gov.uk/). Neutrophils are important in combating staphylococcal infections, as evidenced by host susceptibility to this pathogen when neutrophil function is defective, for example in chronic granulomatous disease (Winkelstein *et al.*, 2000). To further explore this clinically important host-pathogen interaction, I chose to purify peripheral blood neutrophils rather than use a whole blood killing assay (such as that described by Lu *et al.*, 2014), to eliminate the possible confounding effect of other immune cell types such as monocytes, and of antibacterial proteins present in the blood including antibodies and complement. However, neutrophils are sensitive cells whose activation state can be profoundly altered by mechanical and chemical stress during isolation procedures (Watson *et al.*, 1992), for example activation by LPS contamination of Ficoll supplies, was reported by Jahr *et al.*, 1999; hence care must be taken during the preparative process. Our group has extensive experience in neutrophil preparative methods and along with others have characterised and validated the function of density gradient centrifugation-derived neutrophils (e.g., Hoenderdos *et al.*, 2016; Parker *et al.*, 2009; Decleva *et al.*, 2006; Dri *et al.*, 2002). The use of antibody-coated magnetic bead protocols allow negative selection of very pure neutrophils with fewer centrifugation steps, but is expensive and only suitable for low blood volumes (Thomas *et al.*, 2015).

When studying host-pathogen interaction it is important to use conditions that match those *in vivo* as closely as possible. Hypoxia is a physiological state in certain parts of the human body such as the gut, the basal layers of skin, and muscle, and the degree of hypoxia can be enhanced by infection and inflammation (0-3 kPa), hence both bacteria and neutrophils must adapt to operate within such harsh environments (Simmen and Blaser, 1993; Campbell *et al.*, 2014; Monceaux *et al.*, 2016). Many *S. aureus*-infected sites are profoundly hypoxic or even anoxic e.g., abscesses and infections in deep tissues such as osteomyelitis (Wilde *et al.*, 2015). In contrast, most

scientific data on neutrophil function has been obtained by studying isolated cells cultured in ‘normal’ atmospheric oxygen (approx. 21.33 kPa). This does not reflect the pathological situations encountered *in vivo* by both bacteria and immune cells, particularly in deep tissue infections. Therefore, during my work I have employed a hypoxic workstation, which allows cell incubation at controlled levels of hypoxia, and compared neutrophils incubated under these conditions in parallel to those that remain in ‘standard’ culture conditions in atmospheric oxygen. However, the workstation has limited internal space and the capacity to run only single small items of electrical equipment; it is accessed via ‘portal gloves’ which limit dexterity, and it is prone to malfunction. Using the hypoxic chamber therefore poses significant challenges and limits the range and magnitude of experiments that can be undertaken.

Hypoxic conditions have an impact on neutrophils but may also affect bacterial growth and function (Hajdamowicz *et al.*, 2019). I have chosen three strains of *S. aureus* to study: two methicillin-sensitive MSSA strains, namely SH1000 (Horsburgh *et al.*, 2002) and Wood46 (ATCC® 10832D5™) and for comparison JE2 (a clinical methicillin-resistant MRSA strain, USA300; Fey *et al.*, 2013). The JE2 strain is a highly characterised community- acquired MRSA (CA-MRSA) which contains three small plasmids that encode resistance to tetracycline, erythromycin and one of them being cryptic. It carries a type IV staphylococcal chromosomal cassette *mec* (SCC*mec* IV), which encodes resistance to methicillin and other β- lactam antibiotics (Diep *et al.*, 2006), and by expression of encoded by *pvl* genes in a lysogenic bacteriophage of PVL (Narita *et al.*, 2001). Although methicillin-sensitive strains such as SH1000 are easier to treat and often less virulent than MRSA, they are far better characterised, and widely used to study staphylococcal physiology and infection *in vitro* and *in vivo*. There are animal models of SH1000- infection such as murine (McVicker *et al.*, 2014) and zebrafish embryo models (Prajsnar *et al.*, 2008). This strain is the derivative of *S. aureus* 8325 lineage (O’Neill, 2010). First, strain 8325 was modified by curing its three prophages (Φ 11, Φ 12 and Φ 13) to yield strain 8325-4 (Novick, 1967) and reinstatement of an intact *rsbU* gene encoding a regulator of sigma factor B to yield strain SH1000 (Horsburgh *et al.*, 2002).

A previous study (McGovern *et al.*, 2011) suggested that hypoxia may impair neutrophil microbicidal function against *S. aureus* Wood46, but only very limited

observations were made. The main aim of the work in this chapter is to confirm and extend this important observation, hence the inclusion of the laboratory- adapted Wood46 strain. In view of the clinical link between chronic granulomatous disease and recurrent staphylococcal infection and the observation that hypoxia limits the oxidative burst, **I hypothesised that hypoxia would significantly impair the killing of *S. aureus* by isolated human neutrophils.**

A key requirement was to develop a robust killing assay to study intracellular killing of the above *S. aureus* strains over time, which could be undertaken in normoxia and hypoxia in parallel. This necessitated several parameters to be tested and optimised:

- Hypoxic incubation conditions
- Growth kinetics of bacteria in the relevant environments.
- The killing of extracellular (non-phagyocytosed) bacteria (to avoid non-ingested bacteria being counted as 'eaten but not killed').
- The appropriate ratio of bacteria to neutrophils (MOI - multiplicity of infection), as some strains at higher MOIs might induce neutrophil lysis or apoptosis (Yamamoto et al, 2002).
- Quantification of surviving intracellular bacteria was accurate and reproducible.

A schematic of the devised methodology is shown in Fig 3.1.

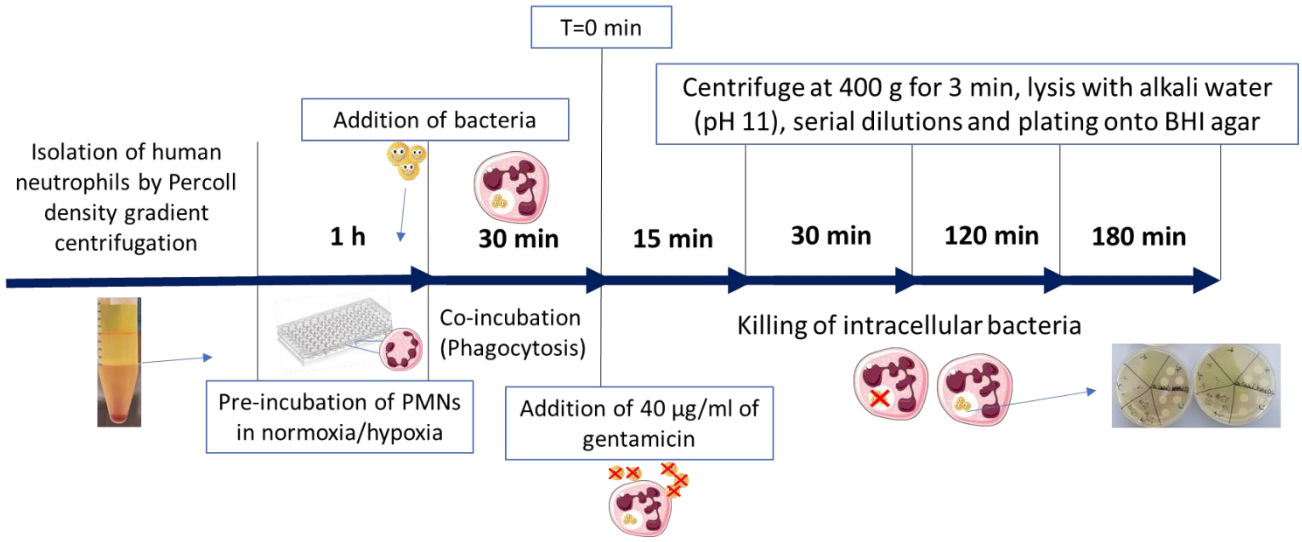

Figure 3.1 Schematic representation of killing assay to assess neutrophil-mediated killing of *S. aureus*

Graphical representation of the optimised methodology used to measure intracellular killing of S. aureus by freshly isolated human neutrophils re-suspended in RPMI/FBS/HEPES medium (pre-equilibrated in normoxia and hypoxia for 24 h). Once isolated, neutrophils were re-suspended in pre-equilibrated RPMI for 1 h in 96 well plates in parallel in normoxia (21% O2, 5% CO2) and hypoxia (0.8% O2, 5% CO2) prior to the addition of bacteria (MOI≈2). Following 30 min of co-incubation of neutrophils with bacteria to allow phagocytosis (designated as timepoint t=0 on all subsequent graphs using this method), 40 µg/mL of gentamicin was added to kill extracellular bacteria (including those adherent to cells but not internalised). At each indicated timepoint samples were transferred to Eppendorf tubes and spun at 400 g for 3 min. PMN pellets were lysed (alkaline water) extracts plated onto agar plates. The number of CFUs represent the number of surviving intracellular bacteria).

The **specific aims** of the work described in this chapter, and the methodology used to address them, are as follows:

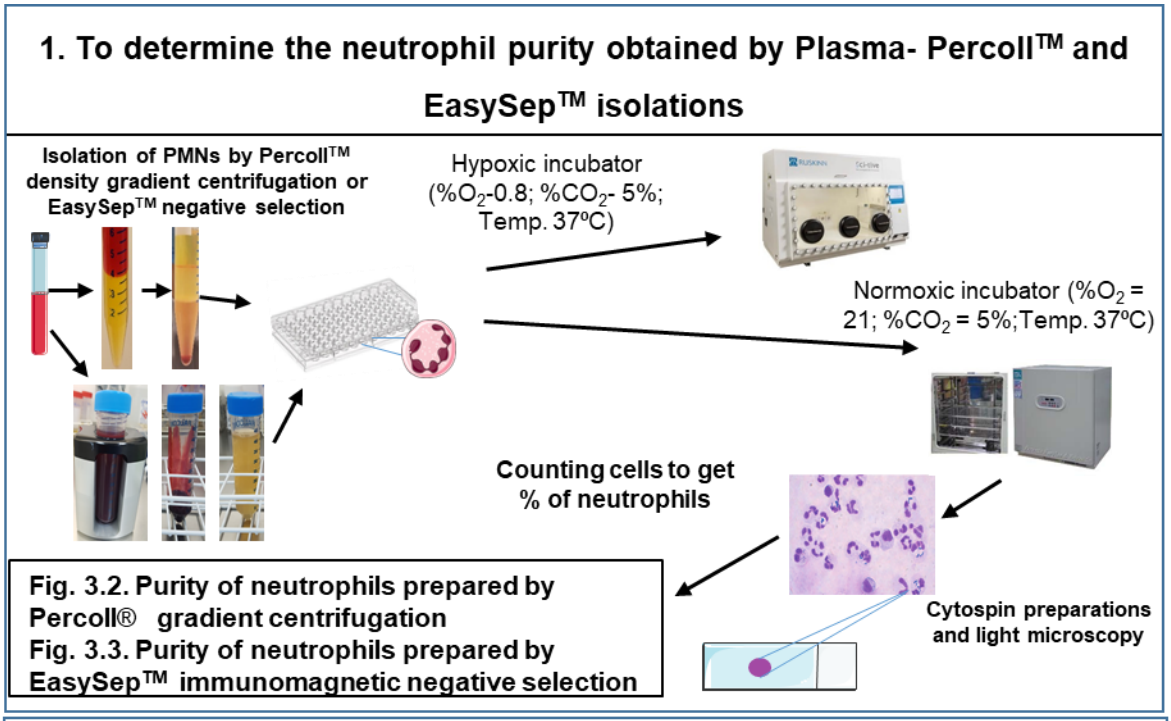

Fig. 3.2. Purity of neutrophils prepared by Percoll® gradient centrifugation
Fig. 3.3. Purity of neutrophils prepared by EasySep™ immunomagnetic negative selection

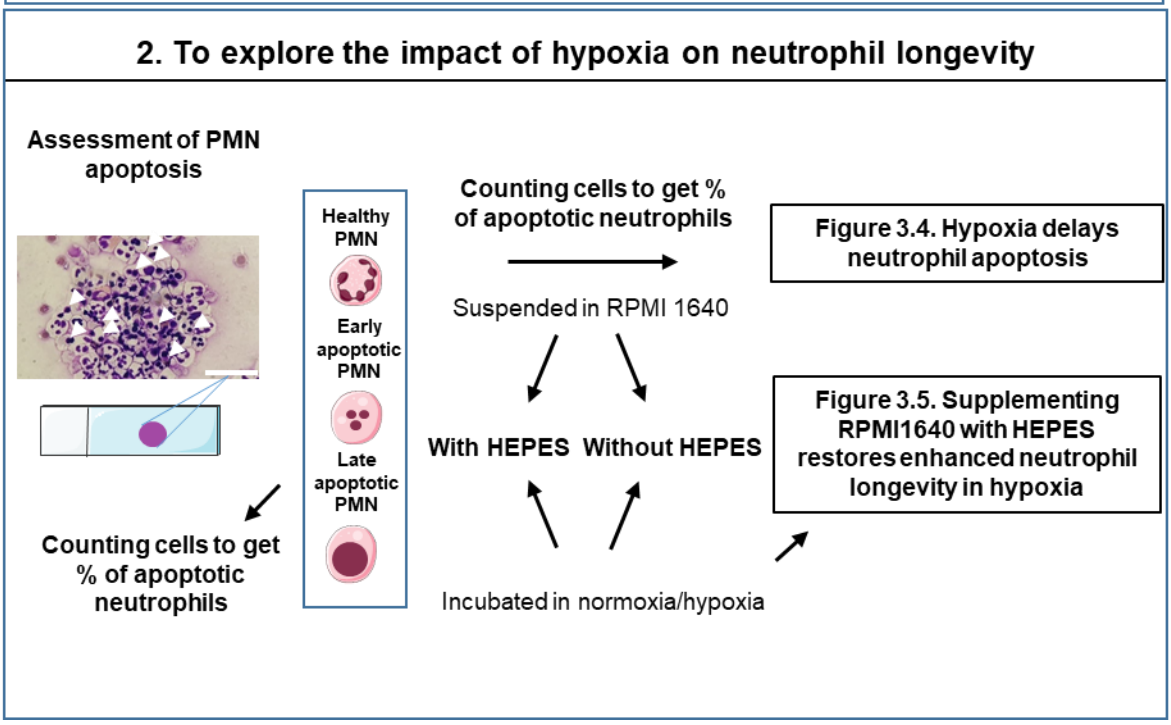

Figure 3.4. Hypoxia delays neutrophil apoptosis

Figure 3.5. Supplementing RPMI1640 with HEPES restores enhanced neutrophil longevity in hypoxia

3. To explore the impact of hypoxia on hypoxia-responsive gene regulation

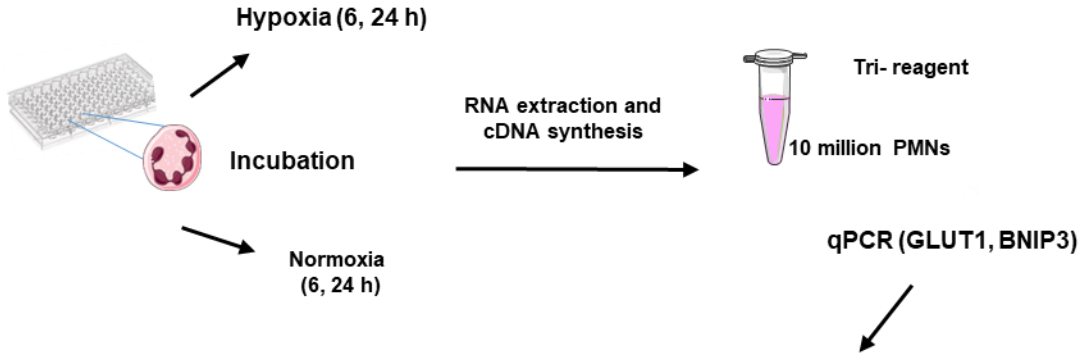

Figure 3.6. Upregulation of BNIP3 and GLUT1 genes in neutrophil response to hypoxia

4. To establish the effect of hypoxia on kinetics of growth of *S. aureus* MSSA (Wood46 and SH1000) and MRSA (JE2) strains in BHI and RPMI media

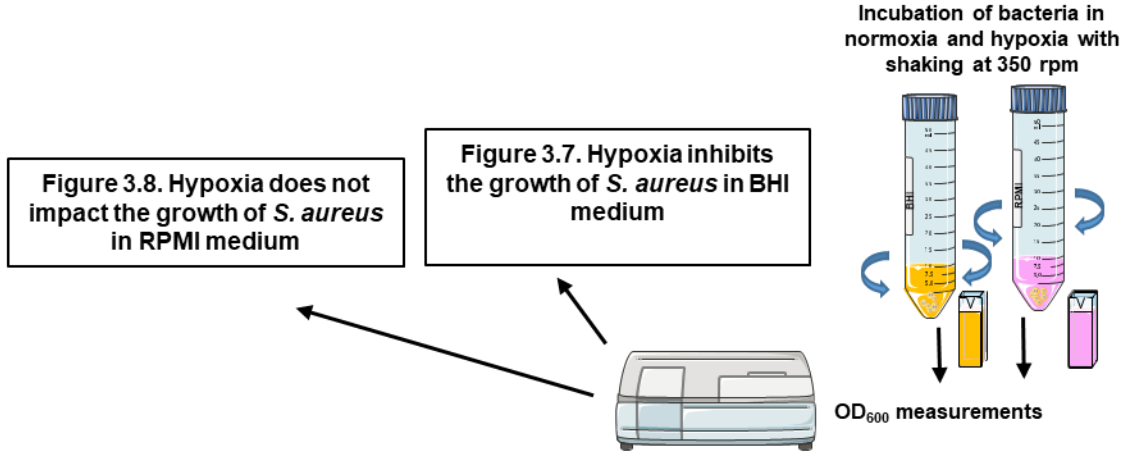

Figure 3.8. Hypoxia does not impact the growth of *S. aureus* in RPMI medium

Figure 3.7. Hypoxia inhibits the growth of *S. aureus* in BHI medium

5. To optimise antimicrobial agent to kill adherent/extracellular *S. aureus*

Lysostaphin (20 µg/ml)/Gentamicin (40 µg/ml)

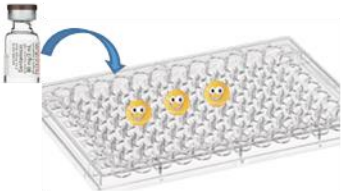

Treatment for 0, 20, 40 min

Plate onto BHI agar plates

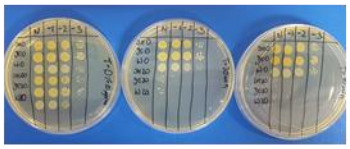

CFU counting

Figure 3.10. Gentamicin kills all tested staphylococcal strains

Figure 3.9. Lysostaphin kills Wood46 and SH1000 strains incompletely and does not effectively kill JE2

6. To explore the effects of hypoxia on neutrophil phagocytosis and killing propensity of MSSA and MRSA strains

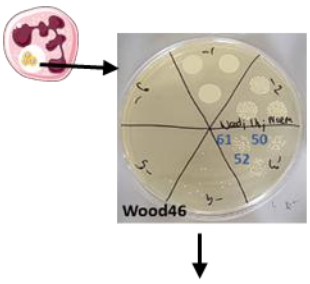

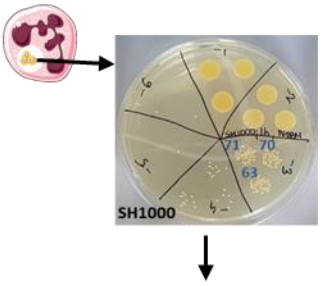

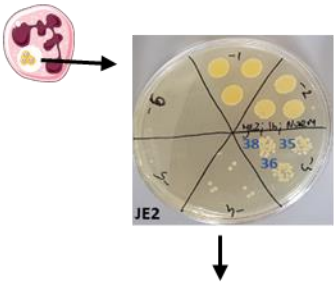

Figure 3.11. Hypoxia impairs neutrophil killing of *S.aureus* Wood46

Figure 3.12. Short- term and long- term hypoxia impairs killing of SH1000

Figure 3.13. Short term hypoxia has a little impact on killing JE2

7. To investigate the effect of hypoxia on ROS production

8. To determine effect of Hif1 alpha stabilisation and inhibition of protein synthesis

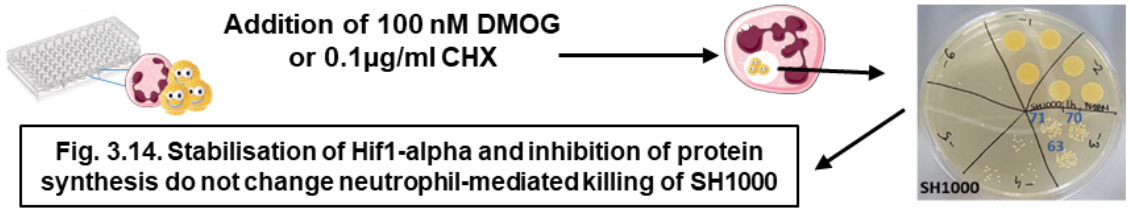

Fig. 3.14. Stabilisation of Hif1-alpha and inhibition of protein synthesis do not change neutrophil-mediated killing of SH1000

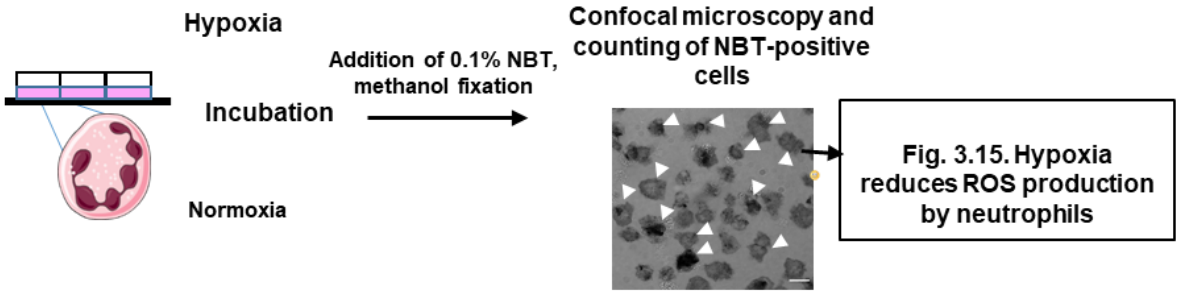

Fig. 3.15. Hypoxia reduces ROS production by neutrophils

3.1.1.1 Impact of hypoxia on neutrophil lifespan

In addition to establishing neutrophil purity, I wished to align the functionality of my isolated neutrophils to that reported in the literature. Hypoxia has been previously reported to delay neutrophil apoptosis (Hannah *et al.*, 1995; Walmsley *et al.*, 2005). I aimed to confirm that hypoxic conditions were maintained inside the hypoxic chamber, and to benchmark the magnitude of the hypoxic survival signal imparted in our newly installed hypoxic chamber with that reported in the literature. The above studies have shown that 0.8% environmental oxygen leads to an oxygen tension of 3 kPa in the culture media that bathes the cells and that this is sufficient to stabilise the transcription factor HIF. Neutrophils isolated as above were incubated at 37ºC in normoxia (21% O_2, 5% CO_2) or hypoxia (0.8% O_2, 5% CO_2) as described in Methods (see Sections 2.3.1. and 2.3.2.) for 6 h and 24 h in RPMI/FBS/1% P/S. At these timepoints, aliquots of cells were removed and immediately subjected to cytospin and Quick-Diff staining. The slides were coded so that the assessor was blinded to the experimental conditions. Around 300 cells from each condition were morphologically assessed and quantified for apoptotic phenotype (condensed, pyknotic nuclei, see Methods, Section 2.4.1) using a light microscope. The fields of quantification were selected randomly, excluding areas where the nuclear morphology could not be assessed due to clumping of cells. Data shown in Figure 3.4 were collected from three independent experiments using cells isolated from individual donors. A similar percentage of apoptotic neutrophils was seen following 6 h incubation in normoxia and hypoxia (9.87 ± 1.91% and 10.21 ± 4.76% SEM, respectively). However, after 24 h significantly fewer apoptotic cells were observed following hypoxic incubation (23.03 ± 1.862% SEM) than normoxic incubation (55.04 ± 8.08% SEM).

These initial results (the basal apoptosis rate in normoxia and the magnitude of the survival effect in hypoxia) are in agreement with previously published data and support the supposition that hypoxia is delivered at the appropriate level in a sustained fashion by the hypoxic chamber. However, in subsequent experiments using a new batch of RPMI/FBS, I noted that on prolonged incubation (24 h) in the hypoxic but not the normoxic environment, the media changed from pink to orange indicating a marked shift to a more acid pH (phenol red is incorporated as an indicator of pH) (Fig. 3.5.A).

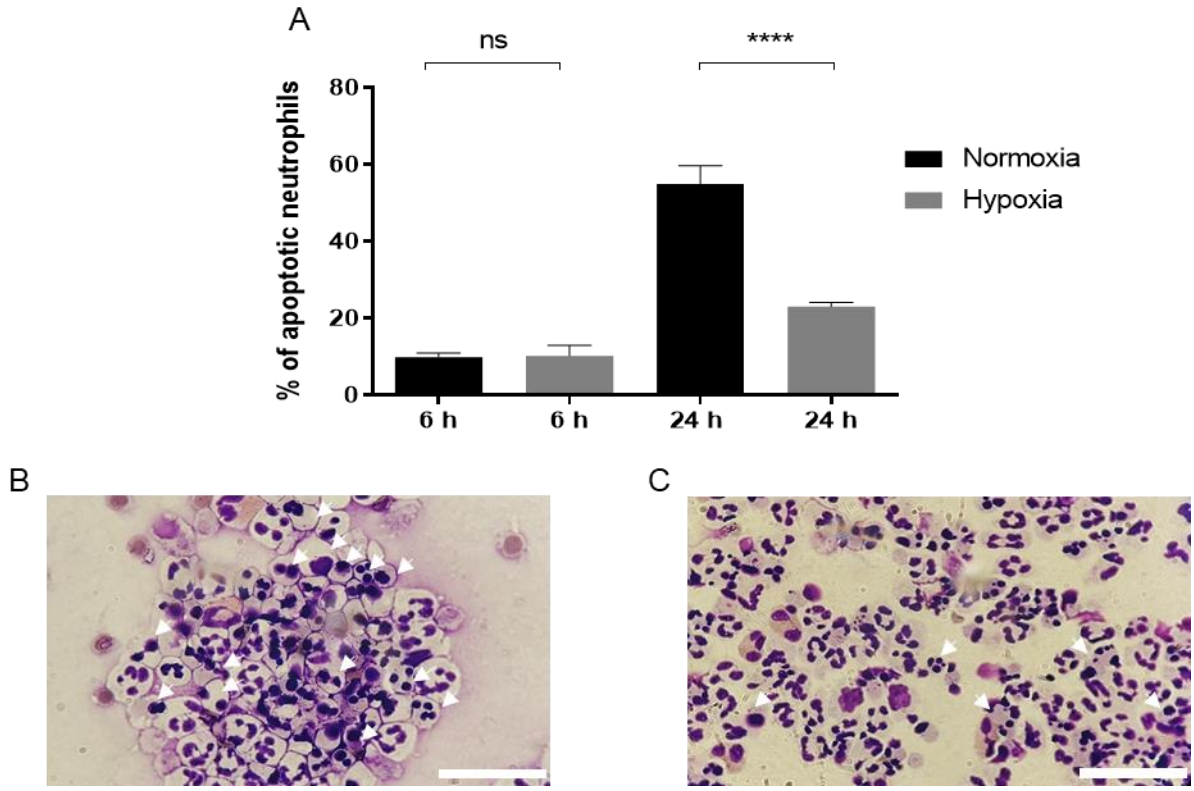

Figure 3.2 Hypoxia delays neutrophil apoptosis

***(A)**. Neutrophils were isolated by plasma-Percoll™ gradient centrifugation and incubated in RPMI 1640 supplemented with 10% FBS at 37ºC in normoxia (21% O_2, 5% CO_2) or hypoxia (0.8% O_2, 5% CO_2) for the indicated times prior to making cytospin preparations. Duplicate cytospins were Quick-Diff stained and approximately 300 neutrophils were counted for each condition and designated as having either apoptotic or non-apoptotic morphology. Data represent mean +/- SEM, n=3; ns p >0.05, **** p <0.0001 tested by one-way ANOVA with Sidak's Multiple Comparison Test. **(B, C).** Representative (of n=3 experiments) micrographs of neutrophils at 24 h in normoxia **(B)** and hypoxia **(C)** with white arrows indicating apoptotic cells. Scale bars, approximately 100 µm.*

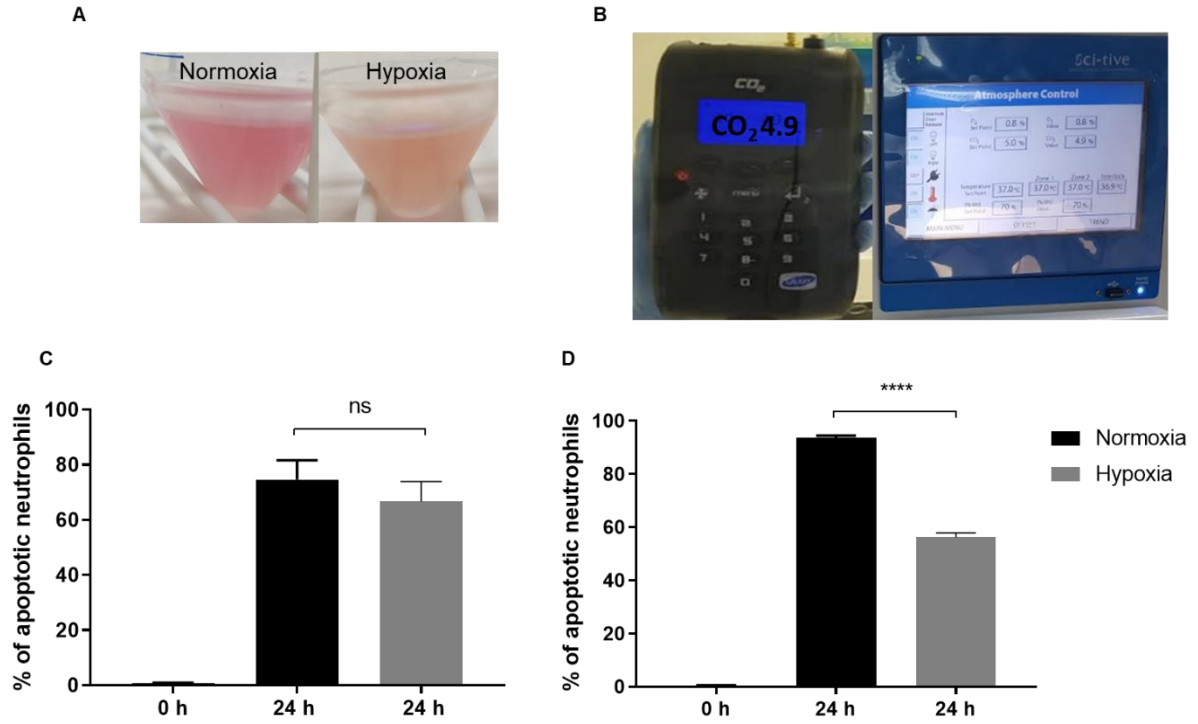

Figure 3.3 Supplementing RPMI 1640 with HEPES restores enhanced neutrophil longevity in hypoxia

*RPMI 1640 medium incubated alone at 37ºC in normoxia (21% O_2, 5% CO_2) or hypoxia (0.8 % O_2, 5% CO_2) for 24 hours **(A)**. CO_2 measurement inside the hypoxic workstation using Galaxy CO_2 Analyzer with accuracy ± 1% measuring range +2% of reading at reference points **(B)**. Neutrophils were resuspended in RPMI 1640 without (RPMI/FBS; **C)** and with 25 mM HEPES (RPMI/FBS/HEPES; **D)** and incubated at 37ºC in normoxia or hypoxia for the indicated times prior to making cytospin preparations. Cytospins were Quick-Diff stained and approximately 300 neutrophils were counted for each condition and assigned to either apoptotic or non-apoptotic morphology. Number of apoptotic PMNs presented as the % of all counted cells. Data represent mean +/- SEM, n=3; ns p >0.05, **** p <0.0001 normoxia vs. hypoxia at 24 h timepoint tested by unpaired t- test.*

A higher than anticipated CO_2 concentration would acidify the media. I confirmed that the embedded monitors within the hypoxic chamber which indicated satisfactory oxygen and carbon dioxide levels (Fig 3.5.B) were giving accurate readings using additional devices placed within the hood to measure the percentages of carbon dioxide and oxygen (not shown). Bacterial contamination of the hypoxic chamber that might induce media acidification and compromise the killing assay results was also excluded as a possible cause of by using sentinel agar plates left in the chamber for 24 h (no bacterial growth observed: not shown).

I then checked whether hypoxia still prolonged neutrophil longevity by repeating the apoptosis assays (Fig. 3.5.C). In direct contrast to my earlier results, when standard RPMI/FBS was used, no significant difference was observed in the percentage of apoptotic neutrophils isolated from three different donors at 24 h in normoxia compared with hypoxia. This likely related to the failure to maintain neutral pH in the hypoxic setting. Media containing HEPES (4-(2-hydroxyethyl)-1-piperazine-ethanesulfonic acid) provide better maintenance of physiological pH in cell culture, even if there are changes in carbon dioxide concentration (Baicu and Taylor, 2002). In the same study it was reported that hypoxia can lead to difficulty in preserving a stable pH in basic cell culture medium. Therefore, I investigated whether supplementing RPMI/FBS with 25 mM HEPES maintained the pH better; using this supplemented media, hypoxia again significantly reduced the percentage of apoptotic neutrophils in comparison to normoxia (Figure 3.5.D) as well as maintaining the pH as judged by the phenol red indicator (the media remained pink overnight in hypoxia and normoxia). These experiments suggested that some batches of standard RPMI1640 do not buffer hypoxic neutrophils sufficiently over 24 h and that batch variation may occur; future experiments were hence performed with RPMI/FBS with addition of 25 mM of HEPES (henceforth referred to as RPMI/FBS/HEPES).

These results demonstrate the importance of close monitoring of the relevant tissue culture media in the setting of hypoxia. Having developed a stable incubation system to maintain milieu that is identical except for the oxygen tension, I proceeded to further explore the impact of hypoxic incubation on neutrophils. To further confirm that I was indeed inducing stable and sustained hypoxia in the hypoxic chamber, I additionally investigated the ability of hypoxic incubation to induce the transcription of genes that are known to be targets of HIF.

3.1.1.2 Regulation of neutrophil gene expression by hypoxia

BCL2/adenovirus E1B 19 kDa- interacting protein 3 (BNIP3) gene is a member of the Bcl-2-family with pro-apoptotic/survival activity and has been shown to be significantly induced by hypoxia in several cell types (Guo *et al.*, 2001), including human peripheral neutrophils (McGovern *et al.*, 2011). Glucose transporter type 1 (GLUT1) also known as solute carrier family 2, facilitated glucose transporter member 1 (SLC2A1) was also reported to be upregulated upon hypoxic conditions in phagocytes (Cramer *et al.*, 2003). Stabilisation of HIF and induction of HIF-dependent transcripts is often used as a surrogate readout of hypoxic exposure. To confirm that hypoxic incubation conditions were sufficient to stabilise HIF-1α and hence upregulate HIF-dependent transcripts in neutrophils, the abundance of BNIP3 and GLUT1 mRNA was examined by qPCR of RNA isolated from cells cultured under normoxic and hypoxic incubation conditions. Neutrophils are terminally differentiated but remain transcriptionally active, although their RNA abundance is relatively low, and hence a substantial number of cells was required for RNA preparation.

qPCR was performed using RNA extracted from 5 x 10^6 of neutrophils incubated at 37ºC in parallel in normoxia (21% O_2, 5% CO_2) and hypoxia (0.8% O_2, 5% CO_2) for 6 and 24 h (Fig. 3.6). The cycle threshold of BNIP3 and GLUT1 was corrected to 18s ribosomal RNA reference gene (for details see Section 2.4.2). The expression of this housekeeping gene was constant over time and the different incubation conditions (data not shown). The relative gene expression obtained in hypoxia was compared to that in normoxia (Fig. 3.6.). Both genes were upregulated by hypoxia with substantially higher fold changes of BNIP3 (214.7 ± 83.9 SEM fold increase at 6 h; 81.6 ± 26.0 SEM fold increase at 24 h) in comparison to GLUT 1 (4.7 ± 1.9 SEM fold increase at 6 h; 4.2 ± 1.3 SEM fold increase at 24 h). Both genes showed a significant upregulation at 6 h; at 24 h the upregulation of BNIP3 was somewhat variable and hence did not reach statistical significance.

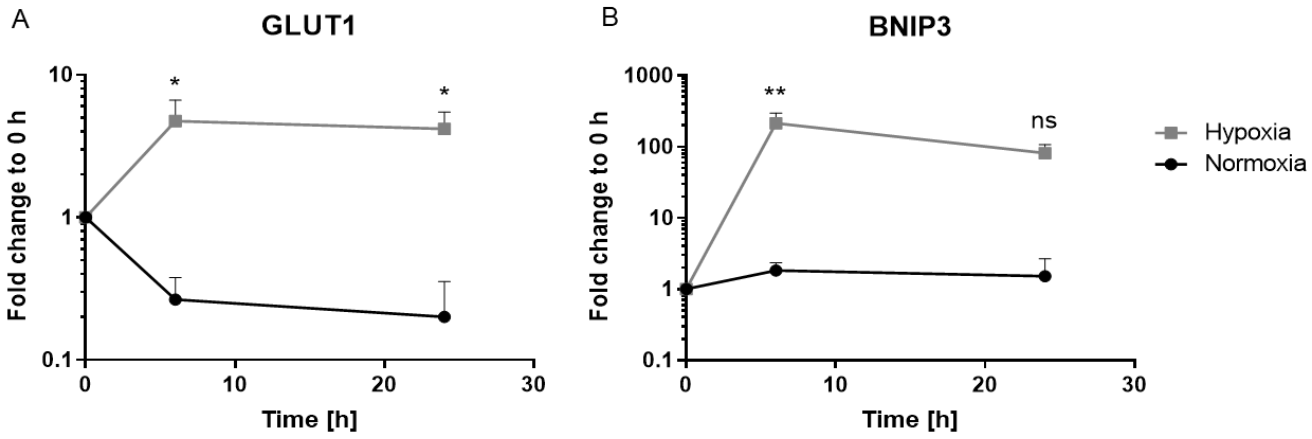

Figure 3.4 Upregulation of BNIP3 and GLUT1 genes in neutrophil response to hypoxia

RNA was extracted from neutrophils (5 x 10^6) incubated in parallel in normoxia (21% O_2, 5% CO_2,) and hypoxia (0.8% O_2, 5% CO_2, 37ºC) in RPMI/FBS for 6 and 24 h. The RNA was then converted to cDNA and the genes of interest quantified by qPCR. The relative gene expression (fold change) of GLUT1 ***(A)*** *and BNIP3* ***(B)*** *is expressed as $2^{-\Delta\Delta CT}$. Data represent mean +/- SEM, n=3; *p<0.05, **p<0.01 ns p= 0.41 normoxia versus hypoxia, one-way ANOVA with Sidak's multiple comparison test.*

The data presented above (reduced neutrophil apoptosis under conditions of hypoxia plus transcriptional up-regulation of hypoxic targets (Figs. 3.5. and 3.6.), together demonstrate that the hypoxic chamber delivers and maintains a level of hypoxia sufficient to lead to a sustained functional effect (prolongation of lifespan) and implies stabilisation of the transcription factor HIF-1α has occurred by 6 hours, in keeping with previously reported outcomes. My experiments aimed to explore the impact of a relatively brief hypoxic incubation on a functional effect previously shown likely to be HIF-independent (McGovern *et al.*, 2011). As I planned to examine the impact of hypoxia on host-pathogen interactions (and in particular on bacterial killing), it was also important to undertake an evaluation of the impact of hypoxia on bacterial growth kinetics; for example, if hypoxia attenuates staphylococcal replication rates, this might be interpreted as an increased ability to ingest or kill bacteria. In addition, this is an important biological effect relevant to the course of infection in a hypoxic setting. The impact of hypoxia on the growth kinetics of the selected bacterial strains was not known, and I therefore set out to quantify these parameters.

3.1.1.3 Effect of hypoxia on *S. aureus* growth in BHI medium

S. aureus is a facultative anaerobe and is able to adapt to low oxygen tensions, a response that is vital for its pathogenesis (Hajdamowicz *et al.*, 2019). BHI medium is a standard bacterial growth broth, which is nutrient-rich and optimised to support bacterial replication. Therefore, the three selected target staphylococcal strains (SH1000, JE2, Wood46) were grown in 10 mL of BHI, in normoxic and hypoxic incubation conditions for 24 h and the growth kinetics were assessed by serial readings of the culture optical density at 600nm (OD_{600}) of 900 µL of bacterial suspension.

From a starting OD_{600} ~ 0.05 at 0 h, in normoxia all strains grew rapidly, attaining the following ODs at 5 h: 7.0 ± 0.3 for SH1000, 6.4 ± 0.38 for JE2 and 5.3 ± 0.19 for Wood46 (±SEM). In contrast, the same strains cultured in parallel in the hypoxic chamber achieved statistically significant lower OD_{600} values in the same timeframe: 3.8 ± 0.29 SEM for SH1000, **p*= 0.01 in comparison with 5 h at normoxia, and 2.7 ± 0.19 SEM for both JE2 (**p*=0.01 compared to normoxia) and Wood46, **p*=0.02 in comparison with normoxia (Fig. 3.7). At 24 h, the differences in OD_{600} between normoxia and hypoxia were maintained or increased and were again statistically significant for all strains (****p*=0.0003 for JE2, ****p*=0.0007 for SH1000 and ***p*= 0.0014 for Wood46). It was therefore concluded that hypoxia inhibits growth of all tested staphylococcal strains in BHI media, a setting where nutrient supply is not limiting (it contains brain-heart infusion extract which includes essential amino acids and other growth factors). However, neutrophils are standardly cultured in precise chemical media such as RPMI that are LPS free, do not include nutrient-rich biological extracts, and are buffered in an attempt to avoid changes in pH. As I anticipated performing bacterial killing assays in RPMI/FBS rather than BHI, I therefore next studied the impact of hypoxia on bacterial growth in RPMI/FBS.

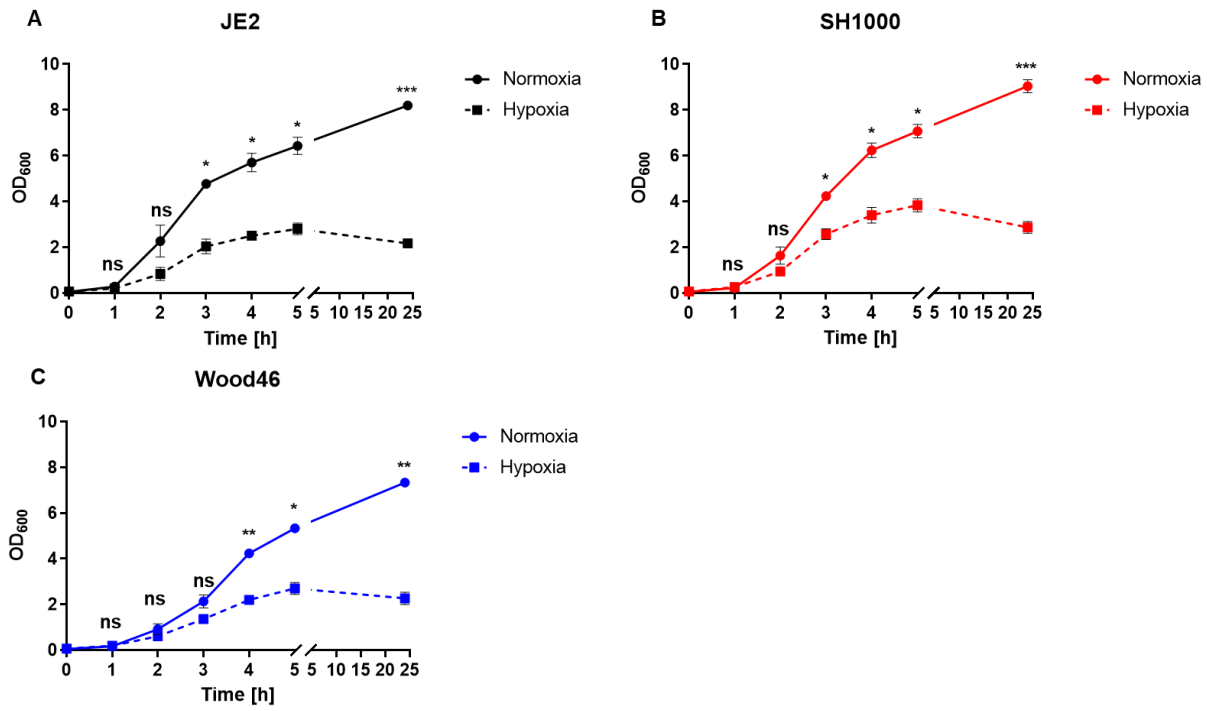

Figure 3.5 Hypoxia inhibits the growth of *S. aureus* in BHI medium

Strains of S. aureus JE2 ***(A)****, SH1000* ***(B)*** *and Wood46* ***(C)*** *were grown for 24 h in 10 mL BHI media at 37ºC, in a humidified 5% CO_2 environment with shaking in normoxia (21% O_2) or hypoxia (0.8% O_2) and OD_{600} was measured at 1, 2, 3, 4, 5 and 24 hours as indicated. Data represent mean +/- SEM, n=3. ns p >0.05, JE2: * p=0.03 for 3 h, *p=0.04 for 4 h, *p=0.01 for 5 h and ***p=0.0003 for 24 h; SH1000: *p=0.04 for 3 h, * p=0.02 for 4 h, * p=0.01 for 5 h and ***p=0.007 for 24 h; Wood46: **p=0.007 for 4 h, *p=0.02 for 5 h and **p=0.0014 for 24 h; tested by two-way ANOVA with Sidak's multiple comparison test.*

3.1.1.4 Effect of hypoxia on growth of *S. aureus* in RPMI 1640 medium

The aim of performing these experiments was to test the kinetics of staphylococcal growth in a eukaryotic cell culture medium, namely RPMI/FBS which is a standard media used to assess neutrophil function, for up to 3 hours (the timeframe planned for bacterial killing assays). The RPMI/FBS/HEPES medium supports cell culture, but the lack of additional nutrients may make it unlikely to be optimal for robust bacterial growth and hence it may impose limitations on bacterial growth.

SH1000, JE2 and Wood46 were grown in 10 mL of RPMI/FBS in normoxia and hypoxia. After 1, 2, and 3 h the OD_{600} for each sample was measured. Bacteria grew slowly to an $OD_{600} < 1$ after 3 h with no significant differences between hypoxia and normoxia (Fig. 3.8). Of note, all bacterial strains grew far more slowly in RPMI/FBS than in BHI broth. Although I did not assess later timepoints in this experiment, this has been undertaken by Rebecca Hull (PhD student, Condliffe group), who showed no difference in staphylococcal growth in RPMI between normoxia and hypoxia up to and including 24 h (personal communication, Rebecca Hull and Professor Alison Condliffe).

These results show that in assays involving a short-term incubation in RPMI/FBS, bacteria will not increase in number differentially under normoxia versus hypoxia sufficient to affect the experiment outcome. Additionally, it appears that nutrient lack restricts growth such that hypoxia is no longer a limiting factor; this likely replicates conditions at sites of infection and hence these conditions were adopted to further assess the host-pathogen interaction. In addition, it allowed me to compare normoxia and hypoxia without otherwise possible changes in number of bacteria. Frozen aliquots were prepared from bacteria grown in RPMI media at approximate OD_{600} of 0.7 for all of strains. These aliquots were tested for CFUs before freezing and when thawed and gave similar number of colonies on BHI agar, showing that freezing process does not kill bacteria (data not shown). In the following experiments frozen aliquots were used to ensure consistency with regards to bacterial preparation and numbers.

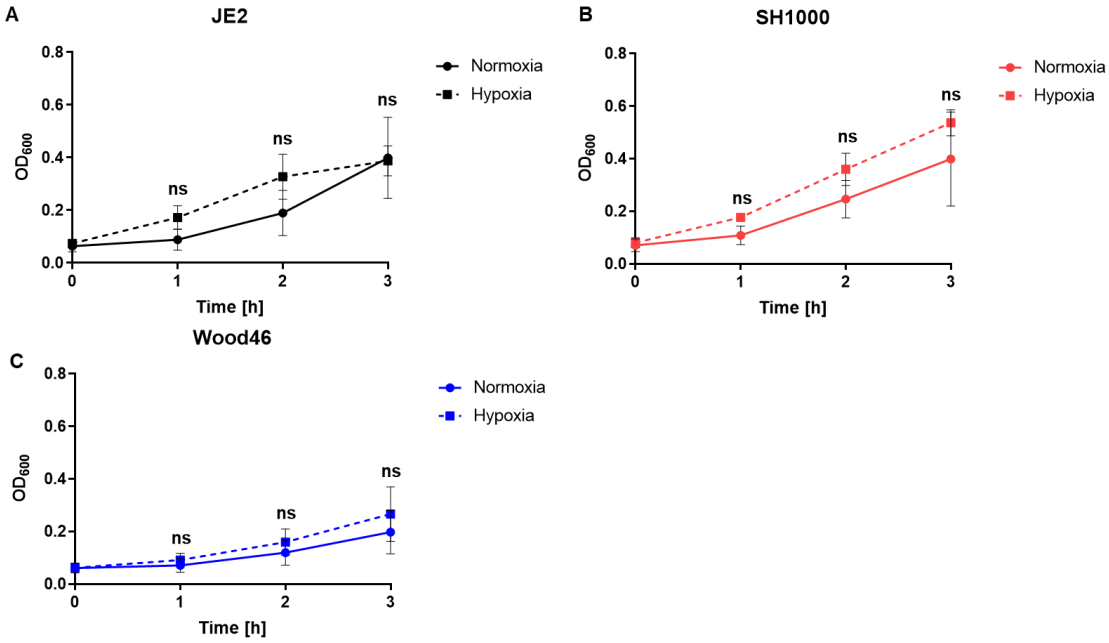

Figure 3.6 Hypoxia does not impact the growth of *S. aureus* strains in RPMI medium

*Strains of S. aureus JE2 (**A**), Wood46 **(B)** and SH1000 **(C)** were grown in 10 mL RPMI/FBS media at 37º, in a humidified 5% CO_2 environment with shaking and OD_{600} was determined at 1, 2 and 3 hours in normoxia (21% O2) and hypoxia (0.8% O2). Error bars represent SEM; n=3, ns p>0.05 OD normoxia versus hypoxia tested by one-way ANOVA with Sidak's multiple comparison test.*

3.1.1.5 Killing of *S. aureus* by lysostaphin

To quantify bacterial intracellular killing rather than phagocytosis or adherence of bacteria to cells, and in order to remove extracellular (non-adherent) and cell-adherent but non-ingested bacteria after co- incubation with neutrophils, an efficient antimicrobial agent has to be used. In addition to killing the majority of extracellular bacteria, the chosen agent should ideally not be incorporated into phagocytes, as this might allow ongoing microbicidal action against ingested organisms and hence confound results.

Lysostaphin, a bacteriolytic enzyme secreted by *Staphylococcus simulans,* has been shown to kill staphylococci by cleaving the pentaglycine bridges of its cell-wall (Schindler and Schuhardt, 1964). It has been also reported that lysostaphin is not toxic to phagocytes and does not enter those cells when used at low concentrations during short incubation period, and it has therefore been used in neutrophil killing assays previously (Easmon *et al.*, 1978). Frozen aliquots of bacteria that had been prepared in RPMI/FBS (see Section 2.5.4) were resuspended in fresh RPMI/FBS at 1 x 10^8 CFU/mL and 10 µL was added to 190 µL of 20 µg/mL of lysostaphin. This concentration has used by other researchers in our laboratory and elsewhere (e.g., Easmon *et al.*, 1978) and shown to be sufficient to kill extracellular staphylococci. The killing of staphylococci was determined after 20 and 40 min of incubation at 37°C by colony counting (Miles and Misra method, Section 2.5.2 in Materials and Methods). As can be seen in Figure 3.9, lysostaphin significantly reduced the number of Wood46 and SH1000 (about a thousand-fold) after 40 min, however approximately 10^4 viable bacteria could still be detected. Importantly, lysostaphin had no significant effect on the numbers of viable JE2 *S. aureus* detected (Fig.3.9.A), indicating that it was unable to kill this strain. There was no significant difference in bacterial killing for any strain between 20 and 40 min, suggesting that increasing the exposure time would not improve the microbicidal activity. A similar pattern was observed using higher concentration (40 µg/mL) of lysostaphin for the same times (data not shown). It was felt to be important to use the same antimicrobial compound able to effectively kill all strains to avoid a potential confounding variable when performing killing assays. I therefore tested an alternative antimicrobial agent, the antibiotic gentamicin, which is used in clinical practice to treat infections caused by *S. aureus*.

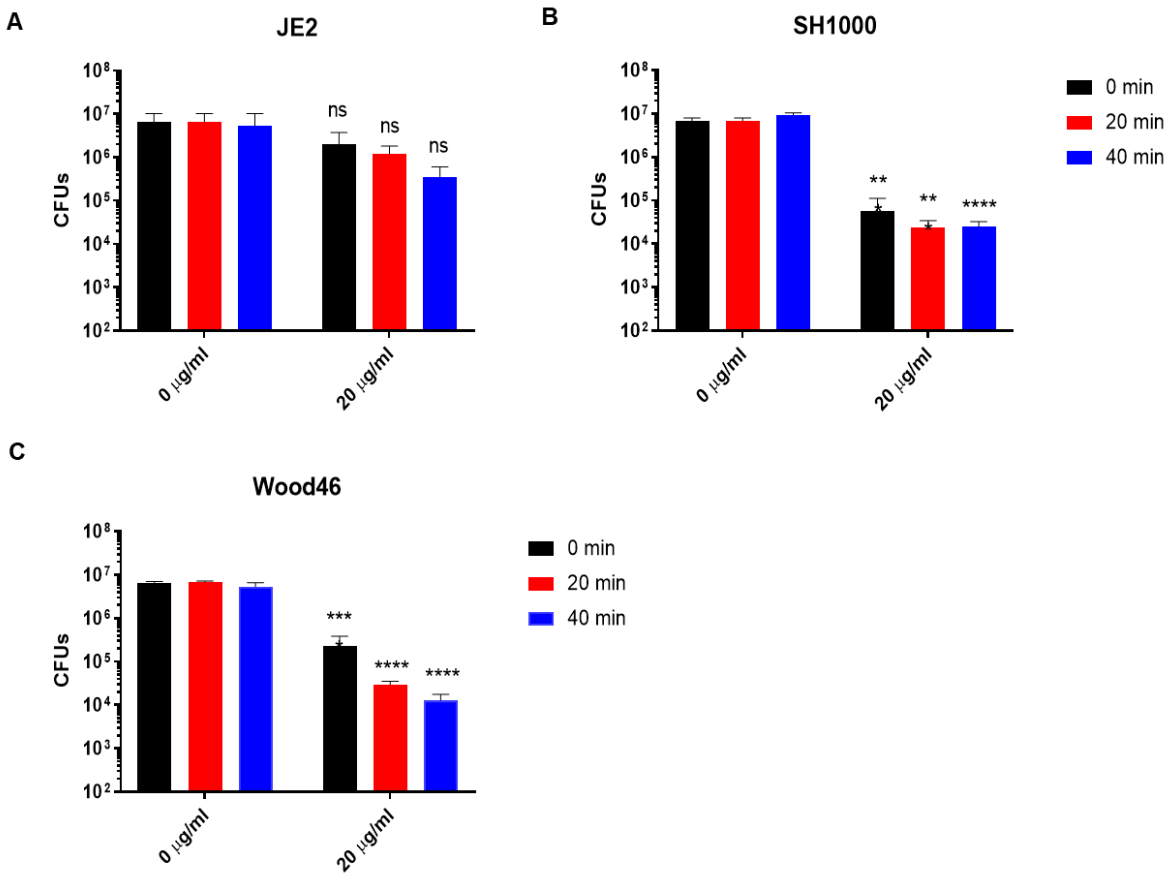

Figure 3.7 Lysostaphin kills Wood46 and SH1000 strains incompletely and does not effectively kill JE2

*10^6 CFU of **(A)** JE2 **(B)** SH1000 and **(C)** Wood46 were incubated with 20 µg/mL lysostaphin or vehicle control in RPMI/FBS medium for 0 min (black bars), 20 min (red bars) and 40 min (blue bars) to assess the ability of lysostaphin to kill bacteria, quantified by the Miles and Misra method. Data represent mean +/- SEM, n=3. ****p<0.0001, ***p<0.001, ns p>0.05 treated (20 µg/mL) versus vehicle control groups, one-way ANOVA with Sidak's multiple comparison test.*

3.1.1.6 Killing of *S. aureus* by gentamicin

Gentamicin is an aminoglycoside antibiotic which irreversibly binds the 30S subunit of the bacterial ribosome, and hence inhibits synthesis of bacterial proteins. It has been used in so-called 'protection' assays to kill non-phagocytosed bacteria during incubation with cells. Concerns have been raised that gentamicin may penetrate eukaryotic cells, and thereby influence intracellular bacterial survival, as reported in macrophages (Hamrick *et al.*, 2003). However, investigations have been undertaken as to whether gentamicin can enter PMNs and affect internalised bacteria, with compelling evidence that *S. aureus* internalised by neutrophils were not killed by gentamicin, even when the antibiotic was used at a very high external concentration (100 µg/mL) (Vaudaux and Waldvogel, 1979).

Using aliquots of Wood46, SH1000 and JE2 prepared in RPMI/FBS, bacteria were resuspended in fresh RPMI/FBS at 1 x 10^8 CFU/mL and 10 µL of bacteria was added to gentamicin (final concentration 40 µg/mL). Viable bacterial numbers were again quantified by using the Miles and Misra method after 20 and 40 min of incubation at 37°C. As shown in Figure 3.10, the number of bacteria of all strains including JE2 significantly decreased (to 10^3 or below) after 20 min of gentamicin treatment with a trend towards a further reduction in detected CFUs obtained after 40 min.

I next moved on to incorporate the use of gentamicin to kill extracellular but not intracellular bacteria in a killing assay.

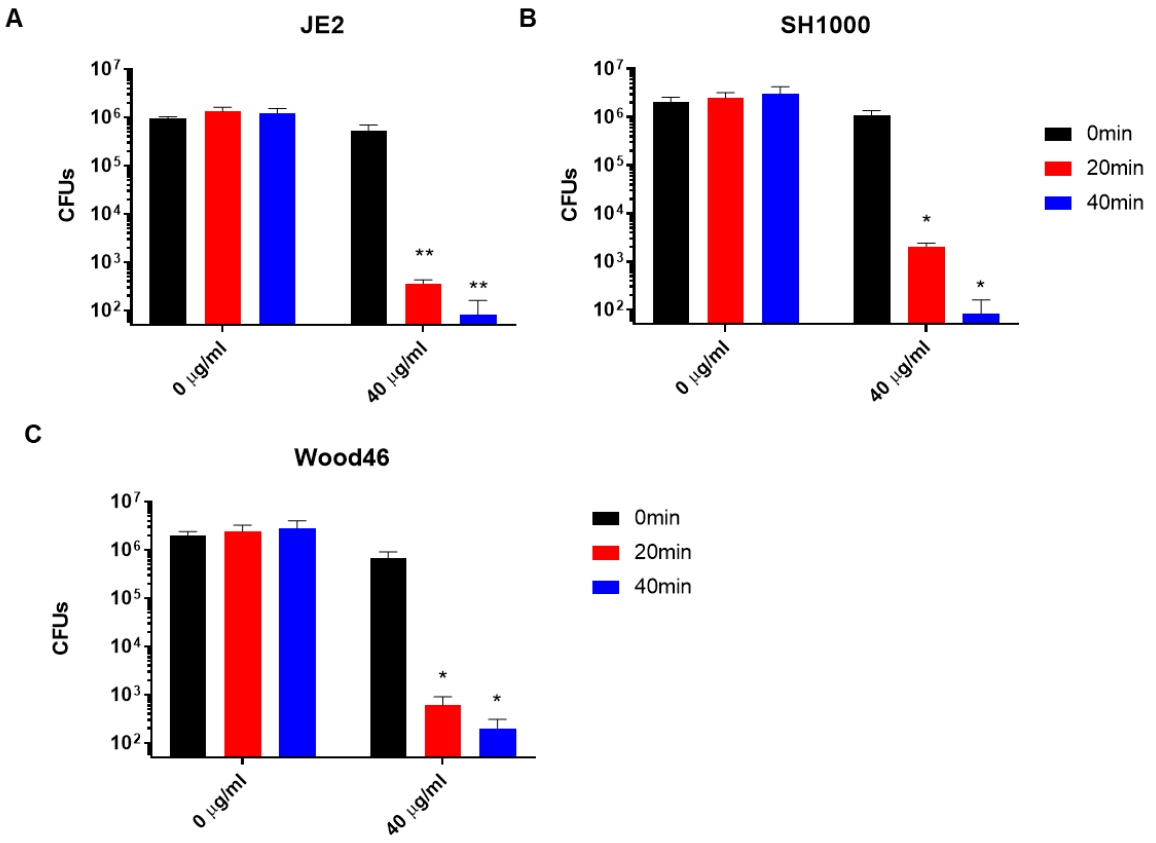

Figure 3.8 Gentamicin kills all tested staphylococcal strains

(A) *JE2* ***(B)*** *SH1000 and* ***(C)*** *Wood46 were added to 40 µg/mL gentamicin or vehicle control in RPMI/FBS medium and incubated for 0 min (black bars), 20 min (red bars) and 40 min (blue bars) to assess the ability to kill bacteria using the Miles and Misra method. Data represent mean +/- SEM, n=3. *p<0.05, **p<0.01 compared with non-treated groups (0 µg/mL), tested by one-way ANOVA with Sidak's multiple comparison test.*

3.1.1.7 Optimised gentamicin protection assay reveals impaired killing of *S. aureus* Wood46 by hypoxic human neutrophils

My initial attempts to undertake a gentamicin protection killing assay in normoxic versus hypoxic conditions yielded somewhat variable results (not shown), hence I had to make several changes to fully optimise the experimental protocol. Firstly, I extended an initial 1 h pre-equilibration period of media in the hypoxic chamber to 24 h to ensure the media (volumes of 100 µl placed in a 96 well plate) was fully hypoxic. As noted previously (see Fig. 3.5), some batches of standard RPMI did not preserve a neutral pH over longer incubation periods. Since this represented a potential experimental confounder, I adopted the use of RPMI supplemented with HEPES as noted above to remove this as a potential source of error.

Finally, I ensured that cells were not inadvertently re-oxygenated during processing. Initially I had removed neutrophils from the hypoxic chamber after co-incubation with bacteria to spin down the cells prior to lysis. Samples were thus exposed to normoxia for five to ten minutes before lysing with alkali water, a procedure also performed in normoxic environment. This could potentially lead to re-oxygenation of hypoxic cells, which might allow accelerated intracellular killing of bacteria. It has been shown that transferring hypoxic neutrophils to normoxia for 30 min restored bacterial killing, (McGovern et al, 2011), although shorter durations of re-oxygenation were not reported. A micro-centrifuge was therefore installed inside the hypoxic incubator so that all steps of the optimised assay up to plating on agar could be completed in the hypoxic conditions. Together these steps were felt to have ensured a more resilient and reliable assay.

I studied the kinetics of phagocytosis, aiming to identify a time at which sufficient bacteria had been ingested (but not killed), and to ensure that phagocytosis did not differ significantly between normoxia and hypoxia. Of note, I was unable to centrifuge the bacteria onto the neutrophils to expedite contact as the hypoxic chamber is not large enough to incorporate a plate spinner. I incubated Wood46 (4.5×10^5 CFU in 10 µL RPMI/FBS/HEPES) with freshly isolated neutrophils (2.25×10^5 /90 µL RPMI/FBS/HEPES), corresponding to MOI ~ 2 as described by McGovern *et al* (2011), for 15, 30, 45 and 60 min at 37˚C in normoxia (21% O_2, 5% CO_2) (Fig. 3.11.A). Neutrophils had ingested large numbers of added bacteria after 30 min, presented as

the $\log_{10}$ of intracellular bacterial CFU (3.76 $\log_{10}$ ± 0.003 $\log_{10}$ CFUs ± SEM), with little further ingestion apparent after this time (Fig.3.11.A), therefore 30 min was subsequently adopted to allow phagocytosis before the addition of gentamicin to kill any uningested organisms. The number of intracellular bacteria at this time (henceforth designated as time t=0) is an indication of the efficiency of phagocytosis. (Fritzenwanger *et al.*, 2011), previously noted increased neutrophil phagocytosis in the setting of hypoxia, but although I observed a trend towards increased phagocytosis in hypoxia compared to normoxia at time t=0 (i.e., after 30 min of neutrophil-bacterial interaction), this did not reach statistical significance, in agreement with McGovern (2011). Importantly, my results demonstrated that following 120 min of co-incubation neutrophils with Wood46, significantly more bacteria survived within hypoxic than normoxic neutrophils (224.7 ± 137 CFUs versus 3175 ± 1514 of CFUs; n=4, Fig.3.11.B), indicating a significant killing deficit in hypoxia. Light microscopy of cytospin preparations at 60 min of co-incubation under normoxia (Fig. 3.11.C) and hypoxia (Fig. 3.11.D) confirmed that neutrophils had indeed ingested staphylococci, and phagocytes containing bacteria appeared fully intact with normal morphology.

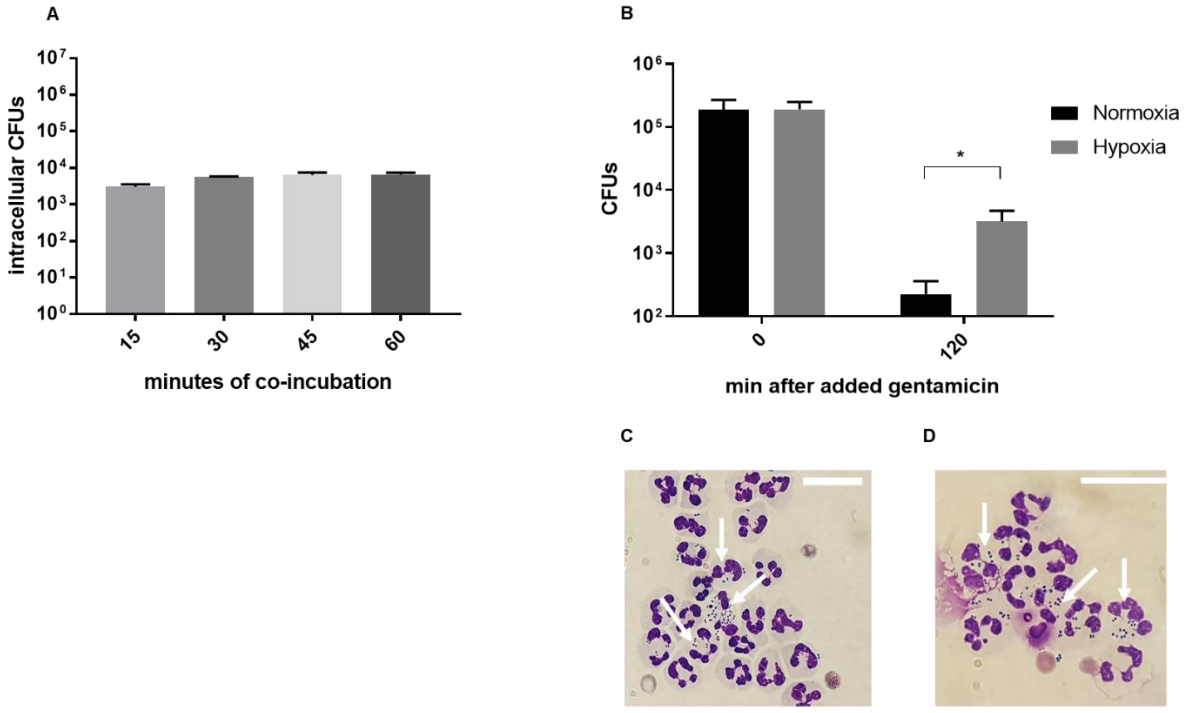

Figure 3.9 Hypoxia impairs neutrophil killing of *S. aureus* Wood46

***(A)**. Phagocytosis of S. aureus Wood46. Bacteria (MOI~2) were co-incubated with freshly isolated neutrophils (2.25 x 10^5 cells/90 µL) in normoxia (21% O_2). Samples were centrifuged to remove free bacteria. Neutrophils were lysed with alkali water after 15, 30, 45 and 60 min of co-incubation. Data represent mean ± SEM of n=2 for log10 of phagocytosed bacteria analysed by Miles and Misra CFUs of intracellularly surviving bacteria **(B).** Neutrophils (2.25 x 10^5 /90 µL) freshly isolated by Percoll gradient centrifugation were re-suspended in medium pre-equilibrated in normoxia (21% O_2) or hypoxia (0.8 % O_2). Then neutrophils were pre-incubated for 1 h before addition of Wood46 (MOI ~ 2). Gentamicin at 40 µg/mL was used after 30 min to kill extracellular bacteria and intracellular killing was measured after 120 mins of co-incubation using the Miles and Misra method. Samples were spun down at the given environments and lysed with alkali water. Data represent mean ± SEM of n=4 experiments. *p=0.029 normoxia vs. hypoxia for 120 min, Mann-Whitney test. **(B, C).** Representative micrographs of cytospin preparations of neutrophils and Wood46 after 60 min of infection in normoxia **(C)** and hypoxia **(D)**, white arrows indicating intracellular bacteria within neutrophils. Scale bars represent approx. 100 µm.*

3.1.1.8 Hypoxia impairs killing of *S. aureus* SH1000 by neutrophils

I next employed the optimised gentamicin protection killing assay to assess intracellular killing of strains of *S. aureus* other than Wood46. For the first time, killing of the MSSA- SH1000 strain by hypoxic PMNs was explored. Freshly isolated neutrophils were suspended in pre-equilibrated normoxic and hypoxic RPMI/FBS/HEPES and were pre-incubated in normoxia (21% O_2, 5% CO_2) and hypoxia (0.8 % O_2, 5% CO_2) for 1 h prior to addition of SH1000 at MOI 5 (based on our laboratories' previous experience with this organism). In addition to assessing killing at 180 min (SH1000 are more robust that Wood46), killing was also assessed at a much later (24 h) timepoint, to explore whether the impact of hypoxia might be to enable longer-term survival of intracellular bacteria. I also assessed the morphology of neutrophils by cytospin to ensure that intact cells were present and to assess if surviving bacteria were retained within the neutrophil.

As for Wood46, there was a non-significant trend towards increased phagocytosis of SH1000 by PMNs in hypoxia compared to normoxia, inferred from the values at time t=0, Figure 3.12.A. As for the Wood46 strain, at 180 min there was a significant increase of *S. aureus* SH1000 surviving inside hypoxic neutrophils compared to viable bacteria within normoxic cells (1271 ± 197.8 *versus* 1316407 ± 554625 CFUs ± SEM respectively; n=6). At 24 h, no viable bacteria were detected in normoxic neutrophil-bacterial co-cultures, but large numbers were present in the equivalent hypoxic co-incubations as shown in Figure 3.12.D; (16.50 ± 5.05 *versus* 3800000 ± 967000 CFUs ± SEM respectively; n=5). Numbers of bacteria detected at 180 min and 24 h in hypoxia were near identical, perhaps suggesting no further killing had occurred over this extended time course. Cytospin preparations performed after 180 min and 24 h co-incubation of neutrophils and SH1000 are presented (Fig.3.12.B, E for normoxia and Fig.3.12.C, F for hypoxia). Viable neutrophils were seen in each condition with internalised bacteria; some neutrophils had ingested large numbers. There appeared to be more viable neutrophils at 24 h following hypoxic incubation, as anticipated.

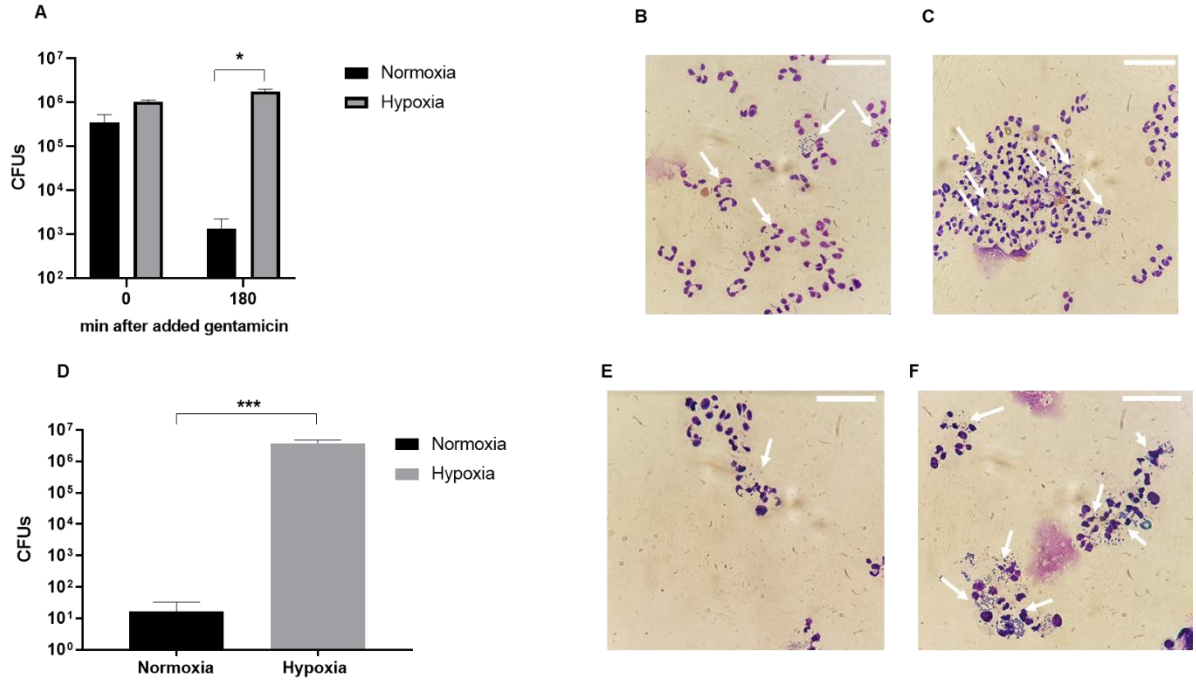

Figure 3.10 Short-term and long-term hypoxia impairs killing of SH1000

***(A)**. Gentamicin protection assay of S. aureus SH1000. Freshly isolated neutrophils (2.25 x 10^5 cells/90 µL) were incubated simultaneously in normoxia (21% O_2) and hypoxia (0.8 % O_2) for 1 h prior to addition of SH1000 (MOI 5) with gentamicin added after 30 min of co-incubation (0 min timepoint in panel A). Samples were spun down in indicated environments and lysed with alkaline water. Bacteria were quantified by Miles Misra method. Data represent mean ± SEM of n=6 experiments, presented as CFUs of intracellular bacteria; * p=0.0260 tested by Mann-Whitney test normoxia vs. hypoxia for 180 min **(B, C).** Representative cytospin preparations of neutrophils after 180 min of infection in normoxia **(B)** and hypoxia **(C)** white arrows indicate neutrophils with intracellular bacteria. Scale bars representing approx. 100 µM. **(D).** 24 h gentamicin protection killing assay. Freshly isolated neutrophils (2.25 x 10^5 cells/90 µL) were incubated simultaneously in normoxia (21% O_2) and hypoxia (0.8 % O_2) for 1 h prior to addition of SH1000 (MOI 2-4) with gentamicin added after 30 min of co-incubation. Samples were spun down in indicated environments at 24h and lysed with alkaline water. Bacteria were quantified by Miles Misra. Data represent mean ± SEM of n=5 experiments, presented as CFUs of intracellular bacteria; *** p=0.0006 tested by Mann-Whitney test normoxia vs. hypoxia for 24 h. **(E, F).** Representative cytospin preparations of neutrophils after 24 h of infection in normoxia **(E)** and hypoxia **(F)** with white arrows indicating neutrophils with ingested bacteria.*

3.1.1.9 Killing of JE2 by normoxic and hypoxic neutrophils is equivalent

The next aim was to test the effect of hypoxia on neutrophil- mediated killing of *S. aureus* JE2, as an example of an MRSA strain.

Briefly, freshly isolated neutrophils at 2.25 x 10^5 cells in 90 µL of RPMI/FBS/HEPES per well were pre-incubated for 1 h prior to the addition of JE2 at ~1.35 x 10^6 CFU/10 µL (~5 MOI, based on previous work conducted in the Foster laboratory) in normoxia (21% O_2, 5% CO_2) and hypoxia (0.8 % O_2, 5% CO_2). An optimised gentamicin protection/killing assay was undertaken as previously described to measure intracellular killing of bacterial cells at 60 and 180 min.

The majority of bacteria were phagocytosed by both normoxic and hypoxic neutrophils, with significantly fewer staphylococci recovered at time t=0 in hypoxia 290000 ± 55076 CFUs ± SEM than in normoxia 892335 ± 99540 CFUs ± SEM ***p= 0.0012*. (Fig.3.13.). This indicates that JE2 was killed in greater number by 30 min (t=0) by hypoxic than normoxic neutrophils. Unexpectedly, the killing of internalised JE2 was similar between normoxic and hypoxic environments at 180 min. Thus overall, the killing of JE2 by hypoxic neutrophils is if anything slightly accelerated but reaches a similar level to that achieved by normoxic neutrophils after 180 min.

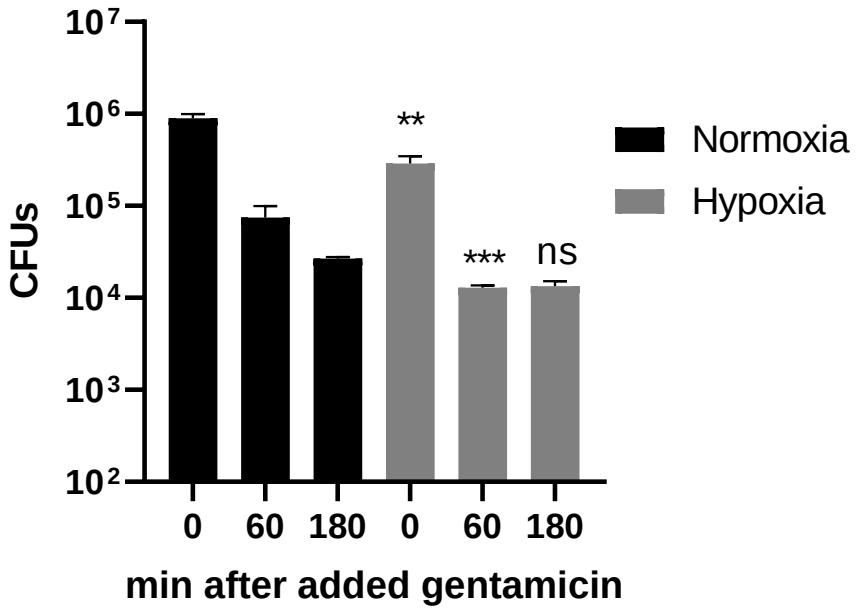

Figure 3.11 Short-term hypoxia has a little impact on killing JE2

*Gentamicin protection killing assay of ingested S. aureus JE2. Human neutrophils (2.25 x 10^5 cells/ 90 µL) were incubated simultaneously in normoxia (21% O_2) and hypoxia (0.8 % O_2), prior to the addition of S. aureus JE2 (MOI~5). Gentamicin was added after 30 min of co-incubation (0 min timepoint). Samples were spun down at the indicated times in normoxia or hypoxia and lysed with alkaline water. Bacteria were quantified by Miles Misra. Data represent mean ± SEM of n=3 experiments, presented as CFUs of intracellular bacteria; **p= 0.0012 0 min normoxia vs hypoxia, ***p= 0.0005 60 min normoxia vs hypoxia; ns p= 0.5 180 min normoxia vs hypoxia.*

3.1.1.10 Effect of pharmacological HIF stabilisation and inhibition of protein synthesis on neutrophil- mediated killing of S. aureus SH1000 upon normoxia and hypoxia

Hypoxia may influence cells directly by limited oxygen availability, but most of its effects are mediated by the HIF transcription factors and hence require HIF stabilisation and subsequent downstream transcriptional/protein synthetic events. Although killing assays are performed over a relatively brief time course, HIF-dependent transcription is readily apparent at 6h of hypoxic incubation (Figure 3.5). I therefore probed the HIF-dependency of the impaired hypoxic killing of *S. aureus* by pharmacological stabilisation of HIF (with Dimethyloxallyl Glycine (DMOG), a cell permeable, competitive inhibitor of prolyl hydroxylase) and the protein synthesis inhibitor cycloheximide (CHX). These experiments were performed after the COVID-19 pandemic lockdown and due to limitations accessing sufficient donors we used negative magnetic bead selection to isolate neutrophils from low volume blood draws. Neutrophils isolated by EasySep^{TM} negative selection (Materials and Methods Section 2.2.2) were re-suspended in normoxic or hypoxic RPMI/FBS/HEPES media at 2.5 x 10^6 /90 µL into 96 well plates with 100 nM DMOG or 1 µg/mL cycloheximide (CHX) or appropriate vehicle controls for 1 h preincubation before adding bacteria *S. aureus* SH1000 at MOI 5. After 30 min (timepoint 0), 40 µg/mL gentamicin was added to kill extracellular bacteria. Intracellular killing was measured at 180 min for DMOG in normoxia and 180/240 min for CHX in normoxia and hypoxia. DMOG did not affect phagocytosis (intracellular bacteria detected at 30 min prior to addition of gentamicin) with 1520458 ± 136266 CFUs ± SEM for vehicle control cells in normoxia compared to 1446833 ± 187084 CFUs ± SEM normoxia in the presence of DMOG. Importantly, no significant differences were found in intracellular bacteria recovery at 180 min between normoxic and DMOG treated cells (26205 ± 13739 CFUs ± SEM versus 27496 ± 6597 CFUs ± SEM), however as expected there were significantly fewer bacteria at 180 min for both groups in comparison with the number of bacteria at 30 min (Fig.3.14. A).

Likewise, the protein synthesis inhibitor CHX, used at concentrations previously optimised for neutrophils in our laboratory, had no impact on the phagocytosis process or killing at any tested timepoints between normoxia and hypoxia (Fig 3.14. B).

The results presented above suggest that stabilisation of the transcription factor HIFα using DMOG (a ‘hypoxia mimetic’ which stabilises HIF but does not restrict oxygen availability), or inhibition of protein synthesis by CHX (which would block events mediated by HIF-dependent transcription) does not impact on killing of *S. aureus*. Hence, impairment of killing of *S. aureus* is likely HIF-independent and due to the lack of molecular oxygen available to fuel the oxidative burst.

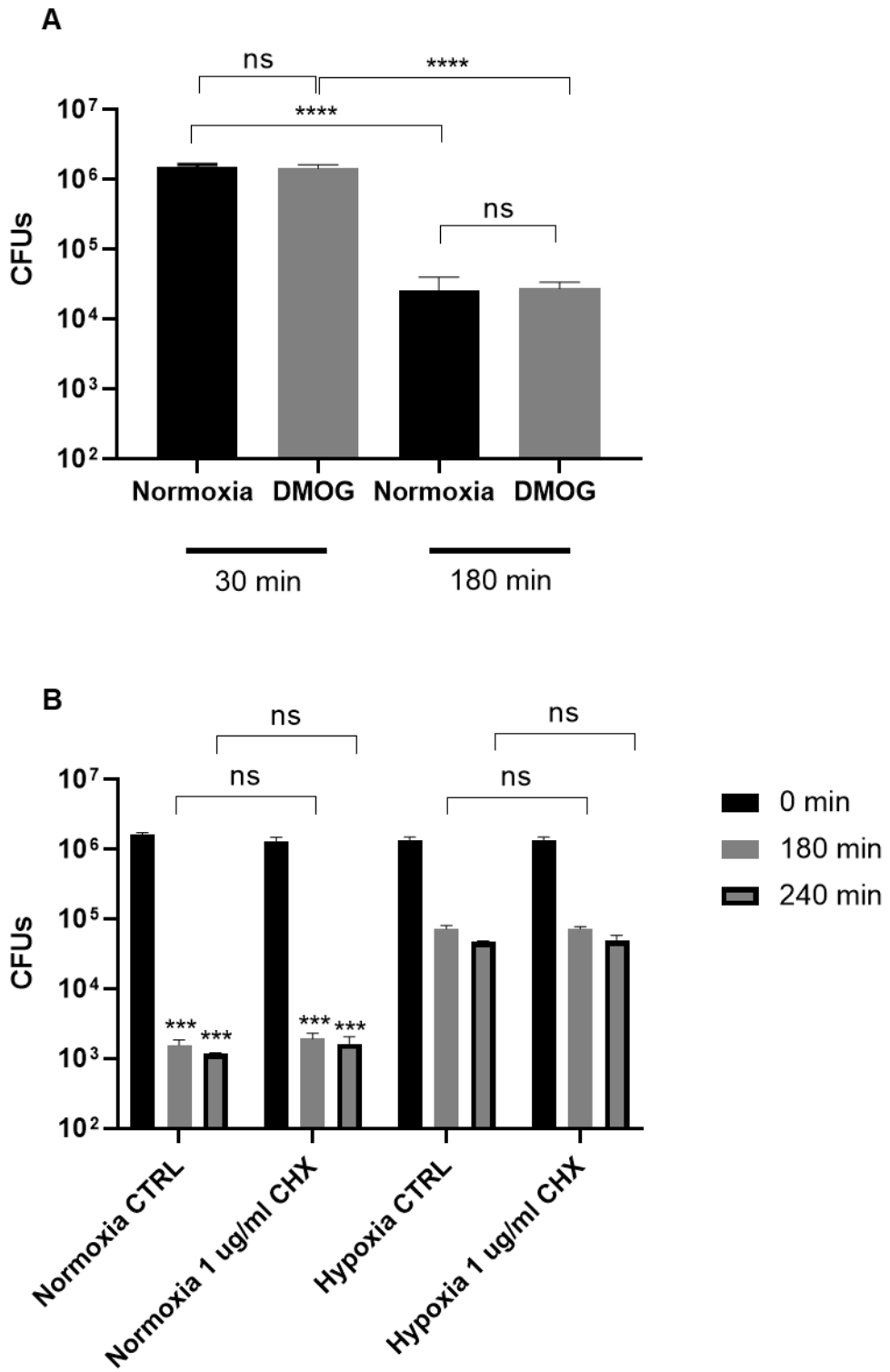

Figure 3.12 Stabilisation of Hif1-alpha and inhibition of protein synthesis do not change neutrophil-mediated killing of SH1000

(A) *Human neutrophils (2.25 x 10^5 cells/ 90 µL) were pre-incubated for 1 hour with 100 µM dimethyloxalylglycine (DMOG) before addition of SH1000 at MOI 5 under normoxic conditions* ***(B)*** *Human neutrophils (2.25 x 10^5 cells/ 90 µL) were resuspended in hypoxic or normoxic*

media and pre-incubated for 1 hour in normoxia or hypoxia with 1 µg/mL cycloheximide (CHX) before adding SH1000 at MOI 5. For all conditions, gentamicin at 40 µg/mL was then added after 30 minutes of co-incubation, and intracellular killing was determined at 180 and (for CHX) 240 minutes by lysing neutrophils, serially diluting lysates, and plating for Miles and Misra analysis. Data represent mean ± SEM of n=3 ***(A)*** *and n=4* ***(B)*** *experiments, presented as CFUs of intracellular bacteria. Analysis by One-way ANOVA with Sidak's multiple comparisons test ns p> 0.05, ****p< 0.0001* ***(A)*** *and by Two-way ANOVA with Tukey's multiple comparisons test ns p>0.05, ***p=0.0001 Normoxia CTRL and Normoxia 1 µg/mL CHX vs Hypoxia CTRL and Hypoxia 1 µg/mL CHX* ***(B)****.*

3.1.1.11 Hypoxia limits intracellular ROS production in human neutrophils

It is challenging to measure intracellular ROS production in the hypoxic workstation as it cannot easily accommodate devices such as microscopes or a flow cytometer to measure ROS in live cells using fluorescent indicators, therefore I used a compound called nitro-blue tetrazolium chloride (NBT) to detect reactive oxygen species. NBT is reduced to diformazan, a dark blue insoluble precipitate, visible under a microscope (see Section 2.7.3. in Materials and Methods). This reaction detects predominantly superoxide radical formation by neutrophils.

Freshly isolated neutrophils were resuspended in normoxic or hypoxic RPMI/FBS/HEPES media and placed onto 8-well glass bottom Ibidi chamber to pre-incubate for 1 h in normoxia and hypoxia in parallel. After this time, bacteria (mCherry-SH1000, 1.12 x 10^6 CFU (MOI 5)) were added and co-incubated for a further 1 h. Afterwards cells were subjected to 0.1 % NBT for 15 min, washed in 1x DPBS and fixed (100 % methanol); all of these steps were undertaken in the hypoxic hood in parallel with standard oxygen conditions. Samples were subsequently imaged using a spinning disk confocal microscope at 60 x oil immersion magnification with the observer blinded to the experimental condition. Formazan precipitates were illuminated by transmission of white light (bright-field channel), therefore contrast in the sample is caused by attenuation of the light by the dense formazan (Fig. 3.15.B, C). Cells containing dark stained areas were classed as ROS positive and were expressed as the percentage of overall number of cells present in the field of view in normoxia and hypoxia. Changes in percentage of positive cells counted in normoxia were compared with those cells in hypoxia from three independent experiments and presented in the Fig.3.15.A. There were significantly fewer NBT positive cells in hypoxia in comparison with normoxia (29.37% to 69.62%, respectively).

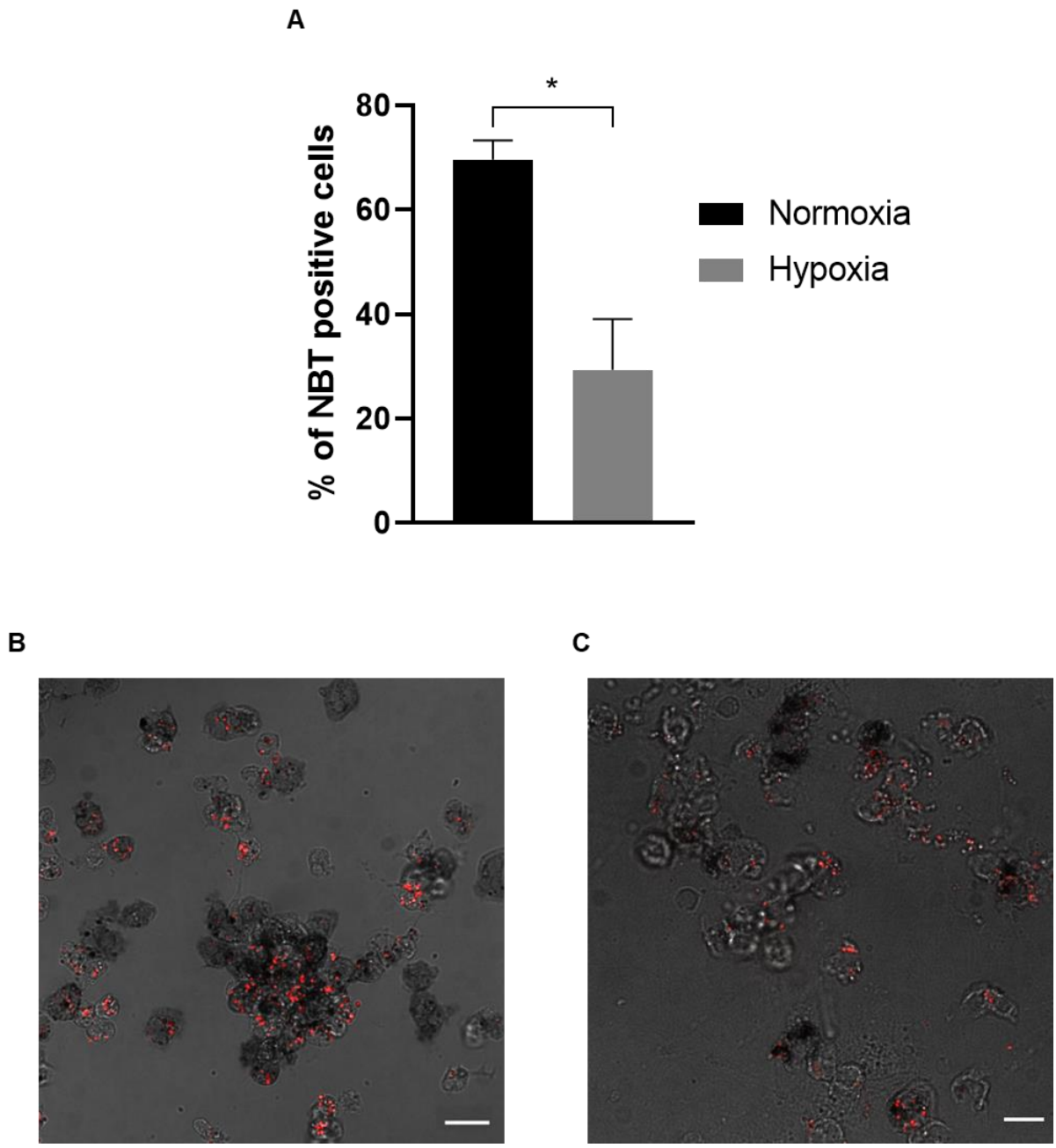

Figure 3.13 Hypoxia reduces ROS production by neutrophils

(A) *2.25x10^6/180 µL neutrophils where incubated 1 hour in IBIDI plates in normoxia and hypoxia, before addition of mCherry-SH1000 at MOI 5. After 1 hour of co-incubation, the 0.1% of NBT was used to stain ROS for 15 min to quantify the percentage of positive cells, which were fixed in methanol. Representative images of cells co-incubated in normoxia* ***(B)*** *and hypoxia* ***(C)*** *with darkly stained areas within neutrophils (reduced NBT to formazan precipitates). Data represent mean ± SEM of n=3 experiments, presented as % of all cells present in the field of view; *p= 0.018 normoxia vs hypoxia. Scale bars represent 10 µM.*

3.1 Discussion

The wide range of infections attributable to *S. aureus* cause substantial morbidity and mortality. Their treatment has become more challenging with the emergence of multidrug resistant strains, such as methicillin resistant *S. aureus* (MRSA), which remains a major cause of hospital-acquired infection globally. Due to the evolution of antibiotic resistance driven by antibiotic use in healthcare and the agricultural industry, there is a global need for the development of alternative therapeutic strategies. Consequently, a deeper understanding of the host-pathogen interface is essential. Exploring the mechanisms underlying host killing of microbes or its failure may inform new treatment strategies for recalcitrant infections, by targeting host cell functions supporting bacterial growth or permitting/augmenting bactericidal functions.

The overarching aim of the work described in this chapter was to explore the interactions between *S. aureus* and human neutrophils under hypoxic conditions, optimising the methodology to assess the ability of neutrophils to kill various strains of *S. aureus* in a hypoxic environment that more accurately mimics *in vivo* infection. Most studies on phagocytic and bactericidal function of human neutrophils have been undertaken in ambient oxygen (Hampton *et al.*, 1994; Lu *et al.*, 2014), whereas analysis of oxygen tensions during infection have shown such areas to be hypoxic, in some situations profoundly hypoxic and even anoxic (Simmen and Blaser, 1993; Wilde *et al.*, 2015). Both neutrophils and bacteria are known to adapt to hypoxia, but little is known about how this affects the outcome of their interactions and in particular whether bacteria can be effectively killed by hypoxic neutrophils. I have shown here that hypoxia significantly reduces the intracellular production of ROS by human neutrophils that have ingested prey, which could explain impairment in killing of *S. aureus* by those cells. This process seems to be HIF-independent, as evidenced by failure to recapitulate by pharmacological stabilisation of HIF (Fig.3.14.A) or by failure to reverse by inhibiting protein synthesis (Fig.3.14.B).

My project relies on the isolation of human neutrophils from healthy donors. In the initial experiments I performed, the plasma/Percoll® density isolation method yielded initially approximately 90% pure neutrophils (Fig. 2.4) which is slightly less pure than published literature (e.g., Haslett *et al.*, 1985), although most subsequent experiments had yields of 95% purity or greater. The contaminating cells observed in the PMN preparation were predominantly eosinophils with a low percentage of monocytes

(<1%), as expected. Monocytes should be separated from neutrophils by Percoll® gradients as their lack of granularity imparts a lower density, but eosinophils are of a similar granularity and hence not separated from neutrophils in this way and the percentage contamination reflects their abundance in the donor's blood. The higher number of eosinophils could be due to seasonal variations - more of these cells were present in blood during spring and summer months, but also reflect differences between donors (Kuhns *et al.*, 2015; Liu and Taioli, 2015), for example atopic individuals have higher circulating eosinophil counts. To reduce eosinophil contamination, positive selection by anti CD16-coupled magnetic beads can be used (CD16 is highly expressed on neutrophils but not on eosinophils, (Parker *et al.*, 2009); however, such methods are expensive, time-consuming (undesirable given the short neutrophil lifespan) and binding to the beads might affect neutrophil function or cause their unwanted activation. Eosinophils can ingest and kill bacteria, but they respond differently in hypoxia compared to neutrophils (Porter *et al.*, 2017). On pragmatic grounds, PMN preparations with eosinophil contamination ≥ 10% were discarded and not used in my assays.

Negative selection methods e.g., EasySep™ Direct Human Neutrophil Isolation Kit that employs antibody/magnetic bead depletion of all other white cell populations avoid many of mentioned above technical problems, but the associated cost and inability to operate on a large scale was initially felt to preclude their routine use. We changed to this method following the COVID pandemic as we had a very restricted pool of donors able to attend the laboratory, requiring us to make frequent low volume bleeds to perform enough experiments. We also noted that post-pandemic, neutrophils obtained by Percoll® density gradient often yielded activated neutrophils; we did change all of our preparative reagents including citrate, Percoll® and dextran, with no improvement. Several of our donors had previously experienced SarsCoV2 infection, and that even though there were clinically well, we speculate their neutrophils were susceptible to activation by the repeated centrifugation steps or a reagent in the isolation procedure. These issues were circumvented using the EasySep™ negative selection method. Prepared neutrophils are at approximately 95% with a small number of monocytes (~5%) as the only other contaminating blood cells (Fig.2.5). All preparations made using this method yielded fully functional, healthy, responsive and basal neutrophils. Of note, the PMNs obtained using this method would include so-called 'low density'

neutrophils (LDNs), which would be absent from populations isolated by density gradient centrifugation. Whilst some authors have suggested that such LDNs are immature or activated in the setting of diseases such as COVID19 (e.g., Morrissey *et al.*, 2021), others have found that LDNs are very similar in functionality to normal density neutrophils (Hardisty *et al.*, 2021) and that differences detected by other authors are specific to the diseases they were investigating. Since if anything the neutrophils obtained by negative selection were more quiescent than those from density gradients, we incline to the latter view. Of note, the results obtained in the killing assays aligned precisely to those I had previously obtained with the Percoll® methodology, with equivalent killing of *S. aureus* in the same timeframe.

The widespread use of fetal bovine serum for cell-culture has often raised concerns. One concern is that FBS serum in culture media causes exposure of cells of none-bovine origin to xenogeneic proteins which could affect several functions of the cells (Bahar Bilgen *et al.*, 2008). Moreover, the variability in composition of FBS from batch to batch may cause not reproducible results (Baker, 2016). In the study of Alipour *et al*., it has been shown that replacing the 10% FBS with equivalent of autologous plasma (which may also contain a wider range individually different mediators) has led to prolongation of neutrophil lifespan after several hours of incubation (>12 h) (Alipour *et al.*, 2020). The use of the same batch of FBS throughout studies avoided this source of variation. In the majority of assays, neutrophils were not incubated for longer than 4 hours (microscopy and gentamicin-protection assays), however I did confirm that the lifespan of neutrophils in normoxia and hypoxia, measured by myself are in line to those in the literature to that similar percentage of normoxic and hypoxic neutrophils survivals with use of same percentage of added FBS (McGovern *et al.*, 2011), but also studies that have used autologous plasma (Hannah *et al.*, 1995).

Using a hypoxic chamber has enabled me to study the impact of reduced oxygen tensions on neutrophils and bacteria separately and on bacterial-neutrophil interactions, recapitulating conditions relevant to infected tissues (McGovern *et al.*, 2011; Thompson *et al.*, 2017). The Ruskinn Sci-tive hypoxic workstation measures the gas composition (pO_2 and pCO_2) maintained inside the air in the chamber, not in the media which are incubated in these conditions. Equilibration of the media with the hypoxic environment will take time depending on the liquid volume and surface area. Our laboratory does not possess a blood gas analyser and attempts to transport

samples to distant blood gas analysers in the Sheffield Teaching Hospitals NHS Trust were unsuccessful, due to re-oxygenation of media samples during transport (Dr Ben Durham, Research Technician, Department of Infection, Immunity and Cardiovascular Disease, personal communication). Media parameters from samples incubated in a Ruskinn incubator using identical settings to those in this study have previously been measured using a blood gas analyser to ensure that media are at an appropriate level of hypoxia (McGovern *et al.*, 2011). However, the hypoxic workstation was newly installed in our laboratory, and I therefore wished to validate that it delivers the desired and effective level of hypoxia. Neutrophils undergo constitutive apoptosis limiting their lifespan, which is a vital process in homeostasis (Atallah *et al.*, 2012) and in the resolution of inflammation *in vivo* (Elks *et al.*, 2011). Previous *in vitro* studies have shown that hypoxia (an oxygen tension of 3 kPa in the media, achieved by equilibration in 0.8% atmospheric oxygen) substantially delays neutrophil apoptosis at 20 hours (Hannah *et al.*, 1995; Walmsley *et al.*, 2005). I therefore quantified neutrophil apoptosis under these conditions. My data (Fig. 3.4) are in full agreement with those published in the literature, showing a significantly decreased number of apoptotic neutrophils at 24 h upon hypoxic incubation. I also showed upregulation of the HIF-target genes BNIP3 and GLUT1(Guo *et al.*, 2001; Cramer *et al.*, 2003; McGovern *et al.*, 2011). Hypoxic transcriptional responses (largely mediated via the HIF pathway, with hypoxia stabilising HIF to enable it to exert transcriptional activity) induced chemically or genetically have been shown to delay the resolution of inflammation by prolongation of neutrophil lifespan and increased neutrophil retention at the inflamed site in zebrafish (Elks *et al.*, 2011). However, transcriptional responses take time to evolve, and hypoxia has more rapid, HIF-independent effects on neutrophil function. For example, hypoxia limits the neutrophil oxidative burst (McGovern *et al.*, 2011) and promotes degranulation (Hoenderdos *et al.*, 2016) in a HIF-independent fashion. I have also shown that there is significantly reduced ROS production by hypoxic neutrophils, the effect that can be mimicked by use of chemical inhibitors (explored in the next Chapter). These changes in neutrophil function occur rapidly in response to oxygen deprivation, as they do not require transcription and translation of new proteins. Neutrophils newly arriving at a hypoxic infection site will not have stabilised HIF for sufficient time to enact changes dependent on HIF-mediated transcriptional activity, and I wanted to explore the impact of short-term hypoxia on bacterial killing.

The relatively short timeframe of the pre-incubation (60 min) and assay time (a further 180-240 min) makes it likely the defect in killing is independent of HIF, which must be stabilised and initiate transcription/translation to exert its effects. This approach also helps to mitigate the potential confounding issues of increased neutrophil survival in hypoxia and the risk that staphylococcal virulence factors might lyse neutrophils. The exception to this is the effect of more prolonged (24 h) hypoxia, which resulted in substantial intracellular survival of *S. aureus* SH1000 (Fig. 3.12.B), further discussed below.

Hypoxia may also affect bacterial properties (Hajdamowicz *et al.*, 2019). Although some previous studies have examined the effect of hypoxia on neutrophils, relatively little is known about how hypoxia might affect staphylococcal growth, virulence factor production and other properties relevant to pathogenicity. *S. aureus* is a facultative anaerobe, and gene expression in response to the switch from aerobic to completely anaerobic conditions has been broadly investigated. Under depleted oxygen conditions, higher expression of genes belonging to the functional categories of glycolysis, fermentation and anaerobic respiration have been observed (Fuchs *et al.*, 2007). The expression of virulence factors by *S. aureus* has been demonstrated to be regulated by the staphylococcal respiratory response AB (SrrAB) two-component system, which in low oxygen tension down-regulates production of *agr* RNAIII, protein A and toxic shock syndrome toxin 1 (TSST-1) (Yarwood *et al.*, 2001). These findings indicate that anoxia (rather than hypoxia) has a negative impact on bacterial metabolism and pathogenicity. The slower growth of staphylococci in hypoxic culture in nutrient-rich medium (Fig. 3.7) that I observed is consistent with this work and that of Ferreira *et al.*, 2013, but the latter examined only a single bacterial strain in a chemically defined medium that is not widely used. Hence it was important for me to establish the impact of the levels of hypoxia that I would routinely use on staphylococcal growth. I therefore assessed bacterial growth in this medium under conditions of normoxia and hypoxia; growth was much slower than in BHI but was equivalent in the different oxygen tension environments (Fig.3.8). RPMI is a synthetic medium commonly used to culture cells and provides a relatively pH-controlled environment in stable CO_2 conditions by bicarbonate buffering. Although as noted in Figure 3.5, the buffering in standard RPMI may not be sufficient at least in longer-term experiments and so I used additional HEPES supplementation to ensure stable pH. It

has a fixed chemical composition and is far less nutrient-rich than conventional BHI medium (see Section 2.1.1 for full composition of media). My results therefore suggest that when growth is not limited by nutrient availability, hypoxia is a restraining factor, however when nutrients are limiting, hypoxia does not further compromise growth. Hence differential bacterial growth should not have confounded comparisons of killing in the different oxygen environments.

The growth restriction suggests that switching to RPMI might re-programme staphylococcal gene expression and functional responses, hence I grew bacteria in RPMI prior to freezing stocks for future sub-culture in RPMI. Using RPMI for bacterial pre-cultivation before adding to cell suspension should avoid the need for rapid bacterial adaptations to a drastically changed nutritional supply, and hence minimise the induction of bacterial stress response. It has previously been demonstrated that growth of *S. aureus* is reproducible in RPMI and that this medium is suitable for laboratory growth experiments to study metabolic pathways (Dorries and Lalk, 2013) or iron acquisition (Sheldon *et al.*, 2014). The level of growth of *S. aureus* in RPMI medium that I observed in my experiments is similar to that reported by Dorries and Lalk and Sheldon *et al*. Of note, my observations that hypoxia impaired bacterial growth in this way underpinned a further PhD studentship currently being undertaken by Ms Rebecca Hull to study the ability of hypoxia to promote the evolution of staphylococcal resistance to innate immune killing.

Whilst the timeframe of my experiment and the MOIs chosen mean that the majority of added bacteria are internalised, minor differences in phagocytic capacity have been reported between normoxic and hypoxic neutrophils, and this was consistent with my observation of a trend to hypoxia-enhanced phagocytosis, although I did not find it to be a significant effect. However, differential rates of ongoing phagocytosis and/or extracellular killing might confound results. In order to determine the intracellular neutrophil killing capacity, *in vitro,* it is thus important to eliminate extracellular bacteria in the suspension to distinguish intracellular killing from ongoing active phagocytosis. This can be done by using an effective antimicrobial agent, ideally one which does not penetrate the eukaryotic cells and can effectively all the strains used in this study. Lysostaphin, the anti-staphylococcal endopeptidase, has been widely used in PMN killing assays in order to remove cell-adherent and extracellular bacteria and shown not to enter these cells (Easmon *et al.*, 1978). I found that lysostaphin applied directly

against bacteria in the absence of neutrophils significantly reduced the number of Wood46 and SH1000 but had no bactericidal effect on the JE2 strain (Fig. 3.9). Resistance of MRSA to this enzyme has in fact been previously reported (Kusuma *et al.*, 2007). Even with Wood46 and SH1000, killing of *S. aureus* was incomplete, despite increasing the lysostaphin concentration, increasing the exposure time and sourcing from different manufacturers. A more effective antimicrobial was therefore felt to be required. Gentamicin killed all strains of *S. aureus* effectively, although there were a small number of residual CFUs (Fig. 3.10). It has been previously demonstrated that gentamicin does not accumulate to a significant degree within human neutrophils (Prokesch and Hand, 1982). The aminoglycosides exhibit limited passive diffusion through the eukaryotic cell membrane due to their large size and negative charge. Their uptake by eukaryotic cells is largely by active pinocytosis, which results in accumulation only after quite prolonged drug exposure (Tulkens, 1990). Thus, gentamicin should not kill intracellular bacteria or affect neutrophil-mediated killing, hence this antibiotic was adopted for use in a gentamicin protection assay.

Using the optimised gentamicin-protection assay protocol I have confirmed short-term hypoxia relevant to infected sites does indeed compromise the ability of neutrophils to kill the MSSA strains Wood46 and SH1000. Importantly, for the first time I have also shown that after a more prolonged (24 h) of co-incubation neutrophils with SH1000 abundant viable bacteria were recovered from hypoxic neutrophils, in comparison to completely eradicated bacteria in normoxia. Cytospins demonstrated the presence of bacteria within largely non-apoptotic neutrophils in hypoxic culture, whilst neutrophils cultured in standard normoxic conditions were mostly apoptotic and contained few visible bacteria which most likely were dead based on culture results. This suggests that hypoxia permits long term intracellular staphylococcal survival. This may be highly clinically relevant; in a zebrafish model of staphylococcal infection, single bacteria were carried to distant sites and were able to establish new foci of infection (Prajsnar *et al.*, 2012). Hypoxic neutrophils are more prone to degranulate (Hoenderdos *et al.*, 2016), which may favour such dissemination and promote the local tissue destruction that is characteristic of the classic staphylococcal abscess.

Although hypoxia impaired the killing of 2 MSSA strains, my results suggest that killing of the MRSA strain is not affected by hypoxia at 180 min, although longer time points

were not examined. I used time t=30 min as the start point of all gentamicin-protection assays as a time-course of phagocytosis suggested that maximal phagocytosis was always achieved (and was equivalent in normoxia and hypoxia). Earlier timepoints as short as 15 min did give similar phagocytosis rates although I cannot exclude differential effects between conditions, it was necessary to introduce this additional delay to allow the processing of normoxic and hypoxic samples in parallel. Whilst the neutrophils might be in a different state in the different incubation conditions, this part of what we were trying to document. Over the timeframe of the assay, there were more surviving intracellular JE2 present than SH1000 or Wood46 in the normoxic neutrophils. This may reflect the increased virulence of this strain and its resistance to killing processes by human cells. It has been demonstrated that MRSA strains of *S. aureus* are rapidly phagocytosed and are able to survive within human neutrophils for many hours. The killing occurs only at early time-points but within the time of further co-incubation, number of surviving staphylococci increases (Gresham *et al.*, 2000). Of note, *S. aureus* actively produces factors to evade killing by human neutrophils and at higher MOIs may kill the phagocytic cells (Voyich *et al.*, 2005). It would be of interest to look at lower MOIs of JE2 and to prolong the incubation periods in the setting of normoxia and hypoxia. It is likely that delayed apoptosis in hypoxia has evolved to allow neutrophils additional time to deal with pathogens in these conditions. Whilst neutrophil-mediated killing of *S. aureus* is almost completely dependent on the generation of ROS (which requires oxygen), many other bacteria such as *E. coli* are killed normally in hypoxia by non-oxidative-dependent mechanisms such as granule-derived proteases and anti-microbial peptides, and perhaps autophagy. Since it is just the ROS-dependent killing mechanisms that have been compromised by hypoxia, the host will still benefit from prolonged neutrophil lifespan in these settings.

Although I employed only a short-term hypoxic pre-incubation, I looked to HIF stabilisation as the mediator of impaired neutrophil-mediated killing in short-term hypoxia as modulation of HIF/hypoxia responses is being explored in the field of cancer biology (reviewed in (Jahanban-Esfahlan *et al.*, 2018; Francis *et al.*, 2018), and hence a HIF-mediated effect might be amenable to pharmacological agents. Perhaps unsurprisingly, the chemical stabilisation of HIF or inhibition of protein synthesis did not alter neutrophil- mediated killing of staphylococci (Fig. 3.14 A, B), suggesting that observed impairment of killing by hypoxic neutrophils is HIF-independent. I wished to

further elucidate the mechanism of impaired killing and hence looked at the impact of hypoxia on intracellular ROS production in response to bacterial ingestion.

The generation of ROS by the neutrophil oxidative burst requires a dramatic oxygen consumption (Reiss and Roos, 1978) and hence this response could be impaired if oxygen availability is limited. Standard methods of measuring intracellular ROS such as the cell-permeable fluorogenic probe 2',7'-dichlorofluorescein diacetate are not feasible in hypoxia, as unfixed cells must be run through the flow cytometer, and this would result in re-oxygenation of neutrophils. Therefore, an older method, the NBT assay, was employed to assess percentage of positive cells for ROS production in normoxia and hypoxia. This method has been used in the past as a test for diagnosing CGD patients in medical laboratories (Roos and Boer, 2014; Gifford and Malawista, 1970), or bacterial and viral infections (Gordon *et al.*, 1973). Using this method, I showed that hypoxia significantly reduced intracellular ROS production of neutrophils in response to staphylococcal ingestion, as predicted (Fig.3.15.). This result supports findings of McGovern *et al.*, (2011) who found that hypoxia inhibits extracellular release of ROS, and re-oxygenation restored both ROS release and the killing of *S. aureus* to the level observed in normoxia.

My findings have relevance for *in vivo* infections that are detrimental to human health. Previous publications have shown that infiltrating neutrophils responding to pro-inflammatory signals consume oxygen, thereby enhancing local tissue hypoxia (Campbell *et al.*, 2014). In the setting of infection, *S. aureus* also worsens tissue hypoxia, consuming oxygen and stabilising HIF1α in a skin infection model (Lone *et al.*, 2015; Werth *et al.*, 2010). Low oxygen tensions modify the host-pathogen interaction to promote infection patterns typical of staphylococcal infection, such as abscess formation. Hypoxia influences several steps involved in the formation of a staphylococcal abscess (Hajdamowicz *et al.*, 2019) by affecting both the neutrophil and the microbe. Hypoxia favouring intracellular persistence may lead to neutrophils disseminating staphylococcal infection in a ‘Trojan horse’ fashion (Prajsnar *et al.*, 2012). As the abscess matures, hypoxia also promotes the secretion of proteases by neutrophils (Hoenderdos and Condliffe, 2013) to liquefy the centre, and staphylococcal virulence factors such as coagulases induce neutrophils necrosis to further contribute to this process (Cheng *et al.*, 2010). Hypoxia may further shape the maturation of an abscess by inducing the production of lysyl-oxidase to promote the formation of a

capsule, sealing off the infection but also preventing resolution of infection (Beerlage *et al.*, 2013). All of these factors perpetuate the hypoxic environment in the centre of the abscess, and this will impair bacterial killing as I have shown.

I therefore wished to further investigate the mechanism of how hypoxia impairs staphylococcal killing. However, the practical challenges of undertaking these complex assays in the hypoxic hood led me to consider other ways of undertaking these experiments. Since I found that the impaired killing of *S. aureus* in hypoxia might be related to the reduction in the oxidative burst imposed by lack of molecular oxygen. I therefore decided to explore this further using chemical inhibition of the oxidative burst to complement my studies in the hypoxic chamber, which is the subject of my next Results Chapter.

4 Exploring the impact of neutrophil ROS production on the staphylococcal-phagosomal environment using chemical inhibition of ROS and hypoxia

4.1 Introduction

Neutrophils recruited to deep-seated tissue infections such as those caused by *S. aureus* must operate within a hypoxic environment to be successful at bacterial clearance. As hypoxia prolongs neutrophil survival and modulates other neutrophil functions, this may influence the outcome of the host-pathogen interaction. I have shown in Chapter 3 that hypoxia impairs the intracellular killing of *S. aureus*, although the impact of hypoxia is dependent on the precise bacterial strain under investigation. Whilst phagocytosis was not impaired, intracellular killing of *S. aureus* SH1000 at both early (90 min) and late (24 h) (Fig.3.12) time points was substantially reduced in the setting of hypoxia comparable to that measured in relevant infections *in vivo* (Simmen and Blaser, 1993; Wilde *et al.*, 2015). These studies reflect the outcome of the interaction at a population level, and do not offer mechanistic insights into the nature of the killing defect. Such insights are challenging to investigate in human neutrophils, whose limited lifespan constrains our ability to manipulate them genetically; hence our understanding of how bacteria are killed within the neutrophil phagosome remains incomplete.

Once phagocytosis has occurred the bacteria resides within an early phagosome, which must mature to generate a bactericidal environment. In macrophages, this process depends on a series of choreographed endosomal fusion events**,** (Vieira *et al.*, 2002) however, neutrophils do not have such a well-orchestrated endosomal pathway, and phagosomal maturation seems to be mediated, at least in part, by fusion of neutrophil granules with the phagosome. This has two major consequences for bactericidal activity; firstly, the granule contents contain an array of antimicrobial proteases, enzymes and peptides that may exhibit direct or indirect antibacterial effects; and secondly, delivery of components of the NADPH oxidase to the phagosomal membrane (together with recruitment of the cytoplasmic oxidase components) facilitates the oxidative (respiratory) burst, with reduction of molecular oxygen to superoxide anions (Fig.1.4.). A range of other ROS are generated by the action of enzymes including superoxide dismutase (SOD) and interaction with granule proteins such as MPO. Due to small volume and circumscribed nature of phagosomes, high levels of oxidants and granule proteins can be achieved (Winterbourn and Kettle,

2013), and there is synergy between oxidative and non-oxidative bactericidal mechanisms, with the precise contribution of these mechanisms to bacterial execution varying between bacterial species. The susceptibility of CGD patients to *S. aureus* suggests that the majority of killing of this organism is oxidase-dependent, a supposition supported by the work of Hampton *et al.* (Hampton *et al.*, 1996); these investigators used IgG-linked superoxide dismutase to estimate that at least three quarters of neutrophil-mediated killing of *S. aureus* was oxidase-dependent.

Whilst the endosomal-mediated delivery of vacuolar ATPase (v-ATPase) renders the macrophage phagosomal environment acidic, the phagosome in human neutrophils initially either undergoes a slight alkalinisation and subsequently returns to neutral (Foote *et al.*, 2019) or a very mildly acidic pH (Dri *et al.*, 2002). This is due to the granular composition of neutrophils which in part influences the intracellular pH in those cells (Nanda *et al.*, 1992). This is despite the rapid electron transfer mediated by the NADPH oxidase and is at least partially due to the action of a voltage gated proton channel, which compensates for the charge imbalance (Okochi *et al.*, 2009). The action of the NADPH oxidase thus influences phagosomal pH, and neutrophils from CGD patients do not display the initial alkalinisation seen in healthy cells (Dri *et al.*, 2002).

Although hypoxia has been shown to curtail the generation of reactive oxygen species, it is challenging to image host-pathogen interaction directly and in a dynamic fashion in the setting of hypoxia, due to the constraints imposed by the hypoxic chamber. Since hypoxia limits the generation of ROS at the phagosomal membrane (McGovern *et al.*, 2011) and since the generation of ROS is a key bactericidal effector for this pathogen, I used inhibition of ROS generation to further study this interaction.

I hypothesised that hypoxia modifies phagosomal development and function via suppression of ROS formation and that this can be modelled by the use of inhibitors of the NADPH oxidase.

Specific aims of this chapter:

1. To quantify the impact of inhibition of the neutrophil oxidative burst on intracellular ROS production in response to ingested S. aureus, and to confirm that inhibition of ROS generation recapitulates the impact of hypoxia on bacterial killing

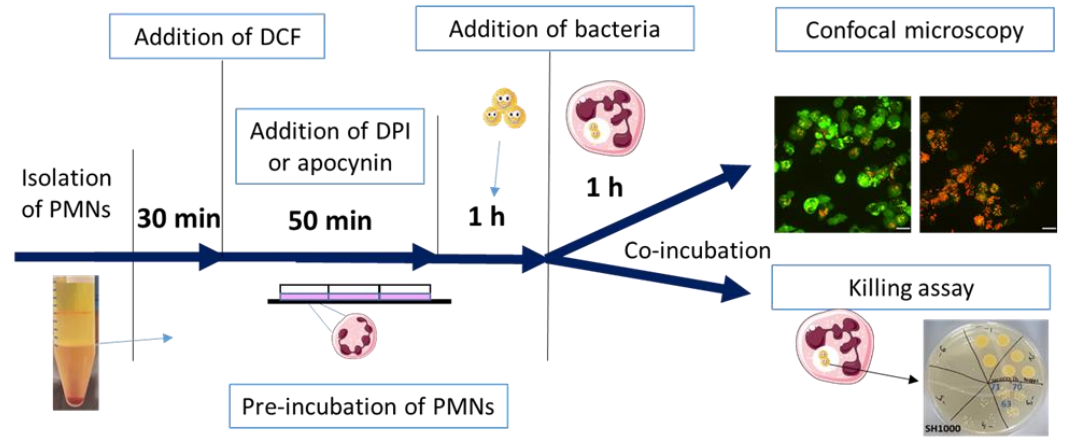

Fig.4.1. DPI inhibits Neutrophils ROS and killing of *S. aureus* SH1000

Fig.4.2. Apocynin promotes *S. aureus* SH1000-induced neutrophil ROS production

2. To investigate the impact of physiological and pharmaceutical inhibition of ROS on phagosomal morphology using confocal and electron microscopy

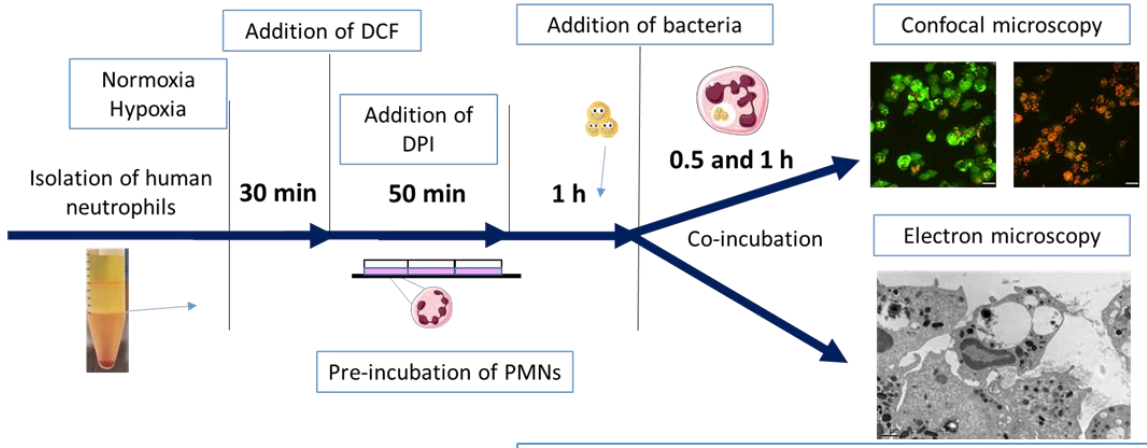

Fig.4.3. Effect of DPI on neutrophil phagosomal morphology

Fig.4.4. and Fig.4.5. Hypoxia and DPI modify neutrophil phagosomal morphology in response to *S. aureus* SH1000 at 0.5 and 1 h

3. To identify the effect of bafilomycin on intraphagosomal environment following infection with *S. aureus*

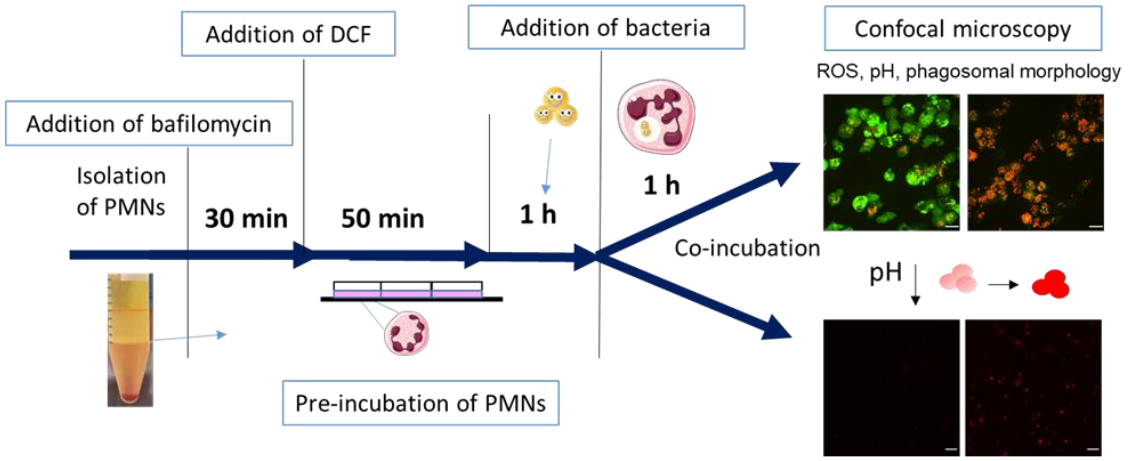

Fig.4.7. Lack of effect of bafilomycin in neutrophil ROS production or phagosomal environment

4. To examine the effect of DPI and bafilomycin on intraphagosomal environment

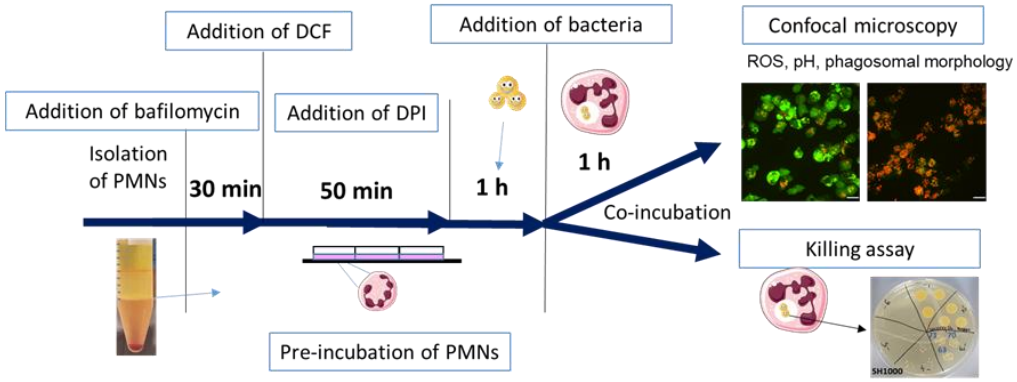

Fig.4.8. Effect of DPI and bafilomycin on neutrophil phagosomal acidification following ingestion of *S. aureus* SH1000

Fig. 4.10. Effect of bafilomycin on killing SH1000 by DPI-treated neutrophils

Fig.4.6. Effect of DPI on neutrophil phagosomal pH following ingestion of *S. aureus* SH1000

Fig. 4.9. Effect of DPI and bafilomycin on phagosomal morphology

5. To explore the effects of modulating intracellular transport processes (inhibition of Class III PI3 kinases) on the phagosomal morphology and killing of *S. aureus*

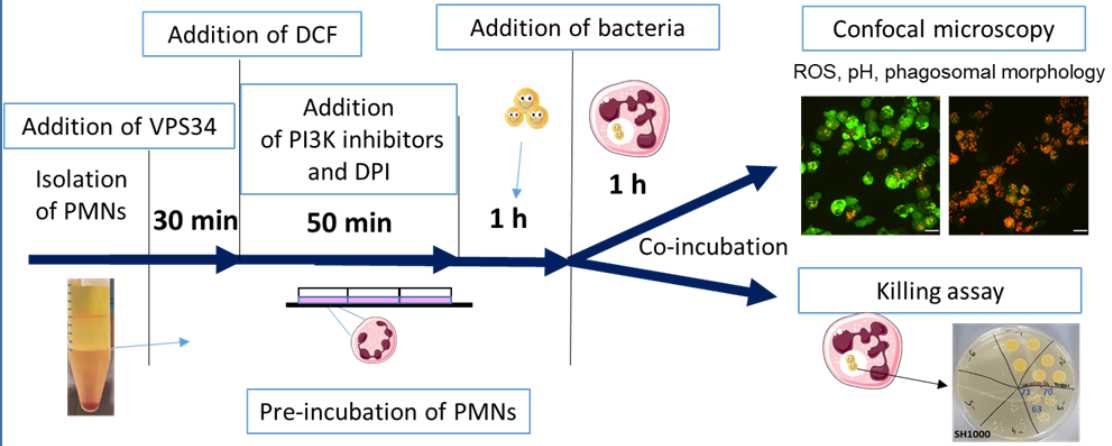

Fig.4.14. Impact of VPS34 inhibitor on ROS production by neutrophils in response to *S. aureus* SH1000

Fig.4.13. Effect of specific PI3K inhibitors on phagosomal pH of *S. aureus*

Fig.4.12. Effect of specific PI3K inhibitors on phagosomal morphology of neutrophils containing *S. aureus* SH1000

Fig.4.11. PI3K inhibitors limit *S. aureus* SH1000-induced neutrophil ROS production

Fig.4.17. VPS34 effect on killing of S. aureus by neutrophils

Fig.4.16. Effect of VPS34 on intraphagosomal pH of neutrophils

Fig.4.15. Effect of VPS34 on phagosomal morphology of neutrophils-containing *S. aureus* SH1000

4.1.1 Diphenyleneiodonium chloride (DPI) inhibits ROS production and killing of SH1000 by human neutrophils

To explore the impact of ROS on intracellular killing, I wished to quantify intracellular ROS production. Flow cytometry has frequently been used for this purpose (e.g., Bass *et al.*, 1983); however it does not allow continuous monitoring in real time, and interactions with bacteria or phagosomal morphology are difficult to explore in parallel. I therefore adapted the standard flow cytometric method using 2',7' –dichlorofluorescein diacetate (DCFDA), which is oxidized by ROS to fluorescent dye 2', 7' –dichlorofluorescein (DCF) seen as a green signal, using live imaging of unfixed cells to capture images and visualise intracellular events in response to bacterial ingestion. Neutrophils (2.25 x 10^5 cells/180 µL) were resuspended in RPMI/FBS/HEPES medium in IBIDI chamber plate and allowed to settle for 30 min, prior to the addition of 5 µM DCFDA. After a further 20 min, diphenyleneiodonium chloride (DPI) at 2 µM (or DMSO 0.01% as vehicle control) was added to inhibit ROS production in neutrophils. Finally, after a further 10 min live or heat-killed bacteria (mCherry-labelled *S. aureus* SH1000 (Pollitt *et al.*, 2018), at MOI 5 were added to DMSO or DPI treated neutrophils. Then, after 1 h of further co-incubation, samples were transferred to a spinning disk confocal microscope to visualise samples at 60 x oil immersion magnification. ROS signals were detected as green (DCF) fluorescence, seen predominantly in close proximity to red labelled bacteria in DMSO controls. In contrast, very limited DCF signal was detected in DPI-treated cells. Images were quantified (Section 2.7.2.) using ImageJ macro (MFI in control cells 2501 ± 379.8 versus 1000 ± 0.16 in DPI-treated cells, p=0.0029 for live bacteria, Fig. 4.1.A and 1844 ± 163 DMSO HK vs 793.8 ± 49.9 DPI HK, Fig.4.1.E). Representative images show strong DCF signal in DMSO controls (Fig. 4.1.B for live bacteria and Fig.4.1.F for HK), in comparison to DPI-treated cells where this signal was barely detected (Fig. 4.1.C for live bacteria and Fig.4.1.F for HK).

After confirming the inhibition of ROS production by DPI, the impact on killing of SH1000 was measured as previously. Briefly, after 50 min of pre-incubation of neutrophils (2.25 x 10^5 cells/90 µL) with DPI 2 µM or DMSO, bacteria (MOI 5) were added. After 30 min of co-incubation, gentamicin was added at 40 µg/mL to kill extracellular bacteria, and following lysis, intracellularly surviving bacteria were quantified by the Miles and Misra method. There was no significant difference at t=0

min, suggesting DPI does not impact phagocytosis (1253633 ± 151940 CFUs for DMSO to 1006600 ± 245832 CFUs for DPI treated cells). However, after 180 min there were significantly more bacteria surviving within DPI treated cells than in DMSO controls (33333 ± 1764 CFUs and 565 ± 75.92 CFUs respectively, Fig. 4.1.D). These data show that DPI not only inhibits ROS production but also impairs killing of SH1000. However, in addition to its effects on the NADPH oxidase, DPI may also inhibit other ROS generation, for example it inhibits nitric oxide synthase and hence the generation of reactive nitrogen species. I therefore decided to explore the impact of apocynin, also reported to inhibit the NADPH oxidase, to see if it had similar effects.

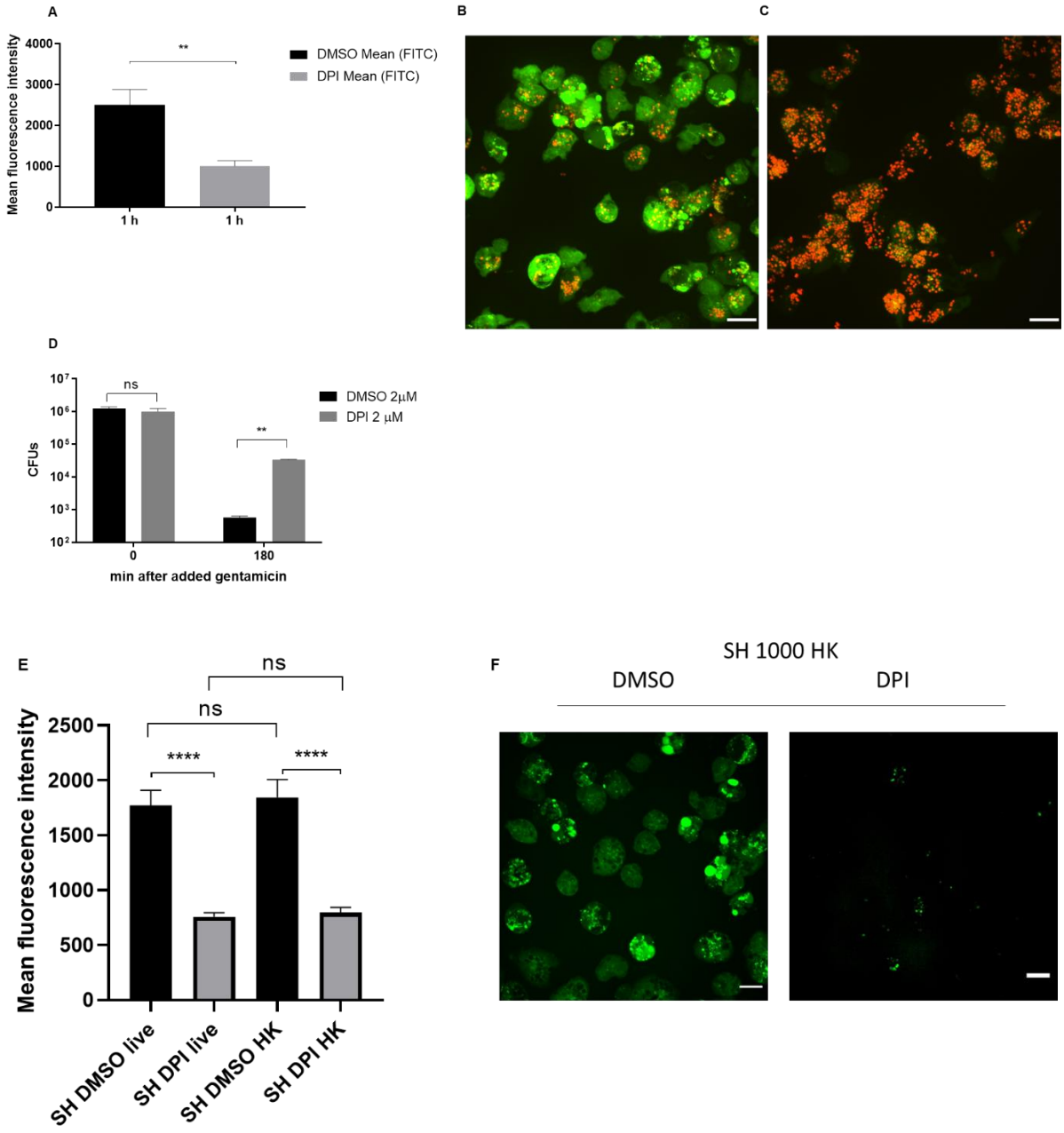

Figure 4.1 DPI inhibits Neutrophil ROS production and killing of *S. aureus* SH1000

(A,E). *Neutrophils isolated by Percoll® gradient centrifugation (2.25 x 10^5 cells/180 µL) were placed in 8-well glass bottom Ibidi chamberand allowed to adhere. DCFDA 5 µM (or vehicle control- 0.01% DMSO) was added after 30 min and DPI 2 µM or vehicle control at 50 min, and finally mCherry S. aureus SH1000 (MOI 5), live or heat-killed, were added at 60 min. Following a further 1 h co-incubation, live imaging was undertaken using a spinning disk confocal microscope at 60 x oil immersion magnification. Images were quantified using an Image J Macro. Data represent mean fluorescence intensity (MFI) from n=3 independent experiments*

*with measurement from 2 randomly chosen fields of view per experiment, **p=0.0029, unpaired t-test.* ***(B, C).*** *Representative images of DMSO control* ***(B)*** *and DPI treated* ***(C)*** *neutrophils containing phagocytosed red (mCherry) live bacteria; the green signal (oxidised DCF i.e., 2'7'-dichlorofluorescein) represents ROS production within neutrophils. Scale bars are 10 µm.* ***(D).*** *Gentamicin protection killing assay. Neutrophils (2. 25 x 10^5 cells/90 µL) were incubated for in normoxia (21% O_2) prior to the addition of DPI 2 µM or vehicle control at 50 min of S. aureus SH1000 (1.12 x 10^6 CFU/10 µL). After 30 min of co-incubation, gentamicin at 40 µg/mL was added to kill extracellular bacteria. At 0 min and 180 min, samples were lysed with alkali water, and CFU were quantified by the Miles and Misra method. Data represent n=3 experiments performed in duplicate, ns p=0.9684 for 0 min DMSO control vs DPI and **p=0.0012 for 180 min for DMSO vs DPI, one-way ANOVA with Sidak's multiple comparison test.* ***(F)*** *Representative images of DCF signal in neutrophils controls and DPI- treated, containing heat-killed SH1000. Scale bars are 10 µm.*

4.1.2 Apocynin promotes ROS production in response to *S. aureus* in human neutrophils

Apocynin has been reported to inhibit the generation of ROS by preventing the translocation of NADPH oxidase cytosolic subunits to the membrane (Barbieri *et al.*, 2004), although it may have other activities including scavenging free radicals (Savla *et al.*, 2021). Freshly isolated neutrophils (Percoll® gradient centrifugation, 2.25 x 10^5 cells/180 µL) were placed onto 8-well glass bottom Ibidi chamber and incubated to allow neutrophils to settle at the bottom of the wells. After 30 min, DCFDA (5 µM) was added to cells. At 50 minutes of pre-incubation, DPI (2 µM) or apocynin (300 µM) or DMSO control (0.01%) were added to neutrophils. At 1 h bacteria (mCherry SH1000) were added at MOI 5 and incubated for a further 1 h with neutrophils before imaging on the spinning disk confocal microscope. Samples were imaged at 60 x oil immersion magnification with the red signal channel to detect bacteria and the green channel to visualise DCF. Quantification (ImageJ macro) of the fluorescein (oxidised DCF) signal was undertaken to determine ROS production. Unexpectedly, as shown in Fig. 4.2.A, there was significantly more oxidised DCF signal seen in apocynin- treated neutrophils than DPI- or DMSO-treated cells (MFI 3253 ± 33.65 compared to 813.4 ± 13 and 1372 ± 9.26 mean fluorescence intensity, respectively). Representative images (Fig. 4.2.B-D) show visually the intense green signal observed in cells treated with apocynin (Fig. 4.2.D). Those data show that apocynin doe not inhibit ROS production/DCFDA oxidation under the experimental conditions required, hence it was not used for future experiments. I therefore returned to using DPI and explored the impact of this compound on phagosomal morphology and acidification.

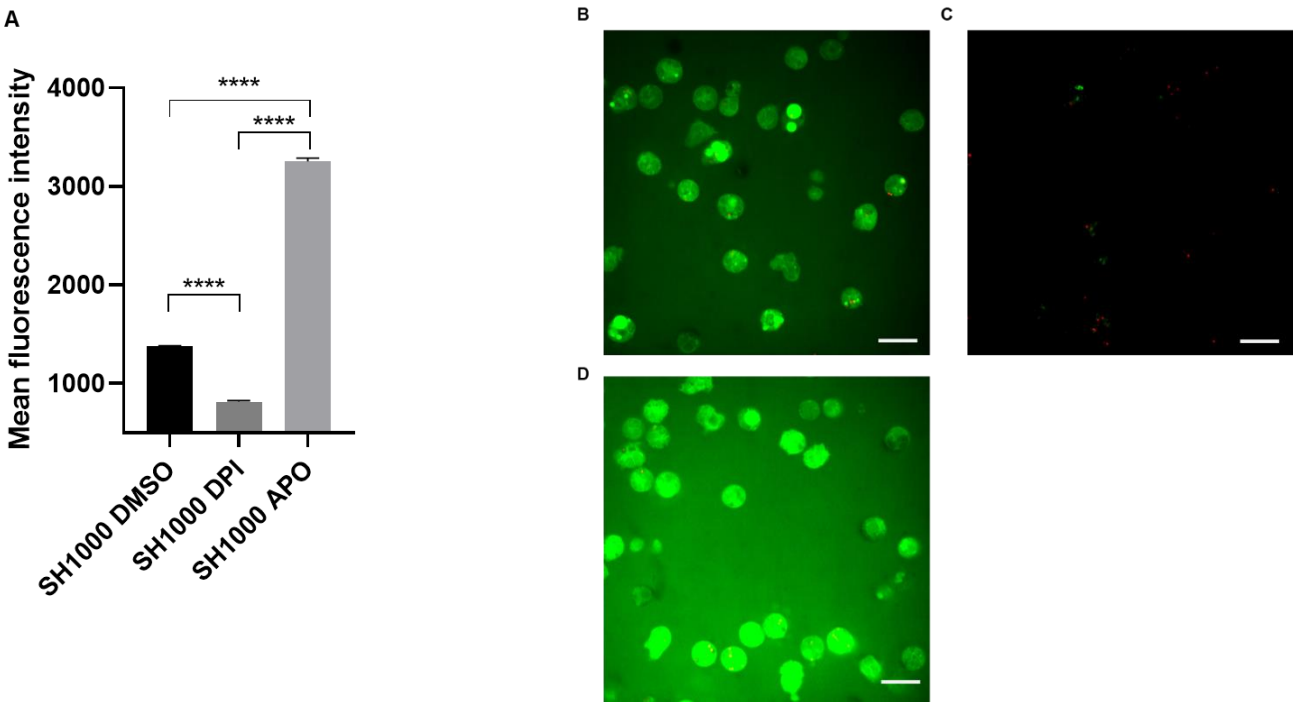

Figure 4.2 Apocynin promotes *S. aureus* SH1000-induced neutrophil ROS production

***(A)**. Neutrophils (2.25 x 10^5 cells/180 µL) isolated by Percoll® gradient centrifugation were placed onto 8-well glass bottom Ibidi chamber and allowed to adhere. DCFDA 5 µM (or vehicle control 0.01% DMSO) was added after 30 min and DPI 2 µM or vehicle control or apocynin at 300 µM at 50 min, and finally mCherry S. aureus SH1000 at MOI 5 were added at 60 min. Following a further 1 h co-incubation, live imaging was undertaken using spinning disk confocal microscope at 60 x oil immersion magnification. Images were quantified using an Image J Macro, and data represent fluorescein mean fluorescence intensity (MFI) from n=3 independent experiments with measurement from 2 randomly chosen fields of view per experiment, ****p<0.0001 DMSO vs DPI, DMSO vs APO, DPI vs APO, one-way ANOVA with Sidak's multiple comparison test. **(B, C)**. Representative images of DMSO control **(B)** DPI treated cells **(C)** and apocynin treated cells **(D)** green signal represents oxidised DCF and red mCherry bacteria. Scale bars are 10 µm.*

4.1.3 Inhibition of ROS production by DPI alters neutrophil phagosomal morphology

Neutrophils isolated by Percoll® gradient centrifugation (2.25 x 10^5 cells/180 µL) were placed onto 8-well glass bottom Ibidi chamber for 50 min before the addition of DPI (2 µM) or vehicle control (0.01% DMSO). pHrodo red stained SH1000 at MOI 5 were added at 1 h, and following a further 1 h, samples were imaged using the spinning disk confocal microscope at 60 x oil immersion magnification. The imaging was performed using live bacteria and heat-killed (see Section 2.7.1). It was not possible to fix cells as the fixation process had impact on neutrophils shape, hence live imaging has been performed. This unbaled imaging of cells incubated in hypoxia. Randomly chosen fields of view were imaged and the morphology of phagosomes with ingested bacteria was studied with the observer blinded to experimental conditions. A clear difference in phagosomal morphology was observed, with some bacteria within very large phagosomes and some sitting within phagosomes only slightly larger than the bacteria themselves. Phagosomes which tightly surrounded bacteria were designated as ‘’tight’’ phagosomes’ and those were far larger than the enclosed bacteria were defined as ‘’spacious’’ phagosomes. A neutrophil containing at least one spacious phagosome was counted as a “spacious phagosome-containing neutrophil”. Calculations were done manually in ImageJ for the percentage of spacious phagosome/s containing neutrophils. Counting was performed from three randomly chosen fields of view from three independent experiments. As noted previously (Fig. 4.1.D), DPI did not reduce phagocytosis, however DPI significantly ($p<0.0001$) reduced the number of tight phagosomes seen compared to those observed in DMSO controls; 47 ± 3.4% of control neutrophils contained spacious phagosomes in comparison to only 6 ± 1.29 % when DPI was used (Fig. 4.3.A). Using heat-killed bacteria led to the same results (Fig. 4.3.D), DPI significantly reduced spacious phagosome formation in comparison to DPI treated neutrophils with live bacteria (1.86 ± 0.94 % to 1.12 ± 0.64%, respectively). Dead bacteria led to also spacious phagosome formation, with similar percentage as when live bacteria were used (Fig.4.3.D). Spacious phagosomes are visible on the image in Fig. 4.3.B and E of DMSO control neutrophils. In contrast there are none of these compartments detected in DPI treated cells (Fig. 4.3.C,F). Continuous live imaging suggested that these differences were stable over time (not shown). These data suggest that inhibiting ROS generation affects phagosomal

development, and I wished to relate this to my initial experiments employing hypoxic incubation.

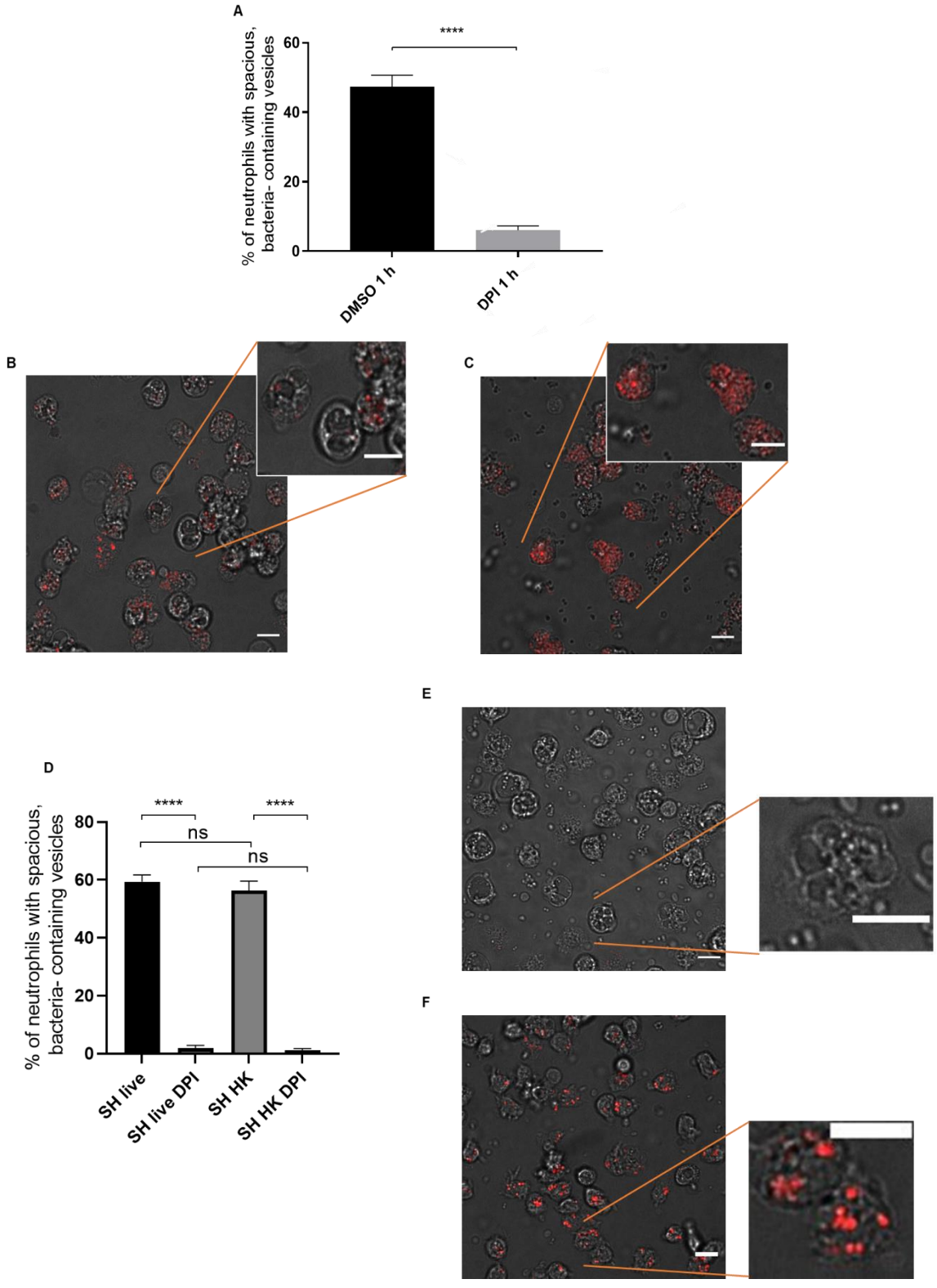

Figure 4.3 Effect of DPI on neutrophil phagosomal morphology

(A, D). *Bacteria were stained with pHrodo red pH-sensitive dye to assess intraphagosomal pH following phagocytosis of S. aureus SH1000 or heat-killed after staining. Neutrophils isolated*

*by Percoll® gradient centrifugation (2.25 x 10^5 cells/180 µL) were placed onto 8-well glass bottom Ibidi chamber and allowed to adhere. DPI 2 µM or DMSO 0.01% vehicle control was added at 50 min, and dually stained S. aureus SH1000 (MOI 5) were added at 60 min. Samples were incubated for a further 30 min before real time imaging by spinning disk confocal microscope at 60 x oil immersion magnification. After 1 h of co-incubation, the number of neutrophils containing spacious phagosomes was manually quantified from n=3 independent experiments from 3 random fields of view per sample. Data represent percentage of neutrophils with spacious SH1000-containing vesicles at 1 h post infection, unpaired Mann- Whitney test **** p<0.0001 DPI vs DMSO.* ***(B, C).*** *Representative images of DMSO control neutrophils containing spacious phagosomes* ***(B,E)*** *and DPI treated cells without those vesicles* ***(C,F).*** *Scale bars are 10 µm.*

4.1.4 Hypoxia induces similar changes to DPI in neutrophil phagosomal morphology in response to *S. aureus* SH1000

As previously noted, microscopy of live hypoxic cells is not easily accomplished as the hypoxic chamber is not set up to allow access for a microscope (in particular the glass front prevents access to the eye piece) and the humidity within the chamber would preclude incorporating the majority of such devices. Light microscopy of fixed cells did not provide sufficient resolution to quantify the abundance of tight and spacious phagosomes (not shown). I therefore used electron microscopy to evaluate phagosomal morphology in the setting of hypoxia and DPI treatment compared to control neutrophils following ingestion of *S. aureus* SH1000. Freshly isolated neutrophils by Percoll® were resuspended in normoxic or hypoxic RPMI/FBS/HEPES and placed in a 96 well plate (2.25 x 10^5 cells/90 µL) for 1 hour of pre- incubation in normoxia and hypoxia. After 50 min of this incubation, DPI at 2 µM or vehicle control (0.01% DMSO) were added to samples in normoxia. At 1 h, *S. aureus* SH1000 at MOI 10 (2.25 x 10^6 CFU/10 µL) were added to neutrophils for further 30 min or 1 h of co-incubation; the higher MOI was used as electron microscopy will only image one plane through each neutrophil and hence the likelihood of 'capturing' a phagosome is reduced. After these times, samples were collected from several wells and combined to give approximately 10^6 neutrophils from each treatment, to obtain a large enough pellet to process for electron microscopy. Pellets of samples from normoxic control, normoxic DPI-treated and hypoxic cells were then fixed (2.5% Glutaldehyde/0.1M Sodium Cacodylate overnight) and postfixed in 2% aqueous Osmium Tetroxide. From this step sample processing was continued by the Electron Microscopy Officer at the University of Sheffield, Dr Christopher Hill (see Section 2.8.). In brief, ultrathin (85 nm) Sections were cut and stained with saturated aqueous Uranyl Acetate followed by Reynold's Lead Citrate. Sections were examined using an FEI Tecnai Transmission Electron Microscope at an accelerating voltage of 80 Kv. Electron micrographs were recorded using Gatan Orius 1000 digital camera and Gatan Digital Micrograph software by myself.

Quantification was performed manually from randomly chosen bacteria within phagosomes using ImageJ software. The observer was blinded to the experimental condition when undertaking the quantification. Since the whole neutrophil was not imaged, I could not use the same quantification method as previously (% of neutrophils

containing at least one spacious phagosome). Instead, the area of the phagosome and of the ingested bacteria (μm^2) was measured and expressed as a ratio to give the percentage of phagosome occupied by the bacterium in the 2-d image (see Section 2.8.2.). Results obtained from transmission electron microscopy agreed with previous observations that DPI altered phagosomal morphology - in DPI-treated neutrophils bacteria occupied a significantly ($p<0.0001$) greater volume of the phagosome (55.49 ± 1.77% at 30 min; 63.12 ± 2.03% and 60 min) compared to bacteria within phagosomes in control neutrophils (29.70 ± 2.47% at 30 min; 32.67 ± 2.18% at 60 min) (Fig. 4.4.A and Fig. 4.5.A). Importantly, the morphology of phagosomes in the hypoxic neutrophils could not be distinguished from the normoxic DPI-treated comparators, and the volume of the phagosome occupied by the bacteria under hypoxic conditions was also near-identical to DPI-treated cells (56.85 ± 2.7% at 30 min, $p= 0.96$; 64.35 ± 2.74% at 1 h, $p= 0.97$), again significantly different ($p<0.0001$) compared with the normoxic control cells (Fig. 4.4.A and Fig.4.5.A). Representative images highlight the clear differences in the volume of phagosomes in each treatment (Fig. 4.4.B-D and Fig.4.5.B-D). These experiments confirmed my light microscopy findings and extended them to hypoxic neutrophils, demonstrating that inhibition of the oxidase by DPI and incubation of neutrophils in hypoxia (which also inhibits the oxidative burst, see Figure 3.15) leads to a reduction in phagosomal volume following ingestion of *S. aureus*. In view of this change in phagosomal morphology, I next wished to determine whether inhibition of the neutrophil oxidative burst would also affect phagosomal pH.

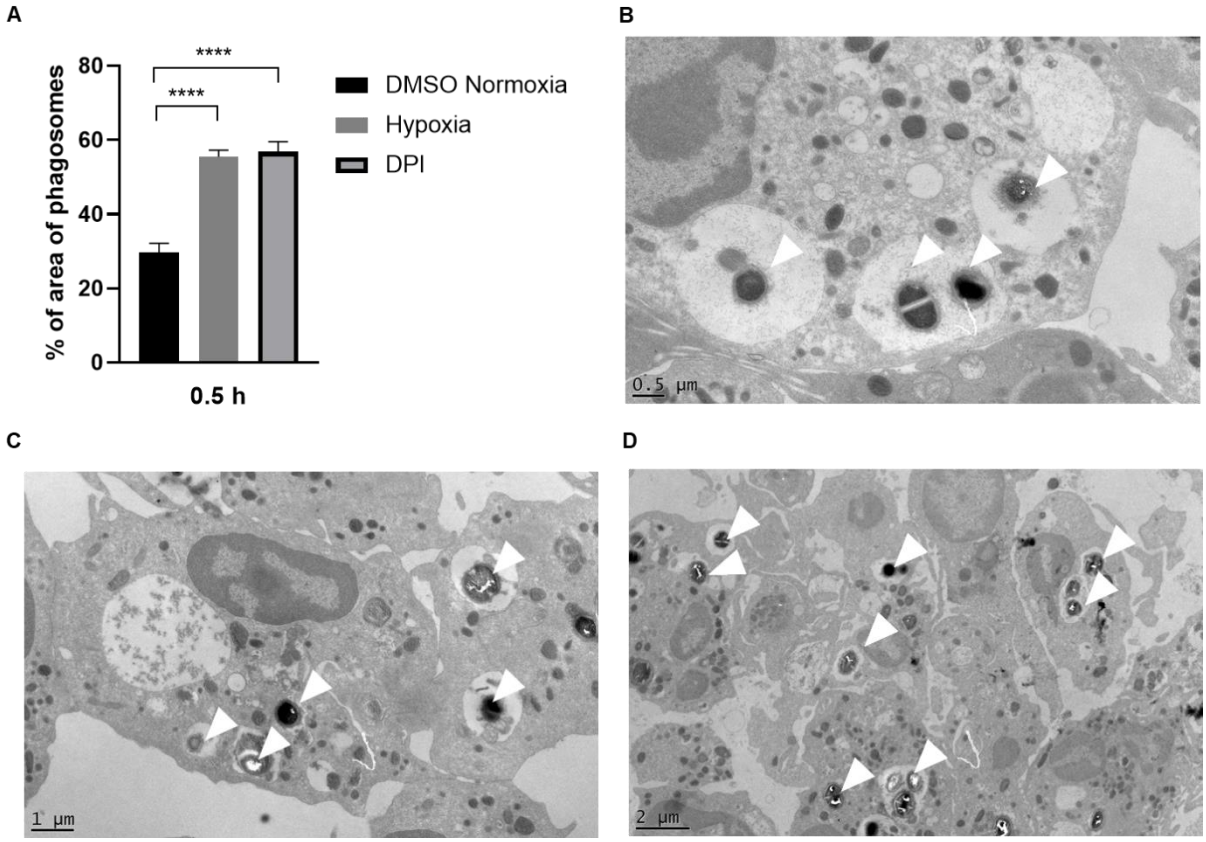

Figure 4.4 Hypoxia and DPI modify neutrophil phagosomal morphology in response to *S. aureus* SH1000 at 30 min

Neutrophils isolated by Percoll® gradient centrifugation (1.12 x 10^6 cells/450 µL) were resuspended in pre-equilibrated normoxic or hypoxic RPMI/FBS/HEPES and pre-incubated for 1 h in normoxia (21 % O_2) or hypoxia (0.8 % O_2) before addition of S. aureus SH1000 (MOI 10); DPI 2 µM or vehicle control (0.01% DMSO) was added to samples incubated in normoxia. After a further 30 min pelleted samples were fixed (2.5 % Glutaldehyde/0.1 M Sodium Cacodylate) and postfixed (2% aqueous Osmium Tetroxide), dehydrated with ethanol, cleared in epoxypropane (EPP) and infiltrated in 50/50 Araldite resin: EPP mixture before being embedded and cured at 60°C for 72 hours. Ultrathin Sections (H 85nm) were cut onto 200 mesh copper grids. These were stained for 10 min with saturated aqueous Uranyl Acetate followed by Reynold's Lead Citrate for 5 min. Sections were examined using a FEI Tecnai Transmission Electron Microscope at an accelerating voltage of 80 Kv. Electron micrographs were recorded using Gatan Orius 1000 digital camera and Gatan Digital Micrograph software. ***(A).*** *Data represent n=2 separate experiments, measurements performed on 21 bacteria/phagosomes analysed using ImageJ software, % area of phagosomes **** p<0.0001 for DMSO vs DPI treated neutrophils and DMSO vs hypoxia. tested by One-way ANOVA with Sidak's multiple comparison.* ***(B-D)****. Representative electron micrographs of DMSO control*

(normoxia) ***(B)****, DPI (normoxia) treated neutrophils* ***(C)*** *and hypoxic neutrophils* ***(D)*** *with white arrows indicating bacteria in the phagosomes. Scale bars as written on the micrographs.*

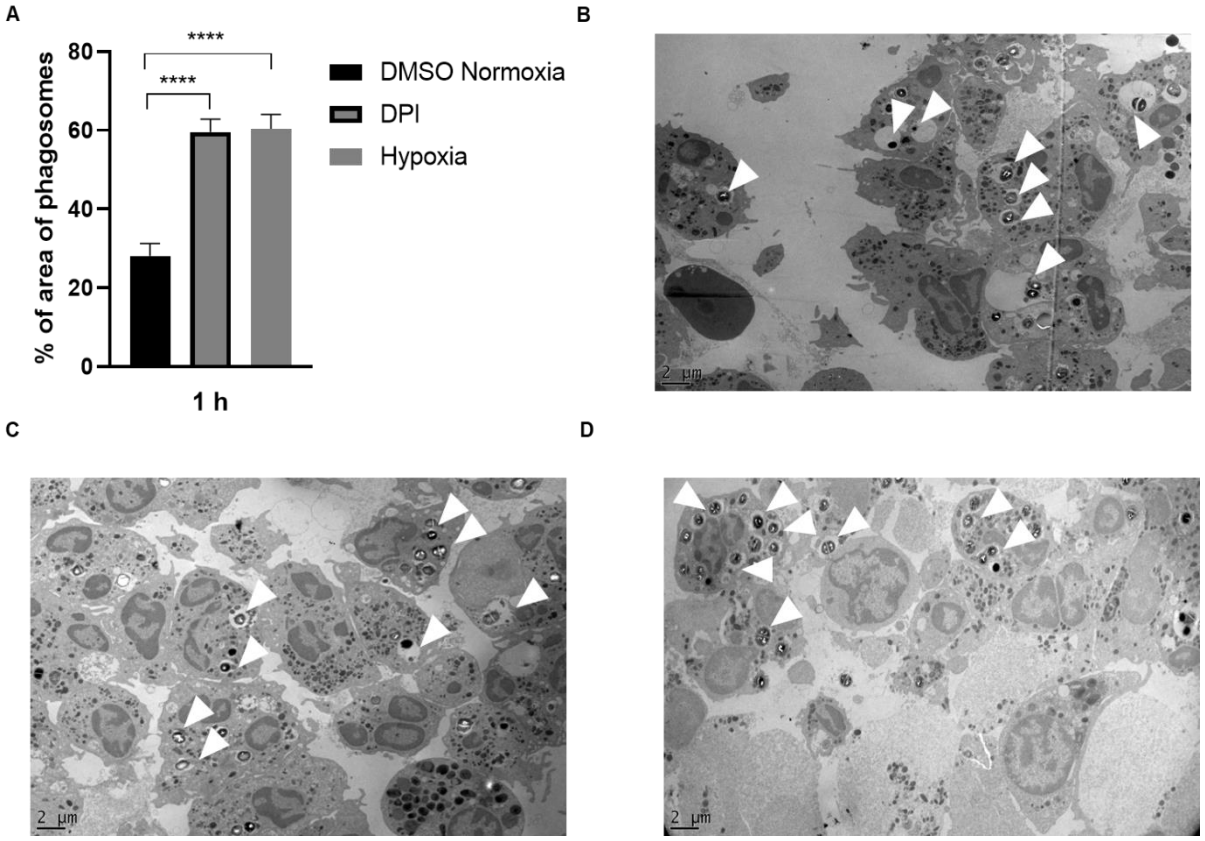

Figure 4.5 Hypoxia and DPI modify neutrophil phagosomal morphology in response to *S. aureus* SH1000 at 1 h

Neutrophils isolated by Percoll® gradient centrifugation (1.12 x 10^6 cells/450 µL) were resuspended in pre-equilibrated normoxic or hypoxic RPMI/FBS/HEPES and pre-incubated for 1 h in normoxia (21 % O_2) or hypoxia (0.8 % O_2) before addition of S. aureus SH1000 (MOI 10); DPI 2 µM or vehicle control (0.01% DMSO) was added to samples incubated in normoxia. After a further 1 h pelleted samples were fixed (2.5 % Glutaldehyde/0.1 M Sodium Cacodylate) and postfixed (2% aqueous Osmium Tetroxide), dehydrated with ethanol, and cleared in epoxypropane (EPP) and then infiltrated in 50/50 Araldite resin: EPP mixture before being embedded and cured at 60°C for 72 hours. Ultrathin Sections (~85nm) were cut onto 200 mesh copper grids. These were stained for 10 min with saturated aqueous Uranyl Acetate followed by Reynold's Lead Citrate for 5 min. Sections were examined using a FEI Tecnai Transmission Electron Microscope at an accelerating voltage of 80 Kv. Electron micrographs were recorded using Gatan Orius 1000 digital camera and Gatan Digital Micrograph software. ***(A).*** *Data represent n=2 independent experiments, measurement performed on 21 bacteria/phagosomes and analysed in ImageJ software, % area of phagosomes **** p<0.0001 for DMSO vs DPI treated neutrophils and DMSO vs hypoxia, tested by One-way ANOVA with*

Sidak's multiple comparison. ***(B-D)****. Representative electron micrographs of DMSO control (normoxia)* ***(B)****, DPI treated neutrophils* ***(C)*** *and hypoxic neutrophils* ***(D)*** *with white arrows indicating bacteria in the phagosomes. Scale bars as written on the micrographs.*

4.1.5 DPI modulates neutrophil phagosomal pH following ingestion of *S. aureus*

S. aureus SH1000 was dually stained with 2 pH sensitive dyes, pHrodo Red and Fluorescein-5-EX S- ester. If the pH drops below the neutral (pH=7), bacteria become redder, indicating acidic environments, whilst if the pH is neutral or above (pH≥7) bacteria are green (Section 2.7.1). Neutrophils (2.25 x 10^5 cells/180 µL) were placed onto 8-well glass bottom Ibidi chamber to sediment at the bottom of the wells. After t=50 min, DPI (2 µM) or vehicle control (0.01% DMSO) were added to cells followed by addition of dually stained bacteria at t=1 h for 1 h more of co-incubation. Samples were imaged on a spinning disk confocal microscope following the further 1 hour of co-incubation. Cells were imaged under 60 x oil immersion magnification for red (532 nm) and green (488 nm) signals from bacteria, and mean fluorescence intensity was quantified from both channels using an ImageJ macro. Bacteria outside the cells remained green, indicating (as expected) the neutral pH of the medium (Fig. 4.6.B-C, white arrows). Intraphagosomal bacteria ingested by neutrophils from DPI treated cells exhibited more intense red signal visually (Fig. 4.6.C) compared with those ingested by DMSO control neutrophils (Fig. 4.6.B). Quantification confirmed greater acidification of bacteria following DPI treatment, as measured from the red and green signals pHrodo and fluorescein, respectively (Fig 4.6.A). There was significantly (p=0.0003) less green (pH≥7) signal from bacteria within phagosomes of DPI treated cells (1114 ± 118.3 MFI) in comparison to those ingested by DMSO controls cell (1919 ± 121.6 MFI). Similarly, a stronger red signal was detected from intraphagosomal bacteria in DPI treated than DMSO treated 1448 ± 186 MFI to 1015 ± 33.5 MFI for DMSO controls (p=0.04*)*. These data suggest DPI treatment leads to enhanced acidification of bacteria within the phagosome in addition to its impact on ROS generation and on phagosomal morphology. To try to unpick these varied effects I decided to next inhibit the vacuolar H^+ ATPase (v-ATPase) which modifies the phagosomal pH.

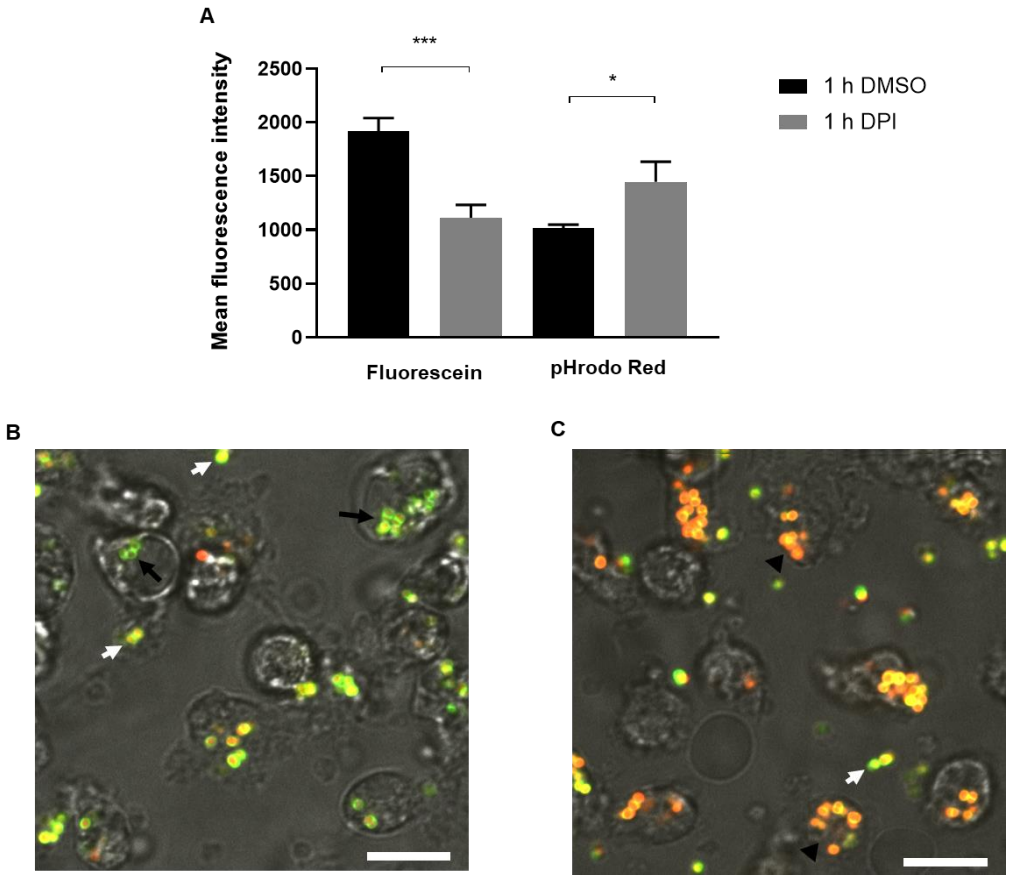

Figure 4.6 Effect of DPI on neutrophil phagosomal pH following ingestion of *S. aureus* SH1000

Bacteria were dually stained with fluorescein (green) and pHrodo Red to assess intraphagosomal pH following phagocytosis of S. aureus SH1000. ***(A).*** *Neutrophils isolated by Percoll® gradient centrifugation neutrophils (2.25 x 10^5 cells/180 µL) were placed onto 8-well glass bottom Ibidi chamber and allowed to adhere. DPI 2 µM or vehicle control (0.01% DMSO) was added at 50 min, and dually stained S. aureus SH1000 (MOI 5) were added at 60 min. Samples were incubated for a further 1 h before imaging in real by spinning disk confocal microscope at 60 x oil immersion magnification. Images were quantified using an Image J Macro, and data represent the indicated mean fluorescence intensity (MFI) from n=3 independent experiments with measurement from 2 randomly chosen fields of view per experiment, ***p=0.0003 for fluorescein DMSO control vs DPI treated cells, *p=0.0473 for pHrodo Red DMSO control vs DPI treated cells, tested by One-way ANOVA with Sidak's multiple comparison test.* ***(B, C).*** *Representative images of DMSO control* ***(B)*** *and DPI treated* ***(C)*** *neutrophils containing phagocytosed pHrodo with red bacteria indicating increased acidification (lower pH, black arrowheads); the green signal (fluorescein) represents bacteria at*

neutral pH within neutrophils (black arrows) or extracellular (white arrows). Scale bars are 10 µm.

4.1.6 Bafilomycin does not modulate ROS production or phagosomal morphology/acidification

Bafilomycin, a macrolide antibiotic isolated from *Streptomyces* species, is an inhibitor of V-ATPase (Bowman *et al.*, 1988). This compound binds to the V0 sector subunit c of the V-ATPase complex and inhibits H+ translocation which causes its accumulation in the cytoplasm (Bowman *et al.*, 2004). The V-ATPase was found to be absent from the resting neutrophil plasma membrane but to be abundant in particular in tertiary granules (Nanda *et al.*, 1992), hence it is likely that delivery of the V-ATPase will occur during phagosomal maturation with the potential to affect the phagosomal environment and in particular the phagosomal pH. Initially, I used bafilomycin alone at a concentration previously reported to modulate the V-ATPase in human neutrophils (Gilman-Sachs *et al.*, 2015). To explore the impact of bafilomycin on ROS production, neutrophils isolated using EasySepTM negative selection were resuspended in RPMI/FBS/HEPES medium with the addition of 0.1 µM bafilomycin, for 1 h of pre-incubation.

To analyse ROS production, DCF 5 µM (or vehicle control 0.01% DMSO) was added after 30 min and pHrodo Red stained *S. aureus* SH1000 (MOI 5) were added at 60 min. Following a further 1 h co-incubation, live imaging was undertaken using spinning disk confocal microscope as previously. As can be seen in Fig. 4.7.A-C, there was no significant difference (ns p=0.32) in ROS production between DMSO control (2326 ± 37.1 MFI SEM) and bafilomycin- treated (2590 ± 172.6 MFI SEM) neutrophils.

To determine the impact of bafilomycin on phagosomal morphology, neutrophils were treated with bafilomycin and fed pHrodo Red-stained *S. aureus* as above and imaged using the spinning disk microscope with manual counting of spacious and tight phagosome-containing neutrophils (Fig. 4.7.D-F). There was a trend to increased spacious phagosomes in bafilomycin treated (58.70 ± 2.94%) compared DMSO control (51.43 ± 1.9%) neutrophils, however it did not reach significance (ns p=0.12).

To assess phagosomal pH in response to bafilomycin, neutrophils were isolated and treated with 0.1 µM bafilomycin or DMSO vehicle control and incubated with pHrodo red *S. aureus* SH1000 exactly as above and imaged using the spinning disk microscope. The MFI of pHrodo red signal of intracellular bacteria was measured with red excitation wavelength of 532 nm. Bafilomycin did not affect the pH of phagocytosed bacteria, with no significant difference (ns p=0.09) between MFI of

pHrodo red signal of intracellular bacteria in DMSO control (487.7 ± 14 MFI SEM) and bafilomycin-treated (527.7 ± 11.71 MFI SEM) neutrophils (Fig 4.7.G-I). The signal remained low indicating the phagosome was not significantly acidified in either the control or bafilomycin-treated cells.

Together these results suggest that bafilomycin does not affect the neutrophil oxidative burst or the phagosomal morphology/pH directly following ingestion of *S. aureus*. I next wished to see if bafilomycin would modify the effect on DPI on the phagosomal environment.

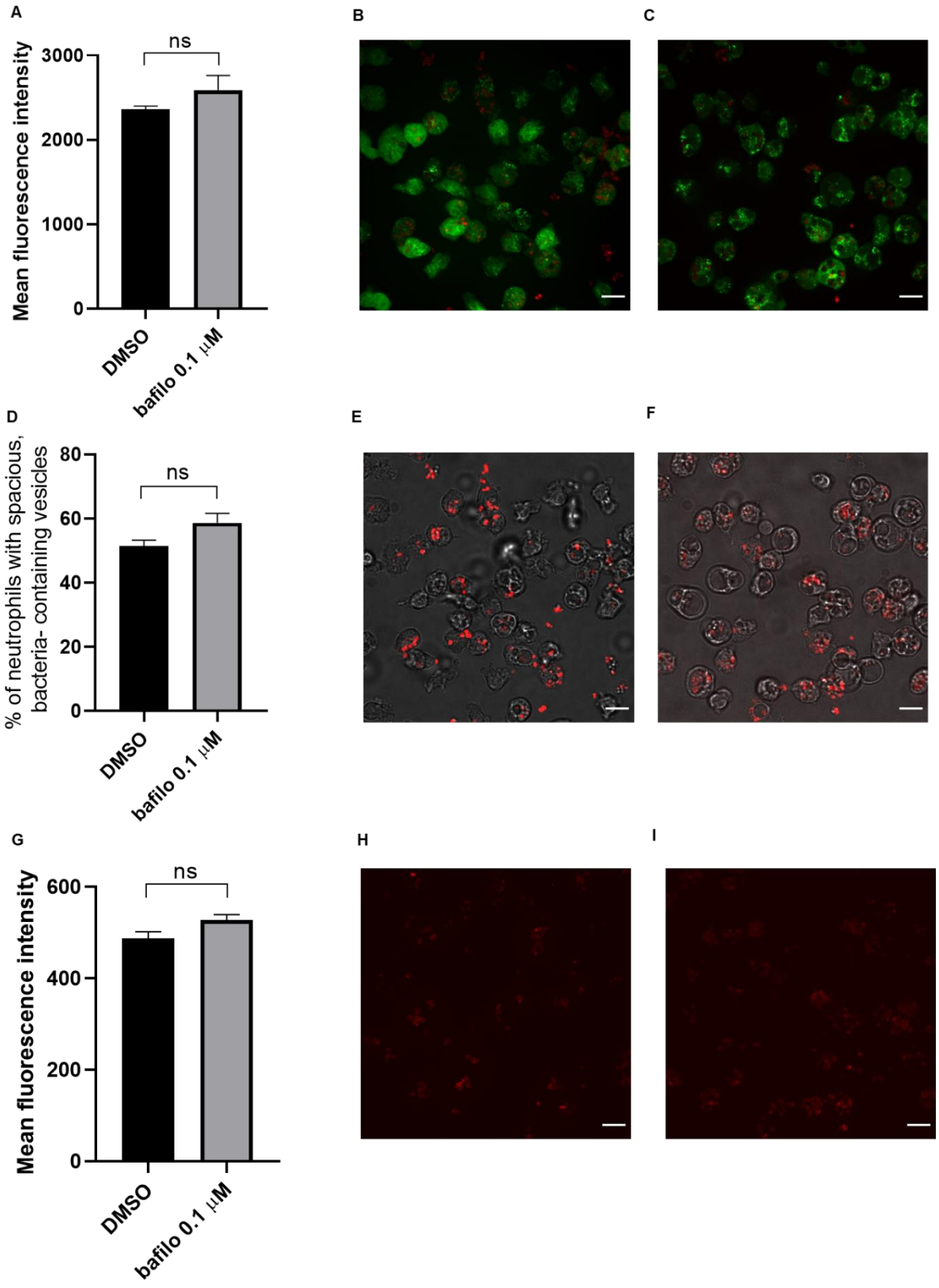

Figure 4.7 Lack of effect of bafilomycin in neutrophil ROS production or phagosomal environment

Neutrophils isolated by EasySep™ (2.25 x 10^5 cells/180 µL) were placed in 8-well glass bottom Ibidi chamber and with addition of bafilomycin 0.1 µM or DMSO vehicle control from the outset.

***(A-C)**. DCF 5 µM (or vehicle control 0.01% DMSO) was added at 30 min and pHrodo Red stained S. aureus SH1000 (MOI 5) were added at 60 min. Following a further 1 h, imaging was undertaken using spinning disk confocal microscope at 60 x oil immersion magnification. A. Images were quantified using an Image J Macro, and data represent fluorescein mean fluorescence intensity (MFI) from n=3 independent experiments with measurement from 2 randomly chosen fields of view per experiment, ns p= 0.32 tested by the Mann- Whitney test (B,C) Representative images of control (B) and bafilomycin treated cells (C), green signal is oxidised DCF and red pHrodo-stained bacteria. Scale bars are 10 µm.*

***(D-F)**. pHrodo Red- stained S. aureus SH1000 (MOI 5) were added at 60 min. Samples were incubated for a further 1 h before real time imaging by spinning disk confocal microscope at 60 x oil immersion magnification. After 1 h of co-incubation the number of neutrophils containing spacious phagosomes was manually quantified from n=3 independent experiments from 3 different fields of view per sample. Data represent percentage of neutrophils with spacious SH1000-containing vesicles at 1 h post infection, Mann- Whitney test was used ns p= 0.12 DMSO vs bafilo (E, F). Representative images of DMSO control (E) and bafilomycin treated neutrophils (F). Scale bars are 10 µm.*

***(G-I)**. pHrodo Red stained S. aureus SH1000 (MOI 5) were added at 60 min. Samples were incubated for a further 1 h before imaging in real time by spinning disk confocal microscope at 60 x oil immersion magnification at 1 hpi. Images acquired after 1 h co-incubation were quantified using an Image J Macro, and data represent mean fluorescence intensity (MFI) from n=3 independent experiments with measurement from 3 randomly selected fields of view per experiment, ns p= 0.09 DMSO control vs DPI with bafilomycin, tested with Mann- Whitney test.*

***(H, I).** Representative images of DMSO (H) or DPI plus bafilomycin treated cells (I). Scale bars are 10 µm.*

4.1.7 Bafilomycin alters the phagosomal pH experienced by ingested *S. aureus* in DPI treated neutrophils

I hypothesised that the impact of DPI on phagosomal acidification is mediated by the V-ATPase and hence predicted that bafilomycin would reverse this effect. I therefore treated cells with both inhibitors. Neutrophils (2.25×10^5 cells/180 µL) were incubated with 0.1 µM bafilomycin or vehicle control in 8-well glass bottom Ibidi chamber. After 50 min of co-incubation, DPI (2 µM) or DMSO control (0.01%) were added to cells followed by addition of pHrodo stained SH1000 at MOI 5 at 1 h. After a further 1 h of co-incubation, cells were imaged at 60 x oil immersion magnification, and MFI for pHrodo was quantified using ImageJ software. As previously, DPI increased the pHrodo fluorescence compared to the control (from 547.7 ± 58.7 MFI to 937.1 ± 112.4 MFI, Fig. 4.8.A). Bafilomycin together with DPI abolished the change in the intraphagosomal pH of environment to the level observed in the vehicle controls (564.8 ± 46.2 and 547.7 ± 58.7 of MFI for red signal, respectively; Fig. 4.8.A, representative images Fig. 4.8.B-D). These data confirm that the decrease of pH by DPI can be abolished by use of bafilomycin and hence is dependent on a functioning V-ATPase. I next wished to determine if this would reverse the DPI-mediated changes in phagosomal morphology or have an impact on bacterial killing.

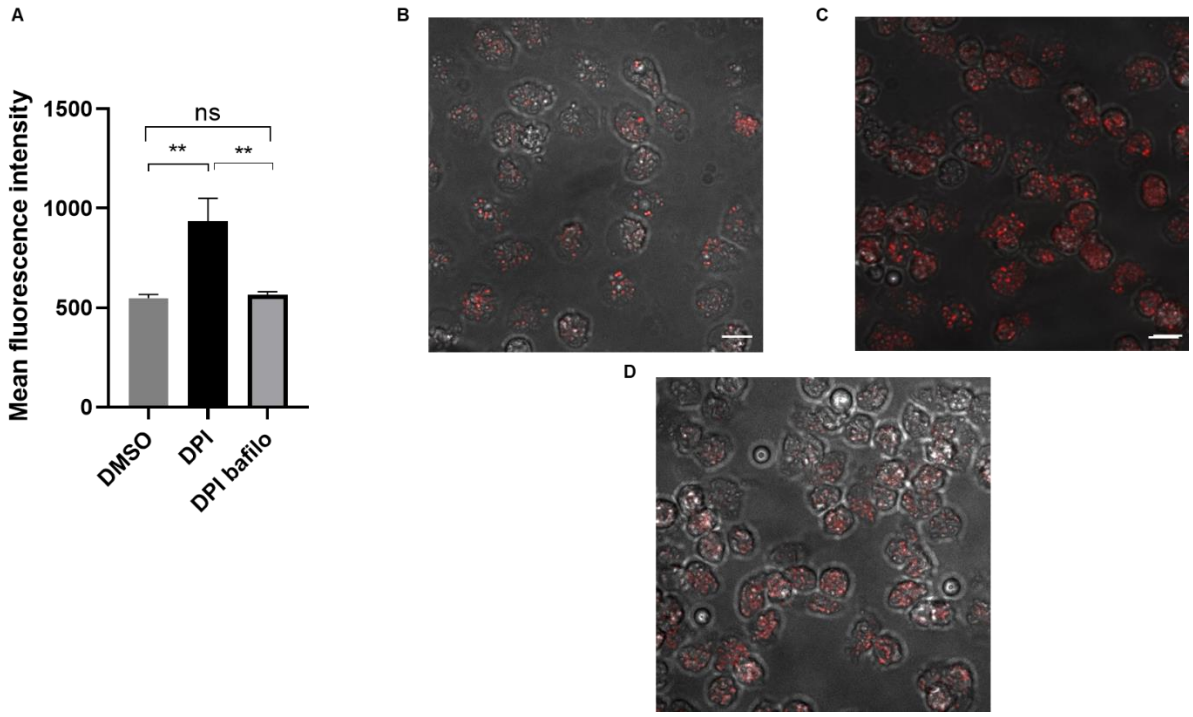

Figure 4.8 Effect of DPI and bafilomycin on neutrophil phagosomal acidification following ingestion of *S. aureus* SH1000

Bacteria were stained with pHrodo red pH-sensitive dye to assess intraphagosomal pH following phagocytosis of S. aureus SH1000. Neutrophils isolated by Percoll® gradient centrifugation (2.25 x 10^5 cells/180 µL) were placed onto 8-well glass bottom Ibidi chamber and allowed to adhere with of 0.1 µM bafilomycin or 0.01% DMSO vehicle present from the outset. DPI 2 µM or vehicle control (DMSO) was added at 50 min, and pHrodo Red stained S. aureus SH1000 (MOI 5) were added at 60 min. Samples were incubated for a further 1 h before imaging in real time by spinning disk confocal microscope at 60 x oil immersion magnification. ***(A)****. Images acquired after 1 h co-incubation were quantified using an Image J macro, and data represent mean fluorescence intensity (MFI) from n=3 independent experiments with measurement from 3 randomly selected fields of view per experiment, ns p=0.9971 DMSO control vs DPI with bafilomycin, **p=0.0012 DMSO vs DPI, **p=0.0019 DPI vs DPI with bafilomycin, One-way ANOVA with Sidak's multiple comparison.* ***(B – D).*** *Representative images of DMSO* ***(B)*** *DPI* ***(C)*** *and DPI plus bafilomycin treated cells* ***(D).*** *Scale bars are 10 µm.*

4.1.8 Bafilomycin does not alter phagosomal morphology of DPI- treated neutrophils following ingestion of *S. aureus*

I considered that the V-ATPase might mediate the effects of DPI on phagosomal morphology either directly or indirectly via the alteration in pH. Therefore, the morphology of phagosomes with ingested *S. aureus* was examined in the context of dual inhibition with DPI and bafilomycin. As previously, neutrophils isolated using Percoll® density gradient centrifugation were placed in 8-well glass bottom Ibidi chamber at 2.25 x 10^5 cells/180 µL and incubated with 0.1 µM bafilomycin or 0.01% DMSO vehicle control. Two µM DPI or vehicle control were added at 50 min and *S. aureus* SH1000 (MOI 5) at 1 h, and co-incubated with neutrophils for another 1h. Randomly chosen fields were imaged and the number of neutrophils containing spacious phagosomes was manually counted from DMSO controls, DPI-treated, and bafilomycin and DPI-treated samples (Fig. 4.9.A). There were significantly fewer (****p<0.0001 for DPI and bafilo DPI) spacious phagosome-positive neutrophils in DPI- and bafilo DPI-treated samples in comparison to DMSO controls (4.38 ± 0.82%, 3.58 ± 0.4% and 46.92 ± 4.2%, respectively). These differences can be clearly seen on the representative microscopic micrographs of neutrophils with ingested bacteria (visible in red), clearly distinguished by their size and shape with bright-field imaging (Fig. 4.9.B-D). Increase of magnification of cells in ImageJ software confirmed lack of spacious phagosomes in DPI- and bafilomycin plus DPI- treated neutrophils, to those (white arrows, Fig. 4.9.B) in DMSO control cells. Given there were no differences observed when bafilomycin was added to DPI, it seems likely that DPI alone has a maximal effect.

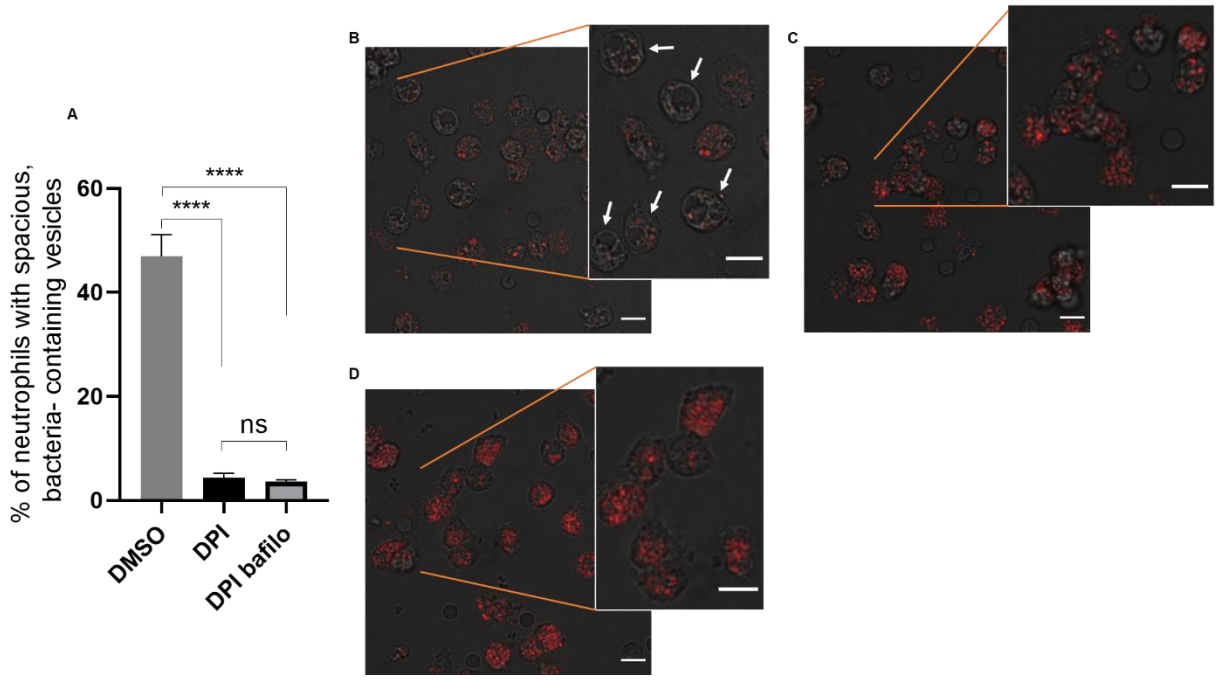

Figure 4.9 Effect of DPI and bafilomycin on phagosomal morphology

(A). *Neutrophils isolated by Percoll® gradient centrifugation (2.25 x 10^5 cells/180 µL) were placed onto 8-well glass bottom Ibidi chamber and allowed to adhere with addition bafilomycin 0.1 µM or 0.01 % DMSO vehicle control. DPI 2 µM or DMSO vehicle control was added at 50 min, and pHrodo Red- stained S. aureus SH1000 (MOI 5) were added at 60 min. Samples were incubated for a further 1 h before imaging by spinning disk confocal microscope at 60 x oil immersion magnification. The number of neutrophils containing spacious phagosomes was manually quantified from n=3 independent experiments from 3 different randomly selected fields of view per sample. Data represent percentage of neutrophils with spacious SH1000-containing phagosomes at 1 h post infection, One-way ANOVA with Sidak's multiple comparison test **** p<0.0001 DPI vs DMSO and DPI bafilo vs DPI; ns p= 0.99.* ***(B, C, D).*** *Representative images of DMSO control neutrophils containing spacious phagosome pointed with white arrows* ***(B)****, DPI* ***(C),*** *DPI and bafilomycin* ***(D)*** *treated cells without those vesicles. Scale bars are 10 µm.*

4.1.9 Effect of bafilomycin on killing of *S. aureus* SH1000 by DPI-treated neutrophils

Next, I wished to assess whether abolishing the effect of DPI on phagosomal pH with bafilomycin reversed the impairment of neutrophil-mediated killing of *S. aureus* seen with this oxidase inhibitor. Neutrophils (2.25 x 10^5 cells/180 µL) were pre-incubated with addition of bafilomycin (0.1 µM) and allowed to sediment to the bottom of 96-well plates. At 50 min, DPI (2 µM) or DMSO control (0.01%) were added followed by addition of SH1000 at MOI 5 at 1 h. After a further 30 minutes of co-incubation (t=0 min), gentamicin at 40 µg/mL was added to kill extracellular bacteria, and intracellular survival was assessed at 0, 60 and 120 min by the Miles and Misra method (Fig. 4.10). As previously, DPI markedly impaired the ability of neutrophils to kill ingested bacteria. However, the addition of bafilomycin to DPI treated cells did not restore the rate of killing of bacteria compared with cells only DPI treated at 60 min (188970 ± 54975 CFUs to 193407 ± 41436 CFUs), and 120 min (135411 ± 32550 CFUs to 71942 ± 15177 CFUs). This indicates that the ability of DPI to prevent neutrophil-mediated intracellular killing of *S. aureus* is not mediated by the change in pH it induces.

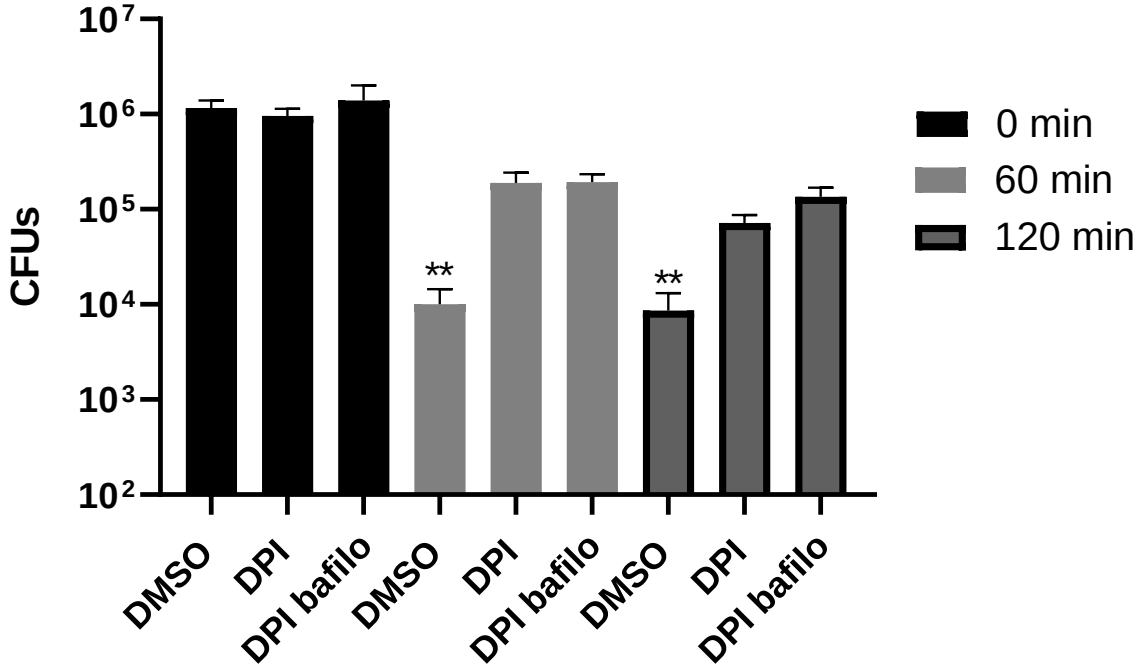

Figure 4.10 Effect of bafilomycin on killing SH1000 by DPI-treated neutrophils

*Neutrophils isolated by Percoll® gradient centrifugation (2.25 x 10^5 cells/180 µL) were placed into 96 well plates with addition of 0.1 µM bafilomycin. DPI 2 µM or vehicle control (0.01% DMSO) was added at 50 min, and S. aureus SH1000 (MOI 5) were added at 60 min. After 30 min of co-incubation, gentamicin at 40 µg/mL was added to kill extracellular bacteria (t=0 on the graph). At each timepoint (0, 30 and 180 min), samples were spun down and neutrophils were lysed with alkali water prior to quantifying bacterial numbers using the Miles and Misra method. Data represent mean of CFUs from n=5 independent experiments. **p= 0.0022 for DMSO vs DPI bafilomycin, **p= 0.0065 for DMSO vs DPI for 1 and 2 h tested by One-way ANOVA with Sidak's multiple comparison.*

4.1.10 Class I Phosphoinositide 3- kinase (PI3K) inhibitors constrain neutrophil ROS production in response to *S. aureus*

Activation of Class 1 PI3Ks leads to the production of phosphatidylinositol (4,5)-bisphosphate (PIP_3) from phosphatidylinositol (4,5)-bisphosphate (PIP_2) (Lehmann *et al.*, 2008). In addition to the ubiquitous isoforms PI3Kα and PI3Kβ, PI3Kγ and PI3Kδ are expressed in neutrophils where they are key to mediating the oxidative burst in response to soluble agonists (Condliffe *et al.*, 2005). In the setting of phagocytosis, generation of PIP_3 has been implicated in early events including closure of the phagocytic cup (Dewitt *et al.*, 2006); however the role of Class I PI3Ks in the oxidative burst at the phagosomal membrane in response to internalised *S. aureus* has been reported to be less important than that of the Class III PI3Ks (which generate PI3P) (Anderson *et al.*, 2008). Here, I investigated the role of Class I PI3-kinases in ROS production by human neutrophils against *S. aureus* SH1000 strain, by using 3 different inhibitors- IC87114 (PI3Kδ) at 10 µM, AS605240 (PI3Kγ) at 5 µM and LY294002 (PAN-class I PI3K inhibitor) at 20 µM. Briefly, neutrophils (2.25 x 10^5 cells/180 µL) were placed into an 8-well glass bottom Ibidi chamber, and after 30 min DCFDA (5 µM) was added to cells followed by the addition of DPI and PI3K inhibitors or vehicle control at 50 minutes. At 1 h, mCherry-labelled SH1000 were added to cells at MOI 5. Following a further 1 h of co-incubation, samples were imaged using the spinning disk confocal microscope (60 x, oil immersion). Images were quantified by the ImageJ macro for oxidised DCF, from two randomly chosen fields of view from each of n=3 independent experiments. As demonstrated in the Fig. 4.10.A, unexpectedly all of the PI3K inhibitors significantly inhibited ROS production as detected by oxidised DCF in close proximity to ingested staphylococci by neutrophils, in comparison to vehicle control. Inhibition of ROS production is shown visually in images (Fig. 4.10.B-F) by reduction of oxidised DCF (green) signal in samples where inhibitors were used relative to DMSO controls. DPI treated cells (Fig. 4.10.C) were used as a positive control and inhibited the generation of ROS more completely (Fig. 4.10.A). I next wanted to establish whether inhibitors of ROS by which act via a different mechanism to DPI (i.e., via inhibition of PI3Ks) also affected phagosomal morphology.

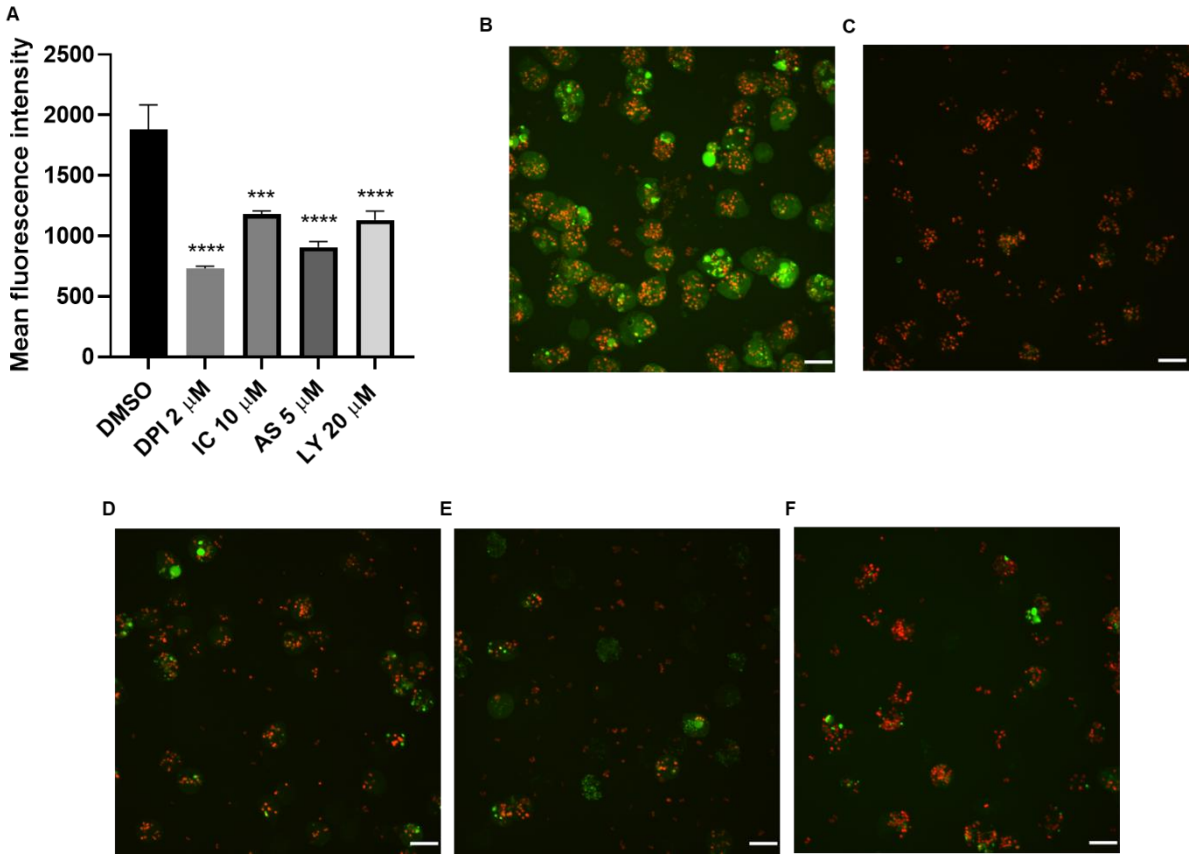

Figure 4.11 Class I PI3K inhibitors reduce *S. aureus* SH1000-induced neutrophil ROS production

(A). *Neutrophils isolated by Percoll® gradient centrifugation (2.25 x 10^5 cells/180 µL) were placed onto 8-well glass bottom Ibidi chamber and allowed to adhere. DCFDA 5 µM (or vehicle control 0.01% DMSO) was added after 30 min and DPI 2 µM or PI3K inhibitors IC87114 (10 µM), AS605240 (5 µM) LY294002 (20 µM) or DMSO vehicle control at 50 min, and finally mCherry S. aureus SH1000 (MOI 5) were added at 1 h. Following a further 1 h co-incubation, imaging was undertaken using a spinning disk confocal microscope at 60 x oil immersion magnification. Images were quantified using an Image J Macro, and data represent fluorescein mean fluorescence intensity (MFI) from n=3 independent experiments with measurement from 2 randomly chosen fields of view per experiment, ***p= 0.003 DMSO control vs IC 10 µM, ****p<0.0001 for vs DMSO control, tested by One-way ANOVA with Sidak's multi comparison test.* ***(B–F).*** *Representative images of DMSO* ***(B)*** *DPI 2 µM* ***(C)*** *IC87114 10 µM* ***(D)*** *AS605240 10 µM* ***(E)*** *and LY294002 20 µM* ***(F)*** *treated neutrophils containing phagocytosed red mCherry bacteria; the green signal (oxidised DCF) represents ROS production within neutrophils. Scale bars are 10 µm.*

4.1.11 PI3K inhibitors alter phagosomal morphology following staphylococcal infection

Inhibition of ROS production by DPI markedly reduced the formation of spacious phagosomes. Since the PI3K inhibitors also decreased ROS production, I explored their impact on phagosomal morphology.

The 3 different inhibitors- IC87114 (PI3Kδ) at 10 µM, AS605240 (PI3Kγ) at 5 µM and LY294002 (PAN-Class 1 PI3K inhibitor) at 20 µM were used. Neutrophils (2.25×10^5 cells/180 µL) were placed onto 8-well glass bottom Ibidi chamber, and at 50 min DPI, and PI3K inhibitors or vehicle control (0.01% DMSO) were added, followed by the addition of mCherry SH1000 MOI 5 at 1 h. Following a further 1 h of co-incubation, samples were imaged and the percentage of neutrophils containing spacious phagosomes was manually quantified from 3 randomly chosen fields of view (around 30-40 neutrophils per field of view, Fig. 4.11). As demonstrated in Fig. 4.11.A, (representative images Fig. 4.11.B-F), all of the inhibitors used significantly reduced the spacious phagosome formation in neutrophils in response to *S. aureus* SH1000. This data suggests that the oxidative burst at the phagosomal membrane might be linked to the phagosomal morphology, and that inhibiting this process reduces the enlargement of phagosomes to the ‘spacious’ morphology.

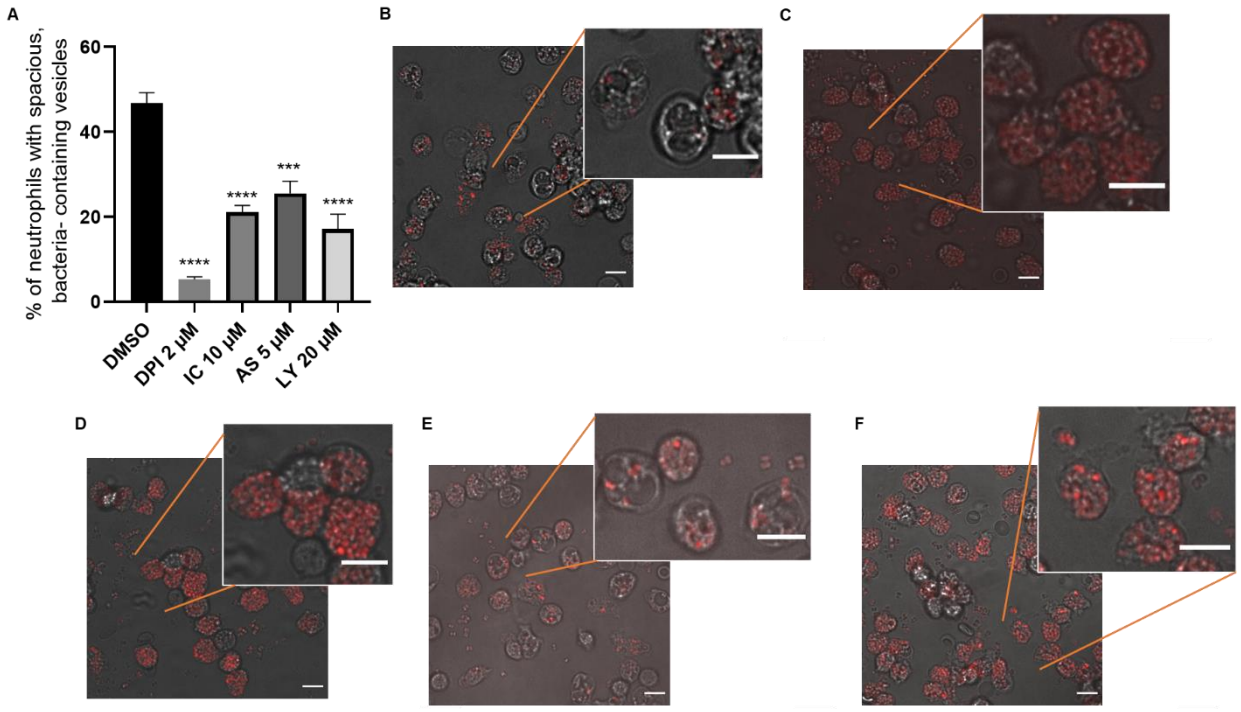

Figure 4.12 Effect of Class I PI3K inhibitors on phagosomal morphology of neutrophils-containing *S. aureus* SH1000

(A). *Neutrophils isolated by Percoll® gradient centrifugation (2.25 x 10^5 cells/180 µL) were placed onto 8-well glass bottom Ibidi chamber and allowed to adhere. DPI 2 µM or PI3K inhibitors IC87114 (10 µM), AS605240 (5 µM) LY294002 (20 µM) and 0.01% DMSO vehicle control were added at 50 min, and mCherry S. aureus SH1000 (MOI 5) were added at 60 min. Following a further 1 h co-incubation, imaging was undertaken using spinning disk confocal microscope at 60 x oil immersion magnification. After 1 h of co-incubation the number of neutrophils containing spacious phagosomes was manually quantified from n=3 independent experiments. Data represent percentage of neutrophils with spacious SH1000-containing vesicles at 1 h post infection, ***p= 0.004 DMSO control vs AS 5 µM, ****p<0.0001 for the rest vs DMSO control, tested by One-way ANOVA with Sidak's multi comparison test.* ***(B–F).*** *Representative images of DMSO* ***(B)*** *DPI 2 µM* ***(C)*** *IC87114 10 µM* ***(D)*** *AS605240 10 µM* ***(E)*** *and LY294002 20 µM* ***(F)*** *neutrophils containing phagocytosed red bacteria. Scale bars are 10 µm.*

4.1.12 Class I PI3K inhibitors do not impact the pH of ingested *S. aureus* SH1000

I observed restrained ROS production and fewer spacious phagosomes when the PI3K inhibitors were used. Since bafilomycin reversed the DPI-induced changes in phagosomal pH but not morphology, I next tested the effect of PI3K inhibitors on the acidification of intraphagosomal *S. aureus* SH1000.

IC87114 (PI3Kδ) at 10 µM, AS605240 (PI3Kγ) at 5 µM and LY294002 (PAN-Class 1 PI3K inhibitor) at 20 µM were used as previously. Neutrophils (2.25×10^5 cells/180 µL) were placed onto 8-well glass bottom Ibidi chamber and at 50 min DPI, and PI3K inhibitors or 0.01% DMSO vehicle control were added, followed by the addition of pHrodo Red-stained SH1000 MOI 5 at 1 h. Following a further 1 h of co-incubation, samples were imaged, and the MFI of the pHrodo signal (532 nm) was quantified using a macro in ImageJ of ingested bacteria from 4 independent experiments. As demonstrated in Fig. 4.12.A, (representative images Fig. 4.12.B-F), out of all the used PI3K inhibitors none caused any pH changes in intracellular *S. aureus* SH1000 compared to controls. As shown previously, DPI significantly increased the MFI of pHrodo in comparison with controls (**p*=0.02).

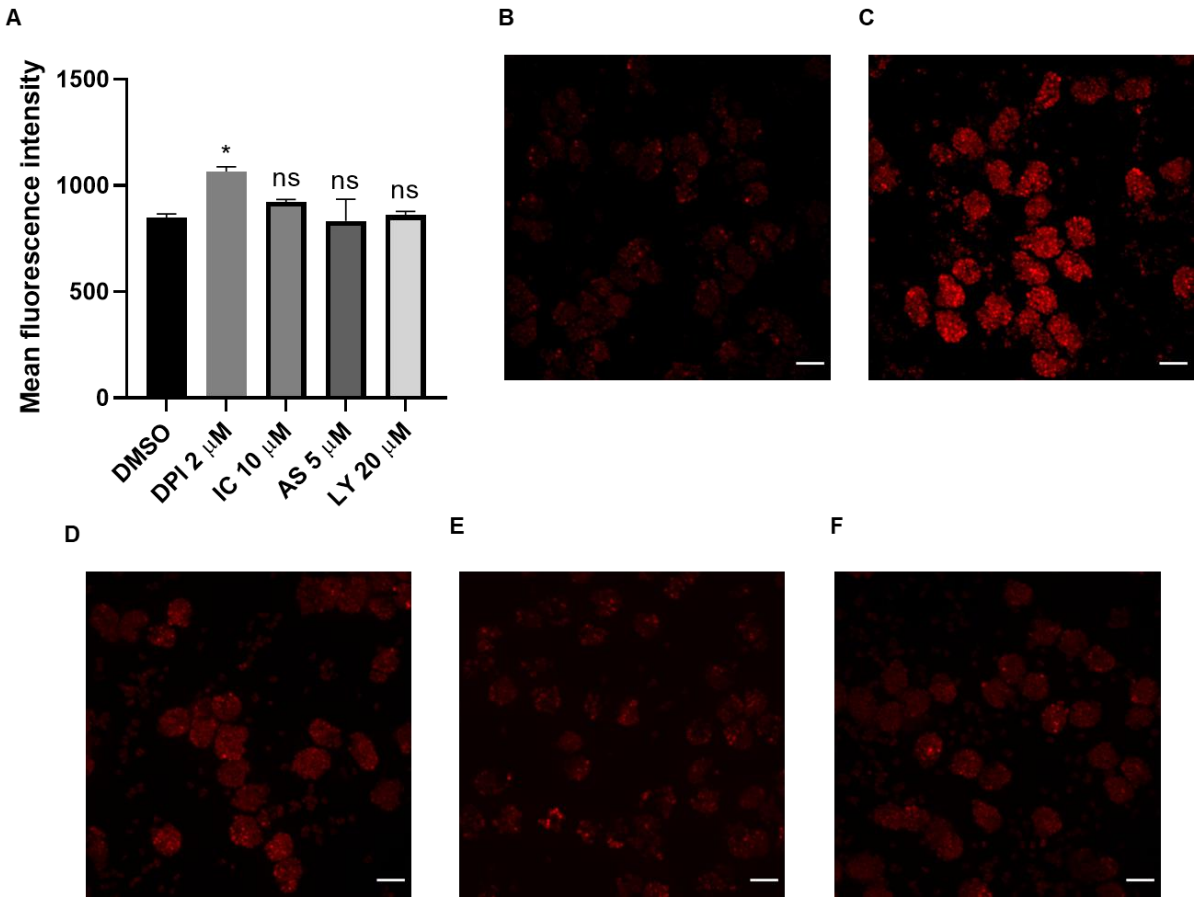

Figure 4.13 Effect of Class I PI3K inhibitors on phagosomal pH of *S. aureus*

(A). *Neutrophils isolated by Percoll® gradient centrifugation (2.25 x 10^5 cells/180 µL) were placed onto 8-well glass bottom Ibidi chamber and allowed to adhere. DPI 2 µM or PI3K inhibitors IC87114 (10 µM), AS605240 (5 µM) LY294002 (20 µM) and 0.01% DMSO vehicle control were added at 50 min, and pHrodo Red stained S. aureus SH1000 (MOI 5) were added at 60 min. Following a further 1 h co-incubation, imaging was undertaken using spinning disk confocal microscope at 60 x oil immersion magnification. After 1 h of co-incubation, the MFI of red signal was read using a macro in ImageJ from n=4 independent experiments. Data represent MFI of pHrodo Red signal of SH1000-containing vesicles at 532 nm wavelength at 1 h post infection, *p=0.02 DMSO control vs DPI 2 µM, ns p=0.75 DMSO control vs IC 10 µM, ns p=0.99 DMSO control vs AS 5 µM and LY 20 µM, tested by One-way ANOVA with Sidak's multi comparison test.* ***(B–F).*** *Representative images of DMSO* ***(B)*** *DPI 2 µM* ***(C)*** *IC87114 10 µM* ***(D)*** *AS605240 10 µM* ***(E)*** *and LY294002 20 µM* ***(F)*** *neutrophils, ingested red bacteria. Scale bars are 10 µm.*

4.1.13 VPS34 inhibition modulates neutrophil ROS production in response to *S. aureus* ingestion

The vacuolar protein sorting 34 (VPS34) is the sole class III PI3K; its function is to phosphorylate phosphatidylinositol (PI) at endosomal membranes to form phosphatidylinositol 3-phosphate (PI3P), PI3P regulates membrane trafficking by recruiting a subset of proteins which possess PI3P-binding phox homology (PX) domains, thereby regulating a range of intracellular processes such as autophagy. VPS34 is recruited to the phagosomal membrane (Ellson *et al.*, 2001), where it generates PI3P and thereby recruits the NADPH oxidase component $p40^{phox}$ to initiate the oxidative burst (Ellson *et al.*, 2006). It has been demonstrated that the potent inhibitor VPS34-IN1 used in this study is very selective and does not significantly inhibit the activity of Class I or class II PI3Ks (Bago *et al.*, 2014; Lindmo and Stenmark, 2006). I speculated that it would modulate the NADPH oxidase, phagosomal morphology and phagosomal pH in view of its reported impact on the oxidase and intracellular trafficking.

Firstly, the impact of the VPS34 inhibitor was tested on neutrophil ROS production in response to staphylococcal ingestion. Neutrophils isolated by EasySep™ were resuspended in RPMI/FBS/HEPES medium and distributed into 8-well glass bottom Ibidi chamber at 2.25 x 10^5 cells/180 µL per each well with addition of VPS34-IN1 at 1, 5 and 10 µM. At 30 min, 5 µM DCF was added to enable ROS detection, and at 1 h pHrodo Red stained *S. aureus* SH1000 were added to neutrophils at MOI 5. Following 30 min of co-incubation, samples were imaged, and images were analysed (ImageJ) (Fig. 4.13.A). VPS34-IN1 led to a concentration-dependent inhibition of staphylococcal induced neutrophil ROS detection, that was not significant at 1 µM but reached significance at 5 and 10 (p=0.014 and p=0.027 versus DMSO controls respectively). Both the quantification and representative images are shown in Figure 4.13 below (Fig. 4.13.A and 4.13.C-E respectively).

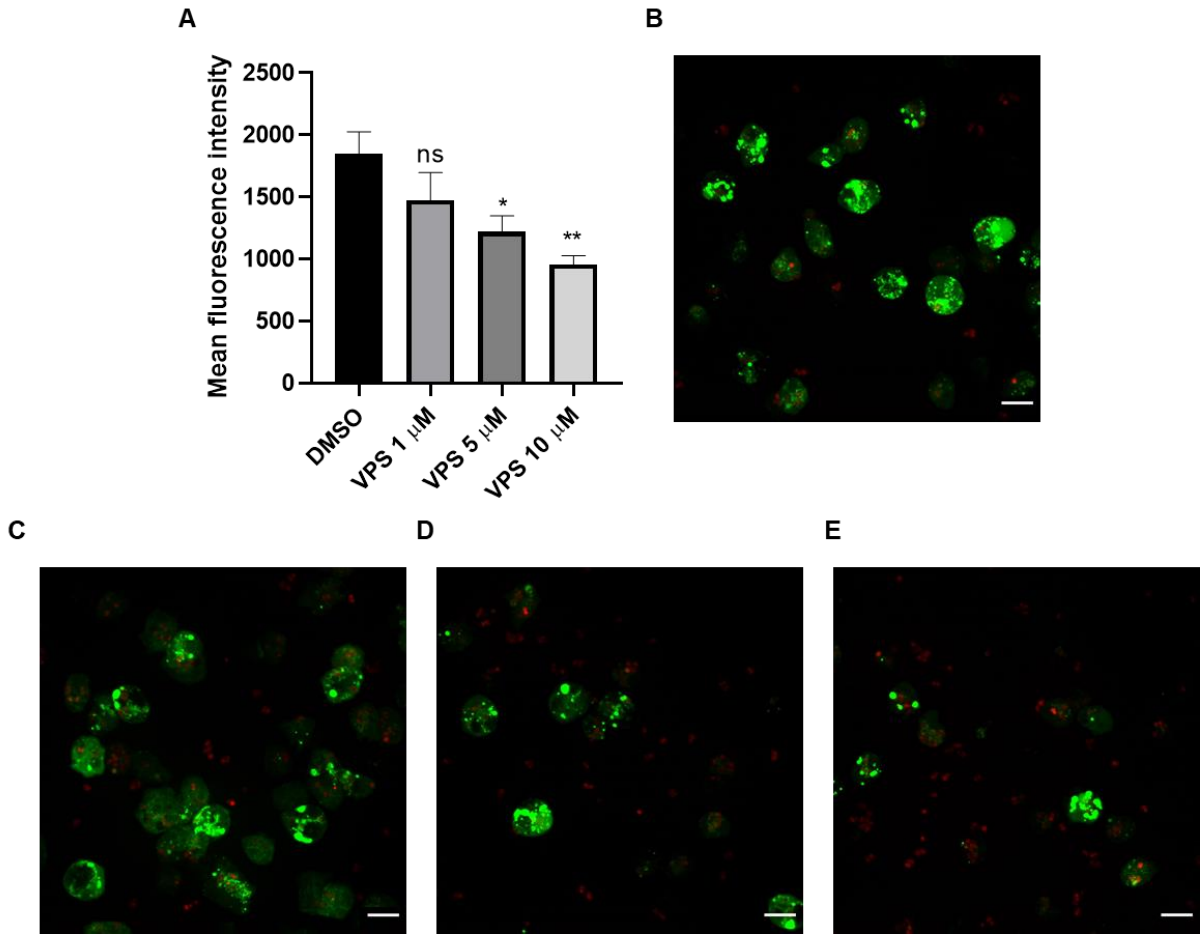

Figure 4.14 Impact of VPS34 inhibitor on ROS production by neutrophils in response to *S. aureus* SH1000

(A). *Neutrophils isolated by EasySep™ (2.25 x 105 cells/180 µL) were placed onto 8-well glass bottom Ibidi chamber with addition of VPS34 inhibitor (VPS34-IN1) at 1, 5 and 10 µM concentration or vehicle 0.01% DMSO controls and allowed to adhere. DCF 5 µM (or vehicle control DMSO) was added after 30 min, and pHrodo Red stained S. aureus SH1000 (MOI 5) were added at 60 min. Following a further 1 h co-incubation, live imaging was undertaken using spinning disk confocal microscope at 60 x oil immersion magnification. Images were quantified using an Image J Macro, and data represent fluorescein mean fluorescence intensity (MFI) from n=3 independent experiments with measurement from 2 randomly chosen fields of view per experiment, **p= 0.0014, *p= 0.0273, ns p= 0.2874, tested by One-way ANOVA with Sidak's multi comparison test.* ***(B, C, D, E****). Representative images of neutrophils treated with DMSO,* ***(B)*** *VPS 1 µM* ***(C)*** *VPS 5 µM* ***(D)*** *VPS 10 µM; green signal is oxidised DCF and red pHrodo-stained bacteria. Scale bars are 10 µm.*

4.1.14 VPS34 inhibition modulates neutrophil phagosomal morphology

To confirm the link between ROS generation and phagosomal morphology, I assessed the impact of VPS34 inhibition on this property. Neutrophils isolated by EasySep™ were placed onto 8-well glass bottom Ibidi chamber with VPS34-IN1 (1 -10 µM) or 0.01% DMSO vehicle control with *S. aureus* (MOI 5) added at 1 h exactly as previously. Samples were imaged (spinning disk confocal microscope), and images were manually analysed to quantify the percentage of spacious phagosome-positive neutrophils from 30-40 neutrophils from 3 fields of view from n=3 independent experiments (Fig. 4.14.A). VPS34-IN1 significantly decreased the percentage of spacious phagosomes at all concentrations in a concentration-dependent fashion. 51.4 ± 1.9% control (DMSO) neutrophils contained spacious phagosomes, with this number falling to 32.51 ± 3.14%, 17.9 ± 0.32% and 7.42 ± 0.67 % at 1, 5 and 10 µM of inhibitor respectively (Fig. 4.14.A). Images from each treatment illustrate these observations, indicating a fall in the number of spacious phagosome- containing neutrophils with increasing concentration of VPS34 (Fig. 4.14.B- E).

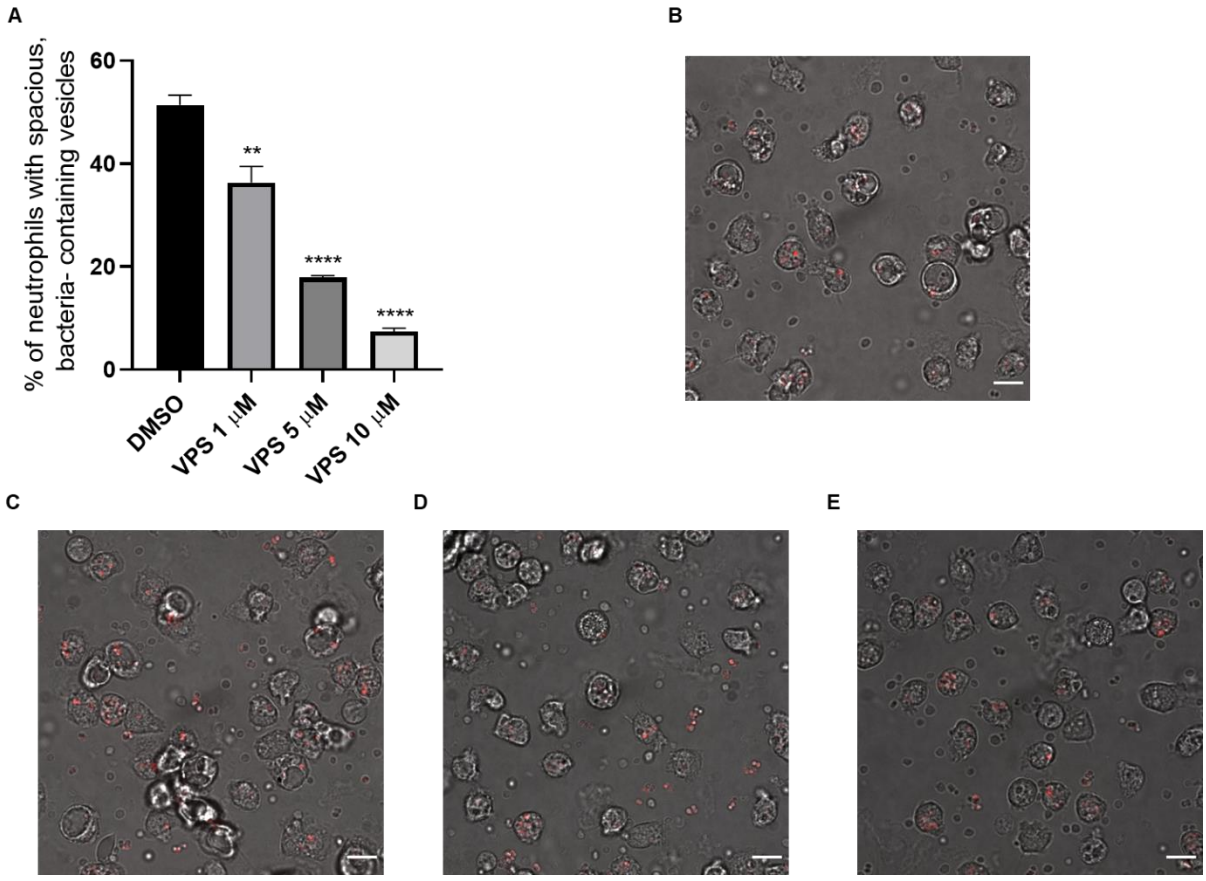

Figure 4.15 Effect of VPS34 inhibitor on phagosomal morphology of neutrophils containing *S. aureus* SH1000

(A). *Neutrophils isolated by EasySep™ (2.25 x 105 cells/180 µL) were placed onto 8-well glass bottom Ibidi chamber with addition of VPS34 inhibitor at 1, 5 and 10 µM concentration or vehicle 0.01% DMSO controls and allowed to adhere. pHrodo Red stained S. aureus SH1000 (MOI 5) were added at 60 min. Following a further 1 h co-incubation, live imaging was undertaken using spinning disk confocal microscope at 60 x oil immersion magnification. The number of neutrophils containing spacious phagosomes was manually quantified from n=3 independent experiments. Data represent percentage of neutrophils with spacious SH1000-containing vesicles at 1 h post infection, ****p< 0.001 for VPS 10 µM and 5 µM vs DMSO and **p= 0.0014 VPS34-IN1 1 µM vs DMSO tested with one-way ANOVA with Sidak's multiple comparison test.* ***(B, C, D, E)*** *Representative images of neutrophils and red bacteria of DMSO* ***(B)****, VPS34-IN1 1 µM* ***(C)****, VPS34-IN1 5 µM* ***(D)*** *and VPS34-IN1 10 µM* ***(E)****. Scale bars are 10 µm.*

4.1.15 VPS34 inhibition does not modify the pH of intra-phagosomal *S. aureus* SH1000

Previous studies with bafilomycin and Class I PI3K inhibitors have linked phagosomal formation to ROS production but not to changes in phagosomal pH. To determine whether VPS34 inhibition likewise affected phagosomal ROS and morphology without altering phagosomal pH, neutrophils isolated by EasySep™ in RPMI/FBS/HEPES were placed onto 8-well glass bottom Ibidi chamber (2.25 x 10^5 cells/180 µL) with VPS34-IN1 at 1, 5 and 10 µM or 0.01% DMSO vehicle control. pHrodo red stained *S. aureus* SH1000 were added to cells at 1h at MOI 5 and imaged after 1 h of co-incubation to assess intraphagosomal pH of bacteria using image J to quantify the MFI. (Fig. 4.15.A). There were no significant differences between treatments suggesting that inhibition of VPS34 does not change the pH of phagocytosed bacteria by neutrophils under the conditions of the experiment. It can be seen visually in the representative images (maximum intensity projections, Fig. 4.15.B-E) that the intensity of red bacteria is similarly low in each image, consistent with the bacteria being in a neutral environment within the neutrophils. The control of bacteria pH was measured by putting cells into acidic and neutral pH for the basis signal to be measured and analysed.

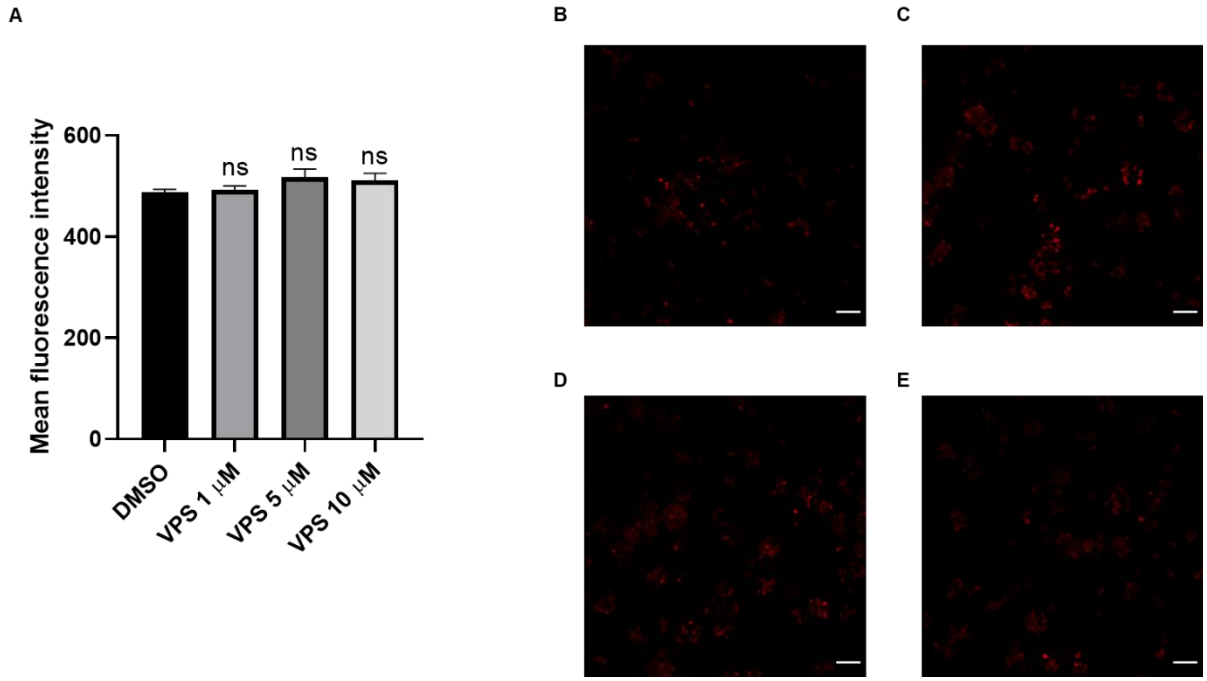

Figure 4.16 Lack of effect of VPS34 on intraphagosomal pH of neutrophils

(A) *Neutrophils isolated by EasySep™ (2.25 x 10^5 cells/180 µL) were placed onto 8-well glass bottom Ibidi chamber with the addition of 1, 5 and 10 µM VPS34 inhibitor or 0.01% DMSO vehicle control. After 1 h, pHrodo red stained SH1000 were added at MOI 5 for further co-incubation and imaged at 1 h using a spinning disk microscope at 60 x oil immersion magnification to quantify MFI of the red signal from intraphagosomal bacteria (532nm excitation wavelength). N=3, ns p= 0.48 for DMSO vs VPS 10 µM, ns p= 0.3 for DMSO vs VPS 5 µM and ns=0.98 for DMSO vs VPS 34-IN1 1µM; tested by One-way ANOVA with Sidak's multi comparison test.* ***(B, C, D, E)*** *Representative images of phagocytosed red bacteria by neutrophils treated with DMSO control* ***(B)****, VPS34-IN1 1 µM* ***(C)****, VPS34-IN1 5 µM* ***(D)*** *and VPS34-IN1 10 µM* ***(E)****; Scale bars are 10 µm.*

4.1.16 Inhibition of VPS34 enhances killing of *S. aureus*

The VPS34 inhibitor led to decreased ROS production and induced tight phagosome formation but did not affect the intraphagosomal pH generated by neutrophils in response to *S. aureus* infection. Here, the effect of this inhibitor was tested on neutrophil-mediated killing of *S. aureus* SH1000, with the anticipated outcome being that VPS34-IN1 would reduce neutrophil bactericidal capacity in keeping with its impact of ROS generation.

Briefly, isolated by EasySep^{TM} neutrophils (2.25 x 10^5 cells/90 µL) were preincubated in 96 well plates with VPS34-IN1 at 1, 5 and 10 µM for 1 h. After this time, *S. aureus* SH1000 at MOI 5 were added. A gentamicin protection killing assay was undertaken exactly as previously. Intracellular bacterial survival was determined at 60 and 180 min after addition of the antibiotic (Fig. 4.16) There were no significant differences in the number of internalised bacteria for any treatment at t=0 (an indirect measurement of phagocytosis), with similar number ~1400000 CFUs recovered with or without inhibitor at this time. At t=60 min, again no significant differences were observed between conditions. Surprisingly, all tested concentrations of VPS34-IN1 significantly increased the killing of *S. aureus* SH1000 (decreased numbers of surviving intracellular bacteria) at 180 min (Fig. 4.16) by approximately 24180 of intracellular CFUs (p=0.0005 for VPS-IN1 10 µM vs DMSO, p<0.0001 for VPS-IN1 5 and 1 µM vs DMSO). Neutrophils at this time appeared healthy and viable, although this was not formally assessed by quantifying apoptosis.

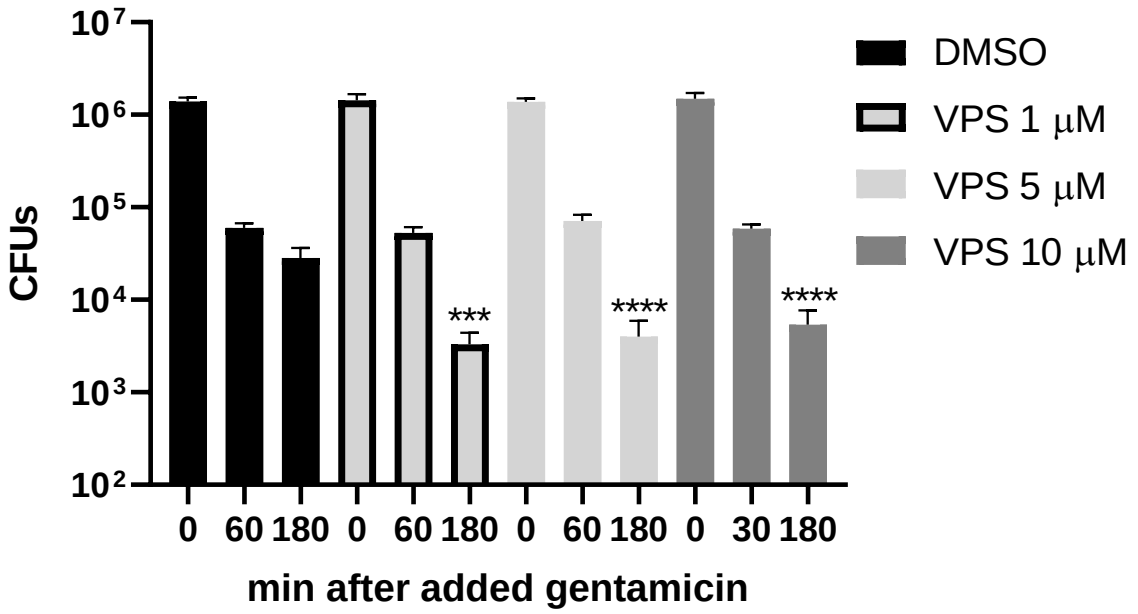

Figure 4.17 Effect of VPS34 Inhibition on killing of *S. aureus* by neutrophils

*Neutrophils isolated by the EasySep™ (2.25 x 10^5 cells/90 µL) were placed into 96 well plate with addition of VPS34 at 1, 5 and 10 µM for 1 h, when S. aureus SH1000 at MOI 5 were added. After 30 min, neutrophils were collected, lysed with alkali water, then plated to quantify the number of internalised bacteria (0 min on the graph); and 40 µg/mL gentamicin was added to the remaining samples to kill extracellular bacteria. After 60 and 180 min, the intracellular killing was measured by lysing neutrophils with alkali water and plating for quantification of CFU of surviving bacteria using Miles and Misra method. Data presented as CFUs from 4 independent experiments, ***p= 0.0005 for 180 min VPS34-IN1 10 µM vs 180 min DMSO, ****p<0.0001 for VPS34-IN1 5 and VPS34-IN1 1 µM vs 180 min DMSO; tested by One-way ANOVA with Sidak's multiple comparison test.*

4.2 **Discussion**

Results obtained in this chapter suggest a crucial role for neutrophil ROS production in both interactions with *S. aureus* and in shaping the phagosomal environment. In the previous chapter, I demonstrated that levels of hypoxia found in the setting of infections such as Staphylococcal abscesses inhibit the killing of these bacteria in a strain-dependent fashion, and that this is associated with inhibition of the generation of ROS (Fig.3.15). However, as noted the hypoxic chamber is not able to support microscopy of live cells, and fluorescent reporters such as DCF and pH-Rodo are not suitable for fixation (I attempted a number of fixation strategies including the use of paraformaldehyde and methanol, without success). Therefore, a pharmacological approach was adopted with the use of the NADPH oxidase inhibitor DPI, which recapitulated the hypoxic effect of inhibition of ROS formation by human neutrophils. I used *S. aureus* SH1000 for these experiments, as a range of mutants are available on this background and as hypoxia impaired killing of this strain (Fig. 3.12; see Section 2.5.1 in Materials and Methods).

In addition to treating neutrophils with DPI, I also tested the effect of different concentrations of DPI on *S. aureus* alone and found that 5 and 10 µM DPI (frequently used in the literature to inhibit neutrophil ROS generation) has a direct microbicidal effect (data not shown), which has been reported previously in the literature (Pandey *et al.*, 2017). Therefore, I used 2 µM DPI, which inhibited human neutrophil ROS production in response to ingestion of *S. aureus* SH100 in (Fig.4.1) with no effect on survival of staphylococci alone (not shown). DPI 2 µM impaired the intracellular killing of *S. aureus,* with more bacteria surviving within DPI- treated neutrophils (Figure 4.1). This finding is in keeping with the literature, however most authors have used a higher concentration of DPI (e.g., Hampton and Winterbourn, 1995 used 10 µM DPI, which might have had a direct bactericidal effect with the potential to confound the results).

Since DPI may affect bacteria as well as neutrophils, and DPI may have off-target effects, for example on nitric oxide synthase and hence the generation of reactive nitrogen species, I considered the use of apocynin as an alternative inhibitor. It has been reported that apocynin inhibits the formation of superoxide anion by NADPH oxidase in human neutrophils, the effect likely to be caused by blocking sulfhydryl groups (Simons *et al.*, 1990) and hence preventing the translocation of the cytosolic subunits to the membrane and assembly of a functional oxidase (Barbieri *et al.*, 2004).

Interestingly, although apocynin was previously reported to inhibit the oxidative burst (reduction in oxygen consumption and chemiluminescence) it did not seem to inhibit the killing of *S. aureus* in the same study (Stolk *et al.*, 1994). However, the strain of *S. aureus* was not specified, high MOI (10) was used, and gentamicin (or equivalent) was not used to kill non-ingested bacteria, hence this assay may have been confounded by an excess of non-phagocytosed organisms. Surprisingly, I found (Fig. 4.2) that apocynin led to significantly increased rather than decreased ROS production in response to phagocytosis of *S. aureus* SH1000, an effect not confined to one batch of this inhibitor (not shown). Similar findings were observed by other lab members testing this compound effect on ROS production in macrophages in response to staphylococcal infection (personal communication, Prof. Simon Foster). Apocynin was shown to increase ROS formation (detected by oxidation of DCFDA, as used in my experiments) in fibroblasts (non-phagocytic cells) (Vejrazka *et al.*, 2005). Vejrazka *et al*. tested if this finding might relate to and interaction pf apocynin with DCFDA, however there was no increase in fluorescent signal when apocynin was mixed with DCFDA in the absence of cells, and apocynin does not fluoresce in unstimulated cells. In the same study, the authors found that apocynin initially stimulated ROS production in macrophages fed opsonised zymosan (up to about 15 min) with subsequent inhibition. They suggested that in macrophages, the effect of apocynin depended on conversion to a dimer in a myeloperoxidase-dependent fashion; pre-activation of apocynin with horseradish peroxidase and hydrogen peroxide inhibited the oxidation of DCFH-DA in fibroblasts and in zymosan-ingesting macrophages (Vejrazka *et al.*, 2005). I attempted to pre-activate apocynin using identical methodology but the 'pre-activated' apocynin still enhanced ROS production in human neutrophils (data not shown). Hence, this compound was not used in further studies, but I did identify other inhibitors of ROS production at the phagosome in later experiments.

Interestingly, DPI had additional effects on human neutrophils in response to *S. aureus* infection. The staining of bacteria with the pH sensitive dye pHrodo Red revealed changes in pH within the phagosome following ingestion by neutrophils (the same change was not seen in non-internalised organisms). When the NADPH-oxidase was fully functional, the pH of intraphagosomal bacteria was not acidic but mildly alkaline, in keeping with the published literature (pH 7.5-8) (Levine *et al.*, 2015; Segal *et al.*, 1981). Although I initially included fluorescein as a pH indicator, it saturates at a pH of

~8 and above, was not generally used in a ratiometric manner, hence I used pH-Rodo for further studies. The alkalisation of ingested pathogens has been linked with the transport of potassium ions (Reeves *et al.*, 2002), together optimising conditions for activation of the neutral proteases released into the phagosome from the more acidic cytoplasmic granules. Activation of the NADPH oxidase results in the transport of electrons into the phagosome and hence membrane depolarisation, requiring charge compensation via the passage of cations into the vacuole which is at least in part mediated by the proton channel Hvcn1 (Levine *et al.*, 2015). I found that when the NADPH-oxidase was inhibited by DPI, bacteria within the phagosome were significantly acidified, further suggesting the important role of functional NADPH-oxidase in modulating intracellular pH in human neutrophils. Acidification of intracellular pathogens (*Candida albicans*) has been reported in human neutrophils treated with DPI and those obtained from patients with X-linked CGD (Foote *et al.*, 2019), although to my knowledge this has not previously been reported in the context of *S. aureus*.

My results suggest that *S. aureus* are efficiently killed by healthy neutrophils, a process which is impaired when the NADPH oxidase is inhibited or when there is a restricted amount of molecular oxygen in hypoxia to prevent an effective oxidative burst. The activation of the microbicidal responses of neutrophils, upon stimulation leads to proton/ H^+ generation (Grinstein and Furuya, 1986). In order to maintain the cytosolic pH at the physiological level, cells must activate a number of H^+ extrusion mechanisms. One of them, an ATP-dependent H^+ pump which belongs to the vacuolar (V^-) class of ATPases, also stimulated upon neutrophils activation (Nanda *et al.*, 1992) is sensitive to macrolide antibiotics such as bafilomycin or concanamycin (Bowman *et al.*, 2004). High, local ROS production has been shown to prevent the accumulation of V-ATPase on neutrophil phagosomes (El Chemaly *et al.*, 2014) hence recruitment of the V-ATPase would be expected to be enhanced by DPI, potentially accounting for the change in pH. Therefore, I tested the impact of inhibition of this pump with bafilomycin alone and together with DPI inhibitor. Used alone, bafilomycin did not have any effect on intracellular pH of *S. aureus* or on phagosomal morphology or ROS production in human neutrophils (Fig. 4.7). However, when used together with DPI, bafilomycin prevented the DPI-induced acidification of bacteria, but did not change the killing of bacteria in DPI-treated neutrophils. This finding is in keeping with the data of

El Chemaly *et al*. (2014) suggesting that ROS limit the changes in phagosomal pH by impairing the recruitment of V-ATPase to the phagosome. These results also suggest that the acidification of phagosomal environment by DPI (and by implication, by hypoxia also) does not play a role in the survival of *S. aureus*. This is consistent with the finding that extracellular *S. aureus* is resistant to acidification and can survive in a wide range of pH (Bore *et al.*, 2007). It may also suggest that neutrophil neutral proteases are less important in killing *S. aureus* than ROS, or that the changes in pH are not sufficient to perturb the function of the relevant proteases involved in *S. aureus* killing, although this was not specifically explored.

When the NADPH-oxidase was fully operational in human neutrophils, *S. aureus* were mostly enclosed within spacious phagosomes. However, when NADPH-oxidase was inhibited by the use of DPI or when ROS production was substantially reduced by hypoxic incubation or other inhibitors, bacteria were found predominantly within tight phagosomes. Similar observations were made by Prajsnar *et al*. using a zebrafish model with cyba/p22^{phox} knockdown or DPI treatment, both of which promoted tight phagosome formation in neutrophils in response to staphylococcal infection (Prajsnar *et al.*, 2021). They proposed the model that when the NADPH oxidase and phagosomal ROS generation are inhibited, bacteria are found in tight, more acidic phagosomes. However, although in this model reduced ROS generation was associated with early (1 and 3 h) failure to kill ingested *S. aureus*, at later time points fish lacking a functional oxidase exhibited longer survival and fewer CFU of *S. aureus*, a finding which is not in keeping with the known susceptibility of humans with CGD to severe Staphylococcal infection or with my data in human neutrophils after more prolonged hypoxic incubation (Figure 3.12.). It is possible that this relates to a difference between human and zebrafish neutrophils.

Stimulation of a neutrophil G-protein coupled FPR receptor with the bacterial formylated peptide fMLP (N-formyl-methionyl-leucyl-phenylalanine) leads to stimulation of Class I phosphatidylinositol (PI)3-kinases (PI3Ks) at the plasma membrane and consequent generation of the ephemeral phospholipid second messenger PIP_3. Class 1 PI3K is involved in cellular signalling of superoxide anion production in neutrophils in response to soluble agonists (Traynor-Kaplan *et al.*, 1989; Coffer *et al.*, 1998; Condliffe *et al.*, 2005), with a reported lesser role in response to ingested bacteria (Anderson *et al.*, 2008). In this study, I tested the role of Class 1

PI3K inhibitors on ROS formation in human neutrophils in response to staphylococcal infection. In contrast to the results of Anderson *et al.*, I found that inhibitors selectively targeting PI3Ks ɣ and δ, as well as a pan-Class 1 PI3K inhibitor, all significantly inhibited ROS production associated with *S. aureus* ingestion (Fig. 4.11). These apparently conflicting results may reflect the significant methodological differences between the studies. Firstly, Anderson *et al*. used the Wood 46 strain, opsonised with serum (which will result in engagement of CD18 and Fcɣ receptors during phagocytosis), and they also primed their neutrophils with TNF/GMCSF; additionally, these investigators assessed ROS generation with luminol-dependent chemiluminescence, which may be more specific for NADPH oxidase activity than DFCDA oxidation. Finally, I used a higher concentration of the inhibitor IC87114 (5 µM versus 500 nM); it is possible the higher concentration led to off-target effects, or the lower concentration did not fully inhibit the target (or both). PI3Kɣ is activated predominantly by G-protein coupled receptors and hence would be unlikely to be activated by bacterial ingestion, hence it is possible the effect of AS605240 in my study was off-target or that was in some way activated by my experimental conditions (e.g., by the paracrine secretion of IL-8; Ryu *et al.*, 2004) However, importantly in my study all of the tested inhibitors led to significant decrease in spacious phagosome formation, data that correlate with the inhibitory effect of these compounds on ROS production (Fig. 4.12). This strongly suggests that the impact of DPI on phagosomal morphology is due to inhibition of the NADPH oxidase, rather than to an off-target effect. However, inhibition of any specific or all class 1 PI3Ks did not alter intraphagosomal pH of *S. aureus*. The impact of the Class 1 PI3K inhibitors on ROS generation was less complete than that of DPI, hence it is possible that this degree of inhibition was insufficient to impair the recruitment of the V-ATPase. It is also possible that the PI3K inhibitors were reducing the generation of other ROS such as nitric oxide (Manda-Handzlik *et al.*, 2020). The concentrations of those Class 1 PI3K inhibitors, used in this study, were based on those widely used in the literature, however I cannot exclude the possibility of off-target effects; in particular the isoform-selective inhibitors are not isoform specific. In most cases the IC_{50} are determines by *in vitro* kinase measurements and do not account for the requirement for diffusion into cells. For instance the *in vitro* IC_{50} for LY294002 is about 500 nM but in a cell based assays the *in vivo* IC_{50} has been estimated at 10 µM (Davies *et al.*, 2000), close to the

concentration that I used. The IC50 for IC87114 is similar and hence the use of 5 µM seems reasonable; this concentration of IC87114 inhibited late (60 s) but not early (6 s) ROS generation in human neutrophils suggesting it does not suppress all PI3K activity at this concentration (Condliffe *et al.*, 2005). The in vitro IC50 for AS605420 is about 8 nM so it is possible that the use of 5 µM of this compound led to some off-target effects, however taking the overall pattern of the PI3K inhibitors together it seems reasonable to conclude that the impact of phagosomal morphology was related to inhibition of the NADPH oxidase due to impaired PIP3 generation. Overall, the impact of NADPH activation on phagosomal pH and morphology and how these factors impact on bacterial killing is incompletely understood and requires further study. Possible interplay with autophagy and LC3-associated phagocytosis are further discussed in the overall discussion in Chapter 6; unfortunately, my attempts to investigate this further were hindered by the fact that several antibodies to LCIII, rubicons and others bound *S. aureus* avidly, hence all phagosomes stained brightly in all conditions, and western blotting of neutrophils that had ingested *S. aure*us for these proteins could not be interpreted (data not shown).

In full agreement with Anderson *et al*., I found that Class III PIK3K (VPS34) inhibitor VPS34-IN1 reduced ROS production in human neutrophils in a concentration-dependent manner in response to *S. aureus* infection (Fig. 4.13). It has been previously shown that PI3P produced by VPS34 regulates NADPH oxidase activity by binding the $p40^{phox}$ homology (PX) domain at its N-terminus (Ellson *et al.*, 2001; Ov *et al.*, 2001). Mutation in the PX domain of $p40^{phox}$ which prevented PI3P binding markedly decreased in phagosomal ROS (Matute *et al.*, 2009; Ellson *et al.*, 2006; Tian *et al.*, 2008). Human CGD patients with $p40^{phox}$ mutations are very rare, the first case of autosomal recessive CGD due to mutation of the NCF4 gene encoding $p40^{phox}$ were reported by Matute *et al*. in 2009. Neutrophils from the affected child were selectively deficient in phagocytosis-induced NADPH oxidase activity during phagocytosis of zymosan or serum-opsonised *S. aureus*, whilst extracellular oxidant production to soluble agonists (PMA or fMLF) was normal (Matute *et al.*, 2009). Neutrophils isolated from $p40^{phox}$ -/- mice demonstrated a 50% reduction in the expression of $p67^{phox}$ with oxidase responses to *S. aureus* reduced by approximately 75% (Ellson *et al.*, 2006). The maximal effect on ROS production above was in response to VPS34-IN1 used at 10 µM, decreasing ROS formation by about 40 % in human neutrophils in response to

S. aureus (Fig. 4.14). This difference may reflect incomplete inhibition of VPS34 and PI3P formation (PI3P may also be formed when PIP3 and other 3-phosphorylated lipids are de-phosphorylated) or differences in methodology used to assess the response.

Wood *et al*. investigated the role of VPS34 inhibition on phagosomal acidification. In contrast to my findings (Figure 4.15) that phagosomal pH was not affected by inhibition of the Class III PI3K, they reported a decrease in pHrodo signal, indicating higher pH of intracellular bacteria than in controls (Wood *et al.*, 2020); however this was in a flow-cytometric assay with trypan blue quenching of extracellular bacteria. It is possible that this methodological difference explains the different results. Furthermore, my results demonstrated that VPS34-IN1 increased staphylococcal killing by human neutrophils (Fig.4.17), whilst Wood et al. showed impairment of killing of *S. aureus* by the same VPS34-IN1 (Wood *et al.*, 2020). The difference observed could be due to variations in methodology. Wood *et al*. used a whole blood assay for phagocytosis and killing by human neutrophils, whereas work presented here was performed on isolated neutrophils. Whole blood assays are influenced by a range of factors including absorption of the inhibitor by red blood cells, and effects of other cell types. Also, the impaired killing of *S. aureus* reported by the Wood *et al*. was shown only at 2 h of co-incubation, in our study we saw significant effect only at a 3 h timepoint. It is possible that the longer co-incubation may result in more effective killing by VPS34IN1 treated neutrophils.

For the first time it has been shown in this study that VPS34 inhibition changes the phagosomal morphology of neutrophils following staphylococcal infection. There were significantly fewer spacious phagosomes found in VPS34-IN1-treated neutrophils in comparison with controls, a concentration-dependent effect that corresponded with the observed dose-dependent reduction in ROS production by this inhibitor. These findings confirm the key role of ROS production on the phagosomal morphology changes. However, there is discordance in the impact of VPS34-IN1 on ROS generation and phagosomal morphology (which are similar to the impact of DPI) and the opposing impact on bacterial killing. Staphylococcal killing is normally very tightly linked to ROS production and this result is both unexpected and unexplained. On n=1 occasion (not shown), I included DPI as a positive control and founded this inhibitor still impaired bacterial killing, suggesting the findings with VPS34 inhibition were not

due to a technical problem with the killing assay. It is possible that the incomplete inhibition of ROS production by the VPS34 inhibitor was insufficient to impair killing; indeed, this would be in keeping with the results of Hampton and Winterbourn, (1995). It is also possible that DPI inhibits nitric oxide generation and other oxidant pathways that are not affected by VPS34-IN1. Further studies would be of value, and interestingly another investigator has found that VPS34-IN1 promoted intracellular killing of *S. aureus* by a mouse macrophage cell line in an unbiased drug screen (Professor Alison Condliffe, personal communication).

Broadly, the data presented in this chapter support the role of ROS production in the intracellular killing of *S. aureus.* In keeping with my results (Chapter 3) showing that hypoxia impaired ROS production and bacterial killing, the chemical inhibition by DPI of the NADPH oxidase (and hence the ROS production) hindered the killing of staphylococci by human neutrophils. Inhibition of NADPH oxidase activity by a range of inhibitors and by hypoxia affected phagosomal morphology with smaller 'tight' as detected by both confocal and electron microscopy. The relationship of oxidase activity and bacterial killing with phagosomal pH was not consistent, suggesting the changes in phagosomal pH detected were not responsible for altered killing. However, the use of the VPS34 inhibitor, which decreases the accumulation of PI3P, reduced ROS production but improved bacterial killing in the setting of staphylococcal ingestion. VPS34-generated PI3P orchestrates the recruitment of a range of proteins involved in the trafficking of proteins to the membranes (Morris *et al.*, 2015; Donner, 2011). The role of VPS34 is broad, and includes autophagy regulation, as it interacts with the essential autophagy gene beclin1, which is critical for autophagosome biogenesis, maturation and apoptosis (Dowdle *et al.*, 2014). The relatively weak autophagy inhibitor hydroxychloroquine has a range of medical uses including treatment of infections (such as malaria), inflammatory diseases (rheumatoid arthritis, systemic lupus erythematosus) and as an adjunct in cancer treatment. There is strong interest in the development of class III PI3K inhibitors for medicinal purposes. The fact that my results suggest improved killing of a clinically relevant pathogen is of significant interest in this context. It is also conceivable, if my results can be recapitulated in (for example) animal models, inhibition of VPS34 could be combined with antibiotics in treatment-resistant staphylococcal infection. However, a further work will be required to investigate this possibility.

5 Exploring the role of staphylococcal virulence factors that combat oxidative stress in oxidative killing by human neutrophils

5.1 Introduction

Killing of ingested pathogens by neutrophils has long been known to be accompanied by a massive rise in non-mitochondrial respiration (Berton *et al.*, 1988). Knowledge of the respiratory burst and the mechanisms employed by bacteria to counter oxidative stress has been substantially expanded by exploring both neutrophils and *S. aureus.* These bacteria encode several antioxidant enzymes, including superoxide dismutases, catalases and peroxiredoxins which enable the pathogens to detoxify the superoxide anions (O_2^-), hydrogen peroxide (H_2O_2) and other ROS produced by host cells to in an attempt to avert intraphagosomal killing during infections (Imlay, 2003; Mishra and Imlay, 2012). Superoxide dismutases (SODs) are metalloproteins which catalyse dismutation (simultaneous oxidation and reduction) of O_2^- (produced by neutrophils by reduction of molecular oxygen during the oxidative burst), thereby converting O_2^- to H_2O_2 (hydrogen peroxide) and O_2 (Valderas *et al.*, 2002; Clements *et al.*, 1999). The SODs evolved to protect cells (both mammalian and bacterial) from direct damage from O_2^-, as well as indirect toxicity by prevention a Fe^{3+}- dependent catalytic reaction which leads to the production of •OH via the Haber-Weiss reaction (Haber *et al.*, 1934). *S. aureus* possesses two SOD-encoding genes, namely *sodA* and *sodM* (Clements *et al.*, 1999). Clements *et al.* observed that these enzymes combine to form three SOD ‘activity zones’ - two homodimers and a heterodimer (Clements *et al.*, 1999). Both SodA and SodM were found to be important in a murine abscess model and were required for nutritional immunity in *S. aureus* when manganese Mn^{2+} was restricted in the host during infection (Karavolos *et al.*, 2003; Garcia *et al.*, 2017). SodA is a manganese (Mn) cofactor enzyme (Clements *et al.*, 1999);it was crucial in oxidative stress resistance and virulence in a mice infection model in the presence of Mn, whereas SodM was the key factor in resistance to nutritional immunity when there is Mn starvation (Garcia *et al.*, 2017).

However, H_2O_2 derived from SOD activity is also a source of oxidative stress. Hydrogen peroxide is produced as a by-product of aerobic growth of bacteria (Imlay, 2003), and by the host in an oxidative response to the infection (Hampton *et al.*, 1996). Host H_2O_2 can kill intracellular pathogens, for instance through the reduction of H_2O_2 by Fe (II) and the subsequent formation of hydroxyl radicals and Fe (III). This Fenton

reaction leads to DNA damage, due to association of Fe (II) with nucleic acids (reviewed by Imlay, 2003). *In vivo* studies have shown that H_2O_2 causes DNA damage, and that this is reduced when the iron chelators are present (Imlay *et al.*, 1988; Repine *et al.*, 1981). Therefore, scavenging of H_2O_2 is important for bacterial aerobic survival. Catalase (KatA) detoxifies H_2O_2 and was suggested to be a major virulence determinant in *S. aureus,* as strains which produced low levels of KatA were more susceptible to neutrophil-mediated killing (Mandell, 1975). However, a single mutation of *katA* in *S. aureus* did not cause attenuation in a murine-abscess model of infection (Messina *et al.*, 2002). A previous study using *E. coli* demonstrated that H_2O_2-scavenging activity was retained in catalase mutants due to the presence of alkyl hydroperoxide reductase (AhpC) (Seaver and Imlay, 2001). Alkyl hydroperoxide reductase is a part of the peroxiredoxin family of enzymes with activity against H_2O_2, peroxynitrite and peroxides, its expression in *S. aureus* is regulated by the peroxide response regulator (PerR) (Horsburgh *et al.*, 2002). It was proposed that lack of attenuation in *katA* mutant of *S. aureus* could be due to compensatory activity of the PerR-dependent increase in *ahpC* (Cosgrove *et al.*, 2007). The PerR-regulated KatA and AhpC proteins have a compensatory function in cellular physiology as both are responsible for oxidative-stress resistance. *In vivo* both play important role in bacterial survival and persistence which can lead to easier dissemination, specifically in nasal colonisation (Cosgrove *et al.*, 2007). In the absence of SodA and SodM, it would be expected that there would be greater accumulation of the highly reactive O_2^- (although spontaneous dismutation does occur) with a consequent reduction in H_20_2, whilst in the absence of KatA and AhpC, H_20_2 would be expected to accumulate with the potential to enhance hydroxyl radical formation (summarised in the fig.5.1.).

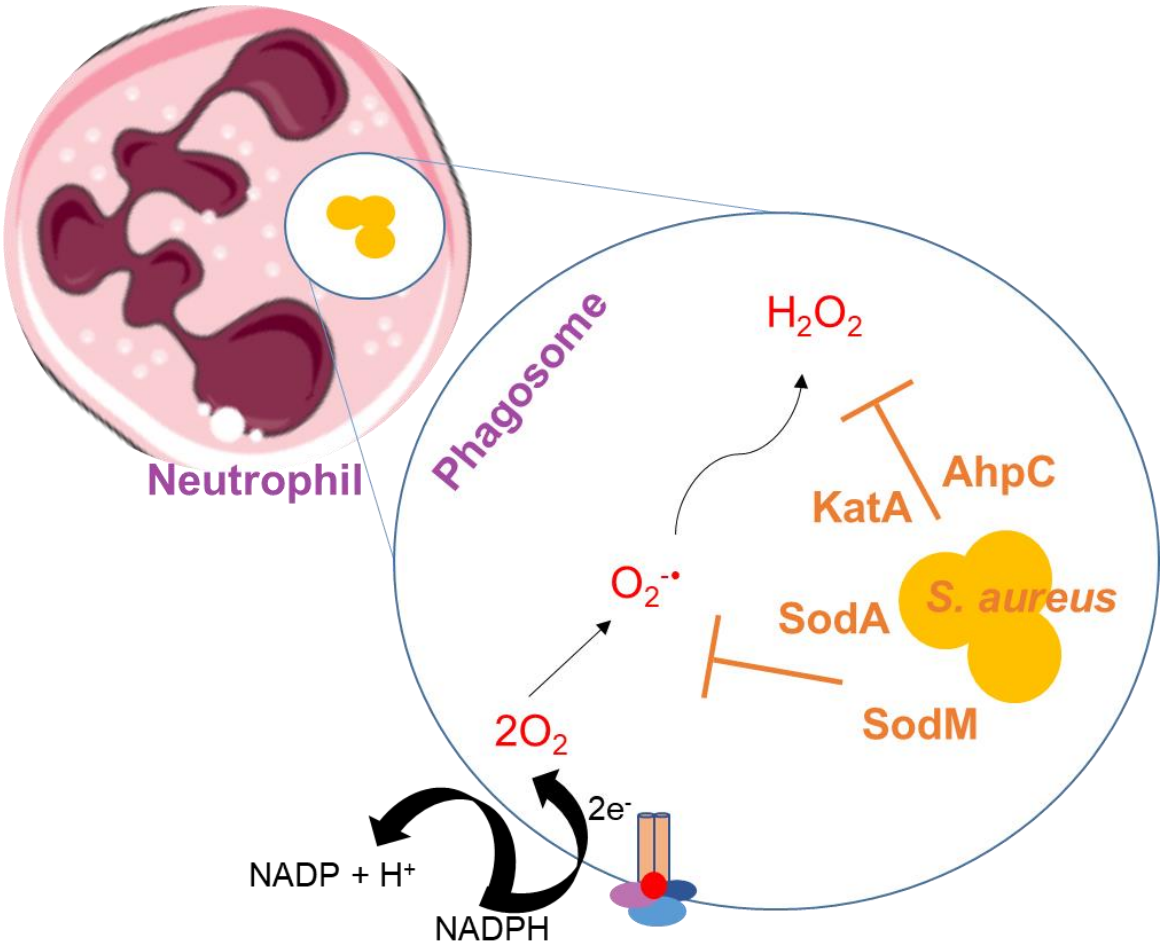

Figure 5.1 Staphylococcal defence against neutrophil oxidative burst

S. aureus has evolved to circumvent oxidative killing by neutrophils by producing enzymes: superoxide dismutases (SodA SodM), catalyse and alkyl hydrogen peroxide (KatA AhpC) which protect these bacteria from killing by host cells ROS ($O^{2-\bullet}$ and H_2O_2).

In this study, double mutants of *S. aureus* SH1000 *sodA sodM* (MHK10AM; Karavolos *et al.*, 2003) and SH1000 *katA ahpC* (KC043; Cosgrove *et al.*, 2007) were used to explore their interactions with human neutrophils. Since the impact of hypoxia on bacterial killing was strain-dependent (Fig 3.11., 3.12., 3.13.), **I hypothesised that changes in neutrophil phagosomal morphology and/or intracellular pH could be influenced by bacterial factors involved in defence against neutrophil- mediated killing.**

Specific Aim:

1. To investigate the impact of staphylococcal strains lacking antioxidant defences on neutrophil phagosomal environment and bactericidal capacity

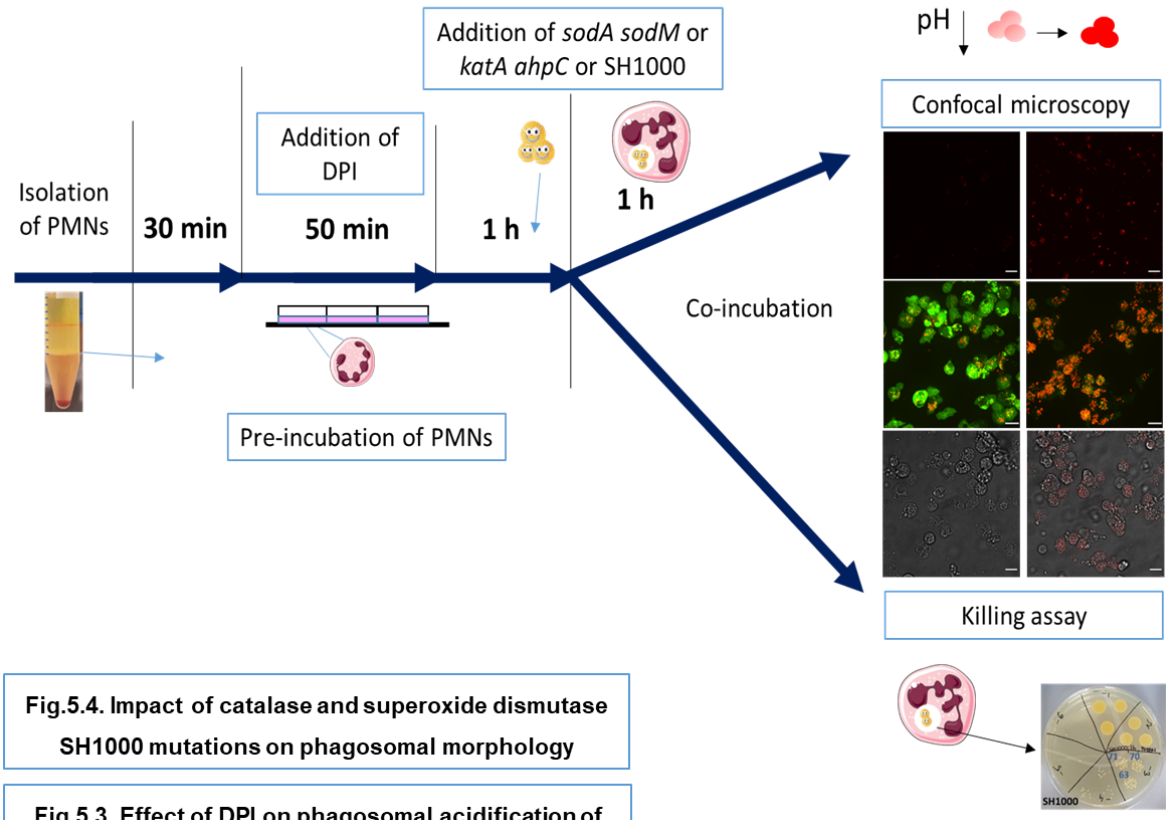

Fig.5.4. Impact of catalase and superoxide dismutase SH1000 mutations on phagosomal morphology

Fig.5.3. Effect of DPI on phagosomal acidification of SH1000 catalase and superoxide dismutase mutants

Fig.5.2. ROS production of neutrophils in response to catalase and superoxide dismutase mutants of S. aureus

Fig.5.6. Neutrophil-mediated killing of SH1000 and SH1000 *katA ahpC* mutant

Fig.5.5. Neutrophil-mediated killing of SH1000 and SH1000 *sodA sodM* mutant

5.1.1 Alkyl hydrogen peroxide, catalase and superoxide dismutase mutants of *S. aureus* SH1000 exhibit impaired control of host ROS generation

Neutrophils isolated by EasySep^{TM} were resuspended in RPMI/FBS/HEPES and distributed onto 8-well glass bottom Ibidi chamber at 2.25 x 10^5 cells/180 µL per each well. After 30 min, 5 µM DCFDA was added, followed by addition of 2 µM DPI (or 0.01% DMSO vehicle) at 50 min. Bacteria (pHrodo red stained wild type SH1000, or *sodA sodM* or *katA ahpC* mutants*)* were added to neutrophils at MOI 5 at 1 h for further co-incubation. After this time, samples were imaged (spinning disk confocal microscope), and the oxidation of DCF was quantified in response to each bacterial strain exactly as previously (Fig.5.2.A). Overall, significantly more intracellular DCF signal indicative of ROS accumulation was observed in response to both of the mutant strains compared with the wild type SH1000. The biggest uplift in signal was seen in response to *S. aureus* SH1000 *katA ahpC* (MFI 7936 ± 340 compared to wild type SH1000 3181 ± 275.1, ****p<0.0001) with a more modest increase in oxidised DCF seen with the *sodA sodM* mutant strain (MFI 4330 ± 256, p=0.0048 compared to wild type SH1000). In all strains the addition DPI significantly reduced ROS accumulation. As can be seen in the representative images (Fig. 5.2.B-D), there was more of the green signal (oxidised DCF) in neutrophils that had ingested the mutant strains rather than the wild type, and that DPI led to near complete inhibition of ROS generation in response to all strains. These data confirm that *S. aureus* actively detoxifies neutrophil ROS generation to reduce the oxidative stress in the phagosomal environment.

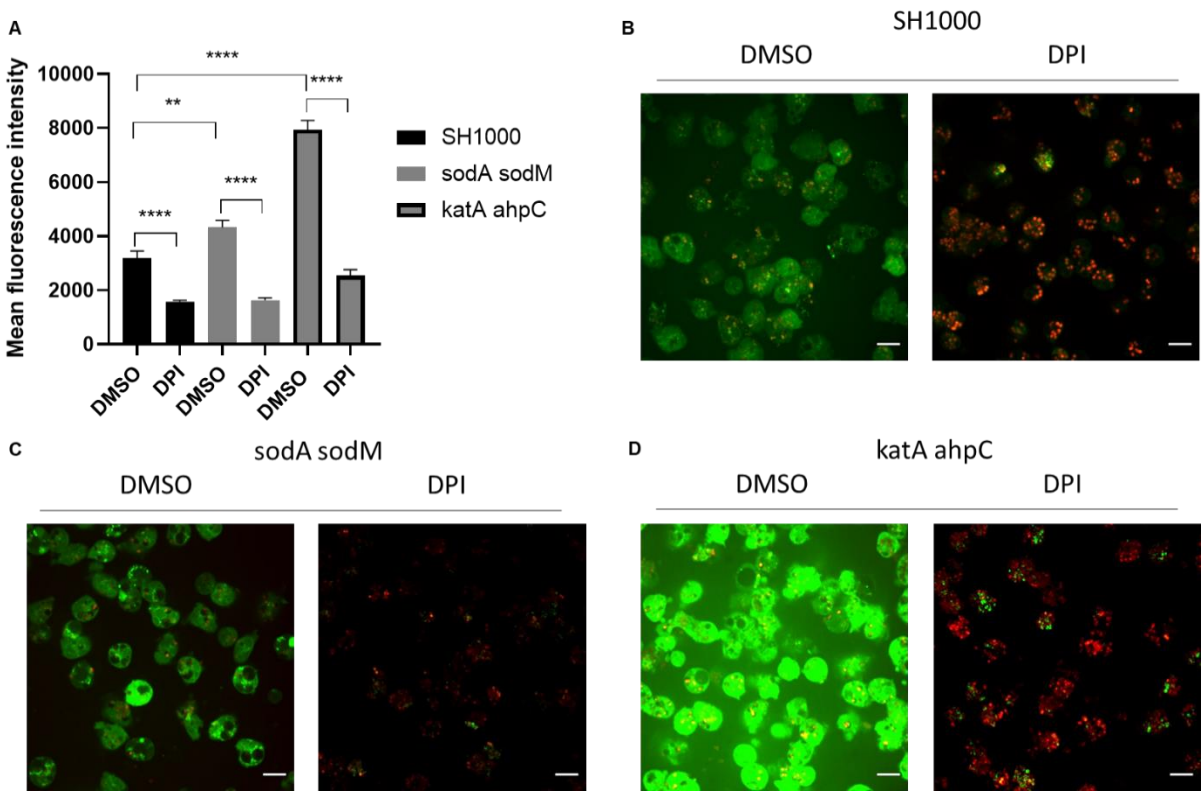

Figure 5.2 ROS levels in neutrophils in response to alkyl hydrogen peroxide, catalase and superoxide dismutase mutants of *S. aureus*

(A). *Neutrophils isolated by EasySep™ (2.25 x 105 cells/180 µL) were placed onto 8-well glass bottom Ibidi chamber and allowed to adhere. DCFDA 5 µM (or vehicle control DMSO) was added after 30 min, DPI 2 µM or DMSO 0.01% vehicle control after 50 min and pHrodo Red stained S. aureus SH1000, sodA sodM or katA ahpC (1.12 x 10^6 CFU/20 µL, MOI 5) were added at 60 min. Following a further 1 h co-incubation, live imaging was undertaken using spinning disk confocal microscope at 60 x oil immersion magnification. Images were quantified using an Image J Macro, and data represent fluorescein mean fluorescence intensity (MFI) from n=3 independent experiments with measurement from 2 randomly chosen fields of view per experiment, ****p< 0.0001 DMSO vs DPI for all strains, **p= 0.0048 DMSO SH1000 vs DMSO sodA sodM, ****p< 0.0001 DMSO SH1000 vs DMSO katA ahpC, tested by One-way ANOVA with Sidak's multi comparison test.* ***(B, C, D)****. Representative images of DMSO control and DPI treated neutrophils infected with* ***(B)*** *SH1000,* ***(C)*** *sodA sodM and* ***(D)*** *katA ahpC, green signal is oxidised DCF and red pHrodo-stained bacteria. Scale bars are 10 µm.*

5.1.2 Alkyl hydrogen peroxide, catalase and superoxide dismutase mutants of *S. aureus* SH1000 have differential effects on intraphagosomal acidification when ROS production is inhibited

Neutrophils isolated by the EasySep^{TM} methodology were placed onto 8-well glass bottom Ibidi chamber at 2.25 x 10^5 cells/180 µL, 2 µM DPI or 0.01% DMSO were added at 50 min followed by addition of pHrodo-stained *S. aureus* SH1000 wild type or mutants (*sodA sodM* or *katA ahpC)* at MOI 5 for 1 h of co-incubation prior to imaging using the spinning disk confocal microscope. Quantification of red fluorescence (MFI) indicating bacterial pH within neutrophils was performed as previously (quantified data shown in Fig. 5.3.A). In the absence of DPI, no differences were observed in intracellular pH of bacteria between either of the mutant strains and wild type controls; the pH in the absence of DPI was not acidic. The pH of intracellular bacteria was significantly reduced in the presence of DPI for wild type SH1000 (Fig. 5.3.A) as previously (Fig. 4.6.) and likewise for the *katA ahpC* mutant strain (Fig.4.18.A, ***p=0.0008 and ****p<0.0001 respectively). However, although there was a trend for increased red fluorescence (representing decreased pH) with the *sodA sodM* mutant in the presence of DPI versus no DPI, this did not reach significance (ns p=0.52). Representative images (Fig. 5.3.B-D) of intracellular bacteria demonstrate more intense red signal for SH1000 and *katA ahpC* but not *sodA sodM* mutants within DPI-treated neutrophils. These data suggest that the effect of DPI on intraphagosomal pH is not directly proportional to ROS generation, since this was suppressed by DPI in response to each strain (Fig. 5.3.). I next explored the phagosomal morphology to discern whether the highly localised impact of the bacterial antioxidant defences would modulate the formation of tight or spacious phagosomes.

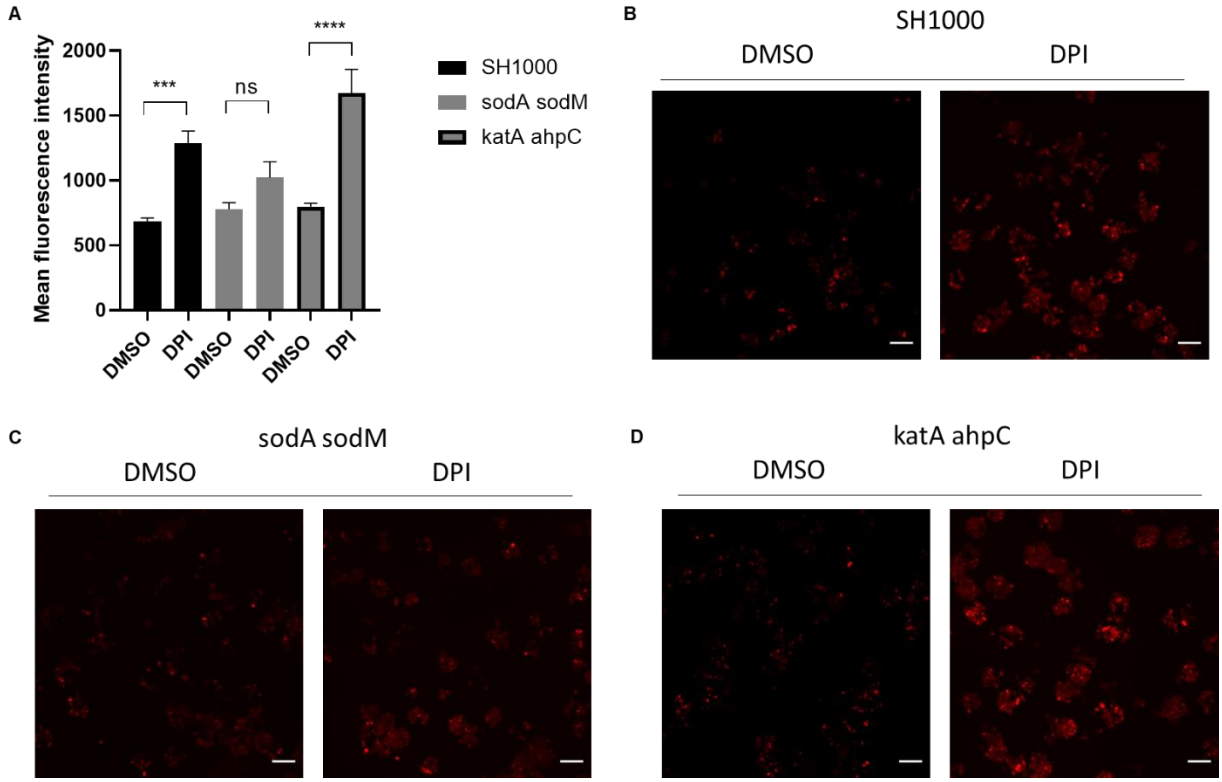

Figure 5.3 Effect of DPI on phagosomal acidification of SH1000 alkyl hydrogen peroxide, catalase and superoxide dismutase mutants

*S. aureus SH1000, sodA sodM and katA ahpC were pHrodo Red-stained to assess intraphagosomal pH of internalised bacteria. Neutrophils isolated by EasySep™ (2.25 x 10^5 cells/180 µL) were placed onto 8-well glass bottom Ibidi chamber and allowed to adhere. DPI 2 µM or DMSO 0.01% vehicle control were added after 50 min and pHrodo Red stained S. aureus SH1000, sodA sodM or katA ahpC (1.12 x 10^6 CFU/20 µL) were added at 60 min. Following a further 1 h co-incubation, live imaging was undertaken using a spinning disk confocal microscope at 60 x oil immersion magnification. Images acquired after 1 h co-incubation were quantified using an Image J macro, and data represent mean fluorescence intensity (MFI) from n=3 independent experiments with measurement from 3 randomly selected fields of view per experiment, ***p=0.0008 DMSO vs DPI for SH1000, ns p= 0.5187 for DMSO vs DPI for sodA sodM, ****p<0.0001 DMSO vs DPI for katA ahpC, tested with one-way ANOVA with Sidak's multiple comparison test.* ***(B, C, D).*** *Representative images of DMSO and DPI treated neutrophils infected with* ***(B)*** *SH1000,* ***(C)*** *sodA sodM and* ***(D)*** *katA ahpC.* *Scale bars are 10 µm.*

5.1.3 Phagosomal morphology is not influenced by alkyl hydrogen peroxide, catalase and superoxide dismutase mutations in *S. aureus* SH1000

Freshly isolated EasySep^{TM} neutrophils (2.25 x 10^5 cells/180 µL) were placed onto 8-well glass bottom Ibidi chamber. At 50 min, 2 µM DPI or 0.01% DMSO vehicle control were added and at 1 h pHrodo red-stained bacteria SH1000 wild type, *sodA sodM* and *katA ahpC* mutants were added at MOI 5. Following a further 1 h, samples were imaged using the spinning disk microscope at 60 x oil magnification to examine phagosomal morphology. The number of spacious phagosome-containing neutrophils was manually quantified by an observer blinded to experimental condition (Fig.5.4.A). For all strains the majority of the bacterial-containing phagosomes observed were spacious, and there was no significant difference between strains. DPI significantly reduced the percentage of spacious phagosome positive neutrophils (****p<0.0001), again with no difference observed between bacterial strains. Data (Fig. 5.4) represent overall quantification (Fig. 5.4.A) and representative microscopic images of all strains with DMSO or DPI treatment (Fig.5.4. B-D). Given these changes in the phagosomal environment, I went to assess the ability of neutrophils to kill these strains both in standard conditions and in the setting of reduced host ROS generation (hypoxia and DPI treatment).

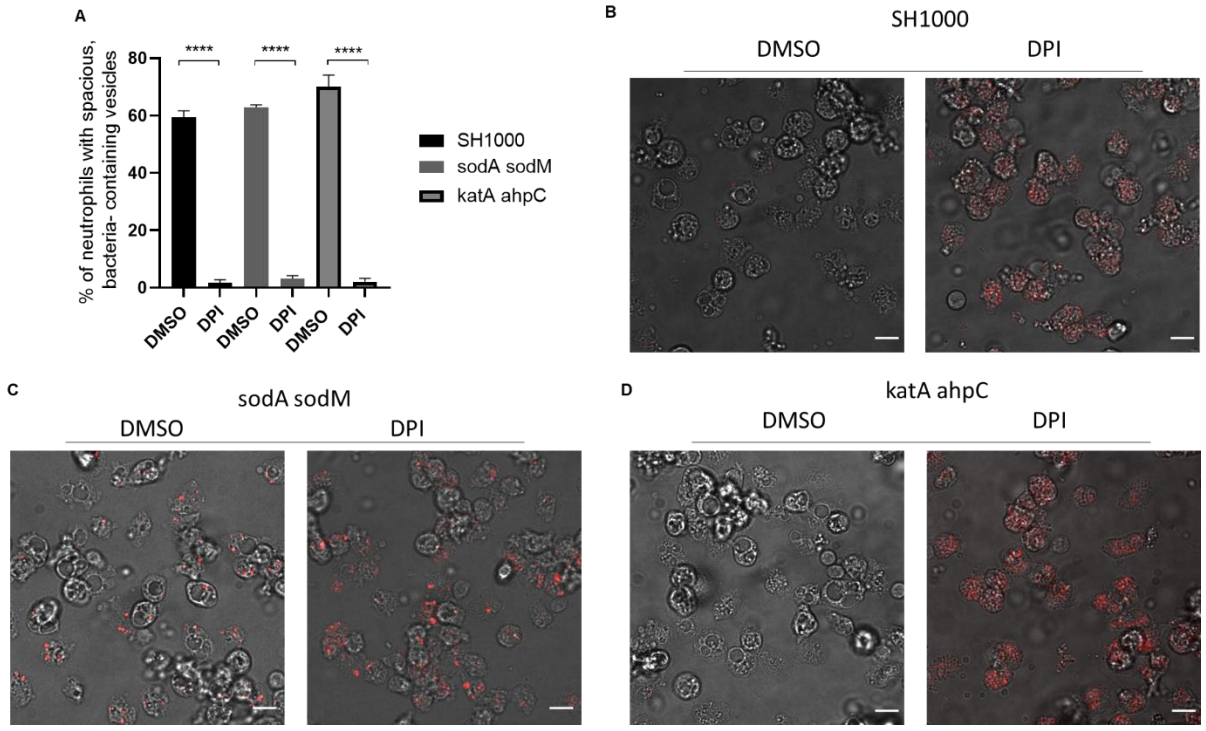

Figure 5.4 Impact of alkyl hydrogen peroxide, catalase and superoxide dismutase SH1000 mutations on phagosomal morphology

(A). *Neutrophils isolated by EasySep™ (2.25 x 105 cells/180 µL) were placed onto 8-well glass bottom Ibidi chamber. pHrodo Red stained S. aureus SH1000, sodA sodM or katA ahpC (1.12 x 10^6 CFU/20 µL) were added at 60 min. Following a further 1 h co-incubation, live imaging was undertaken using a spinning disk confocal microscope at 60 x oil immersion magnification. After 1 h of co-incubation the number of neutrophils containing spacious phagosomes was manually quantified (n=4 independent experiments from 3 fields of view for each). Data represent percentage of neutrophils with spacious S. aureus-containing vesicles at 1 h post infection, ****p< 0.001 tested with one-way ANOVA with Sidak's multiple comparison test.* ***(B, C, D, E)*** *Representative images of DMSO and DPI treated neutrophils infected with* ***(B)*** *SH1000,* ***(C)*** *sodA sodM and* ***(D)*** *katA ahpC. Scale bars are 10 µm.*

5.1.4 Increased killing of *sodA sodM* SH1000 by neutrophils in normoxia but not hypoxia

Since there were differences in the phagosomal environment generated in response to wild type and the chosen mutant strains of *S. aureus,* I next tested if there was any variation in the intracellular survival of these strains; since killing assays do not require live imaging, I was able to assess this outcome in hypoxia as well as normoxia. Neutrophils isolated using the EasySep^{TM} negative selection method (2.25 x 10^5 cells/90 µL) in 96-well plates were pre-incubated for 1 hour in normoxia or hypoxia (in pre-equilibrated RPMI/FBS/HEPES media as previously) to allow cells to sediment at the bottom of the plates. At 50 min, DPI (2 µM) or DMSO vehicle control were added followed by SH1000 and *sodA sodM* at MOI 5 at 1 hour. After 30 min of co-incubation (t=0), gentamicin (40 µg/mL) was added to kill extracellular bacteria, and intracellular survival was measured at 60 and 180 min by Miles and Misra method (Fig. 5.5). Similar numbers of bacteria had been internalised at 30 min (t=0 on the graphs) with no differences between treatments or strains (Fig. 5.5.A-B). In line with previously acquired data with neutrophils isolated by Percoll® density gradient centrifugation (Fig. 4.1.D), there were significantly more surviving *S. aureus* SH1000 in DPI-treated and hypoxic neutrophils in comparison with normoxia at 180 min (833 ± 901.6 CFUs in normoxia, 26663 ± 5591 CFUs in hypoxia, ***p*=0.005 and 5.12 ± 0.24 $\log_{10}$ of CFU in DPI-treated cells, *****p*<0.0001, Fig. 5.5.A). A similar pattern was observed when the *sodA sodM* mutant was used, with more surviving bacteria in DPI and hypoxic neutrophils than in normoxic cells (40665 ± 79253, 25103 ± 6225 CFUs, *****p*<0.0001 and 1.95 ± 0.5 $\log_{10}$ of CFU, ***p*=0.007 respectively, Fig. 5.5.B). Comparison of intracellularly surviving SH1000 and *sodA sodM* mutants revealed that the mutant was killed more effectively than the wild type (591.4 ± 574.9 CFUs versus 3141 ± 901.6 CFUs surviving intracellular bacteria respectively) at 180 min post-infection (Fig. 5.5.C), but this effect was not observed when ROS generation was inhibited by DPI or in the setting of hypoxia (Fig. 5.5.D-E) implying that the inability to remove ROS is responsible for this increased susceptibility to intracellular killing.

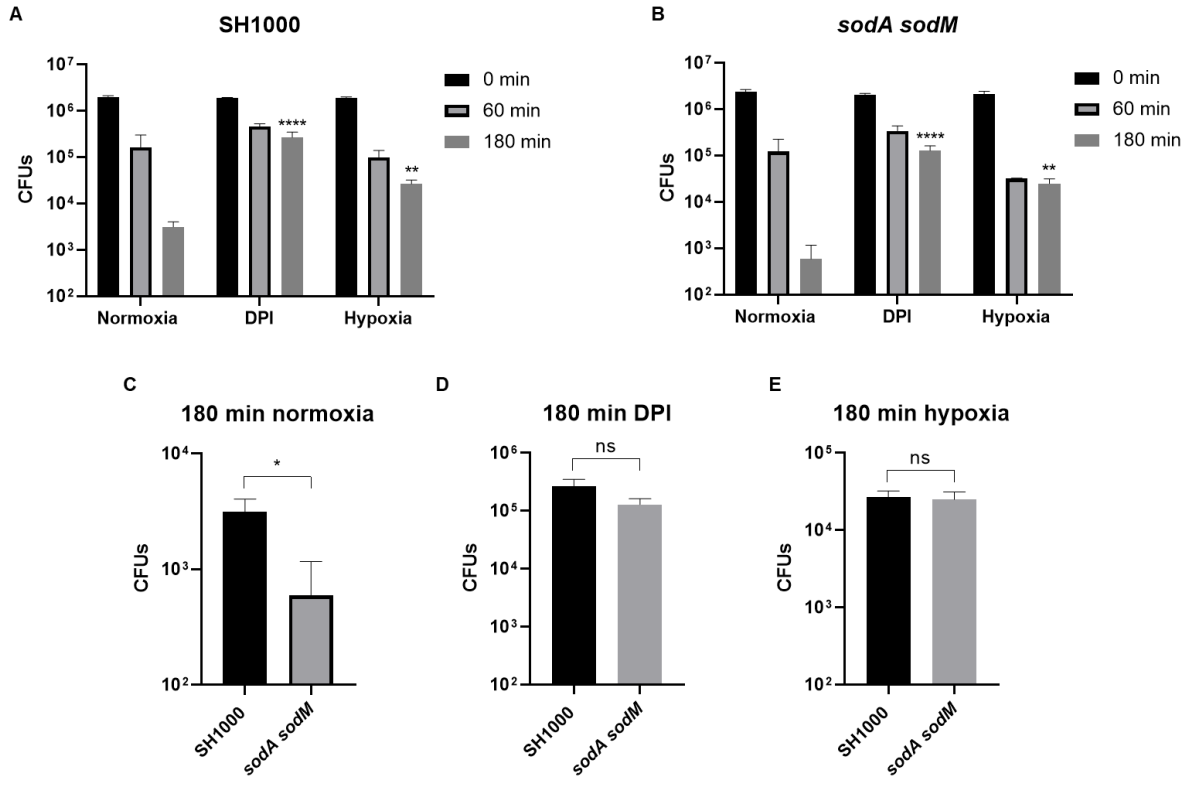

Figure 5.5 Neutrophil-mediated killing of SH1000 and SH1000 *sodA sodM* mutant

Freshly isolated EasySep™ neutrophils were resuspended in normoxic or hypoxic RPMI/FBS/HEPES and were placed in 96 well plates at 2.25 x 10^5 cells/90 µL. DPI 2 µM or DMSO 0.01% vehicle control was added at 50 min, and S. aureus SH1000 or sodA sodM (~MOI 5) were added at 60 min. After 30 min of co-incubation, gentamicin at 40 µg/mL was added to kill extracellular bacteria. At each timepoint (0, 60,180 min) samples were spun down, and neutrophils were lysed with alkali water to use Miles and Misra method to quantify CFUs of intracellularly surviving bacteria. Data represent mean of log_{10} CFU from n=4 independent experiments. ***(A)*** *****p<0.0001 for 180 min SH1000 normoxia vs DPI, **p= 0.005 for 180 min SH1000 normoxia vs hypoxia,* ***(B)*** *****p<0.0001 for 180 min sodA sodM normoxia vs DPI, **p= 0.007 for sodA sodM normoxia vs hypoxia; tested by Two-way ANOVA with Tukey's multiple comparison test.* ***(C)*** **p= 0.0337 for 180 min normoxia SH1000 vs sodA sodM,* ***(D)*** *ns p= 0.3438 for 180 min DPI SH1000 vs sodA sodM and* ***(E)*** *ns p= 0.4452 for 180 min hypoxia SH1000 vs sodA sodM; tested by unpaired student t-test.*

5.1.5 SH1000 *katA ahpC* mutant is not more susceptible to killing by neutrophils

Neutrophil-mediated killing was also tested on the double mutant of catalase and alkyl hydrogen peroxide reductase (*katA ahpC*). A gentamicin protection killing assay was performed using wild type SH1000 and the *katA ahpC* mutant exactly as described above for the *sodA sodM* mutant strain (and the results are shown in Fig. 5.6). As previously, there was no difference in the number of bacteria detected at t=3 in between strains or in the setting of any treatment condition (Fig 5.6.A-B). as previously, there were significantly more surviving *S. aureus* SH1000 in DPI-treated and hypoxic neutrophils in comparison with normoxia at 180 min (29122.5 ± 4279.77 of intracellular CFUs in hypoxia and 4957.8 ± 947 of intracellular CFUs in normoxia, *p=0.03 for hypoxia vs normoxia and 249270 ± 79083 of intracellular CFUs with DPI, ****p<0.0001 for DPI vs normoxia) of co-incubation (Fig.5.6.A). Similarly, killing of the *katA ahpC* mutant was significantly impaired in DPI-treated and hypoxic neutrophils compared with normoxic cells (15677 ± 5248, 49874 ± 16928 of intracellular CFUs and 3.29 ± 0.16 $\log_{10}$ of intracellular CFU, respectively. Fig. 5.6.B). Surprisingly given the marked increase in intracellular ROS detected in this setting (Figure 5.2), comparison of intracellularly surviving SH1000 and *katA ahpC* at 180 min showed no significant differences in neutrophil killing in normoxia, as well as in hypoxia or in the setting of DPI (Fig. 5.6.C-E).

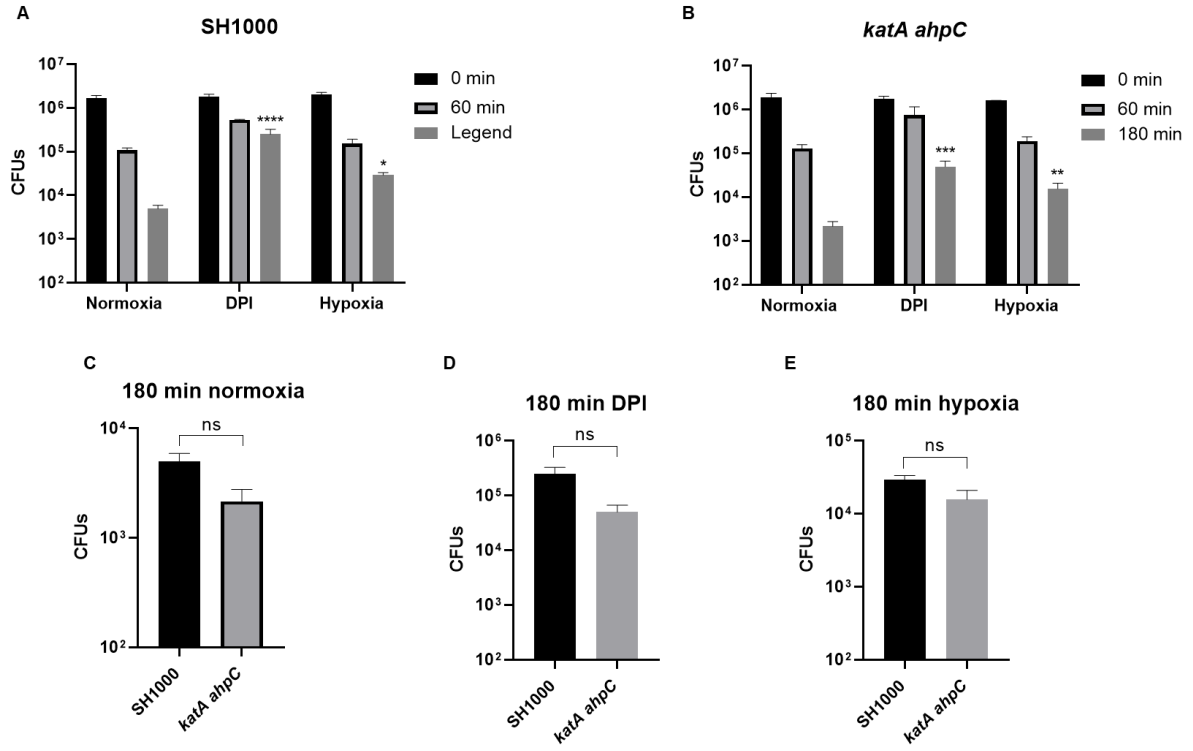

Figure 5.6 Neutrophil-mediated killing of SH1000 and its *katA ahpC* mutant

Freshly isolated EasySep™ neutrophils were resuspended in normoxic or hypoxic RPMI/FBS/HEPES and then were placed in 96 well plates (2.25 x 10^5 cells/180 µL). DPI 2 µM or 0.01% DMSO vehicle control was added at 50 min, and S. aureus SH1000 or katA ahpC (~MOI 5) were added at 60 min. After 30 min of co-incubation gentamicin at 40 µg/mL was added to kill extracellular bacteria. At each timepoint (0, 60, 180 min) samples were spun down and neutrophils were lysed with alkali water to use Miles and Misra method to quantify CFUs of intracellularly surviving bacteria. Data represent mean of log 10 of CFU from n=4 independent experiments. ***(A)*** *****p< 0.0001 for 180 min SH1000 normoxia vs DPI, *p= 0.0344 for 180 min SH1000 normoxia vs hypoxia,* ***(B)*** ****p= 0.0002 for 180 min katA ahpC normoxia vs DPI, **p= 0.0062 for katA ahpC normoxia vs hypoxia; tested by Two-way ANOVA with Tukey's multiple comparison test.* ***(C)*** *ns p= 0.0840 for 180 min normoxia SH1000 vs katA ahpC,* ***(D)*** *ns p= 0.0634 for 180 min DPI SH1000 vs katA ahpC and* ***(E)*** *ns p= 0.2843 for 180 min hypoxia SH1000 vs katA ahpC; tested by unpaired student t-test.*

5.2 Discussion

Superoxide is the immediate product of the NADPH oxidase, and is highly reactive, however the targets it might oxidise to kill bacteria are largely unknown. As it is subject to spontaneous as well as catalytic dismutation, it has been difficult to study independently from its far more stable dismutation product, H_2O_2. In the presence of hydrogen peroxide, the iron liberated from Fe-S clusters (molecular ensembles of iron and sulphide which are common in electron transport systems such as the NADPH oxidase) engenders an intracellular environment that permits Fe-dependent (Fenton) oxidation reactions by which the highly reactive hydroxyl radicals (HO•) are generated. Such radicals react rapidly with molecules in close proximity. As DNA is a charged molecule that attracts positively charged molecules such as Fe^{2+} to its phosphodiester backbone, generated HO• often react with DNA, inducing lethal mutations (Keyer and Imlay, 1996). Other ROS targets that can be modified or oxidised in the context of Fe are amino acids and proteins. For instance, H_2O_2 can react with the Fe^{2+} of a protein that contains iron, to cause carbonylation that leads to the formation of protein aggregates (Dukan *et al.*, 1999; Davies, 2005).

Staphylococci have evolved to avoid killing by human neutrophils, e.g., by producing detoxifying enzymes that catalyse the dismutation of O_2^- and reduce it further to water and oxygen. I measured ROS accumulation in human neutrophils in response to double mutants with inactivated *sodA sodM* and *katA ahpC* in the SH1000 background. ROS detection was higher in response to *sodA sodM* and *katA ahpC* than to the wildtype (Fig. 5.2), confirming that these enzymes would normally remove significant levels of ROS from the phagosomal environment. This effect was not observed when the heat-killed bacteria were used (data not shown), confirming it is an active bacterial-dependent phenomenon. In the absence of these bacterial antioxidant enzymes, there is likely accumulation of superoxide and in particular H_2O_2, both ROS that can oxidise DCFDA to DCF (Holtz, 2009) as bacteria lack other enzymes to detoxify or scavenge endogenously produced H_2O_2 (Valderas *et al.*, 2002; Clements *et al.*, 1999; Cosgrove *et al.*, 2007). However, DPI was able to fully inhibit ROS production in response to mutants to the same extent as to the wildtype, suggesting the origin of the 'additional' ROS was derived from the host oxidase not the bacteria. I also investigated how these bacteria might affect intraphagosomal pH (Fig. 5.3.). All of bacterial strains were found to be within the same neutral/alkaline environment in

the setting of normoxia and all became acidic in NADPH oxidase inhibited cells. Significantly more acidified wild type (SH1000) and *katA ahpC* mutant bacteria were seen in DPI treated neutrophils, with further minor but non-significant increase in the pHrodo signal associated with the *sodA sodM* mutant. However, there were no differences in the percentage of spacious phagosomes in controls between any of the mutant strains and the wild type (Fig. 5.4.). Together these data suggest that the changes in phagosomal morphology relate to activation of the NADPH oxidase rather than the accumulation of ROS or consequent changes in phagosomal pH.

It has been shown that in a mouse abscess model of infection, the *sodA sodM* mutant is less virulent compared to the wild type strain (Karavolos *et al.*, 2003). Similar results were obtained in this study, demonstrating impaired survival of *sodA sodM* in healthy human neutrophils in comparison to the parental strain (Fig. 5.5.C). However, there were no significant differences in survival rate between the SH1000 strain and its *katA ahpC* mutant, which was surprising in the light of the markedly increased ROS signal seen in association with ingestion of this strain. As noted, in the absence of *sodA* and *sodM,* there might be greater accumulation of the highly reactive O_2^- (although spontaneous dismutation does occur) with a relative reduction in H_2O_2, whilst in the absence of *katA* and *ahpC*, H_2O_2 would be expected to accumulate to a greater extent. My results might imply a greater role for O_2^- than H_2O_2 in bacterial killing (at least of *S. aureus*) within the phagosome. The predominant accumulation of H_2O_2 and its derivatives could be less toxic to the bacteria than the ephemeral but reactive O_2^-. An alternative explanation is that even in the presence of functional katA ahpC there is sufficient ROS to kill all susceptible organisms under the experimental conditions used. There was a reduction in nasal colonisation when both *katA* and *ahpC* were inactivated in a cotton rat model, however the mutant was not attenuated in murine models of septic arthritis of atopic dermatitis (Cosgrove *et al.*, 2007). This may reflect the hypoxic nature of the environment, in keeping with the full suppression of ROS by DPI in response to all mutations and their equivalent killing in hypoxia (Figs. 5.5. and 5.6.). Thus, hypoxia may impair the ability to kill intracellular staphylococci in general but might also remove the selective advantage of strains more able to ‘detoxify’ the phagosomal ROS. This observation led to the award of a PhD student (Ms Rebecca Hull) to study the evolution of *S. aureus* in a hypoxic environment. Interestingly, hypoxia promotes mutations in a subset of bacterial genes that regulate bacterial DNA

replication, translation and transcription, enabling the bacteria to adapt to the hypoxic environment, with similar changes not observed in normoxic evolution conditions (Ms Rebecca Hull, personal communication). It would be of interest to correlate such mutations with those occurring in staphylococcal infections that are particularly hypoxic, such as deep-seated abscesses and bone and joint infections.

The mechanism by which ROS generated by NADPH oxidase protect the host from *S. aureus* infection is complex and only partially understood (discussed in Buvelot *et al.*, 2017). Given the many *S. aureus* virulence factors that remove or detoxify ROS, the sensitivity of this organism to ROS (as illustrated by the frequent infections in CGD) is particularly puzzling. While direct killing of *S. aureus* by ROS might be a part of the story, this paradox suggest it does not explain the entire picture. Two additional mechanisms might be particularly relevant: ROS-dependent deregulation of *S. aureus* gene expression. An example of this is that the ROS HOCL (hypochlorous acid) can modify the staphylococcal autoinducing peptide AIP (Pang *et al.*, 2010) to affect quorum sensing; hence the absence of ROS may affect *S. aureus* virulence at the population level rather than just at the level of the individual organism. In addition, it has been suggested that there is ROS-dependent regulation of host immune cells by modification of cytokine production, although this is controversial; for example Dostert et al. (2008) suggested the NAPDH oxidates promotes inflammasome/caspase 1 activation (Dostert *et al.*, 2008), however other studies have suggested the opposite (Meissner *et al.*, 2010), and this effect may be context dependent. More research is required to understand the complex interactions between *S. aureus*, ROS and also phagosomal pH (see below).

6 General discussion and future directions

Laboratory investigations are routinely conducted in atmospheric oxygen as to do otherwise presents substantial logistic challenges. However, this acceptance of atmospheric oxygen as 'normoxia' does not reflect the complex environment in which biological processes occur. As discussed, many body tissues are 'physiologically hypoxic', and infections further generate 'pathological hypoxia' which can be extreme. In this project, I have attempted to explore an important host-pathogen interaction in a way that more accurately recapitulates the *in vivo* setting, both with regard to oxygen tension and nutrient deprivation. It should be noted that other adverse conditions in infection sites (such as acidosis and high lactate levels) have not been pursued in this work. I have also not explored the ability of neutrophils to deal with *S. aureus* growing in biofilms in the setting of hypoxia. All of these parameters would be relevant to the host-pathogen interaction and could be explored in the future.

Key results from my work include (summarised in Table 6.1 below):

a) Short-term hypoxia (0.8% oxygen, equating to 3 kPa) impaired the ability of neutrophils to kill internalised *S. aureus* (both Wood 46 and SH1000), associated with a reduction in the respiratory burst at the phagosomal membrane.

b) Short-term hypoxia as above altered the morphology of the *S. aureus*-containing phagosome.

c) The above changes were recapitulated by DPI, which inhibits the generation of ROS. DPI additionally lowered the pH of the *S. aureus*-containing phagosome.

d) *S. aureus* mutants that lack antioxidant defences did not modify phagosomal morphology or pH, suggesting that these effects are secondary to the activation of the host NADPH oxidase.

Treatment of neutrophils ingesting *S. aureus*	ROS generation	Phagosomal pH	Phagosomal morphology	Bacterial killing
Normoxia	+++++	Neutral/alkaline	Spacious	Efficient
Hypoxia	++	?	Tight	Impaired
DPI	+	Acidic	Tight	Impaired
Class 1 PI3K inhibition	++	Neutral/alkaline	Tight	?
Class III (VPS34) inhibition	++	Neutral/alkaline	Tight	Improved

Table 6.1 The impact of oxygen availability, NADPH oxidase inhibition and Class I or Class III Pi3K inhibition on neutrophil phagosomal environment and killing of *S. aureus*.

My work would suggest that phagosomal pH is not key to the killing of S aureus within the neutrophil phagosome. This is in keeping with the work of Flannagan *et al*., who found that exposure to acidic pH was required for optimal growth of *S. aureus* inside the macrophage phagolysosomes, dependent on the induction of the 2-component GraS system (Flannagan *et al.*, 2018). Along similar lines, the survival of small colony variants (SCVs) of S. epidermidis was promoted by phagosomal acidification and SCV killing was augmented phagosome alkalisation (Magryś *et al.*, 2018). Similarly, early macrophage phagosomal acidification was found to support intracellular survival and replication of *Brucella* spp (Köhler Stephan *et al.*, 2002). Thus, some bacteria not only survive but exploit the acidic phagosomal milieu. In contrast acidification is key to the execution of other pathogens. For example, V-ATPase-mediated phagosomal proton delivery is reduced during phagocytosis of wild-type *S. pyogenes*, leading to impaired acidification and killing; but mutant bacteria lacking virulence factors regulated by the transcriptional regulator Mga, are phagocytosed and killed in acidified phagosomes (Nordenfelt *et al.*, 2012). Treatment with various ion channel blockers increased macrophage phagosome acidification, leading to *M. tuberculosis* growth restriction (Machado *et al.*, 2016). Finally, patient with cystic fibrosis suffer from severe chronic lung infection with *Pseudomonas aeruginosa*; impaired function or absence of the chloride channel cystic fibrosis transmembrane regulator (the genetic defect causing cystic fibrosis) is associated with impaired phagosomal acidification and killing of this pathogen in both neutrophils (Hayes *et al.*, 2020) and macrophages (Di *et al.*, 2006).

Thus, phagosomal pH differentially regulates pathogen killing depending on virulence factor profiles.

Methodological challenges and study limitations

Neutrophils are sensitive to changes in pH, temperature and other factors that have to be taken under consideration before performing any experiments on those cells. Our initial experiments were undertaken using a standard density gradient centrifugation. However, following the COVID pandemic limited donor availability and issues with cell activation necessitated switching to a negative selection method. Fortunately, the results (in particular the number of bacteria killed in normoxia and hypoxia and the impact of DPI on phagosomal morphology and pH) aligned precisely between the 2 methods. Neutrophil lifespan after isolation is very limited, as cultured neutrophils quickly undergo apoptosis (Summers *et al.*, 2010; Scheel-Toellner *et al.*, 2004). A further challenge is that hypoxia modifies this response by delaying apoptosis (Fig. 3.4), with the potential to confound results if longer incubations are used; for these reasons I have studied largely short-term interactions, although many of the infections with *S. aureus* are chronic. Mature neutrophils do not proliferate and are not genetically tractable. Several neutrophil-like cell lines have been studied by a range of groups; however they often differ from mature neutrophils in terms of their morphology, surface molecule expression, signalling pathways and functions. The main advantage of using such cells is that they can be manipulated by siRNA or genetic editing techniques. However, due to the limitations noted above, these cell lines were not utilised in my work. As discussed below, my plans to collaborate to use neutrophils from relevant knockout mice were not achieved due to the COVID-19 pandemic. I note that the use of pharmacological inhibitors in my experiments is subject to limitations, including incomplete inhibition and off-target effects.

Using the hypoxic workstation constrains the assays that can be performed within this environment due to the small working space and limited electrical sockets; hence only a few small items of equipment can be housed within. The high humidity and lack of contact with the exterior meant I was unable to introduce a microscope into the chamber to visualise hypoxic cells, and many of my assays require direct imaging of live cells (including the measurement of intracellular ROS and pH). I was able to confirm the impact of hypoxia on intracellular ROS production using the NBT assay (Fig. 3.15), once used as the diagnostic method to detect CGD now regarded as

obsolete and superseded by FACS-based methods. Although light microscopy of fixed cells did not provide adequate resolution to confirm the impact of hypoxia on phagosomal morphology, I undertook these studies using electron microscopy and showed the appearance of Staphylococcal-containing phagosomes in hypoxic cells was indistinguishable from that of neutrophils treated with DPI. I was unable to find a method to measure phagosomal pH of hypoxic neutrophils. We did explore the option of using a specially manufactured 'mini-hypoxic' glass chamber (OxyGenie™, Baker Ruskinn), however we found that the glass of the chamber was too thick to allow sufficient resolution for imaging. Had this methodology proved feasible we would have used it to image not only human neutrophils in real time but also zebrafish infected with *S. aureus* in a hypoxic environment.

I used laboratory strains of *S. aureus*, as clinical strains are markedly heterogeneous and hence may not give consistent results in the laboratory setting. Whilst this facilitates experimental reproducibility, of course some clinical strains may interact with neutrophils in a different way, for example strains that produce abundant leukocidins may kill the neutrophils that ingest them rather than be killed by them. Thus, my results may not be applicable to all clinical stains, consistent with the lack of impact of hypoxia on the killing of the JE2 *S. aureus* strain (Fig. 3.13) in contrast to the marked limitation of killing by hypoxia of the Wood 46 and SH1000 strains (Figs. 3.11 and 3.12 respectively). However, my focus on SH1000 meant that I was able to test some of the many mutants of this strain available to explore the ability of bacterial antioxidants to modulate the phagosomal environment. My results (presented in Chapter 5) suggest that the predominant determinant of the host-pathogen interaction in this setting is the efficacy of the host NADPH oxidase response.

Despite these challenges I have undertaken an array of studies to characterise the impact of hypoxia and inhibition of the NADPH oxidase on the phagosomal environment, to understand the mechanisms of impaired killing of *S. aureus* in hypoxia at levels thought to be relevant to *in vivo* infection.

Bacteria possess homologues of the PI3K signalling proteins including VPS34, hence I cannot exclude the possibility that the effects of the VPS34 inhibitor were due to direct effects on bacteria. I used VPS34-I, which is highly selective for VPS34 and does not affect Class 1 PI3Ks (Bago *et al.*, 2014); although it has an *in vitro* IC_{50} of 25nM, in a cell-based assay VPS34-I had approximately 80% efficacy (Bago *et al.*,

2014). I used this inhibitor 10 µM based on the above and on the work of Conway-Morris *et al*., 2020, who recapitulated the inhibitory effect of C5a on human neutrophils (since phosphoproteomic analysis implicated VPS34 in this immunosuppressive effect) using 10 µM VPS34. Whilst this implies the concentration of inhibitor that I used inhibited the neutrophil VPS34, it does not exclude an additional effect on bacterial signalling. It would be of interest to explore this by pre-incubating bacteria with 10 µM VPS34-IN1 and determining whether this affected the phagosomal morphology in neutrophils that were naïve for this treatment. Given the selectivity of this compound and the fact that the stated concentration precisely re-capitulated an in-vivo response supported by phosphoproteomic changes, it is unlikely that the inhibitor affected other pathways although this has not been formally tested and a concentration-response curve would have been undertaken had time permitted.

Impact of Hypoxia, Hypoxia Duration and Hypoxia-Inducible Factors (HIFs) on the NADPH Oxidase and killing of *Staphylococcus aureus*

In this study, I have explored impact of short-term (a few hours) hypoxia, using a hypoxic chamber to generate 0.8% oxygen (leading to an oxygen tension of 3 kPa in the tissue culture media), as previously optimised by our group (McGovern *et al.*, 2011). I confirmed the effect of hypoxia on neutrophil functions such as delayed apoptosis (Fig. 3.4) and upregulation of hypoxia responsive genes BNIP3 and GLUT1 (Fig. 3.6). Interestingly, I also found that growth of *S. aureus* is dramatically restricted by hypoxia when bacteria are in BHI media (Fig. 3.7), but in a medium that has limited nutrients (RPMI), both growth of bacteria was significantly reduced, independent of oxygen availability (Fig. 3.8). This phenomenon is currently being further explored by another PhD student in our group, who has found a 3-way interaction between hypoxia, antibiotics, and the time of exposure to these conditions leading to evolution of the *S. aureus* in these environmental settings (Ms Rebecca Hull and Prof Alison Condliffe, personal communication). This shows that the complex interactions at an infection site need to be carefully unpicked to predict the outcome of a host-pathogen interaction and to explore factors that might improve such interactions *in vivo*.

The observed impairment of killing of *S. aureus* SH1000 neutrophils experiencing short-term hypoxia (3 hours, Fig. 3.12.A) was almost certainly caused by the accompanying and highly significant reduction in intracellular ROS production in these

neutrophils (Fig. 3.14). At this early time, the impaired killing was shown to be likely HIF-independent (Fig. 3.15). We chose this short-term time point as longer-term hypoxic exposure prolongs neutrophil survival (Fig. 3.4), which might have confounded the results. Importantly, killing was also markedly impaired following longer term hypoxic incubation (24 h, Fig. 3.12.D), despite the enhanced survival of neutrophils in hypoxia which might be expected to allow them time to overcome the bacterial invaders. By 24 h, normoxic neutrophils had killed all phagocytosed bacteria, whereas cytospins showed intact bacteria within hypoxic neutrophils at 24 h of co-incubation, suggesting survival within an intracellular niche in this setting. This was surprising, as over this timeframe stabilisation of the transcription factor HIF occurs, leading to the transcription of hypoxia responsive genes which are thought to promote the resolution of infection (for example, see Peyssonnaux *et al.*, 2005; Okumura *et al.*, 2012). Using an *in vivo* model of infection and inflammation in zebrafish, the beneficial role of HIF-1α stabilisation on killing of *Mycobacterium marinum* (closely related to the pathogen causing human tuberculosis) by macrophages was clearly demonstrated. Ogryzko *et al.* demonstrated that hypoxia signalling, mediated by the Hif-1α transcription factor, primes macrophages to generate increased levels of IL-1β and upregulates neutrophils antimicrobial nitric oxide (NO) production, underpinning protection against mycobacterial infection (Ogryzko *et al.*, 2019). In contrast, *S. aureus* can resist the antimicrobial effects of NO, thanks to the contribution of four regulators *srrAB, fur, codY,* and *rot;* mutants lacking these were shown to be substantially sensitive to NO (Grosser *et al.*, 2016). Although animal models in which HIFs have been genetically modified have been extremely helpful in elucidating the mechanisms by which HIF-dependent transcriptional responses affect the host-pathogen interaction, it is important to note that HIF stabilisation does not completely equate to hypoxia. HIF stabilisation cannot overcome the lack of molecular oxygen to restore the oxidative burst, and *S. aureus* is particularly sensitive to ROS as shown by the propensity of patients with CGD to suffer staphylococcal infection. Other pathogens will respond differently to the hypoxic intra-phagosomal environment, hence the results from one pathogen cannot be extrapolated to another.

Whilst the hypoxic neutrophil transcriptome has been studied in some settings (e.g.,Thompson *et al.*, 2017), to explore the neutrophil-staphylococcal interaction in

hypoxia more fully it would be fascinating to undertake ‘dual RNA-seq’ (Westermann and Vogel, 2018) to explore the transcriptional responses of both the host neutrophil and the internalised bacteria; the impact of hypoxia on prolonging neutrophil lifespan would make this feasible. Transposon sequencing of surviving bacteria would be an alternative approach, and results could be compared to data from *in vivo* models of chronic staphylococcal infection. For example, in a murine osteomyelitis model, 65 genes were recognised as essential for the survival of bacteria during this chronic infection, of which 45 genes were categorised into metabolic pathways. The staphylococcal respiratory response (SrrAB) system which coordinates staphylococcal response to hypoxia and other stresses (Kinkel *et al.*, 2013) regulates many of these genes. Both the histidine kinase (*srrB*) and the response regulator (*srrA*) components of SrrAB locus (which differentially regulates *S. aureus* genes under aerobic and hypoxic growth) were recognised as essential for staphylococcal survival in bone, implying its importance in survival during chronic infection such as osteomyelitis, which is a profoundly hypoxic setting (Wilde *et al.*, 2015). A wide range of clinical isolates of *S. aureus* from human disease have also been sequenced (Copin *et al.*, 2018) and are available for data mining.

The NADPH Oxidase and Phagosomal pH

In order to measure the phagosomal pH, I stained bacteria with the pHrodo red dye, which changes its fluorescence intensity in response to changes in the surrounding pH (strong fluorescent signal in acidic pH, weak fluorescent signal in alkaline pH, (Lindner *et al.*, 2020). This staining allows continuous monitoring of pH changes, as the signal is still responsive if bacteria are killed whilst they remain intact. Such reporters have limitations however, for example the pH ranges that are accurately reported may be limited (e.g., an alternative reporter, SNARF-1 which can only accurately determine the pH of particles in the pH range of 7-8 (Levine *et al.*, 2015; Loiselle and Casey, 2003; Hayes *et al.*, 2020)), hence it is challenging to measure intraphagosomal pH accurately. pHrodo is able to detect changes in pH between 4 and 9, hence its use in my study. Changes in the pH within neutrophil phagosomes can affect the activity of various microbicidal granule proteins that operate in the specific range of pH, optimally at 7-8 pH for NE, MPO and α-defensins (Hayes *et al.*, 2020). It has been previously demonstrated that the defective function of the NADPH

oxidase in neutrophils from CGD patients led to massive fall in intraphagosomal pH resulting in the impairment of killing of *S. aureus* (Segal *et al.*, 1981). Unfortunately, I was not able to measure the pH of hypoxic neutrophil phagosomes as the live cells could not be imaged within the hypoxic chamber, and fixation impaired the fluorescent signal of the pHrodo-labelled bacteria. Whilst a fall in pH could contribute to the increase in staphylococcal survival within hypoxic and DPI treated neutrophils (by impairing the activation of antimicrobial granule proteins), it is unlikely to be the principal factor limiting staphylococcal killing, since reversing the rise of pH in DPI-treated neutrophils with bafilomycin (Fig. 4.8) did not improve killing of intracellular bacteria (Fig. 4.10). This reversal does however suggest that in situations when the NADPH oxidase is active, the activity of the bafilomycin-sensitive V-ATPase is limited, that DPI permits its activation by inhibition of ROS generation allowing influx of protons to acidify the phagosome, and that bafilomycin is hence able to prevent this proton influx. The failure of PI3K inhibitors (Class I or Class III) to modulate phagosomal pH (Figs. 4.13 and 4.16) despite a significant reduction in ROS generation (Figs. 4.11 and 4.14) does challenge this interpretation and prediction, however the inhibition of ROS generation was less complete than seen with DPI and it is possible that a 'threshold' effect applies. An alternative explanation is that the effect on pH is an off-target effect of DPI, but the observations in CGD patients argue against this.

Hv1/VSOP (hydrogen voltage-gated channel 1/ voltage- sensor domain-only protein) is expressed in neutrophils and mediates charge compensation during the respiratory burst and regulation of pH (Okochi *et al.*, 2009). It has been shown that Hv1/VSOP counteracts the charge imbalance induced by activation of the NADPH oxidase, enabling sustained oxidase activity (DeCoursey *et al.*, 2003). This action of Hv1/VSOP contributes to pH homeostasis; neutrophils lacking Hv1/VSOP generated phagosomes with dysregulated pH, with large population of alkaline (37%) and a smaller proportion (14%) of acidic phagosomes. With zymosan particles as prey, inhibition of the NADPH oxidase by DPI led to near-universal acidification of phagosomes, whether Hv1 was expressed or not, confirming that Hv1 is acting to compensate the NADPH oxidase-induced proton flux (El Chemaly *et al.*, 2014). El-Chamaly *et al*. concluded that ongoing activity of the oxidase prevents phagosomal acidification by the V-ATPase, an inhibition that is less pronounced in Hv1-deficient neutrophils. My results are consistent with this. However, the work of Foote *et al.*

(Foote *et al.*, 2019) suggests that a wide range of ion channels including chloride channels also contribute to the regulation of phagosomal pH (and morphology - see below). However, since pH in the phagosomal milieu does not seem to be key to staphylococcal execution, this avenue would not be a priority for future work on the impact of hypoxia on the neutrophil-staphylococcal interaction.

The NADPH Oxidase and Phagosomal Morphology

'Spacious' phagosomes have been described in relation to several pathogens in different cellular environments. Most data have been collected from macrophages, infected with a range of pathogens including *Salmonella enterica* subsp. *enterica* serovar *Typhimurium* (Alpuche-Aranda *et al.*, 1994), *Mycobacterium tuberculosis* (Schnettger *et al.*, 2017), *S. aureus* (Gresham *et al.*, 2000), *Listeria monocytogenes* (Birmingham *et al.*, 2008) or *Cryptococcus neoformans* (Alvarez and Casadevall, 2006). However, the macrophage phagosome is a very different environment to the neutrophil phagosome - it is highly acidic and phagosomal maturation proceeds by fusion with late endosomes. The maturation of the neutrophil phagosome is less well documented but relies more on the fusion of granules with pH maintained in the near-normal range as described above. Hence results from macrophages cannot be extrapolated to neutrophils.

It has been suggested that spacious phagosome formation is due to entry into the cell via macropinocytosis with a formation of a macropinosome via a form of regulated membrane ruffling (Hewlett *et al.*, 1994). The environment of spacious phagosomes serves as a niche for improved survival and replication of most of the mentioned above pathogens. However, it is far more likely that in the majority of cases, the formation of spacious phagosomes reflects a more specific interference by the pathogen of the phagosome maturation process within the macrophage (summarised by Haas, 2007). There is little knowledge about macropinocytosis as a route for ingestion of pathogens in neutrophils. Pinocytosis exists in those cells and is known to be enhanced when neutrophils are primed by cytokines (Botelho *et al.*, 2002). However, multiple studies have suggested that *S. aureus* is internalised by the neutrophil by phagocytosis (and indeed this has been observed by members of our group using zebrafish (Ms Claire Muir and Prof Alison Condliffe, personal communication) and by super-resolution live imaging (Yin Ho and Dr Lynne Prince, personal communication) hence this does not

seem like a profitable direction for future study. It is possible that the generation of ROS is essential for the maturation of the neutrophil phagosome, for example by the docking of granules to the phagosomal membrane; however, although I did not set out to determine this my electron microscopy images did not suggest this was the case and I did observe (admittedly in only a limited number of examples) docking of granules with the phagosome in all conditions tested.

In vivo studies using the optically transparent zebrafish model have shown that *S. aureus* (SH1000 strain) is phagocytosed into spacious, LC3- positive, non-acidic phagosomes (LAPosomes) in wild type neutrophils, whereas in *cyba* ($p22^{phox}$) knockdown or DPI-treated fish, bacteria were found within tight, LC3-negative and acidic phagosomes (Prajsnar *et al.*, 2021). The impact of DPI on phagosomal morphology is highly reminiscent of my observations (Figs. 4.3, 4.4 and 4.5) of its impact on human neutrophils ingesting the same pathogen (and same strain). In the study undertaken by Prajsnar *et al*. however, knockout of *cyba* (resulting in a non-functional NADPH oxidase or the use of DPI) enhanced survival of infected fish relative to controls. The authors concluded that the 'normal' spacious phagosomes serve as a niche for bacterial persistence and promote dissemination of infection (Prajsnar *et al.*, 2021). In complete contrast, in my study of isolated human neutrophils, both hypoxia and DPI- treated cells formed predominantly tight phagosomes (acidified in the context of DPI) but killed *S. aureus* incompletely (Figs. 3.11, 3.12 and 4.1 respectively). Furthermore, in the zebrafish neutrophils only live bacteria led to the formation of spacious phagosomes, whilst I found that bacterial viability did not affect this response in human neutrophils (Fig.4.3.D). The reason for these contrasting outcomes is uncertain. Whilst it is possible that they reflect species differences, in general observations from zebrafish neutrophils have translated well to the human setting. It is possible that the inhibition of the NADPH oxidase at the whole organism level is relevant, as the generation of ROS will be inhibited in a range of cell types, and the potential for ROS-mediated damage will also be abolished. Of note, in the whole organism study, although the difference in phagosome morphology was observed early (1 h post-infection - 1 hpi), survival was measured over 100 h with no divergence prior to 48 h. Consistent with my results, at 3 hpi fish lacking a functional oxidase had a higher bacterial burden, consistent with impaired killing; however, at 28 hpi this finding was reversed. This is in contrast to my data that the hypoxic neutrophils at 24

h failed to kill internalised bacteria (Fig. 3.12). One possible explanation is that I studied only intracellular killing - the difference could relate to bacteria which were not ingested in the *in vivo* zebrafish model. It should also be noted that the study by Prasjnar *et al*. used zebrafish in which *irf8* had been knocked down to polarise development to neutrophils rather than macrophages - this lack of macrophages could be relevant to the later failure to control infection and would not be captured in my studies of isolated human neutrophils.

The spacious phagosomes appeared to occupy more of the cell in the live cell imaging than EM images. This may in part be due to the fact I used Z-stacks and the images I present represent multiple planes, whilst the EM images represent a single plane. Furthermore, preparation for EM requires stringent and lengthy fixation, embedding, sectioning, and contrast staining steps prior to imaging which can affect cellular morphology (as discussed by Gilbert and Parmley, 1998); hence it is possible that the large spacious phagosomal morphology was particularly susceptible to such disturbances. Regarding the genesis of spacious phagosomes, it has been suggested (Hewlett *et al.*, 1994) that spacious phagosome formation is due to uptake by pinocytosis rather than phagocytosis. Although the identical time course of phagocytosis under normoxia and hypoxia makes this unlikely, it has not been specifically investigated. Of note, the impact of hypoxia on micropinocytosis on tumour cells has been studied; of interest, Gundel *et al*., (Gündel *et al.*, 2017) found that hypoxia compromised micropinocytosis (uptake of FITC-dextran) by a prostate cancer cell line (AT-1) but not a breast cancer cell line (Walker cells). A possible mechanism was recently suggested by Su et al., (Hua Su *et al.*, 2021), who noted that in a pancreatic cancer cell line, blockade of autophagy or hypoxia activated micropinocytosis via the transcription factor Nrf2. The impact of hypoxia on neutrophil micropinocytosis has not been reported to my knowledge, and it would be of interest to investigate this by undertaking experiments in normoxia and hypoxia in the presence of FITC-dextran. However, since FITC-dextran would also be internalised by phagocytosis it would not be feasible to use this method to determine which of these 2 processes led to the internalisation of *S. aureus* in normoxia versus hypoxia, and likewise compounds such as PI3K inhibitors that impair micropinocytosis would also likely affect phagocytosis. It is also possible that the generation of spacious phagosomes reflect the fusion of granules/lysosomes with the phagosome and that

these processes inhibited in hypoxia leading the tight phagosomes formation. However, in my EM images I did see granules fusing with phagosomes in all conditions (normoxia, hypoxia and DPI treatment), although these were rare events and seen only once or twice in each setting. It seems unlikely that these factors are the only ones relevant, but it would be of interest to explore the morphology of *E. coli*-associated phagosomes, since these bacteria are killed effectively in hypoxia likely by the fusion of granules with the phagosome.

As noted above (Section: The NADPH Oxidase and Phagosomal pH) the impact of hypoxia and DPI on phagosomal morphology is likely affected via its effect on a range of ion channels, and it is likely that this leads to alteration in osmotic gradients and hence the passive transfer of water into the phagosome. This is supported by the work of Foote *et al*., (Foote *et al.*, 2019) who found that genetic deletion of a range of ion channels modulated phagosomal pH and morphology. It would be of interest to document the impact of hypoxia on neutrophils from such genetic backgrounds, although these are mouse models and I have not confirmed that spacious/tight phagosomal morphology is the same in mouse neutrophils.

I observed that ROS production was associated with spacious phagosome formation, and these structures could plausibly be 'LAPosomes' (Prajsnar *et al.*, 2021), however more work would be needed to confirm this. I attempted to do this by immunochemical staining of fixed cells for LC3 as well as by western blotting, but both approaches were unsuccessful. Immunostaining was not helpful as multiple antibodies were found to bind non-specifically but very strongly to bacteria within the phagosomes, hence all phagosomes appeared strongly positive, and it was not possible to distinguish staining at the membrane from staining within the phagosome. Similar problems were encountered with western blotting, further compounded by the proteolytic capacity of neutrophils. Provisional agreement had been reached for a collaboration with Dr Ezra Askoy (Queen Mary University, London) as she has mice lacking some of the LAP machinery (including Rubicon knockout mice). I had intended to repeat my studies initially looking at phagosomal morphology in neutrophils from these mice, but the COVID pandemic meant that this was no longer feasible. It is hoped that this will be pursued in future.

Wood *et al.*, (2020) reported that inhibition of VPS34 led to changes in intraphagosomal pH following ingestion of *S. aureus* (MSSA, strain ASASM6)

measured by the pHrodo signal using flow cytometry, and also impaired killing of bacteria in whole blood killing assay (Wood *et al.*, 2020), in contrast to my findings with isolated neutrophils using the same inhibitor. I found that VPS34-IN1 in fact improved neutrophil- mediated killing of *S. aureus* (Fig. 4.17), with no effect on intraphagosomal pH (Fig. 4.16) but reduced ROS production (Fig. 4.14). VPS34 generates the phospholipid PI3P, which function is to control extent of recruitment of cytoplasmic oxidase subunits to the phagosome membrane (PI3P binds to $p40^{phox}$, which is complexed to $p67^{phox}$) and hence regulates ROS production and sustainability (Song *et al.*, 2017). Whilst the different results might reflect the substantial methodological differences, the augmented killing of bacteria in the setting of reduced ROS generation was unexpected and counter-intuitive, but highly reproducible. Furthermore, a PhD student working in a separate group in Sheffield has found that the VPS34-IN1 augments killing of *S. aureus* by primary human macrophages and is indeed using this as a positive control in a drug screen (Ms Faith Tolliday, personal communication). We speculate that VPS34IN1 is inhibiting LC3 processing and hence affecting LAP; which leads to enhanced killing of *S. aureus,* perhaps by preventing the subsequent induction of xenophagy (Prajsnar *et al.*, 2021). It would be interesting to test its effect on later stages of infection, where this inhibitor could inhibit autophagy and maybe increase survival of bacteria. It would be also worth exploring the impact of the VPS34 inhibitor on intracellular killing of other staphylococcal strains (e.g., JE2), but also add this inhibitor to hypoxic neutrophils.

In summary I have shown that modulation of ROS generation by hypoxia or DPI modulates phagosomal ROS generation, morphology and phagosomal pH, and that these effects will alter the outcome of the host-pathogen interaction with impaired killing seen when ROS production is impaired and the phagosomal shifts from a spacious to a tight morphology (see Figure 6.1 below). These results offer new insights into the likely nature of interactions between innate immune cells and bacteria in the setting of typical ‘pathological’ hypoxia which characterises the majority of infections in the *in vivo* setting. The ability of VPS43-IN1 to enhance neutrophil-mediated staphylococcal killing is of interest and the mechanism of this unexpected result will be further explored in future projects.

.

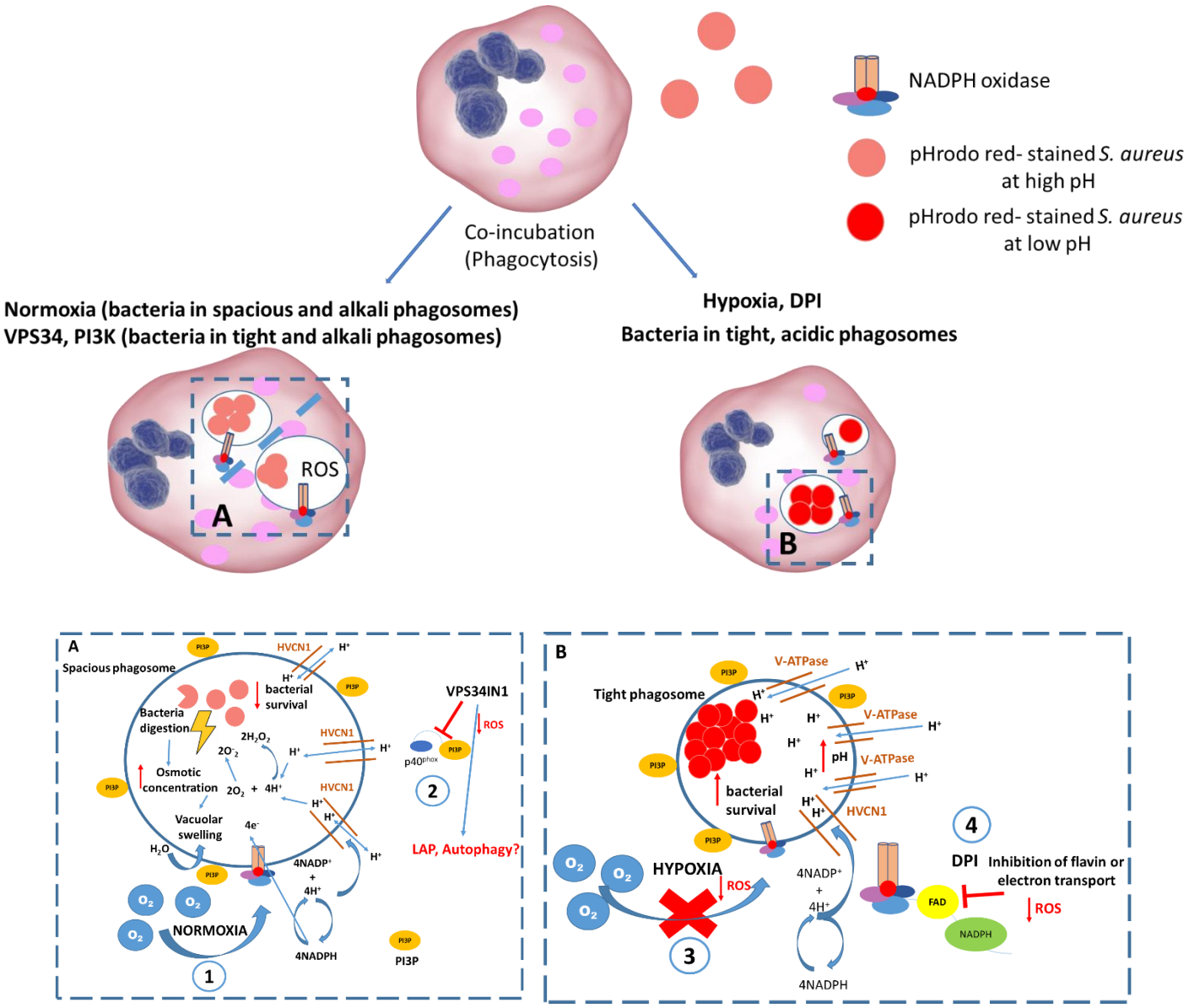

Figure 6.1 Summary and Model of neutrophil-*S. aureus* interactions

*S. aureus is phagocytosed by human neutrophils and this is not affected by VPS34-IN1 (VPS34 in the figure), Class 1 PI3K inhibition (PI3K), hypoxia or DPI. In normoxia **(1)** there is sufficient molecular oxygen to support the oxidative burst by activated NADPH oxidase in neutrophils. Bacteria are thus enclosed within neutral/alkaline phagosomes as charge compensation by channels such as Hv1 is ongoing but the access of the VTPase is blocked. The spacious nature of the phagosomes may relate to osmotic entry of water into the phagosome secondary to the NADPH oxidase activity, fusion with other organelles such as granules and LC3-containing membranes. When VPS34IN1 or Class I PI3K inhibitors are used **(2)**, they reduce recruitment of components of the oxidase (p40^{phox}subunit or p47^{phox}) and hence reduce ROS production, reducing osmotic flux and leading to tighter phagosome*

formation. Importantly, inhibition of VPS34 may reduce fusion of LC3-positive membranes to reduce LAPosome generation and hence improve killing of bacteria at early timepoints. In hypoxia, oxygen availability is limiting, and ROS production is impaired ***(3)****, reducing the capacity for killing of S. aureus passively limiting phagosomal swelling. By extrapolation from results with the NADPH oxidase inhibitor DPI* ***(4)*** *as well as neutrophils from patients with CGD, I predict that hypoxic neutrophils will also display acidification of phagosomes, but this has not been tested directly.*

References

A. L. Cheung, J. M. Koomey, C. A. Butler, S. J. Projan, V. A. Fischetti (1992) Regulation of exoprotein expression in Staphylococcus aureus by a locus (sar) distinct from agr. *Proceedings of the National Academy of Sciences of the United States of America*. **89**(14), 6462.

Ab, G.-C., Mt, N., Ab, W., Lh, P.-S., Em, S. (2012) ETosis: A Microbicidal Mechanism beyond Cell Death. *Journal of parasitology research*. **2012**.

Accarias, S., Genthon, C., Rengel, D., Boullier, S., Foucras, G., Tabouret, G. (2016) Single- cell analysis reveals new subset markers of murine peritoneal macrophages and highlights macrophage dynamics upon Staphylococcus aureus peritonitis. *Innate Immunity*. **22**(5), 382–392.

Adams, W., Espicha, T., Estipona, J. (2021) Getting Your Neutrophil: Neutrophil Transepithelial Migration in the Lung. *Infection and Immunity*.

Aleyd, E., van Hout, M.W.M., Ganzevles, S.H., Hoeben, K.A., Everts, V., Bakema, J.E., van Egmond, M. (2014) IgA enhances NETosis and release of neutrophil extracellular traps by polymorphonuclear cells via Fcα receptor I. *Journal of Immunology (Baltimore, Md.: 1950)*. **192**(5), 2374–2383.

Alipour, R., Fatemi, A., Alsahebfosul, F., Andalib, A., Pourazar, A. (2020) Autologous plasma versus fetal calf serum as a supplement for the culture of neutrophils. *BMC Research Notes*. **13**(1), 39.

Alpuche-Aranda, C.M., Racoosin, E.L., Swanson, J.A., Miller, S.I. (1994) Salmonella stimulate macrophage macropinocytosis and persist within spacious phagosomes. *The Journal of Experimental Medicine*. **179**(2), 601–608.

Alvarez, M., Casadevall, A. (2006) Phagosome extrusion and host-cell survival after Cryptococcus neoformans phagocytosis by macrophages. *Current biology: CB*. **16**(21), 2161–2165.

Anderson, K.E., Boyle, K.B., Davidson, K., Chessa, T.A.M., Kulkarni, S., Jarvis, G.E., Sindrilaru, A., Scharffetter-Kochanek, K., Rausch, O., Stephens, L.R., Hawkins, P.T. (2008) CD18-dependent activation of the neutrophil NADPH oxidase during phagocytosis of Escherichia coli or Staphylococcus aureus is regulated by class III but not class I or II PI3Ks. *Blood*. **112**(13), 5202–5211.

Arazna, M., Pruchniak, M.P., Demkow, U. (2013) Neutrophil extracellular traps in bacterial infections: strategies for escaping from killing. *Respiratory Physiology & Neurobiology*. **187**(1), 74–77.

Atallah, M., Krispin, A., Trahtemberg, U., Ben-Hamron, S., Grau, A., Verbovetski, I., Mevorach, D. (2012) Constitutive Neutrophil Apoptosis: Regulation by Cell Concentration via S100 A8/9 and the MEK – ERK Pathway. *Plos One*. **7**(2), e29333.

Austin, E.D., Sullivan, S.B., Whittier, S., Lowy, F.D., Uhlemann, A.-C. (2016) Peripheral Intravenous Catheter Placement Is an Underrecognized Source of

Staphylococcus aureus Bloodstream Infection. *Open forum infectious diseases*. **3**(2), ofw072–ofw072.

Babior, B.M., Kipnes, R., Curnutte, J. (2014) Biological Defense Mechanisms THE PRODUCTION BY LEUKOCYTES OF SUPEROXIDE, A POTENTIAL BACTERICIDAL AGENT. *Journal of Immunology*. **193**(11), 5359–5362.

Baddela, V.S., Baufeld, A., Yenuganti, V.R., Vanselow, J., Singh, D. (2014) Suitable housekeeping genes for normalization of transcript abundance analysis by real-time RT-PCR in cultured bovine granulosa cells during hypoxia and differential cell plating density. *Reproductive Biology and Endocrinology*. **12**(1), 118.

Bago, R., Malik, N., Munson, M.J., Prescott, A.R., Davies, P., Sommer, E., Shpiro, N., Ward, R., Cross, D., Ganley, I.G., Alessi, D.R. (2014) Characterization of VPS34-IN1, a selective inhibitor of Vps34, reveals that the phosphatidylinositol 3-phosphate-binding SGK3 protein kinase is a downstream target of class III phosphoinositide 3-kinase. *Biochemical Journal*. **463**(Pt 3), 413–427.

Bahar Bilgen, Ester Orsini, Roy K Aaron, Deborah McK Ciombor (2008) FBS suppresses TGF-beta1-induced chondrogenesis in synoviocyte pellet cultures while dexamethasone and dynamic stimuli are beneficial. *J Tissue Eng Regen Med* .. **1**(6), 436–442.

Baicu, S.C., Taylor, M.J. (2002) Acid–base buffering in organ preservation solutions as a function of temperature: new parameters for comparing buffer capacity and efficiency. *Cryobiology*. **45**(1), 33–48.

Bainton, D.F., Farquhar, M.G. (1968) Differences in enzyme content of azurophil and specific granules of polymorphonuclear leukocytes. I. Histochemical staining of bone marrow smears. *The Journal of Cell Biology*. **39**(2), 286–298.

Bainton, D.F., Ullyot, J.L., Farquhar, M.G. (1971) The development of neutrophilic polymorphonuclear leukocytes in human bone marrow. *The Journal of experimental medicine*. **134**(4), 907–934.

Baker, M. (2016) Reproducibility: Respect your cells! *Nature*. **537**(7620), 433–435.

Barbieri, S.S., Cavalca, V., Eligini, S., Brambilla, M., Caiani, A., Tremoli, E., Colli, S. (2004) Apocynin prevents cyclooxygenase 2 expression in human monocytes through NADPH oxidase and glutathione redox-dependent mechanisms. *Free Radical Biology & Medicine*. **37**(2), 156–165.

Bass, D.A., Parce, J.W., Dechatelet, L.R., Szejda, P., Seeds, M.C., Thomas, M. (1983) Flow cytometric studies of oxidative product formation by neutrophils: a graded response to membrane stimulation. *J Immunol*. **130**(4), 1910–7.

Beaumel, S., Picciocchi, A., Debeurme, F., Vivès, C., Hesse, A.-M., Ferro, M., Grunwald, D., Stieglitz, H., Thepchatri, P., Smith, S.M.E., Fieschi, F., Stasia, M.J. (2017) Down-regulation of NOX2 activity in phagocytes mediated by ATM-kinase dependent phosphorylation. *Free Radical Biology & Medicine*. **113**, 1–15.

Beerlage, C., Greb, J., Kretschmer, D., Assaggaf, M., Trackman, P.C., Hansmann, M.-L., Bonin, M., Eble, J.A., Peschel, A., Brüne, B., Kempf, V.A.J. (2013) Hypoxia-inducible factor 1-regulated lysyl oxidase is involved in Staphylococcus aureus abscess formation. *Infection and Immunity*. **81**(7), 2562–2573.

Belambri, S.A., Rolas, L., Raad, H., Hurtado-Nedelec, M., Dang, P.M.-C., El-Benna, J. (2018) NADPH oxidase activation in neutrophils: Role of the phosphorylation of its subunits. *European Journal of Clinical Investigation*. **48 Suppl 2**, e12951.

Berton, G., Dusi, S., Bellavite, P. (1988) The Respiratory Burst of Phagocytes. In A. J. Sbarra & R. R. Strauss, eds. *The Respiratory Burst and Its Physiological Significance*. Boston, MA: Springer US, pp. 33–52.

Birmingham, C.L., Canadien, V., Kaniuk, N.A., Steinberg, B.E., Higgins, D.E., Brumell, J.H. (2008) Listeriolysin O allows Listeria monocytogenes replication in macrophage vacuoles. *Nature*. **451**(7176), 350–354.

Bore, E., Langsrud, S., Langsrud, Ø., Rode, T.M., Holck, A. (2007) Acid-shock responses in Staphylococcus aureus investigated by global gene expression analysis. *Microbiology (Reading, England)*. **153**(Pt 7), 2289–2303.

Borregaard, N., Heiple, J.M., Simons, E.R., Clark, R.A. (1983) Subcellular localization of the b-cytochrome component of the human neutrophil microbicidal oxidase: translocation during activation. *The Journal of Cell Biology*. **97**(1), 52–61.

Botelho, R.J., Tapper, H., Furuya, W., Mojdami, D., Grinstein, S. (2002) FcγR-Mediated Phagocytosis Stimulates Localized Pinocytosis in Human Neutrophils. *The Journal of Immunology*. **169**(8), 4423–4429.

Bowman, E.J., Graham, L.A., Stevens, T.H., Bowman, B.J. (2004) The Bafilomycin/Concanamycin Binding Site in Subunit c of the V-ATPases from *Neurospora crassa* and *Saccharomyces cerevisiae*. *Journal of Biological Chemistry*. **279**(32), 33131–33138.

Bowman, E.J., Siebers, A., Altendorf, K. (1988) Bafilomycins: a class of inhibitors of membrane ATPases from microorganisms, animal cells, and plant cells. *Proceedings of the National Academy of Sciences*. **85**(21), 7972–7976.

Branitzki-Heinemann, K., Mollerherm, H., Vollger, L., Husein, D.M., de Buhr, N., Blodkamp, S., Reuner, F., Brogden, G., Naim, H., Von Kockritz-Blickwede, M. (2016) Formation of neutrophil extracellular traps under Low oxygen Level. *Frontiers in Immunology*. **7**.

Bratton, D.L., Henson, P.M. (2011) Neutrophil clearance: when the party is over, clean-up begins. *Trends in Immunology*. **32**(8), 350–357.

Braun, R.D., Lanzen, J.L., Snyder, S.A., Dewhirst, M.W. (2001) Comparison of tumor and normal tissue oxygen tension measurements using OxyLite or microelectrodes in rodents. *American journal of physiology. Heart and circulatory physiology*. **280**(6), H2533.

Brinkmann, V., Reichard, U., Goosmann, C., Fauler, B., Uhlemann, Y., Weiss, D.S., Weinrauch, Y., Zychlinsky, A. (2004) Neutrophil extracellular traps kill bacteria. *Science (New York, N.Y.)*. **303**(5663), 1532–5.

Burian, E.A., Sabah, L., Kirketerp-Møller, K., Ibstedt, E., Fazli, M.M., Gundersen, G. (2021) The Safety and Antimicrobial Properties of Stabilized Hypochlorous Acid in Acetic Acid Buffer for the Treatment of Acute Wounds-a Human Pilot Study and In Vitro Data. *The International Journal of Lower Extremity Wounds*, 15347346211015656.

Buvelot, H., Posfay-Barbe, K.M., Linder, P., Schrenzel, J., Krause, K.H. (2017) Staphylococcus aureus, phagocyte NADPH oxidase and chronic granulomatous disease. *Fems Microbiology Reviews*. **41**(2), 139–157.

Campbell, E.L., Bruyninckx, W.J., Kelly, C.J., Glover, L.E., McNamee, E.N., Bowers, B.E., Bayless, A.J., Scully, M., Saeedi, B.J., Golden-Mason, L., Ehrentraut, S.F., Curtis, V.F., Burgess, A., Garvey, J.F., Sorensen, A., Nemenoff, R., Jedlicka, P., Taylor, C.T., Kominsky, D.J., Colgan, S.P. (2014) Transmigrating Neutrophils Shape the Mucosal Microenvironment through Localized Oxygen Depletion to Influence Resolution of Inflammation. *Immunity*. **40**(1), 66–77.

Cheng, A.G., Kim, H.K., Burts, M.L., Krausz, T., Schneewind, O., Missiakas, D.M. (2009) Genetic requirements for Staphylococcus aureus abscess formation and persistence in host tissues. *FASEB journal : official publication of the Federation of American Societies for Experimental Biology*. **23**(10), 3393.

Cheng, A.G., McAdow, M., Kim, H.K., Bae, T., Missiakas, D.M., Schneewind, O. (2010) Contribution of Coagulases towards Staphylococcus aureus Disease and Protective Immunity. *PLoS Pathogens*. **6**(8).

Clauditz, A., Resch, A., Wieland, K.-P., Peschel, A., Götz, F. (2006) Staphyloxanthin plays a role in the fitness of Staphylococcus aureus and its ability to cope with oxidative stress. *Infection and Immunity*. **74**(8), 4950–4953.

Clements, M.O., Watson, S.P., Foster, S.J. (1999) Characterization of the Major Superoxide Dismutase of Staphylococcus aureus and Its Role in Starvation Survival, Stress Resistance, and Pathogenicity. *Journal of Bacteriology*. **181**(13), 3898–3903.

Coffer, P.J., Geijsen, N., M'rabet, L., Schweizer, R.C., Maikoe, T., Raaijmakers, J.A., Lammers, J.W., Koenderman, L. (1998) Comparison of the roles of mitogen-activated protein kinase kinase and phosphatidylinositol 3-kinase signal transduction in neutrophil effector function. *The Biochemical Journal*. **329 (Pt 1)**, 121–130.

Condliffe, A.M., Davidson, K., Anderson, K.E., Ellson, C.D., Crabbe, T., Okkenhaug, K., Vanhaesebroeck, B., Turner, M., Webb, L., Wymann, M.P., Hirsch, E., Ruckle, T., Camps, M., Rommel, C., Jackson, S.P., Chilvers, E.R., Stephens, L.R., Hawkins, P.T. (2005) Sequential activation of class IB and class IA PI3K is important for the primed respiratory burst of human but not murine neutrophils. *Blood*. **106**(4), 1432–40.

Copin, R., Shopsin, B., Torres, V.J. (2018) After the deluge: mining Staphylococcus aureus genomic data for clinical associations and host-pathogen interactions. *Current Opinion in Microbiology*. **41**, 43–50.

Cosgrove, K., Coutts, G., Jonsson, I.-M., Tarkowski, A., Kokai-Kun, J.F., Mond, J.J., Foster, S.J. (2007) Catalase (KatA) and Alkyl Hydroperoxide Reductase (AhpC) Have Compensatory Roles in Peroxide Stress Resistance and Are Required for Survival, Persistence, and Nasal Colonization in Staphylococcus aureus. *Journal of Bacteriology*. **189**(3), 1025–1035.

Cowland, J.B., Borregaard, N. (2016) Granulopoiesis and granules of human neutrophils. *Immunological Reviews*. **273**(1), 11–28.

Cramer, T., Yamanishi, Y., Clausen, B.E., Forster, I., Pawlinski, R., Mackman, N., Haase, V.H., Jaenisch, R., Corr, M., Nizet, V., Firestein, G.S., Gerber, H.P., Ferrara, N., Johnson, R.S. (2003) HIF-1 alpha is essential for myeloid cell-mediated inflammation. *Cell*. **112**(5), 645–657.

Cross, A.R., Jones, O.T. (1986) The effect of the inhibitor diphenylene iodonium on the superoxide-generating system of neutrophils. Specific labelling of a component polypeptide of the oxidase. *Biochemical Journal*. **237**(1), 111–116.

Dahlgren, C., Karlsson, A., Bylund, J. (2019) Intracellular Neutrophil Oxidants: From Laboratory Curiosity to Clinical Reality. *Journal of Immunology (Baltimore, Md.: 1950)*. **202**(11), 3127–3134.

Dancey, J.T., Deubelbeiss, K.A., Harker, L.A., Finch, C.A. (1976) Neutrophil kinetics in man. *Journal of Clinical Investigation*. **58**(3), 705–715.

Dang, P.M., Dewas, C., Gaudry, M., Fay, M., Pedruzzi, E., Gougerot-Pocidalo, M.A., El Benna, J. (1999) Priming of human neutrophil respiratory burst by granulocyte/macrophage colony-stimulating factor (GM-CSF) involves partial phosphorylation of p47(phox). *The Journal of Biological Chemistry*. **274**(29), 20704–20708.

Dang, P.M.-C., Stensballe, A., Boussetta, T., Raad, H., Dewas, C., Kroviarski, Y., Hayem, G., Jensen, O.N., Gougerot-Pocidalo, M.-A., El-Benna, J. (2006) A specific p47phox -serine phosphorylated by convergent MAPKs mediates neutrophil NADPH oxidase priming at inflammatory sites. *The Journal of Clinical Investigation*. **116**(7), 2033–2043.

Davies, M.J. (2005) The oxidative environment and protein damage. *Biochimica Et Biophysica Acta*. **1703**(2), 93–109.

Davies, S.P., Reddy, H., Caivano, M., Cohen, P. (2000) Specificity and mechanism of action of some commonly used protein kinase inhibitors. *The Biochemical journal*. **351**(Pt 1), 95–105.

Decleva, E., Menegazzi, R., Busetto, S., Patriarca, P., Dri, P. (2006) Common methodology is inadequate for studies on the microbicidal activity of neutrophils. *Journal of Leukocyte Biology*. **79**(1), 87–94.

DeCoursey, T.E., Morgan, D., Cherny, V.V. (2003) The voltage dependence of NADPH oxidase reveals why phagocytes need proton channels. *Nature*. **422**(6931), 531–534.

Dewas, C., Dang, P.M.-C., Gougerot-Pocidalo, M.-A., El-Benna, J. (2003) TNF-alpha induces phosphorylation of p47(phox) in human neutrophils: partial phosphorylation of p47phox is a common event of priming of human neutrophils by TNF-alpha and granulocyte-macrophage colony-stimulating factor. *Journal of Immunology (Baltimore, Md.: 1950)*. **171**(8), 4392–4398.

Dewitt, S., Tian, W., Hallett, M.B. (2006) Localised PtdIns(3,4,5)P3 or PtdIns(3,4)P2 at the phagocytic cup is required for both phagosome closure and Ca2+ signalling in HL60 neutrophils. *Journal of Cell Science*. **119**(Pt 3), 443–451.

Di, A., Brown, M.E., Deriy, L.V., Li, C., Szeto, F.L., Chen, Y., Huang, P., Tong, J., Naren, A.P., Bindokas, V., Palfrey, H.C., Nelson, D.J. (2006) CFTR regulates phagosome acidification in macrophages and alters bactericidal activity. *Nature Cell Biology*. **8**(9), 933–944.

Diep, B.A., Gill, S.R., Chang, R.F., Phan, T.H., Chen, J.H., Davidson, M.G., Lin, F., Lin, J., Carleton, H.A., Mongodin, E.F., Sensabaugh, G.F., Perdreau-Remington, F. (2006) Complete genome sequence of USA300, an epidemic clone of community-acquired meticillin-resistant Staphylococcus aureus. *The Lancet*. **367**(9512), 731–739.

Donner, A. (2011) Deubiquitinating p53. *Nature Chemical Biology*. **7**(12), 856–856.

Dorries, K., Lalk, M. (2013) Metabolic footprint analysis uncovers strain specific overflow metabolism and D-isoleucine production of Staphylococcus aureus COL and HG001. *Plos One*. **8**(12), e81500.

Dostert, C., Pétrilli, V., Van Bruggen, R., Steele, C., Mossman, B.T., Tschopp, J. (2008) Innate immune activation through Nalp3 inflammasome sensing of asbestos and silica. *Science (New York, N.Y.)*. **320**(5876), 674–677.

Dowdle, W.E., Nyfeler, B., Nagel, J., Elling, R.A., Liu, S., Triantafellow, E., Menon, S., Wang, Z., Honda, A., Pardee, G., Cantwell, J., Luu, C., Cornella-Taracido, I., Harrington, E., Fekkes, P., Lei, H., Fang, Q., Digan, M.E., Burdick, D., Powers, A.F., Helliwell, S.B., D'Aquin, S., Bastien, J., Wang, H., Wiederschain, D., Kuerth, J., Bergman, P., Schwalb, D., Thomas, J., Ugwonali, S., Harbinski, F., Tallarico, J., Wilson, C.J., Myer, V.E., Porter, J.A., Bussiere, D.E., Finan, P.M., Labow, M.A., Mao, X., Hamann, L.G., Manning, B.D., Valdez, R.A., Nicholson, T., Schirle, M., Knapp, M.S., Keaney, E.P., Murphy, L.O. (2014) Selective VPS34 inhibitor blocks autophagy and uncovers a role for NCOA4 in ferritin degradation and iron homeostasis in vivo. *Nature Cell Biology*. **16**(11), 1069–1079.

Dri, P., Presani, G., Perticarari, S., Albèri, L., Prodan, M., Decleva, E. (2002) Measurement of phagosomal pH of normal and CGD-like human neutrophils by dual fluorescence flow cytometry. *Cytometry*. **48**(3), 159–166.

Dukan, S., Belkin, S., Touati, D. (1999) Reactive Oxygen Species Are Partially Involved in the Bacteriocidal Action of Hypochlorous Acid. *Archives of Biochemistry and Biophysics*. **367**(2), 311–316.

Dunman, P.M., Murphy, E., Haney, S., Palacios, D., Tucker-Kellogg, G., Wu, S., Brown, E.L., Zagursky, R.J., Shlaes, D., Projan, S.J. (2001) Transcription profiling-based identification of Staphylococcus aureus genes regulated by the agr and/or sarA loci. *Journal of bacteriology*. **183**(24), 7341–7353.

Easmon, C.S., Lanyon, H., Cole, P.J. (1978) Use of lysostaphin to remove cell-adherent staphylococci during in vitro assays of phagocyte function. *Br J Exp Pathol*. **59**(4), 381–5.

Eisenbeis, J., Saffarzadeh, M., Peisker, H., Jung, P., Thewes, N., Preissner, K.T., Herrmann, M., Molle, V., Geisbrecht, B.V., Jacobs, K., Bischoff, M. (2018) The Staphylococcus aureus Extracellular Adherence Protein Eap Is a DNA Binding Protein Capable of Blocking Neutrophil Extracellular Trap Formation. *Frontiers in cellular and infection microbiology*. **8**, 235–235.

El Chemaly, A., Nunes, P., Jimaja, W., Castelbou, C., Demaurex, N. (2014) Hv1 proton channels differentially regulate the pH of neutrophil and macrophage phagosomes by sustaining the production of phagosomal ROS that inhibit the delivery of vacuolar ATPases. *Journal of Leukocyte Biology*. **95**(5), 827–839.

El-Benna, J., Dang, P.M.-C., Gougerot-Pocidalo, M.-A. (2008) Priming of the neutrophil NADPH oxidase activation: role of p47phox phosphorylation and NOX2 mobilization to the plasma membrane. *Seminars in Immunopathology*. **30**(3), 279–289.

Elks, P.M., Brizee, S., van der Vaart, M., Walmsley, S.R., van Eeden, F.J., Renshaw, S.A., Meijer, A.H. (2013) Hypoxia Inducible Factor Signaling Modulates Susceptibility to Mycobacterial Infection via a Nitric Oxide Dependent Mechanism (HIF Signaling Modulates Mycobacterial Infection) D. S. Schneider, ed. . **9**(12), e1003789.

Elks, P.M., van Eeden, F.J., Dixon, G., Wang, X., Reyes-Aldasoro, C.C., Ingham, P.W., Whyte, M.K.B., Walmsley, S.R., Renshaw, S.A. (2011) Activation of hypoxia-inducible factor-1 alpha (Hif-1 alpha) delays inflammation resolution by reducing neutrophil apoptosis and reverse migration in a zebrafish inflammation model. *Blood*. **118**(3), 712–722.

Elks, P.M., Renshaw, S.A., Meijer, A.H., Walmsley, S.R., van Eeden, F.J. (2015) Exploring the HIFs, buts and maybes of hypoxia signalling in disease: lessons from zebrafish models. *Disease Models & Mechanisms*. **8**(11), 1349–1360.

Ellson, C.D., Anderson, K.E., Morgan, G., Chilvers, E.R., Lipp, P., Stephens, L.R., Hawkins, P.T. (2001) Phosphatidylinositol 3-phosphate is generated in phagosomal membranes. *Current Biology*. **11**(20), 1631–1635.

Ellson, C.D., Davidson, K., Ferguson, G.J., O'Connor, R., Stephens, L.R., Hawkins, P.T. (2006) Neutrophils from p40phox-/- mice exhibit severe defects in NADPH

oxidase regulation and oxidant-dependent bacterial killing. *The Journal of Experimental Medicine*. **203**(8), 1927–1937.

Faurschou, M., Borregaard, N. (2003) Neutrophil granules and secretory vesicles in inflammation. *Microbes and Infection*. **5**(14), 1317–1327.

Ferreira, M.T., Manso, A.S., Gaspar, P., Pinho, M.G., Neves, A.R. (2013) Effect of Oxygen on Glucose Metabolism: Utilization of Lactate in Staphylococcus Aureus as Revealed by In Vivo NMR Studies. *Plos One*. **8**(3), e58277.

Fey, P.D., Endres, J.L., Yajjala, V.K., Widhelm, T.J., Boissy, R.J., Bose, J.L., Bayles, K.W. (2013) A Genetic Resource for Rapid and Comprehensive Phenotype Screening of Nonessential Staphylococcus aureus Genes. *Mbio*. **4**(1), e00537-12.

Flannagan, R.S., Kuiack, R.C., McGavin, M.J., Heinrichs, D.E. (2018) Staphylococcus aureus Uses the GraXRS Regulatory System To Sense and Adapt to the Acidified Phagolysosome in Macrophages. *mBio*. **9**(4), e01143-18.

Foldager, C.B., Munir, S., Ulrik-Vinther, M., Søballe, K., Bünger, C., Lind, M. (2009) Validation of suitable house keeping genes for hypoxia-cultured human chondrocytes. *BMC Molecular Biology*. **10**, 94.

Fontayne, A., Dang, P.M.-C., Gougerot-Pocidalo, M.-A., El-Benna, J. (2002) Phosphorylation of p47phox sites by PKC alpha, beta II, delta, and zeta: effect on binding to p22phox and on NADPH oxidase activation. *Biochemistry*. **41**(24), 7743–7750.

Foote, J.R., Patel, A.A., Yona, S., Segal, A.W. (2019) Variations in the Phagosomal Environment of Human Neutrophils and Mononuclear Phagocyte Subsets. *Front Immunol*. **10**, 188.

Foster, T.J., Höök, M. (1998) Surface protein adhesins of Staphylococcus aureus. *Trends in Microbiology*. **6**(12), 484–488.

Francis, A., Venkatesh, G.H., Zaarour, R.F., Zeinelabdin, N.A., Nawafleh, H.H., Prasad, P., Buart, S., Terry, S., Chouaib, S. (2018) Tumor Hypoxia: A Key Determinant of Microenvironment Hostility and a Major Checkpoint during the Antitumor Response. . **38**(6), 505–524.

Fritzenwanger, M., Jung, C., Goebel, B., Lauten, A., Figulla, H.R. (2011) Impact of short-term systemic hypoxia on phagocytosis, cytokine production, and transcription factor activation in peripheral blood cells. *Mediators of inflammation*. **2011**, 429501–429501.

Fuchs, T.A., Abed, U., Goosmann, C., Hurwitz, R., Schulze, I., Wahn, V., Weinrauch, Y., Brinkmann, V., Zychlinsky, A. (2007) Novel cell death program leads to neutrophil extracellular traps. *The Journal of Cell Biology*. **176**(2), 231–241.

Ganz, T., Selsted, M.E., Szklarek, D., Harwig, S.S., Daher, K., Bainton, D.F., Lehrer, R.I. (1985) Defensins. Natural peptide antibiotics of human neutrophils. *The Journal of Clinical Investigation*. **76**(4), 1427–1435.

Garcia, R.C., Segal, A.W. (1988) Phosphorylation of the subunits of cytochrome b-245 upon triggering of the respiratory burst of human neutrophils and macrophages. *The Biochemical Journal*. **252**(3), 901–904.

Garcia, Y.M., Barwinska-Sendra, A., Tarrant, E., Skaar, E.P., Waldron, K.J., Kehl-Fie, T.E. (2017) A Superoxide Dismutase Capable of Functioning with Iron or Manganese Promotes the Resistance of Staphylococcus aureus to Calprotectin and Nutritional Immunity. *PLOS Pathogens*. **13**(1), e1006125.

Gardete, S., Tomasz, A. (2014) Mechanisms of vancomycin resistance in Staphylococcus aureus. *The Journal of clinical investigation*. **124**(7), 2836–2840.

Geer, A. van de, Nieto-Patlán, A., Kuhns, D.B., Tool, A.T.J., Arias, A.A., Bouaziz, M., Boer, M. de, Franco, J.L., Gazendam, R.P., Hamme, J.L. van, Houdt, M. van, Leeuwen, K. van, Verkuijlen, P.J.H., Berg, T.K. van den, Alzate, J.F., Arango-Franco, C.A., Batura, V., Bernasconi, A.R., Boardman, B., Booth, C., Burns, S.O., Cabarcas, F., Bensussan, N.C., Charbit-Henrion, F., Corveleyn, A., Deswarte, C., Azcoiti, M.E., Foell, D., Gallin, J.I., Garcés, C., Guedes, M., Hinze, C.H., Holland, S.M., Hughes, S.M., Ibañez, P., Malech, H.L., Meyts, I., Moncada-Velez, M., Moriya, K., Neves, E., Oleastro, M., Perez, L., Rattina, V., Oleaga-Quintas, C., Warner, N., Muise, A.M., López, J.S., Trindade, E., Vasconcelos, J., Vermeire, S., Wittkowski, H., Worth, A., Abel, L., Dinauer, M.C., Arkwright, P.D., Roos, D., Casanova, J.-L., Kuijpers, T.W., Bustamante, J. (2018) Inherited p40^{phox} deficiency differs from classic chronic granulomatous disease. *The Journal of Clinical Investigation*. **128**(9), 3957–3975.

Gibson, J.F., Prajsnar, T.K., Hill, C.J., Tooke, A.K., Serba, J.J., Tonge, R.D., Foster, S.J., Grierson, A.J., Ingham, P.W., Renshaw, S.A., Johnston, S.A. (2020) Neutrophils use selective autophagy receptor Sqstm1/p62 to target Staphylococcus aureus for degradation in vivo in zebrafish. *Autophagy*, 1–10.

Gifford, R.H., Malawista, S.E. (1970) A simple rapid micromethod for detecting chronic granulomatous disease of childhood. *The Journal of Laboratory and Clinical Medicine*. **75**(3), 511–519.

Gilbert, C.S., Parmley, R.T. (1998) Morphology of human neutrophils: A comparison of cryofixation, routine gluteraldehyde fixation, and the effects of dimethyl sulfoxide. *The Anatomical Record*. **252**(2), 254–263.

Gilman-Sachs, A., Tikoo, A., Akman-Anderson, L., Jaiswal, M., Ntrivalas, E., Beaman, K. (2015) Expression and role of a2 vacuolar-ATPase (a2V) in trafficking of human neutrophil granules and exocytosis. *Journal of Leukocyte Biology*. **97**(6), 1121–1131.

Godement, M., Zhu, J., Cerf, C., Vieillard-Baron, A., Maillon, A., Zuber, B., Bardet, V., Geri, G. (2021) Neutrophil Extracellular Traps in SARS-CoV2 Related Pneumonia in ICU Patients: The NETCOV2 Study. *Frontiers in Medicine*. **8**, 615984.

Goldmann, O., Medina, E. (2012) The expanding world of extracellular traps: not only neutrophils but much more. *Frontiers in Immunology*. **3**, 420.

Gordon, A.M., Rowan, R.M., Brown, T., Carson, H.G. (1973) Routine application of the nitroblue tetrazolium test in the clinical laboratory. *Journal of Clinical Pathology*. **26**(1), 52–56.

Görgens, A., Radtke, S., Möllmann, M., Cross, M., Dürig, J., Horn, P.A., Giebel, B. (2013) Revision of the Human Hematopoietic Tree: Granulocyte Subtypes Derive from Distinct Hematopoietic Lineages. *Cell Reports*. **3**(5), 1539–1552.

Gresham, H.D., Lowrance, J.H., Caver, T.E., Wilson, B.S., Cheung, A.L., Lindberg, F.P. (2000) Survival of Staphylococcus aureus inside neutrophils contributes to infection. *Journal of Immunology*. **164**(7), 3713–3722.

Grinstein, S., Furuya, W. (1986) Cytoplasmic pH regulation in phorbol ester-activated human neutrophils. *American Journal of Physiology-Cell Physiology*. **251**(1), C55–C65.

Groemping, Y., Rittinger, K. (2005) Activation and assembly of the NADPH oxidase: a structural perspective. *The Biochemical Journal*. **386**(Pt 3), 401–416.

Grosser, M.R., Weiss, A., Shaw, L.N., Richardson, A.R. (2016) Regulatory Requirements for Staphylococcus aureus Nitric Oxide Resistance. *Journal of Bacteriology*. **198**(15), 2043–2055.

Guenther, F., Stroh, P., Wagner, C., Obst, U., Hansch, G.M. (2009) Phagocytosis of staphylococci biofilms by polymorphonuclear neutrophils: S. aureus and S. epidermidis differ with regard to their susceptibility towards the host defense. *The International Journal of Artificial Organs*. **32**(9), 565–573.

Guerra, F.E., Borgogna, T.R., Patel, D.M., Sward, E.W., Voyich, J.M. (2017) Epic Immune Battles of History: Neutrophils vs. Staphylococcus aureus. *Frontiers in cellular and infection microbiology*. **7**, 286–286.

Guimarães-Costa, A.B., Nascimento, M.T.C., Wardini, A.B., Pinto-da-Silva, L.H., Saraiva, E.M. (2012) ETosis: A Microbicidal Mechanism beyond Cell Death. *Journal of Parasitology Research*. **2012**, 929743.

Gündel, D., Allmeroth, M., Reime, S., Zentel, R., Thews, O. (2017) Endocytotic uptake of HPMA-based polymers by different cancer cells: impact of extracellular acidosis and hypoxia. *International journal of nanomedicine*. **12**, 5571–5584.

Günther, F., Wabnitz, G.H., Stroh, P., Prior, B., Obst, U., Samstag, Y., Wagner, C., Hänsch, G.M. (2009) Host defence against Staphylococcus aureus biofilms infection: Phagocytosis of biofilms by polymorphonuclear neutrophils (PMN). *Molecular Immunology*. **46**(8), 1805–1813.

Guo, H., Hall, J.W., Yang, J., Ji, Y. (2017) The SaeRS Two-Component System Controls Survival of Staphylococcus aureus in Human Blood through Regulation of Coagulase. *Front Cell Infect Microbiol*. **7**, 204.

Guo, K., Searfoss, G., Krolikowski, D., Pagnoni, M., Franks, C., Clark, K., Yu, K.T., Jaye, M., Ivashchenko, Y. (2001) Hypoxia induces the expression of the pro-apoptotic gene BNIP3. *Cell Death Differ*. **8**(4), 367–76.

Gupta, A.K., Hasler, P., Holzgreve, W., Gebhardt, S., Hahn, S. (2005) Induction of neutrophil extracellular DNA lattices by placental microparticles and IL-8 and their presence in preeclampsia. *Human Immunology*. **66**(11), 1146–1154.

Haas, A. (2007) The phagosome: compartment with a license to kill. *Traffic (Copenhagen, Denmark)*. **8**(4), 311–330.

Haas, P.-J., de Haas, C.J.C., Kleibeuker, W., Poppelier, M.J.J.G., van Kessel, K.P.M., Kruijtzer, J.A.W., Liskamp, R.M.J., van Strijp, J.A.G. (2004) N-terminal residues of the chemotaxis inhibitory protein of Staphylococcus aureus are essential for blocking formylated peptide receptor but not C5a receptor. *Journal of Immunology (Baltimore, Md.: 1950)*. **173**(9), 5704–5711.

Haber, F., Weiss, J., Pope, W.J. (1934) The catalytic decomposition of hydrogen peroxide by iron salts. *Proceedings of the Royal Society of London. Series A - Mathematical and Physical Sciences*. **147**(861), 332–351.

Häger, M., Cowland, J.B., Borregaard, N. (2010) Neutrophil granules in health and disease. *Journal of Internal Medicine*. **268**(1), 25–34.

Hajdamowicz, N.H., Hull, R.C., Foster, S.J., Condliffe, A.M. (2019) The Impact of Hypoxia on the Host-Pathogen Interaction between Neutrophils and Staphylococcus aureus. *International journal of molecular sciences*. **20**(22), 5561.

Hampton, M.B., Kettle, A.J., Winterbourn, C.C. (1998) Inside the Neutrophil Phagosome: Oxidants, Myeloperoxidase, and Bacterial Killing. *Blood*. **92**(9), 3007–3017.

Hampton, M.B., Kettle, A.J., Winterbourn, C.C. (1996) Involvement of superoxide and myeloperoxidase in oxygen-dependent killing of Staphylococcus aureus by neutrophils. *Infect Immun*. **64**(9), 3512–3517.

Hampton, M.B., Vissers, M.C.M., Winterbourn, C.C. (1994) A SINGLE ASSAY FOR MEASURING THE RATES OF PHAGOCYTOSIS AND BACTERIAL KILLING BY NEUTROPHILS. *Journal of Leukocyte Biology*. **55**(2), 147–152.

Hampton, M.B., Winterbourn, C.C. (1995) Modification of neutrophil oxidant production with diphenyleneiodonium and its effect on bacterial killing. *Free Radic Biol Med*. **18**(4), 633–9.

Hamrick, T.S., Diaz, A.H., Havell, E.A., Horton, J.R., Orndorff, P.E. (2003) Influence of Extracellular Bactericidal Agents on Bacteria within Macrophages. *Infection and Immunity*. **71**(2), 1016–1019.

Hannah, S., Mecklenburgh, K., Rahman, I., Bellingan, G.J., Greening, A., Haslett, C., Chilvers, E.R. (1995) Hypoxia prolongs neutrophil survival in vitro. *FEBS Letters*. **372**(2–3), 233–237.

Hardisty, G.R., Llanwarne, F., Minns, D., Gillan, J.L., Davidson, D.J., Gwyer Findlay, E., Gray, R.D. (2021) High Purity Isolation of Low Density Neutrophils Casts Doubt on Their Exceptionality in Health and Disease. *Frontiers in Immunology*. **12**, 625922.

Haslett, C., Guthrie, L.A., Kopaniak, M.M., Johnston, R.B., Henson, P.M. (1985) Modulation of multiple neutrophil functions by preparative methods or trace concentrations of bacterial lipopolysaccharide. *Am J Pathol*. **119**(1), 101–10.

Hayashi, F., Means, T.K., Luster, A.D. (2003) Toll-like receptors stimulate human neutrophil function. *Blood*. **102**(7), 2660–2669.

Hayes, E., Murphy, M.P., Pohl, K., Browne, N., McQuillan, K., Saw, L.E., Foley, C., Gargoum, F., McElvaney, O.J., Hawkins, P., Gunaratnam, C., McElvaney, N.G., Reeves, E.P. (2020) Altered Degranulation and pH of Neutrophil Phagosomes Impacts Antimicrobial Efficiency in Cystic Fibrosis. *Frontiers in Immunology*. **11**.

Hewlett, L.J., Prescott, A.R., Watts, C. (1994) The coated pit and macropinocytic pathways serve distinct endosome populations. *The Journal of cell biology*. **124**(5), 689–703.

Hill, H., Quie, P., Pabst, H., Ochs, H., Clark, R., Klebanoff, S., Wedgwood, R. (1974) DEFECT IN NEUTROPHIL GRANULOCYTE CHEMOTAXIS IN JOB'S SYNDROME OF RECURRENT 'COLD' STAPHYLOCOCCAL ABSCESSES. *Originally published as Volume 2, Issue 7881*. **304**(7881), 617–619.

Hirano, K., Chen, W.S., Chueng, A.L.W., Dunne, A.A., Seredenina, T., Filippova, A., Ramachandran, S., Bridges, A., Chaudry, L., Pettman, G., Allan, C., Duncan, S., Lee, K.C., Lim, J., Ma, M.T., Ong, A.B., Ye, N.Y., Nasir, S., Mulyanidewi, S., Aw, C.C., Oon, P.P., Liao, S., Li, D., Johns, D.G., Miller, N.D., Davies, C.H., Browne, E.R., Matsuoka, Y., Chen, D.W., Jaquet, V., Rutter, A.R. (2015) Discovery of GSK2795039, a Novel Small Molecule NADPH Oxidase 2 Inhibitor. *Antioxidants & Redox Signaling*. **23**(5), 358–374.

Hoenderdos, K., Condliffe, A. (2013) The Neutrophil in Chronic Obstructive Pulmonary Disease: Too Little, Too Late or Too Much, Too Soon? *American Journal of Respiratory Cell and Molecular Biology (Online)*. **48**(5), 531–9.

Hoenderdos, K., Lodge, K.M., Hirst, R.A., Chen, C., Palazzo, S.G.C., Emerenciana, A., Summers, C., Angyal, A., Porter, L., Juss, J.K., Callaghan, C., Chilvers, E.R., Condliffe, A.M. (2016) Hypoxia upregulates neutrophil degranulation and potential for tissue injury. *Thorax*. **71**(11), 1030.

Holland, P.C., Sherratt, H.S. (1972) Biochemical effects of the hypoglycaemic compound diphenyleneiodonnium. Catalysis of anion-hydroxyl ion exchange across the inner membrane of rat liver mitochondria and effects on oxygen uptake. *The Biochemical Journal*. **129**(1), 39–54.

Holtz, R.W. (2009) Chapter 13 - In Vitro Methods to Screen Materials for Anti-aging Effects. In N. Dayan, ed. *Skin Aging Handbook*. Personal Care & Cosmetic Technology. Norwich, NY: William Andrew Publishing, pp. 329–362.

Hong, X., Qin, J., Li, T., Dai, Y., Wang, Y., Liu, Q., He, L., Lu, H., Gao, Q., Lin, Y., Li, M. (2016) Staphylococcal Protein A Promotes Colonization and Immune Evasion of the Epidemic Healthcare-Associated MRSA ST239. *Front Microbiol*. **7**, 951.

Horsburgh, M., Aish, J., White, I., Shaw, L., Lithgow, J., Foster, S. (2002) [sigma] super(B) Modulates Virulence Determinant Expression and Stress Resistance: Characterization of a Functional rsbU Strain Derived from Staphylococcus aureus 8325- 4 S. Foster, ed. *Journal of Bacteriology*. **184**(19), 5457–5467.

Hsu, A.P., Donkó, A., Arrington, M.E., Swamydas, M., Fink, D., Das, A., Escobedo, O., Bonagura, V., Szabolcs, P., Steinberg, H.N., Bergerson, J., Skoskiewicz, A., Makhija, M., Davis, J., Foruraghi, L., Palmer, C., Fuleihan, R.L., Church, J.A., Bhandoola, A., Lionakis, M.S., Campbell, S., Leto, T.L., Kuhns, D.B., Holland, S.M. (2019) Dominant activating RAC2 mutation with lymphopenia, immunodeficiency, and cytoskeletal defects. *Blood*. **133**(18), 1977–1988.

Hua Su, Fei Yang, Rao Fu, Xin Li, Randall French, Evangeline Mose, Xiaohong Pu, Brittney Trinh, Avi Kumar, Junlai Liu, Laura Antonucci, Jelena Todoric, Yuan Liu, Yinling Hu, Maria T. Diaz-Meco, Jorge Moscat, Christian M. Metallo, Andrew M. Lowy, Beicheng Sun, Michael Karin (2021) Cancer cells escape autophagy inhibition via NRF2-induced macropinocytosis. . **39**(5), P678-693.E11.

Huang, J., Canadien, V., Lam, G.Y., Steinberg, B.E., Dinauer, M.C., Magalhaes, M.A.O., Glogauer, M., Grinstein, S., Brumell, J.H. (2009) Activation of antibacterial autophagy by NADPH oxidases. *Proceedings of the National Academy of Sciences*. **106**(15), 6226–6231.

Huang, L., Arany, Z., Livingston, D., Bunn, H. (1996) Activation of hypoxia- inducible transcription factor depends primarily upon redox- sensitive stabilization of its alpha subunit H. Bunn, ed. *Journal of Biological Chemistry*. **271**(50), 32253–32259.

Imlay, J.A. (2003) Pathways of Oxidative Damage. *Annual Review of Microbiology*. **57**(1), 395–418.

Imlay, J.A., Chin, S.M., Linn, S. (1988) Toxic DNA damage by hydrogen peroxide through the fenton reaction in vivo and in vitro. *Science*. **240**(4852), 640–642.

Jaakkola, P., Mole, D.R., Tian, Y.M., Wilson, M.I., Gielbert, J., Gaskell, S.J., Von Kriegsheim, A., Hebestreit, H.F., Mukherji, M., Schofield, C.J., Maxwell, P.H., Pugh, C.W., Ratcliffe, P.J. (2001) Targeting of HIF- alpha to the von Hippel- Lindau ubiquitylation complex by O2-regulated prolyl hydroxylation. *Science (New York, N.Y.)*. **292**(5516), 468.

Jahanban-Esfahlan, R., Guardia, M. de la, Ahmadi, D., Yousefi, B. (2018) Modulating tumor hypoxia by nanomedicine for effective cancer therapy. *Journal of Cellular Physiology*. **233**(3), 2019–2031.

Jahr, H., Pfeiffer, G., Hering, B.J., Federlin, K., Bretzel, R.G. (1999) Endotoxin-mediated activation of cytokine production in human PBMCs by collagenase and Ficoll. *J Mol Med (Berl)*. **77**(1), 118–20.

Jin, H.L., Sun, J., Zhu, K., Liu, X., Zhang, Q., Shen, Q., Gao, Y., Yu (2017) The prognostic value of neutrophil-lymphocyte ratio is superior to derived neutrophil-lymphocyte ratio in advanced gastric cancer treated with preoperative chemotherapy and sequential R0 resection: a 5-year follow-up. *OncoTargets Ther.*. **10**, 2655–2664.

Kanai, F., Liu, H., Field, S.J., Akbary, H., Matsuo, T., Brown, G.E., Cantley, L.C., Yaffe, M.B. (2001) The PX domains of p47phox and p40phox bind to lipid products of PI(3)K. *Nature Cell Biology*. **3**(7), 675–678.

Karavolos, M.H., Horsburgh, M.J., Ingham, E., Foster, S.J. (2003) Role and regulation of the superoxide dismutases of Staphylococcus aureus. *Microbiology (Reading, England)*. **149**(Pt 10), 2749–2758.

Kennedy, A.D., DeLeo, F.R. (2009) Neutrophil apoptosis and the resolution of infection. *Immunologic Research*. **43**(1–3), 25–61.

Keshari, R.S., Jyoti, A., Dubey, M., Kothari, N., Kohli, M., Bogra, J., Barthwal, M.K., Dikshit, M. (2012) Cytokines induced neutrophil extracellular traps formation: implication for the inflammatory disease condition. *PloS One*. **7**(10), e48111.

van Kessel, K.P.M., Bestebroer, J., van Strijp, J.A.G. (2014) Neutrophil-mediated phagocytosis of Staphylococcus aureus. *Frontiers in Immunology*. **5**, 12.

Keyer, K., Imlay, J.A. (1996) Superoxide accelerates DNA damage by elevating free-iron levels. *Proceedings of the National Academy of Sciences of the United States of America*. **93**(24), 13635–13640.

Kinkel, T.L., Roux, C.M., Dunman, P.M., Fang, F.C. (2013) The Staphylococcus aureus SrrAB Two-Component System Promotes Resistance to Nitrosative Stress and Hypoxia. *Mbio*. **4**(6), 9.

Kirchner, T., Möller, S., Klinger, M., Solbach, W., Laskay, T., Behnen, M. (2012) The impact of various reactive oxygen species on the formation of neutrophil extracellular traps. *Mediators of Inflammation*. **2012**, 849136.

Kitahara, M., Eyre, H.J., Simonian, Y., Atkin, C.L., Hasstedt, S.J. (1981) Hereditary myeloperoxidase deficiency. *Blood*. **57**(5), 888–893.

Kobayashi, S., Voyich, J., Braughton, K., Whitney, A., Nauseef, W., Malech, H., Deleo, S. (2004) Gene Expression Profiling Provides Insight into the Pathophysiology of Chronic Granulomatous Disease S. Kobayashi, ed. *Journal of Immunology*. **172**(1), 636–643.

Kobayashi, S.D., Malachowa, N., DeLeo, F.R. (2018) Neutrophils and Bacterial Immune Evasion. *Journal of Innate Immunity*. **10**(5–6), 432–441.

Koh, M.Y., Powis, G. (2012) Passing the baton: the HIF switch. *Trends in Biochemical Sciences*. **37**(9), 364–372.

Köhler Stephan, Foulongne Vincent, Ouahrani-Bettache Safia, Bourg Gisèle, Teyssier Jacques, Ramuz Michel, Liautard Jean-Pierre (2002) The analysis of the intramacrophagic virulome of Brucella suis deciphers the environment encountered

by the pathogen inside the macrophage host cell. *Proceedings of the National Academy of Sciences*. **99**(24), 15711–15716.

Koymans, K.J., Bisschop, A., Vughs, M.M., van Kessel, K.P.M., de Haas, C.J.C., van Strijp, J.A.G. (2016) Staphylococcal Superantigen-Like Protein 1 and 5 (SSL1 & SSL5) Limit Neutrophil Chemotaxis and Migration through MMP-Inhibition. *International journal of molecular sciences*. **17**(7), 1072.

Kubica, M., Guzik, K., Koziel, J., Zarebski, M., Richter, W., Gajkowska, B., Golda, A., Maciag-Gudowska, A., Brix, K., Shaw, L., Foster, T., Potempa, J. (2008) A Potential New Pathway for Staphylococcus aureus Dissemination: The Silent Survival of S. aureus Phagocytosed by Human Monocyte-Derived Macrophages. *Plos One*. **3**(1), 16.

Kuhns, D.B., Long Priel, D.A., Chu, J., Zarember, K.A. (2015) Isolation and Functional Analysis of Human Neutrophils. *Curr Protoc Immunol*. **111**, 7.23.1-16.

Kusuma, C., Jadanova, A., Chanturiya, T., Kokai-Kun, J.F. (2007) Lysostaphin-resistant variants of Staphylococcus aureus demonstrate reduced fitness in vitro and in vivo. *Antimicrobial Agents and Chemotherapy*. **51**(2), 475–82.

Kyme, P., Thoennissen, N.H., Tseng, C.W., Thoennissen, G.B., Wolf, A.J., Shimada, K., Krug, U.O., Lee, K., Müller-Tidow, C., Berdel, W.E., Hardy, W.D., Gombart, A.F., Koeffler, H.P., Liu, G.Y. (2012) C/EBPε mediates nicotinamide-enhanced clearance of Staphylococcus aureus in mice. *The Journal of Clinical Investigation*. **122**(9), 3316–3329.

Lam, G.Y., Cemma, M., Muise, A.M., Higgins, D.E., Brumell, J.H. (2013) Host and bacterial factors that regulate LC3 recruitment to Listeria monocytogenes during the early stages of macrophage infection. *Autophagy*. **9**(7), 985–995.

Lando, D., Peet, D.J., Gorman, J.J., Whelan, D.A., Whitelaw, M.L., Bruick, R.K. (2002) FIH-1 is an asparaginyl hydroxylase enzyme that regulates the transcriptional activity of hypoxia-inducible factor. *Genes & Development*. **16**(12), 1466–1471.

Leffell, M.S., Spitznagel, J.K. (1974) Intracellular and Extracellular Degranulation of Human Polymorphonuclear Azurophil and Specific Granules Induced by Immune Complexes. *Infection and Immunity*. **10**(6), 1241–1249.

Lehmann, D.M., Seneviratne, A.M., Smrcka, A.V. (2008) Small molecule disruption of G protein beta gamma subunit signaling inhibits neutrophil chemotaxis and inflammation. *Mol Pharmacol*. **73**(2), 410–8.

Lekstrom-Himes, J., Kuhns, D., Alvord, W., Gallin, J. (2005) Inhibition of Human Neutrophil IL- 8 Production by Hydrogen Peroxide and Dysregulation in Chronic Granulomatous Disease J. Lekstrom-Himes, ed. *Journal of Immunology*. **174**(1), 411–417.

Leliefeld, P.H.C., Pillay, J., Vrisekoop, N., Heeres, M., Tak, T., Kox, M., Rooijakkers, S.H.M., Kuijpers, T.W., Pickkers, P., Leenen, L.P.H., Koenderman, L. (2018)

Differential antibacterial control by neutrophil subsets. *Blood advances*. **2**(11), 1344–1355.

Lerche, C.J., Christophersen, L.J., Kolpen, M., Nielsen, P.R., Trøstrup, H., Thomsen, K., Hyldegaard, O., Bundgaard, H., Jensen, P.Ø., Høiby, N., Moser, C. (2017) Hyperbaric oxygen therapy augments tobramycin efficacy in experimental Staphylococcus aureus endocarditis. *International Journal of Antimicrobial Agents*. **50**(3), 406–412.

Lerena, M.C., Colombo, M.I. (2011) Mycobacterium marinum induces a marked LC3 recruitment to its containing phagosome that depends on a functional ESX-1 secretion system. *Cellular Microbiology*. **13**(6), 814–835.

Levine, A.P., Duchen, M.R., de Villiers, S., Rich, P.R., Segal, A.W. (2015) Alkalinity of neutrophil phagocytic vacuoles is modulated by HVCN1 and has consequences for myeloperoxidase activity. *Plos One*. **10**(4), e0125906.

Li, C., Wu, Y., Riehle, A., Ma, J., Kamler, M., Gulbins, E., Grassmé, H. (2017) Staphylococcus aureus Survives in Cystic Fibrosis Macrophages, Forming a Reservoir for Chronic Pneumonia. *Infection and Immunity*. **85**(5), e00883-16.

Li, X.J., Marchal, C.C., Stull, N.D., Stahelin, R.V., Dinauer, M.C. (2010) p47phox Phox Homology Domain Regulates Plasma Membrane but Not Phagosome Neutrophil NADPH Oxidase Activation. *The Journal of Biological Chemistry*. **285**(45), 35169–35179.

Lindmo, K., Stenmark, H. (2006) Regulation of membrane traffic by phosphoinositide 3-kinases. *Journal of Cell Science*. **119**(4), 605–614.

Lindner, B., Burkard, T., Schuler, M. (2020) Phagocytosis assays with different pH-sensitive fluorescent particles and various readouts. *BioTechniques*. **68**(5), 245–250.

Liu, B., Taioli, E. (2015) Seasonal Variations of Complete Blood Count and Inflammatory Biomarkers in the US Population - Analysis of NHANES Data. *Plos One*. **10**(11), e0142382.

Liu, C.-I., Liu, G.Y., Song, Y., Yin, F., Hensler, M.E., Jeng, W.-Y., Nizet, V., Wang, A.H.-J., Oldfield, E. (2008) A cholesterol biosynthesis inhibitor blocks Staphylococcus aureus virulence. *Science (New York, N.Y.)*. **319**(5868), 1391–1394.

Lodge, K.M., Cowburn, A.S., Li, W., Condliffe, A.M. (2020) The Impact of Hypoxia on Neutrophil Degranulation and Consequences for the Host. *International Journal of Molecular Sciences*. **21**(4), 1183.

Lodge, K.M., Thompson, A.A.R., Chilvers, E.R., Condliffe, A.M. (2017) Hypoxic regulation of neutrophil function and consequences for Staphylococcus aureus infection. *Microbes and Infection*. **19**(3), 166–176.

Loiselle, F.B., Casey, J.R. (2003) Measurement of Intracellular pH. In Q. Yan, ed. *Membrane Transporters: Methods and Protocols*. Methods in Molecular Biology. Totowa, NJ: Humana Press, pp. 259–280.

Lone, A.G., Atci, E., Renslow, R., Beyenal, H., Noh, S., Fransson, B., Abu-Lail, N., Park, J.-J., Gang, D.R., Call, D.R. (2015) Staphylococcus aureus induces hypoxia and cellular damage in porcine dermal explants. *Infection and Immunity*. **83**(6), 2531.

Lu, T., Porter, A.R., Kennedy, A.D., Kobayashi, S.D., DeLeo, F.R. (2014) Phagocytosis and Killing of Staphylococcus aureus by Human Neutrophils. *Journal of Innate Immunity*. **6**(5), 639–649.

Machado, D., Pires, D., Perdigão, J., Couto, I., Portugal, I., Martins, M., Amaral, L., Anes, E., Viveiros, M. (2016) Ion Channel Blockers as Antimicrobial Agents, Efflux Inhibitors, and Enhancers of Macrophage Killing Activity against Drug Resistant Mycobacterium tuberculosis. *PloS one*. **11**(2), e0149326–e0149326.

Magryś, A., Deryło, K., Bogut, A., Olender, A., Tchórzewski, M. (2018) Intraphagolysosomal conditions predispose to Staphylococcus epidermidis small colony variants persistence in macrophages. *PloS one*. **13**(11), e0207312–e0207312.

Malanoski, G.J., Samore, M.H., Pefanis, A., Karchmer, A.W. (1995) Staphylococcus aureus Catheter- Associated Bacteremia: Minimal Effective Therapy and Unusual Infectious Complications Associated With Arterial Sheath Catheters. *Archives of Internal Medicine*. **155**(11), 1161–1166.

Manda-Handzlik, A., Bystrzycka, W., Cieloch, A., Glodkowska-Mrowka, E., Jankowska-Steifer, E., Heropolitanska-Pliszka, E., Skrobot, A., Muchowicz, A., Ciepiela, O., Wachowska, M., Demkow, U. (2020) Nitric oxide and peroxynitrite trigger and enhance release of neutrophil extracellular traps. *Cellular and molecular life sciences: CMLS*. **77**(15), 3059–3075.

Mandell, G.L. (1975) Catalase, superoxide dismutase, and virulence of Staphylococcus aureus. In vitro and in vivo studies with emphasis on staphylococcal--leukocyte interaction. *The Journal of Clinical Investigation*. **55**(3), 561–566.

Mashruwala, A.A., Guchte, A. van de, Boyd, J.M. (2017) Impaired respiration elicits SrrAB-dependent programmed cell lysis and biofilm formation in Staphylococcus aureus. *eLife*. **6**, e23845.

Matute, J.D., Arias, A.A., Wright, N.A.M., Wrobel, I., Waterhouse, C.C.M., Li, X.J., Marchal, C.C., Stull, N.D., Lewis, D.B., Steele, M., Kellner, J.D., Yu, W., Meroueh, S.O., Nauseef, W.M., Dinauer, M.C. (2009) A new genetic subgroup of chronic granulomatous disease with autosomal recessive mutations in p40 phox and selective defects in neutrophil NADPH oxidase activity. *Blood*. **114**(15), 3309–3315.

Maxwell, P.H., Wiesener, M.S., Chang, G.W., Clifford, S.C., Vaux, E.C., Cockman, M.E., Wykoff, C.C., Pugh, C.W., Maher, E.R., Ratcliffe, P.J. (1999) The tumor suppressor protein VHL targets hypoxia-inducible factors for oxygen-dependent proteolysis. *Nature*. **399(6733)**, 271–275.

McDonough, M.A., Li, V., Flashman, E., Chowdhury, R., Mohr, C., Lienard, B.M.R., Zondlo, J., Oldham, N.J., Clifton, I.J., Lewis, J., McNeill, L.A., Kurzeja, R.J.M., Hewitson, K.S., Yang, E., Jordan, S., Syed, R.S., Schofield, C.J. (2006) Cellular

oxygen sensing: Crystal structure of hypoxia-inducible factor prolyl hydroxylase (PHD2). *Proceedings of the National Academy of Sciences of the United States of America*. **103**(26), 9814–9819.

McGovern, N.N., Cowburn, A.S., Porter, L., Walmsley, S.R., Summers, C., Thompson, A.A.R., Anwar, S., Willcocks, L.C., Whyte, M.K.B., Condliffe, A.M., Chilvers, E.R. (2011) Hypoxia Selectively Inhibits Respiratory Burst Activity and Killing of Staphylococcus aureus in Human Neutrophils. *Journal of Immunology*. **186**(1), 453–463.

McVicker, G., Prajsnar, T.K., Williams, A., Wagner, N.L., Boots, M., Renshaw, S.A., Foster, S.J. (2014) Clonal expansion during Staphylococcus aureus infection dynamics reveals the effect of antibiotic intervention. *PLoS pathogens*. **10**(2), e1003959.

Meissner, F., Seger, R.A., Moshous, D., Fischer, A., Reichenbach, J., Zychlinsky, A. (2010) Inflammasome activation in NADPH oxidase defective mononuclear phagocytes from patients with chronic granulomatous disease. *Blood*. **116**(9), 1570–1573.

Menegazzi, R., Decleva, E., Dri, P. (2012) Killing by neutrophil extracellular traps: fact or folklore? *Blood*. **119**(5), 1214–1216.

Messina, C.G.M., Reeves, E.P., Roes, J., Segal, A.W. (2002) Catalase negative Staphylococcus aureus retain virulence in mouse model of chronic granulomatous disease. *FEBS letters*. **518**(1–3), 107–110.

Mishra, S., Imlay, J. (2012) Why do bacteria use so many enzymes to scavenge hydrogen peroxide? *Archives of Biochemistry and Biophysics*. **525**(2), 145–160.

Mitroulis, I., Kambas, K., Chrysanthopoulou, A., Skendros, P., Apostolidou, E., Kourtzelis, I., Drosos, G.I., Boumpas, D.T., Ritis, K. (2011) Neutrophil extracellular trap formation is associated with IL-1β and autophagy-related signaling in gout. *PloS One*. **6**(12), e29318.

Monceaux, V., Chiche-Lapierre, C., Chaput, C., Witko-Sarsat, V., Prevost, M.-C., Taylor, C.T., Ungeheuer, M.-N., Sansonetti, P.J., Marteyn, B.S. (2016) Anoxia and glucose supplementation preserve neutrophil viability and function. *Blood*. **128**(7), 993–1002.

Morris, D.H., Yip, C.K., Shi, Y., Chait, B.T., Wang, Q.J. (2015) BECLIN 1-VPS34 COMPLEX ARCHITECTURE: UNDERSTANDING THE NUTS AND BOLTS OF THERAPEUTIC TARGETS. *Frontiers in Biology*. **10**(5), 398–426.

Morrissey, S.M., Geller, A.E., Hu, X., Tieri, D., Ding, C., Klaes, C.K., Cooke, E.A., Woeste, M.R., Martin, Z.C., Chen, O., Bush, S.E., Zhang, H.-G., Cavallazzi, R., Clifford, S.P., Chen, J., Ghare, S., Barve, S.S., Cai, L., Kong, M., Rouchka, E.C., McLeish, K.R., Uriarte, S.M., Watson, C.T., Huang, J., Yan, J. (2021) A specific low-density neutrophil population correlates with hypercoagulation and disease severity in hospitalized COVID-19 patients. *JCI insight*. **6**(9), 148435.

Murray, J., Barbara, J.A., Dunkley, S.A., Lopez, A.F., Van Ostade, X., Condliffe, A.M., Dransfield, I., Haslett, C., Chilvers, E.R. (1997) Regulation of neutrophil apoptosis by tumor necrosis factor-alpha: requirement for TNFR55 and TNFR75 for induction of apoptosis in vitro. *Blood*. **90**(7), 2772–83.

Nanda, A., Gukovskaya, A., Tseng, J., Grinstein, S. (1992) Activation of vacuolar-type proton pumps by protein kinase C. Role in neutrophil pH regulation. *Journal of Biological Chemistry*. **267**(32), 22740–22746.

Narita, S., Kaneko, J., Chiba, J., Piémont, Y., Jarraud, S., Etienne, J., Kamio, Y. (2001) Phage conversion of Panton-Valentine leukocidin in Staphylococcus aureus: molecular analysis of a PVL-converting phage, phiSLT. *Gene*. **268**(1–2), 195–206.

Nauseef, W.M. (1988) Myeloperoxidase deficiency. *Hematology/Oncology Clinics of North America*. **2**(1), 135–158.

Nguyen, T.L., Durán, R.V. (2016) Prolyl hydroxylase domain enzymes and their role in cell signaling and cancer metabolism. *The International Journal of Biochemistry & Cell Biology*. **80**, 71–80.

Nis Pedersen, J., Kasper, H., Caroline Marie, A., Michael, P., Kurt, F., Rikke, L.M., Eskild, P. (2017) Hyperbaric Oxygen Therapy is Ineffective as an Adjuvant to Daptomycin with Rifampicin Treatment in a Murine Model of Staphylococcus aureus in Implant- Associated Osteomyelitis. *Microorganisms*. **5**(2), 21.

Nordenfelt, P., Grinstein, S., Björck, L., Tapper, H. (2012) V-ATPase-mediated phagosomal acidification is impaired by Streptococcus pyogenes through Mga-regulated surface proteins. *Danger signals and immunity*. **14**(14), 1319–1329.

Nordenfelt, P., Tapper, H. (2011) Phagosome dynamics during phagocytosis by neutrophils. *Journal of Leukocyte Biology*. **90**(2), 271–284.

Nordenfelt, P., Tapper, H. (2010) The role of calcium in neutrophil granule-phagosome fusion. *Communicative & Integrative Biology*. **3**(3), 224–226.

Novick, R. (1967) Properties of a cryptic high-frequency transducing phage in Staphylococcus aureus. *Virology*. **33**(1), 155–166.

Ogryzko, N.V., Lewis, A., Wilson, H.L., Meijer, A.H., Renshaw, S.A., Elks, P.M. (2019) Hif-1α-Induced Expression of Il-1β Protects against Mycobacterial Infection in Zebrafish. *Journal of Immunology (Baltimore, Md.: 1950)*. **202**(2), 494–502.

Okochi, Y., Sasaki, M., Iwasaki, H., Okamura, Y. (2009) Voltage-gated proton channel is expressed on phagosomes. *Biochemical and Biophysical Research Communications*. **382**(2), 274–279.

Okumura, C.Y.M., Hollands, A., Tran, D.N., Olson, J., Dahesh, S., von Köckritz-Blickwede, M., Thienphrapa, W., Corle, C., Jeung, S.N., Kotsakis, A., Shalwitz, R.A., Johnson, R.S., Nizet, V. (2012) A new pharmacological agent (AKB-4924) stabilizes hypoxia inducible factor-1 (HIF-1) and increases skin innate defenses against

bacterial infection. *Journal of Molecular Medicine (Berlin, Germany)*. **90**(9), 1079–1089.

Okura, Y., Yamada, M., Kuribayashi, F., Kobayashi, I., Ariga, T. (2015) Monocyte/ macrophage- Specific NADPH Oxidase Contributes to Antimicrobial Host Defense in X- CGD. *Journal of Clinical Immunology*. **35**(2), 158–167.

O'Neill, A.J. (2010) Staphylococcus aureus SH1000 and 8325-4: comparative genome sequences of key laboratory strains in staphylococcal research. *Letters in Applied Microbiology*. **51**(3), 358–361.

Ov, V., Rj, B., L, R., Sm, B., T, M., Hw, D., A, S., Jm, B., Lc, C., S, G. (2001) Distinct roles of class I and class III phosphatidylinositol 3-kinases in phagosome formation and maturation. *The Journal of Cell Biology*. **155**(1), 19–25.

Palazon, A., Goldrath, A.W., Nizet, V., Johnson, R.S. (2014) HIF Transcription Factors, Inflammation, and Immunity. *Immunity*. **41**(4), 518–528.

Pandey, M., Singh, A.K., Thakare, R., Talwar, S., Karaulia, P., Dasgupta, A., Chopra, S., Pandey, A.K. (2017) Diphenyleneiodonium chloride (DPIC) displays broad-spectrum bactericidal activity. *Scientific reports*. **7**(1), 11521–11521.

Pang, Y.Y., Schwartz, J., Thoendel, M., Ackermann, L.W., Horswill, A.R., Nauseef, W.M. (2010) agr-Dependent Interactions of Staphylococcus aureus USA300 with Human Polymorphonuclear Neutrophils. *Journal of Innate Immunity*. **2**(6), 546–559.

Park, B., Liu, G.Y. (2020) Staphylococcus aureus and Hyper-IgE Syndrome. *International Journal of Molecular Sciences*. **21**(23).

Parker, L.C., Prince, L.R., Buttle, D.J., Sabroe, I. (2009) The Generation of Highly Purified Primary Human Neutrophils and Assessment of Apoptosis in Response to Toll-Like Receptor Ligands. In C. E. McCoy & L. A. J. O'Neill, eds. *Toll-Like Receptors: Methods and Protocols*. Totowa, NJ: Humana Press, pp. 191–204.

Parkin, J., Cohen, B. (2001) An overview of the immune system. *The Lancet*. **357**(9270), 1777–1789.

Pereira, H.A., Shafer, W.M., Pohl, J., Martin, L.E., Spitznagel, J.K. (1990) CAP37, a human neutrophil-derived chemotactic factor with monocyte specific activity. *The Journal of Clinical Investigation*. **85**(5), 1468–1476.

Perera, N.C., Wiesmüller, K.-H., Larsen, M.T., Schacher, B., Eickholz, P., Borregaard, N., Jenne, D.E. (2013) NSP4 Is Stored in Azurophil Granules and Released by Activated Neutrophils as Active Endoprotease with Restricted Specificity. *The Journal of Immunology*. **191**(5), 2700–2707.

Peyssonnaux, C., Datta, V., Cramer, T., Doedens, A., Theodorakis, E.A., Gallo, R.L., Hurtado-Ziola, N., Nizet, V., Johnson, R.S. (2005) HIF-1 alpha expression regulates the bactericidal capacity of phagocytes. *Journal of Clinical Investigation*. **115**(7), 1806–1815.

Pintard, C., Ben Khemis, M., Liu, D., Dang, P.M.-C., Hurtado-Nedelec, M., El-Benna, J. (2020) Apocynin prevents GM-CSF-induced-ERK1/2 activation and -neutrophil survival independently of its inhibitory effect on the phagocyte NADPH oxidase NOX2. *Biochemical Pharmacology*. **177**, 113950.

Pollitt, E.J.G., Szkuta, P.T., Burns, N., Foster, S.J. (2018) Staphylococcus aureus infection dynamics. *Plos Pathogens*. **14**(6), e1007112.

Porter, L.M., Cowburn, A.S., Farahi, N., Deighton, J., Farrow, S.N., Fiddler, C.A., Juss, J.K., Condliffe, A.M., Chilvers, E.R. (2017) Hypoxia causes IL-8 secretion, Charcot Leyden crystal formation, and suppression of corticosteroid-induced apoptosis in human eosinophils. *Clinical & Experimental Allergy*. **47**(6), 770–784.

Prajsnar, T.K., Cunliffe, V.T., Foster, S.J., Renshaw, S.A. (2008) A novel vertebrate model of Staphylococcus aureus infection reveals phagocyte-dependent resistance of zebrafish to non-host specialized pathogens. *Cellular Microbiology*. **10**(11), 2312–2325.

Prajsnar, T.K., Hamilton, R., Garcia-Lara, J., McVicker, G., Williams, A., Boots, M., Foster, S.J., Renshaw, S.A. (2012) A privileged intraphagocyte niche is responsible for disseminated infection of Staphylococcus aureus in a zebrafish model. *Cellular Microbiology*. **14**(10), 1600–1619.

Prajsnar, T.K., Serba, J.J., Dekker, B.M., Gibson, J.F., Masud, S., Fleming, A., Johnston, S.A., Renshaw, S.A., Meijer, A.H. (2021) The autophagic response to Staphylococcus aureus provides an intracellular niche in neutrophils. *Autophagy*. **17**(4), 888–902.

Prokesch, R.C., Hand, W.L. (1982) Antibiotic entry into human polymorphonuclear leukocytes. *Antimicrobial Agents and Chemotherapy*. **21**(3), 373–80.

Raad, H., Paclet, M.-H., Boussetta, T., Kroviarski, Y., Morel, F., Quinn, M.T., Gougerot-Pocidalo, M.-A., Dang, P.M.-C., El-Benna, J. (2009) Regulation of the phagocyte NADPH oxidase activity: phosphorylation of gp91phox/NOX2 by protein kinase C enhances its diaphorase activity and binding to Rac2, p67phox, and p47phox. *FASEB journal: official publication of the Federation of American Societies for Experimental Biology*. **23**(4), 1011–1022.

Recsei, P., Kreiswirth, B., Reilly, M., Schlievert, P., Gruss, A., Novick, R. (1986) Regulation of exoprotein gene expression in Staphylococcus aureus by agr. *Molecular and General Genetics MGG*. **202**(1), 58–61.

Reeves, E., Nagl, M., Godovac-Zimmermann, J., Segal, A. (2003) Reassessment of the microbicidal activity of reactive oxygen species and hypochlorous acid with reference to the phagocytic vacuole of the neutrophil granulocyte E. Reeves, ed. *Journal of Medical Microbiology*. **52**(8), 643–651.

Reeves, E.P., Lu, H., Jacobs, H.L., Messina, C.G.M., Bolsover, S., Gabella, G., Potma, E.O., Warley, A., Roes, J., Segal, A.W. (2002) Killing activity of neutrophils is mediated through activation of proteases by K+ flux. *Nature*. **416**(6878), 291–297.

Regier, D.S., Waite, K.A., Wallin, R., McPhail, L.C. (1999) A phosphatidic acid-activated protein kinase and conventional protein kinase C isoforms phosphorylate p22(phox), an NADPH oxidase component. *The Journal of Biological Chemistry*. **274**(51), 36601–36608.

Reiss, M., Roos, D. (1978) Differences in Oxygen Metabolism of Phagocytosing Monocytes and Neutrophils. *Journal of Clinical Investigation*. **61**(2), 480–488.

Remijsen, Q., Vanden Berghe, T., Wirawan, E., Asselbergh, B., Parthoens, E., De Rycke, R., Noppen, S., Delforge, M., Willems, J., Vandenabeele, P. (2011) Neutrophil extracellular trap cell death requires both autophagy and superoxide generation. *Cell Research*. **21**(2), 290–304.

Repine, J.E., Fox, R.B., Berger, E.M. (1981) Hydrogen peroxide kills Staphylococcus aureus by reacting with staphylococcal iron to form hydroxyl radical. *The Journal of Biological Chemistry*. **256**(14), 7094–7096.

Rigby, K.M., DeLeo, F.R. (2012) Neutrophils in innate host defense against Staphylococcus aureus infections. *Seminars in Immunopathology*. **34**(2), 237–259.

Röhm, M., Grimm, M.J., D'Auria, A.C., Almyroudis, N.G., Segal, B.H., Urban, C.F. (2014) NADPH oxidase promotes neutrophil extracellular trap formation in pulmonary aspergillosis. *Infection and Immunity*. **82**(5), 1766–1777.

Rong, W., Kevin, R.B., Dorothee, K., Thanh-Huy, L.B., Shu, Y.Q., Min, L., Adam, D.K., David, W.D., Seymour, J.K., Andreas, P., Frank, R.D., Michael, O. (2007) Identification of novel cytolytic peptides as key virulence determinants for community- associated MRSA. *Nature Medicine*. **13**(12), 1510.

Roos, D., Boer, M. (2014) Molecular diagnosis of chronic granulomatous disease. *Clinical and Experimental Immunology*. **175**(2), 139–149.

Roth, I.L., Salamon, P., Freund, T., Gadot, Y.B.-D., Baron, S., Hershkovitz, T., Shefler, I., Hanna, S., Confino-Cohen, R., Bentur, L., Hagin, D. (2020) Novel NCF2 Mutation Causing Chronic Granulomatous Disease. *Journal of Clinical Immunology*. **40**(7), 977–986.

Ryu, J.-S., Kang, J.-H., Jung, S.-Y., Shin, M.-H., Kim, J.-M., Park, H., Min, D.-Y. (2004) Production of interleukin-8 by human neutrophils stimulated with Trichomonas vaginalis. *Infection and Immunity*. **72**(3), 1326–1332.

Sabroe, I., Prince, L.R., Jones, E.C., Horsburgh, M.J., Foster, S.J., Vogel, S.N., Dower, S.K., Whyte, M.K.B. (2003) Selective roles for Toll- like receptor (TLR) 2 and TLR4 in the regulation of neutrophil activation and life span. *Journal of immunology (Baltimore, Md. : 1950)*. **170**(10), 5268.

Savill, J.S., Wyllie, A.H., Henson, J.E., Walport, M.J., Henson, P.M., Haslett, C. (1989) Macrophage phagocytosis of aging neutrophils in inflammation. Programmed cell death in the neutrophil leads to its recognition by macrophages. *Journal of Clinical Investigation*. **83**(3), 865–875.

Savla, S.R., Laddha, A.P., Kulkarni, Y.A. (2021) Pharmacology of apocynin: a natural acetophenone. *Drug Metabolism Reviews*. **0**(0), 1–21.

Scheel-Toellner, D., Wang, K., Craddock, R., Webb, P.R., McGettrick, H.M., Assi, L.K., Parkes, N., Clough, L.E., Gulbins, E., Salmon, M., Lord, J.M. (2004) Reactive oxygen species limit neutrophil life span by activating death receptor signaling. *Blood*. **104**(8), 2557–2564.

Schindler, C.A., Schuhardt, V.T. (1964) LYSOSTAPHIN: A NEW BACTERIOLYTIC AGENT FOR THE STAPHYLOCOCCUS. *Proceedings of the National Academy of Sciences of the United States of America*. **51**, 414–21.

Schnettger, L., Rodgers, A., Repnik, U., Lai, R.P., Pei, G., Verdoes, M., Wilkinson, R.J., Young, D.B., Gutierrez, M.G. (2017) A Rab20-Dependent Membrane Trafficking Pathway Controls M. tuberculosis Replication by Regulating Phagosome Spaciousness and Integrity. *Cell Host & Microbe*. **21**(5), 619-628.e5.

Seaver, L.C., Imlay, J.A. (2001) Alkyl hydroperoxide reductase is the primary scavenger of endogenous hydrogen peroxide in Escherichia coli. *Journal of Bacteriology*. **183**(24), 7173–7181.

Segal, A.W., Geisow, M., Garcia, R., Harper, A., Miller, R. (1981) The respiratory burst of phagocytic cells is associated with a rise in vacuolar pH. *Nature*. **290**(5805), 406–409.

Sheldon, J.R., Marolda, C.L., Heinrichs, D.E. (2014) TCA cycle activity in Staphylococcus aureus is essential for iron-regulated synthesis of staphyloferrin A, but not staphyloferrin B: the benefit of a second citrate synthase. *Molecular Microbiology*. **92**(4), 824–39.

Simmen, H.-P., Blaser, J. (1993) Analysis of pH and pO2 in abscesses, peritoneal fluid, and drainage fluid in the presence or absence of bacterial infection during and after abdominal surgery. *The American Journal of Surgery*. **166**(1), 24–27.

Simons, J.M., Hart, B.A., Ip Vai Ching, T.R., Van Dijk, H., Labadie, R.P. (1990) Metabolic activation of natural phenols into selective oxidative burst agonists by activated human neutrophils. *Free Radical Biology & Medicine*. **8**(3), 251–258.

Sitkovsky, M., Lukashev, D. (2005) Regulation of immune cells by local-tissue oxygen tension: HIF1[alpha] and adenosine receptors. *Nature Reviews. Immunology*. **5**(9), 712–21.

Soderberg-Warner, M., Rice-Mendoza, C.A., Mendoza, G.R., Stiehm, E.R. (1983) Neutrophil and T lymphocyte characteristics of two patients with hyper-IgE syndrome. *Pediatric Research*. **17**(10), 820–824.

Stapels, D.A.C., Ramyar, K.X., Bischoff, M., von Köckritz-Blickwede, M., Milder, F.J., Ruyken, M., Eisenbeis, J., McWhorter, W.J., Herrmann, M., van Kessel, K.P.M., Geisbrecht, B.V., Rooijakkers, S.H.M. (2014) Staphylococcus aureus secretes a unique class of neutrophil serine protease inhibitors. *Proceedings of the National Academy of Sciences of the United States of America*. **111**(36), 13187–13192.

Stolk, J., Hiltermann, T.J., Dijkman, J.H., Verhoeven, A.J. (1994) Characteristics of the inhibition of NADPH oxidase activation in neutrophils by apocynin, a methoxy-substituted catechol. *American Journal of Respiratory Cell and Molecular Biology*. **11**(1), 95–102.

Summers, C., Rankin, S.M., Condliffe, A.M., Singh, N., Peters, A.M., Chilvers, E.R. (2010) Neutrophil kinetics in health and disease. *Trends in Immunology*. **31**(8), 318–324.

Takeda, N., Dea, E.L., Doedens, A., Kim, J.-W., Weidemann, A., Stockmann, C., Asagiri, M., Simon, M.C., Hoffmann, A., Johnson, R.S. (2010) Differential activation and antagonistic function of HIF-{ alpha} isoforms in macrophages are essential for NO homeostasis. *Genes & development*. **24**(5), 491.

Thammavongsa, V., Kim, H., Missiakas, D., Schneewind, O. (2015) Staphylococcal manipulation of host immune responses. *Nature Reviews. Microbiology*. **13**(9), 529–543.

Thomas, H.B., Moots, R.J., Edwards, S.W., Wright, H.L. (2015) Whose Gene Is It Anyway? The Effect of Preparation Purity on Neutrophil Transcriptome Studies. *PLOS ONE*. **10**(9), e0138982.

Thompson, A.A.R., Dickinson, R.S., Murphy, F., Thomson, J.P., Marriott, H.M., Tavares, A., Willson, J., Williams, L., Lewis, A., Mirchandani, A., Dos Santos Coelho, P., Doherty, C., Ryan, E., Watts, E., Morton, N.M., Forbes, S., Stimson, R.H., Hameed, A.G., Arnold, N., Preston, J.A., Lawrie, A., Finisguerra, V., Mazzone, M., Sadiku, P., Goveia, J., Taverna, F., Carmeliet, P., Foster, S.J., Chilvers, E.R., Cowburn, A.S., Dockrell, D.H., Johnson, R.S., Meehan, R.R., Whyte, M.K.B., Walmsley, S.R. (2017) Hypoxia determines survival outcomes of bacterial infection through HIF-1alpha dependent re-programming of leukocyte metabolism. *Science immunology*. **2**(8), eaal2861.

Tian, W., Li, X.J., Stull, N.D., Ming, W., Suh, C.-I., Bissonnette, S.A., Yaffe, M.B., Grinstein, S., Atkinson, S.J., Dinauer, M.C. (2008) Fc gamma R-stimulated activation of the NADPH oxidase: phosphoinositide-binding protein p40phox regulates NADPH oxidase activity after enzyme assembly on the phagosome. *Blood*. **112**(9), 3867–3877.

Tkalcevic, J., Novelli, M., Phylactides, M., Iredale, J.P., Segal, A.W., Roes, J. (2000) Impaired immunity and enhanced resistance to endotoxin in the absence of neutrophil elastase and cathepsin G. *Immunity*. **12**(2), 201–210.

Tong, S.Y.C., Davis, J.S., Eichenberger, E., Holland, T.L., Fowler, V.G. (2015) Staphylococcus aureus Infections: Epidemiology, Pathophysiology, Clinical Manifestations, and Management. *Clinical Microbiology Reviews*. **28**(3), 603–661.

Traynor-Kaplan, A.E., Thompson, B.L., Harris, A.L., Taylor, P., Omann, G.M., Sklar, L.A. (1989) Transient increase in phosphatidylinositol 3,4-bisphosphate and phosphatidylinositol trisphosphate during activation of human neutrophils. *The Journal of Biological Chemistry*. **264**(26), 15668–15673.

Treffon, J., Chaves-Moreno, D., Niemann, S., Pieper, D.H., Vogl, T., Roth, J., Kahl, B.C. (2020) Importance of superoxide dismutases A and M for protection of Staphylococcus aureus in the oxidative stressful environment of cystic fibrosis airways. *Cellular Microbiology*. **22**(5), e13158.

Tulkens, P.M. (1990) Intracellular pharmacokinetics and localization of antibiotics as predictors of their efficacy against intraphagocytic infections. *Scand J Infect Dis Suppl*. **74**, 209–17.

Ulfig, A., Leichert, L.I. (2021) The effects of neutrophil-generated hypochlorous acid and other hypohalous acids on host and pathogens. *Cellular and molecular life sciences : CMLS*. **78**(2), 385–414.

Valderas, M.W., Gatson, J.W., Wreyford, N., Hart, M.E. (2002) The Superoxide Dismutase Gene sodM Is Unique to Staphylococcus aureus: Absence of sodM in Coagulase-Negative Staphylococci. *Journal of Bacteriology*. **184**(9), 2465–2472.

Valenti, P., Antonini, G. (2005) Lactoferrin: an important host defence against microbial and viral attack. *Cellular and molecular life sciences: CMLS*. **62**(22), 2576–2587.

Vaudaux, P., Waldvogel, F.A. (1979) Gentamicin antibacterial activity in the presence of human polymorphonuclear leukocytes. *Antimicrobial Agents and Chemotherapy*. **16**(6), 743–749.

Vejrazka, M., Micek, R., Stipek, S. (2005) Apocynin inhibits NADPH oxidase in phagocytes but stimulates ROS production in non-phagocytic cells. *Biochimica et Biophysica Acta (BBA) - General Subjects*. **1722**(2), 143–147.

Vieira, O.V., Botelho, R.J., Grinstein, S. (2002) Phagosome maturation: aging gracefully. *Biochem J*. **366**(Pt 3), 689–704.

von Vietinghoff, S., Ley, K. (2008) Homeostatic regulation of blood neutrophil counts. *Journal of Immunology (Baltimore, Md.: 1950)*. **181**(8), 5183–5188.

Vogt, K.L., Summers, C., Condliffe, A.M. (2019) The clinical consequences of neutrophil priming. *Curr Opin Hematol*. **26**(1), 22–27.

Voyich, J.M., Braughton, K.R., Sturdevant, D.E., Whitney, A.R., Saïd-Salim, B., Porcella, S.F., Long, R.D., Dorward, D.W., Gardner, D.J., Kreiswirth, B.N., Musser, J.M., DeLeo, F.R. (2005) Insights into mechanisms used by Staphylococcus aureus to avoid destruction by human neutrophils. *J Immunol*. **175**(6), 3907–19.

Walmsley, S.R., Print, C., Farahi, N., Peyssonnaux, C., Johnson, R.S., Cramer, T., Sobolewski, A., Condliffe, A.M., Cowburn, A.S., Johnson, N., Chilvers, E.R. (2005) Hypoxia-induced neutrophil survival is mediated by HIF-1 alpha-dependent NF-kappa B activity. *Journal of Experimental Medicine*. **201**(1), 105–115.

Watson, F., Robinson, J.J., Edwards, S.W. (1992) Neutrophil function in whole blood and after purification: changes in receptor expression, oxidase activity and responsiveness to cytokines. *Biosci Rep*. **12**(2), 123–33.

Watts, A., Ke, D., Wang, Q., Pillay, A., Nicholson-Weller, A., Lee, J. (2005) Staphylococcus aureus Strains That Express Serotype 5 or Serotype 8 Capsular Polysaccharides Differ in Virulence A. Watts, ed. *Infection and Immunity*. **73**(6), 3502–3511.

Weiss, S.J. (1989) Tissue Destruction by Neutrophils. *New England Journal of Medicine*. **320**(6), 365–376.

Werth, N., Beerlage, C., Rosenberger, C., Yazdi, A.S., Edelmann, M., Amr, A., Bernhardt, W., von Eiff, C., Becker, K., Schafer, A., Peschel, A., Kempf, V.A. (2010) Activation of hypoxia inducible factor 1 is a general phenomenon in infections with human pathogens. *Plos One*. **5**(7), e11576.

Westermann, A.J., Vogel, J. (2018) Host-Pathogen Transcriptomics by Dual RNA-Seq. *Methods in Molecular Biology (Clifton, N.J.)*. **1737**, 59–75.

Wilde, A.D., Snyder, D.J., Putnam, N.E., Valentino, M.D., Hammer, N.D., Lonergan, Z.R., Hinger, S.A., Aysanoa, E.E., Blanchard, C., Dunman, P.M., Wasserman, G.A., Chen, J., Shopsin, B., Gilmore, M.S., Skaar, E.P., Cassat, J.E. (2015) Bacterial Hypoxic Responses Revealed as Critical Determinants of the Host-Pathogen Outcome by TnSeq Analysis of Staphylococcus aureus Invasive Infection. *Plos Pathogens*. **11**(12), 24.

Wimley, W.C., Selsted, M.E., White, S.H. (1994) Interactions between human defensins and lipid bilayers: evidence for formation of multimeric pores. *Protein Science: A Publication of the Protein Society*. **3**(9), 1362–1373.

Winkelstein, J.A., Marino, M.C., Johnston, R.B., Boyle, J., Curnutte, J., Gallin, J.I., Malech, H.L., Holland, S.M., Ochs, H., Quie, P., Buckley, R.H., Foster, C.B., Chanock, S.J., Dickler, H. (2000) Chronic granulomatous disease. Report on a national registry of 368 patients. *Medicine*. **79**(3), 155.

Winterbourn, C.C., Kettle, A.J. (2013) Redox reactions and microbial killing in the neutrophil phagosome. *Antioxid Redox Signal*. **18**(6), 642–60.

Wood, A.J.T., Vassallo, A.M., Ruchaud-Sparagano, M.-H., Scott, J., Zinnato, C., Gonzalez-Tejedo, C., Kishore, K., D'Santos, C.S., Simpson, A.J., Menon, D.K., Summers, C., Chilvers, E.R., Okkenhaug, K., Morris, A.C. (2020) C5a impairs phagosomal maturation in the neutrophil through phosphoproteomic remodeling. *JCI Insight*. **5**(15).

Yarwood, J.M., McCormick, J.K., Schlievert, P.M. (2001) Identification of a novel two-component regulatory system that acts in global regulation of virulence factors of Staphylococcus aureus. *Journal of Bacteriology*. **183**(4), 1113–23.

Yasui, K., Komiyama, A. (2001) Roles of phosphatidylinositol 3-kinase and phospholipase D in temporal activation of superoxide production in FMLP-stimulated human neutrophils. *Cell Biochemistry and Function*. **19**(1), 43–50.

Yu, H.-H., Yang, Y.-H., Chiang, B.-L. (2021) Chronic Granulomatous Disease: a Comprehensive Review. *Clinical Reviews in Allergy & Immunology*. **61**(2), 101–113.

Zhang, J., Zhang, Q. (2018) VHL and Hypoxia Signaling: Beyond HIF in Cancer. *Biomedicines*. **6**(1).